# EMULSION CHAMBER TECHNOLOGY EXPERIMENT (ECT)

**Final Report**
**on Contract NAS8-38428**

## SUMMARY

The experimental objective of ECT was to develop space-borne emulsion chamber technology so that cosmic rays and nuclear interactions may subsequently be studied at extremely high energies with long exposures in space.

A small emulsion chamber was built and flown on flight STS-62 of the *Columbia* in March 1994. Analysis of the several hundred layers of radiation-sensitive material has shown excellent post-flight condition and suitability for cosmic ray physics analysis at much longer exposures. Temperature control of the stack was 20 ± 1°C throughout the active control period and no significant deviations of temperature or pressure in the chamber were observed over the entire mission operations period. The unfortunate flight attitude of the orbiter (almost 90% Earth viewing) prevented any significant number of heavy particles ($Z \geq 10$) reaching the stack and the inverted flow of shower particles in the calorimeter has not allowed evaluation of absolute primary cosmic ray-detection efficiency nor of the practical time limits of useful exposure of these calorimeters in space to the level of detail originally planned. Nevertheless, analysis of the observed backgrounds and quality of the processed photographic and plastic materials after the flight show that productive exposures of emulsion chambers are feasible in low orbit for periods of up to one year or longer. The engineering approaches taken in the ECT program were proven effective and no major environmental obstacles to prolonged flight are evident.

## ACKNOWLEDGMENTS

The successful accomplishment of the ECT experiment on STS-62 required the participation and effort of many individuals at several institutions. Notable among these were:

Tom Parnell, Mark Christl, Ellen Roberts, and Walt Fountain, (Marshall Space Flight Center, Space Sciences Lab, Cosmic Ray Laboratory)

Dave Cockrell, Jimmy Johnson, John Owens, Lou Ann Fikes, David Siersma, James McGee, (Marshall Space Flight Center, Engineering)

Steve Sutherlin and John Webber, (Orbital Sciences Corporation, Thermal and Electrical Engineering)

Gerard Durback, Joanne Baker, Neal Barthelme, (Goddard Space Flight Center, Engineering)

Eugene Benton, Allan Frank, Eric Benton, (ERIL Research, Dosimetry Program)

Takahiro Tominaga, Bei-Lei Dong, and Kanaya Chevli, (University of Alabama in Huntsville, Cosmic Ray Laboratory)

Francis Wessling, Reinhold Freiseis, Ron Eakes, Lisa Hughes, (University of Alabama in Huntsville, Engineering)

## CONTENTS

## 1. Introduction

Emulsion chambers have proven an efficient means of measuring the charge composition and energy spectrum of cosmic rays in the region above $10^{13}$eV (ref 1,2,3,4)). Such measurements require detector exposure factors of thousands of $m^2$ hours exposure above the atmosphere to provide adequate statistics. So far these have been, and continue to be, obtained using balloons. However, definitive measurements of abundances above $10^{15}$eV require exposures of detectors of area several $m^2$ for periods of many months, and ultimately will require flight on an orbital platform. An engineering test flight of a 40 x 50 $cm^2$ emulsion chamber was undertaken on the Space Shuttle to evaluate the effects of radiation background, launch, thermal and other environments on a heavy calorimeter of this type. Since the detector stack was composed of parallel sheets of total mass-thickness ~ 120g $cm^{-2}$, it also provided a thick structure easily modeled for radiation transport calculations. The stack included arrays of small dosimetry detectors to provide a means of calibrating the transport codes in the orbital radiation field at high shielding depths.

This paper describes the technical results of the first orbital flight of an emulsion chamber. The flight experiment was performed in March, 1994, on NASA's Space Shuttle *Columbia*, and designated STS-62. The Emulsion Chamber Technology (ECT) mission was planned to ***assess the major uncertainties of space exposure of an emulsion calorimeter*** through the flight of one sub-unit of a chamber. Deployment of an actual experiment for astrophysical research purposes would require an assembly of many such chambers. Verification of the effectiveness of the emulsion chamber technology in space is vital for large-scale cosmic ray experiments on the STS and the International Space Station platforms. The secondary objective of the ECT flight was to obtain radiation data for studying the effects of shielding on the penetrative particles of interest, utilizing the emulsion chamber's self-shielding materials that are much greater than the maximum value in ordinary manned space vehicles.

Our emulsion chambers contain a fine-grain, three-dimensional tracking telescope and a sampling calorimeter, which have proven powerful in observing very high energy cosmic ray protons and nuclei. This method was well established for balloon flight experiments by the Japanese American Cooperative Emulsion Experiment (JACEE) collaboration for direct observation of cosmic rays toward the "knee" region (E ~ $10^{15}$ eV) (1). Very low intensities of cosmic rays in the "knee" region (~ 100/$m^2$ year sr at E ~ $10^{15}$ eV) call for a large-area and long-duration space experiments.

Long-duration space experiments, however, pose several logistic and technological challenges for emulsion chambers. Among many issues, the following three must at least be studied and overcome for successful experiments: (1) assess the feasibility of track registration and analyses with emulsions and X-ray films under conditions of high background density of slow protons coming from the radiation belts, (2) protection from hostile thermal environments to secure uniform and regular track registration quality, and (3) provision of the mechanical strength for safeguard of emulsions from extreme vibration and shock loads during launch of the Shuttle.

## 2. Instrumentation

The ECT emulsion chamber utilized over 120 double-sided emulsion plates with 70 X-ray films, 20 sheets of CR-39 plate, and 12 radiation lengths of lead absorbers (**Fig. 1**). A complete description of the flight stack configuration is given in **Appendix D**. The vertical material

thickness was 120 g/cm$^2$. All the materials were tightly mounted in a hermetically sealed, anodized aluminum chamber which was milled out of 2 blocks (**Fig. 2**). The ceiling or lid was an aluminum honeycomb panel. Thin Kapton-film heaters were mounted on the top and the bottom of the chamber. A dozen thermistors were mounted inside and outside the chamber, which, with an electronic control unit, regulated the uniform temperature of $20.0 \pm 0.1^0$ C, at all the points in the chamber (**Fig. 3**) during the period while the system was powered. Ground procedures were designed so that the chamber temperature should not exceed $30^0$C at any time. No excursions above $24^0$C were encountered.

ECT was mounted in the *Columbia* on a cross-bay structure termed the Mission Particular Experiment Support Structure (MPESS) which was configured by Goddard Space Flight Center to carry a total of six experiments for the Office of Aeronautics and Space Technology (OAST). This configuration was termed OAST-2. **Figs. 4, 5, and 6** show ECT and the OAST-2 in the bay of *Columbia*. The other experiments are identified in **Fig. 7**.

## 3. Flight Profile of STS-62

STS-62 was launched at 7:53 a.m. CST on March 4, 1994. The mission lasted a total of 335.3 hours or 13.97 days. The orbiter *Columbia* had a mean altitude of 296 km and an orbital inclination of 39.0 deg. While the cargo bay doors were open for most of the flight, the bay was mostly facing the Earth.

ECT was designed to measure cosmic rays and should ideally always have been facing deep space and away from Earth. Practically, on the Space Shuttle, that is never possible for a variety of reasons. At the time of mission planning, OAST-2 was secondary payload consisting of 6 experiments. The original ECT requirement was 80 hours space viewing, based on 50% Space:50% Earth viewing over a possible 6 to 7 day flight. This minimum was subsequently reduced to 35-40 hours deep-space viewing. Later, the mission was extended to 14 days without changing the ECT minimums. Because of United States Microgravity Payload (USMP) requirements and thermal problems with at least two OAST-2 payloads, the mission was changed from a basically gravity-gradient (-XLV) orientation to a mostly Earth-viewing flight. More than 10 days were spent in this latter orientation (-ZLV), with about 80 hours -XLV (equivalent to 40 hours deep-space). There were additional periods of several hours uninterrupted deep-space viewing which permitted testing of the cold case thermal control system but did not substantially add to the deep-space viewing fraction of the total exposure.

The result of this orientation mix was that only 12% of the orbital time was spent facing deep space, with the consequence that almost 90% of all cosmic ray showers entered ECT from the bottom, with most of the heavies having already interacted with materials in the Shuttle or the ECT support structure.

This produced two major impacts:

1. The fraction of heavy nuclei detected was very low compared with that originally expected.

2. The effect of retrograde showers through the calorimeter was quite different from normal (i.e. balloon) experience, preventing direct comparison of proton and helium fluxes and thus calibration of event-retrieval efficiency. Also, the particle

background distribution is different in the stack making extrapolations to much longer flight times of several months problematical.

The complex mass distribution of the materials in the Shuttle bay (see **Figs. 8** and **9**) has prevented the planned simplification of calculations using NASA radiation-transport codes.

It should be emphasized however that, despite these complications to our original analysis plan, many events were traced, and detailed analyses performed as discussed below. The engineering approaches used in the ECT experiment were adequate to protect the emulsion materials and would provide the design basis for a space exposure using emulsion calorimetry for a flight period many times longer.

## 4. Data Analysis

### 4.a) Materials for Data Analysis

All the photographic plates and solid state track detectors in the ECT were analyzed. To evaluate the performance of the emulsion chamber materials in space flight, an approximately-identical emulsion chamber of the 1994 Antarctic balloon flight experiment (JACEE-12: a 10-day circumpolar flight) performed only 3 months prior to the STS-62 flight, was analyzed for comparison.

The differences observed in these materials are largely a result of the thermal, mechanical and radiation environments of the space flight and a balloon flight. **Table A1** illustrates the major differences of the ECT shuttle flight and the Antarctic balloon flight exposure. The Antarctic balloon flight was made in the stratosphere (~38 km above the ground) and did not receive any trapped-belt proton background. However, the year 1994, in which both STS-62 and JACEE-12 were flown, was close to solar minimum and background particle fluxes were high in both ECT and JACEE-12 chambers, due to trapped particles and low energy cosmic rays respectively. Comparisons of materials from these two flight materials exposed at solar-minimum help define the background problem and give solid bases for projecting the emulsion chamber capabilities for future long-duration orbital flights.

Materials in the Ground Control Unit for the ECT's STS-62 flight were developed and analyzed together with the flight materials. Other materials used in the analysis include those used in the Materials Compatibility Tests that were performed during the Production Phase (1991 - 93).

**Table A1.** Flight parameters of the STS-62 (ECT) and the Antarctic circumpolar experiment (JACEE-12).

| | Flight Dates | Duration of Flight | Altitude (Average) | Temperature during Flight | Developments Processed in |
|---|---|---|---|---|---|
| ECT | 3/4~18/94 | 14 Days | 296 km | 20 ± 0.1 °C | May, 1994 |
| JACEE-12 | 1/3~14/94 | 10 Days | 38 km | -5 ± 3°C* | April, 1994 |

*Diurnal temperature variation at a particular plate. This does not include stable variations in plate temperatures from top to bottom (~15°C) in the stack, nor the cool-down period (~1 day) immediately following balloon launch.

### 4.b) X-ray Films

Assessment of the performance of the X-ray films was made by scanning, mapping, and photometry of the recorded high energy shower events. While ~1000 high energy events were typically observed by visual scanning in one block of an emulsion chamber in the JACEE-12 Antarctic 10-day flight, the number of events recorded by similar selection criteria in the ECT experiment was about 500, mainly because most energetic particles entered from the bottom of the instrument. In fact, the observed number of events above a detection threshold energy of about 3 TeV (sum of gamma ray energies emanating from the interaction) was about 400 events, or 40% of expectation for full-time deep-space experiment. Most primaries entered the bottom of the chamber, having interacted in the material of the bottom of the shuttle bay, in the MPESS structure and the experiment mounting plate. Interactions occurring at a distance from the emulsion chamber produce diffuse showers that are not detected except at very high primary energies.

The scanning and analysis on this point were made at the UAH Cosmic Ray Laboratory by using an in-house designed CCD photometer. A sample of events are shown in a photograph of a flight X-ray film where several high energy cascades are clearly visible. The background darkness discussed in the following section appear as a general gray field in the X-ray films, as shown in a TV picture (**Fig. 10a**).

All 32 layers of x-ray film in the calorimeter were scanned. The scanned events were projected onto a single map, which gave the direction and incoming zenith angle of each event at a glance, as shown in **Fig. 10b**. Using this event-map and x-ray films, each event spot on x-ray films was measured for optical density ($D_{shower}$). The background density ($D_{bg}$) is also measured around the shower event. The optical density where a shower is located is

$$D = D_{shower} + D_{bg}, \text{ where} \quad (1)$$

$$D \equiv \log_{10} I_o/I, \quad (2)$$

and $I_o$ and I are incident and transmitted light intensity measured by a photometer. These measured data at various radiation lengths in the emulsion calorimeter were plotted as a function of the material thickness (t). Automatic shower fitting for each event was performed at NASA MSFC. **Fig. 11** illustrates four such examples. For each shower spot, both D and $D_{bg}$ were measured. To eliminate contamination from the shower in the $D_{bg}$ measurements, the $D_{bg}$ measurements were performed at about 1 cm away from the shower. All the D data for the shower events thus include two values of D: $D_{shower}$ and $D_{bg}$. Only the $D_{shower}$'s are used for shower curve analysis. The maximum optical density of an event ($D_{max}$) is the $D_{shower}$ value at the maximum point in the fitted curve (shower maximum). It is approximately proportional to the number of shower electrons ($N_e$), and it can be related to the total shower energy as a power function of the shower energy ($\Sigma E\gamma$):

$$D_{max} \propto [\Sigma E\gamma]^{0.8}. \quad (3)$$

The world-wide convention of equation (1) that defines the shower density $D_{shower}$ from directly measurable film density D and background density $D_{bg}$ is approximate and valid only for low optical density measurements. It is increasingly inaccurate for higher energy events that have high D and/or $D_{bg}$ values. This is because the quasi-linear response function of the Optical Density

of X-ray films gradually deviates from linearity at very high electron densities ($\rho$), and ultimately saturates to the asymptotic density ($D_0$),

$$D = D_0 \left(1 - \frac{1}{1+\alpha\rho}\right).\text{where } \alpha \text{ is a constant representing silver grain size} \qquad (4)$$

High energy events that have high optical density, $D_{shower} > 2$, in high background-density exposures are subject to corrections corresponding to the exact definition of the subtraction formulae (6) for the optical density of the shower, $D_{shower}$. The electron density of the shower ($\rho_{shower}$) and background ($\rho_{bg}$) have to be used in subtracting the background density from the electron density ($\rho_{observed}$) observed in X-ray films. The correct electron density and the optical density of the shower at all ranges of the optical density are :

$$\rho_{shower} = \rho_{observed} - \rho_{bg} = \frac{D_0(D - D_{bg})}{\alpha(D_0 - D)(D_0 - D_{bg})}, \qquad (5)$$

and

$$D_{shower} = D_0 \left(1 - \frac{1}{1+\alpha\rho_{shower}}\right) = \kappa\,(D - D_{bg}), \qquad (6)$$

where

$$\kappa \equiv \left[\left(1 - \frac{D_{bg}}{D_0}\right) - \frac{D_{bg}}{D_0}\left(1 - \frac{D}{D_0}\right)\right]^{-1}. \qquad (7)$$

The ECT experiment is the first to recognize the limitation of the approximate formulae (1) in high density environment. We note here that the exact formulae (6) should be used in any future space experiment where background density $D_{bg}$ is not small. For example, for a film with a background $D_{bg} \sim 1.0$, the correct value of D shower (from equation 6) may equal 3.5, while the value from equation (1) is $D_{shower} \sim 3.0$.

### 4. b):1. High Energy Event Detection and Energy Spectrum.

A total of 383 events was measured by photometric shower densitometry with the selection criterion that the event must have more than 6 layers of the $D_{shower}$ values above the minimum set value, $D_{shower}$ (t) > 0.15. The average number of the events detected with the same criterion for the Antarctic 10-day balloon flight (JACEE-12; 1994) was 864 events. This criterion approximately corresponds to events with the shower energy greater than 3 TeV (primary energy ~ 12 TeV for protons, 40 TeV for irons). The detected events have various zenith angles ranging from $0^o$ to $87^o$. The spectrum analysis was made only for events with the zenith angle from $0^o$ to $80^o$, as the D fit for events with zenith angles from $80^o$ to $87^o$ was relatively poor, due to the fact that some of these data were at the edges of X-ray films and there were some uncertainties in $D_{bg}$ data at the edges when measured at the point away from the shower spot. The raw ECT data on the $D_{max}$ differential distribution is shown in **Fig. 12a**. The integral $D_{max}$ spectrum of high energy cosmic rays from measured events is (**Fig. 12b**):

$$I(> D_{max}) = 1005\,(D_{max}/0.1)^{-1.88 \pm 0.096}. \qquad (8)$$

The integral energy spectrum I(>ΣEγ (TeV)) can be obtained from the $D_{max}$ spectrum by using the relationship, $D_{shower} \propto [\Sigma E\gamma]^{0.8}$,

$$I(>\Sigma E\gamma\ (TeV)) \propto (>\Sigma E\gamma)^{-1.50 \pm 0.08}. \quad (9)$$

The ECT result formulae (9) is consistent with the all-particle energy spectrum for high energy cosmic rays observed on several JACEE balloon flight experiments, namely:

$$I(>\Sigma E\gamma\ (TeV)) \propto (>\Sigma E\gamma)^{-(1.45 - 1.55)}. \quad (10)$$

This close correlation between measured spectral indices of the gamma-ray inelasticity for the space-flight and balloon flight data confirms the spectrographic capability of the emulsion chamber for high energy cosmic rays. Although a large part of the flight time was earth-facing, and the majority of high charge events interacted with the materials of the shuttle bay floor, the emulsion chamber recorded and identified most of them as interactions originating outside the chamber. Those inversely-developing shower events were degraded in the detectable shower energy ($\Sigma E\gamma$) due to spreading of showers in the path between the vertex (cargo bay floor) and the ECT calorimeter. The inversely-developing events in the integral energy spectrum are reduced in intensity by the reduced ($\Sigma E\gamma$) value which were measured within a finite photometric slit size (250 μm x 250 μm). The loss in the intensity in such a raw (uncorrected) energy spectrum was about 60%, if compared with the prediction for the full-time deep-space flight (~ 1000 events).

Low energy cosmic ray protons (E < 10 TeV) and shower electrons were major components of the track background in the emulsion chamber. In spite of the fact that a large portion of cosmic rays entered the ECT chamber after passing through the materials of the cargo bay floor, secondary tracks (leading cosmic ray particles, fragments, produced mesons, and showers) were still at relatively high energies, and were not absorbed by these materials. They were accompanied as "inversely developing showers" as shown later in **Fig. 19**. Hence, the total background intensity due to cosmic rays experienced for the inverted exposure of ECT is approximately equivalent to a 14-day deep-space orientation flight, at least in the majority of the bulk of the chamber.

The recognition of this fact is important as a preamble in the evaluation and extrapolation procedures of the Emulsion Chamber Technology in space for future long-duration orbital flights.

### 4.b):2 Background Analysis

#### 4.b):2.1 Background Density, Position Dependence and Fluence

The background optical density was in the order of 2.4 in the central part of the x-ray films when a conventional, regular development method (20 °C isothermal) was adopted. That of the Antarctic, long-duration balloon flights (10 days) in the similar period (JACEE-12) was 2.2. Both ECT and JACEE-12 received the highest cosmic ray background intensity at the solar minimum period, when the geomagnetic cut-off was the lowest and the lowest energy cosmic ray particles entered the detectors without magnetic rejection. These values of the background densities are approaching the limit of efficient use of X-ray films. The actual films were processed with drastic reduction of background density to D = 0.2 ~ 0.6 by a new, low-temperature method, described in the next section.

The background density of x-ray films depends on the position of the film in the emulsion chamber, as a natural consequence of different fluence at different location. The $D_{bg}$ data in films at various depth in the calorimeter are shown in **Figs. 13-1 through 13-8**, where all the edges indicate higher values of $D_{bg}$. Because radiation-belt protons would stop within materials less than 20 g/cm$^2$, the mid-part of the chamber received high energy cosmic rays and cascade electrons but much less trapped proton radiation; while the edges and the upper portion of the chamber received more proton background and exhibit higher darkness on x-ray films. This can be clearly seen in these figures.

A comment is due for both ECT and JACEE-12 films: the edge density is higher than that of the central area, due to slow protons and soft components that stopped within the chamber. This enhanced darkness in ECT x-ray films at the edges is shown in **Fig. 13**. These edge darkness values were higher than D = 2.5 if processed by a regular development method, causing difficulty using the normal technique with naked eyes and a regular-luminosity light-box. While the use of a high luminosity lamp and a scanning densitometer still allows analysis of these high-density x-ray films, the low-temperature development reduced these darknesses to D ~ 0.5, and the analysis was made easy using the standard eye-scanning method.

The absolute value of the $D_{bg}$ by the UAH's CCD photometer was calibrated by the PMT photometer at the NASA/MSFC prior to the STS-62 flight. The uniform background and shower are different in calibrations, because the shower has lateral structure and the CCD and PMT have different saturation functions at high densities. Calibration with uniform density (wedge) is given in **Fig. 14a,** and that for showers, in **Fig. 14b**. We use this (**Fig. 15a**) internal calibration for the general discussion on background endurance in (a)-1 and in other sections. The relationship can be approximated for showers as $D_{CCD} = 1.55\ D_{PMT}$ (up to $D_{PMT} < 1.0$). Densities of the high density shower events were measured by both CCD and PMT. On the other hand, the relationship for uniform background is approximated by a 5-th order polynomial (dotted line). The PMT saturates at $D_{PMT} = 4.2$, while CCD saturates at $D_{CCD} = 2.2$ ($D_{PMT} \approx 3.3$). The fluctuations of the photometry for both CCD and PMT were $\sigma = 0.05 \sim 0.06$. Throughout this report, we will omit this error value for simplicity. The $D_{bg}$ values cited in the following descriptions are all those of the CCD measurements, unless otherwise specified.

The thickness (t) dependence of the darkness for the ECT x-ray films is shown by the darkness data in **Figs. 13**. The Antarctic balloon data, on the other hand, indicated a gradual increase of $D_{bg}$ with increasing material thickness in the calorimeter, as a result of the cascade development of electron showers in the lead calorimeter. (The balloon flight detector did not receive trapped-belt proton radiation.) However, the ECT chamber received all the orbital radiation particles (**Fig. 14c**) in more complicated manner. When compared with the balloon flight data, the following was observed:

(1) The (t) dependence of the $D_{bg}$ was quasi-symmetric with the highest values in the center of the calorimeter. The ECT was exposed to cosmic rays and radiation mainly with opposite orientation of the field-of-view to that on balloons.. Consequently, the $D_{bg}$ does not monotonically increase toward the bottom of the chamber. Detailed transport calculations have not been performed to see if this result can be replicated.

(2) The increase and an eventual decrease of the $D_{bg}$ with increasing depth was more pronounced than the similar fluence data from emulsions and CR-39 that measured the

This observation might offer a plausible explanation to account for the enhanced depth-dependence of x-ray film data, although we cannot quantitatively fully understand the ECT flight data at this point. The analysis is complicated by the mixing of different radiation profiles due to the mixed profiles of the shuttle orientation. The ECT data of $D_{bg}$ in the central location of the x-ray films are shown in **Table X1**. Compared with this table is the data from the emulsions measured at the center of each plate (**Table X2**).

**Table X1.** Three-dimensional data summary of the X-ray film optical density.

| Depth ($g/cm^2$) | C01 | C04 | C12 | C15 | C18 | C21 | C33 |
|---|---|---|---|---|---|---|---|
| A | 0.69 ± 0.14 | 0.59 ± 0.17 | 0.53 ± 0.16 | 0.55 ± 0.13 | 0.50 ± 0.17 | 0.53 ± 0.16 | 0.59 ± 0.13 |
| B | 0.73 ± 0.13 | 0.62 ± 0.16 | 0.59 ± 0.14 | 0.59 ± 0.13 | 0.55 ± 0.15 | 0.55 ± 0.15 | 0.59 ± 0.13 |
| C | 0.63 ± 0.16 | 0.59 ± 0.17 | 0.51 ± 0.16 | 0.51 ± 0.13 | 0.50 ± 0.16 | 0.53 ± 0.16 | 0.58 ± 0.13 |

A: Center of the left side, B: Center of the film, C: Top edge at the left side.

**Table X2.** Density of Fog, Grains, and Tracks (at center of the plate).

| Vertical Depth | 2.29 $g/cm^2$ | 33.17 $g/cm^2$ | 113.41 $g/cm^2$ | Ground Control |
|---|---|---|---|---|
| Plate Number | P-03 | P-69 | C-35 | #1 |
| Fog/1000$\mu m^3$ | 1.61 ± 0.14 | 1.49 ± 0.14 | 1.71 ± 0.15 | 1.24 ± 0.13 |
| Grains/100$\mu m$ | 26.09 ± 4.20 | 30.93 ± 2.96 | 31.37 ± 2.80 | 32.42 ± 1.92 |
| Tracks $10^5/cm^2$ | 4.30 ± 0.16 | 3.56 ± 0.36 | 2.53 ± 0.27 | 0.418 ± 0.19 |

### 4. b)2:2 Background Analysis : Isothermal, Low-temperature DevelopmentMethod Required for Space Flight X-ray Films

When the background density is very high (such as $D_{bg} > 2$), visual contrast in x-ray films becomes very poor for shower detection, and an undesirable saturation of the linear response curve of x-ray films on the shower energy becomes significant. $D_{bg} < 2.0$ is recommended for efficient scanning and preservation of a linear response of $D_{max}$ for energy determination. Considering the possibility of much higher background density, as would result by exposing the EC on Space Station for 1/2 to 1 year, we experimented and established a new, low-temperature development recipe for the ECT experiment (5 °C isothermal for 3 minutes). **Table X3** shows a comparison of conventional recipe and the ECT's new recipe.

**Table X3.** Comparison of recipes for X-ray film development

| Low-Temperature Method | Development | Stop | Fix |
|---|---|---|---|
| Chemicals | Konidol | Acetic Acid 3% | Konifix |
| Temperature °C | 5 | 5 | 5 |
| Duration (minutes) -variable | 1 ~ 7 | 1 ~ 3 | 30 ~ 40 |

| Conventional Method | Development | Stop | Fix |
|---|---|---|---|
| Chemicals | Konidol | Acetic Acid 3% | Konifix |
| Temperature °C | 20 | 20 | 20 |
| Duration (minutes) -variable | 5 ~ 20 | 1 | 20 |

The new ECT prescription seems to respond well to the particle-background density problem posed by long-duration space flights, by reducing the $D_{bg}$ from 2.1 to 0.5 without compromising the number of detectable events. (We used longer development time of 5 minutes in the actual development of the ECT X-ray films, with the average $D_{bg}$ value of 0.2 by CCD and 1.1 by PMT.) The method works by reducing *the size* of the developed silver-halide crystal without much reducing *the number* of latent image-grains. Since $D_{bg}$ varies with the background track density, $N_e$ (bg) approximately according to:

$$D_{bg} \propto \log N_e (bg), \qquad (11)$$

we project that the effectiveness of x-ray films in recording and analyzing events will be maintained up to backgrounds of ~80 times ($10^{(2.4-0.5)}$) that of the ECT exposure. We conclude that, with suitable adjustment of development procedures, chambers can be effectively deployed (in a similar orbit) for up to (80 x 15) = 1200 days.

At the higher orbit (400 km) and inclination (57°) expected for the International Space Station, the background density can be about 3 times higher than the STS-62 orbit (300 km, 39°), and the maximum useful duration would be about 400 days. This number is subject to the nature of the background. The number quoted here is for trapped belt radiation, which affects the validity of x-ray films in the edges and at the shallow depth in the emulsion chambers.

### 4. b):2.3 Background Analysis: Materials Compatibility Studies

Aluminum and other "active" metals have long been known (ref 5) to have potentially damaging effects on silver bromide emulsions, and emulsion lore is rife with stories of plates and pellicles ruined by contact with or proximity to such metals. The JACEE Collaboration in 10 balloon flights had avoided that problem by constructing the emulsion containers entirely from non-metallic materials such as rubber sheet, polymethylmethacrylate (lucite) and plywood. The rigors of rocket launch, and the requirements of demonstrably safe mechanical confinement and attachment, resulted in the basic container design being a hermetically sealed aluminum box. While this conferred some advantages, such as more accurate plate positioning and maintenance of constant humidity in the plate materials, it did require a focused effort to assure compatibility of materials with emulsion gel plates and x-ray films. These detectors must be able to be stored in the flight housing for 1 year without significant degradation.

A program was devised and carried out in which small pieces of the detector materials were exposed to the box construction materials for various periods from 1 to 18 months. Of

principal concern was Al. Tests were conducted with bare Al and with various kinds of surface coating on the metal. Tests were conducted both with the dissimilar materials both in direct contact, and in close proximity within small sealed chambers.

**Table X4** lists the materials and conditions of exposure of films. Diagnosis is defined by the words "Normal" or "Damaged".

**Table X4.** Various tested materials, Optical Density (PMT) and physical conditions.

| *Hermetic* | **Sample 1 (1.0 months)** | **Sample 2 (2.5 months)** | **Sample 3* (4.5 months)** | **Sample 4 (18 months)** |
|---|---|---|---|---|
| **Controls** | 1.46 | 1.50 | 0.91 | 2.02 |
| **with Krylon** | 1.47 | 1.46 | 0.89 | - |
| **with Epoxy** | 1.45 | 1.58 | 0.94 | - |
| **with Aluminum** | 1.38 | 1.56 | 0.94 | - |

All samples were normal conditions; * short development processing; - Data not available

**Table X5** shows the optical densities of the test films. The sample names, 1, 2, 3, 4 , and F, correspond to the duration of the exposure for the test, 1.0 month, 2.5 months, 4.5 months, 8.5 months and 18 months, respectively. The sample 4C was for 8.5 months.

**Table X5.** Optical Density (PMT data) of the ground control X-ray films.

| *Material\Period* | *Sample 1* | *Sample 2* | *Sample 3* | *Sample 4* | *Sample 4C* | *Sample F* |
|---|---|---|---|---|---|---|
| Control | 1.57 | 1.55 | 1.55 | 2.02 | - | 1.38 |
| Aluminum# | 2.52@ | 2.19@ | 2.20@ | 3.48@ | 2.07@ | 1.78@ |
| Anodized Al.# | 1.76# | 1.80# | 1.93# | 2.17# | 1.69# | 1.52# |
| Alodined Al.# | 1.69## | 1.55## | 1.57## | 1.97## | 1.98## | 1.65## |
| Black Lucite | 1.45 | 1.44 | 1.49 | 1.55 | 1.92 | 1.80 |
| Clear Lucite 1/4" | 1.43 | 1.51 | 1.52 | 1.80 | 2.02 | 1.47 |
| Si Rubber | 1.49 | 1.54 | 1.49 | 1.64 | 1.78 | 1.52 |
| Clear Lucite 1/16" | 1.67 | 1.62 | 1.61 | 1.72 | 1.87 | 1.55 |
| Viton O-ring | 1.61 | 1.60 | 1.56 | 1.78 | 1.68 | 1.45 |
| Gold Plated AL. | 1.41 | 1.50 | 1.50 | 1.72 | - | 1.50 |
| Parafilm | - | - | - | 1.73 | - | 1.66 |
| Anodized Al. painted 1 | - | - | - | 1.84 | - | 1.50 |
| Anodized Al. painted 2 | - | - | - | 1.78 | - | 1.49 |
| Pb (cleaned) | - | - | - | - | - | 1.78 |
| Pb (painted) | - | - | - | - | - | 1.65 |

@: All contact pieces were damaged, progressively worsened; non-contact part was fogged but not damaged.
#: All contact samples were somewhat damaged; non-contact sample were not damaged.
##: Some contact samples were damaged; non-contact samples were not damaged.
All other samples without @, #, and ## symbols were in "Normal" condition.

Aluminum and alodined aluminum were shown to destroy emulsions and X-ray films on contact, while anodized aluminum was inert. Anodized aluminum was selected for the space flight emulsion chamber based upon these material compatibility tests. The actual shuttle flight result confirmed the ground test results. It is reasonable to extrapolate further, based on the ground tests and the ECT flight, that all the materials in the flight emulsion chamber in a ECT pressurized vessel should be safe for long duration space flights at least up to 18 months.

### 4.c) Emulsions

Measurements of the high energy cosmic ray events, background track density, chemical fog, and grain density were performed using high magnification microscopes. Similar measurements were performed with ground control unit and balloon-borne emulsions to compare the quality and capabilities with the space-flight emulsions.

### 4.c):1 Quality of Tracks (Examination by Berriman-Curve Test)

The contrast for track recognition in emulsions was excellent and clear track measurements were achieved. Grain density relative to the fog density is a measure for evaluating the quality of the track recognition contrast (Berriman curve **Fig. 15**). "Excellent" quality of emulsions are indicated by a domain above the solid curve in the figure, while the dotted curve represents the "good recognition". They were measured at the central part of the emulsions, because the majority of the emulsion measurements for cosmic rays depend on the quality in the central part where the event tracking will be made. All the ECT emulsions turned out to be "excellent contrast" as demonstrated in **Fig. 15** (Berriman curve) and **Fig. 16** (photograph).

**Table E1** provides the measured densities of grains and fogs, as well as the background track densities. In average, the grain density of the ECT flight emulsions for relativistic, minimum-ionizing, $Z = 1$ particles was $29.5 \pm 1.8$ grains/100μm, while the fog density was $1.60 \pm 0.08$ fogs/1000μm$^3$, while those of the ground-control emulsions for the same period were $32.42 \pm 1.92$ grains/100μm and $1.24 \pm 0.13$ fogs/1000μm$^3$, respectively. The grain density of both materials are similar within the statistical errors, while the fog density is clearly enhanced by 29% (to $3\sigma$ level) in the flight emulsions. This difference is small enough to assure the high quality of flight emulsions.

**Table E1**. ECT background measurements (on emulsion properties).

| Plate Number | Location from the top (g/cm$^2$) | Fog density (fogs/1000 μm$^3$) | Grain density (grains/100 μm) | Background ($10^5$ tracks/cm$^2$) |
|---|---|---|---|---|
| P-03* | 2.29 | $1.61 \pm 0.14$ | $26.09 \pm 4.20$ | $4.30 \pm 0.16$ |
| P-69** | 33.2 | $1.49 \pm 0.14$ | $30.93 \pm 2.96$ | $3.56 \pm 0.36$ |
| C-35** | 113.4 | $1.71 \pm 0.15$ | $31.37 \pm 2.80$ | $2.53 \pm 0.27$ |
| Control** | GROUND | $1.24 \pm 0.13$ | $32.42 \pm 1.92$ | $0.42 \pm 0.19$ |

* measured at 1 cm from the edge of the plate.
** measured at the center of each plate.

The ECT in-flight temperature set-point was selected at 20°C. This is near the upper limit of safe working temperatures for emulsions (30°C maximum). Emulsion fog is often induced by high temperature and by some active chemicals in the environment surrounding the emulsions. It is possible that the small observed difference in fog densities is mainly due to thermo-chemical fog

induced during some part of the transportation and storage period when several days of high temperature (21 - 22.5°C) were recorded for the flight emulsions. The ground-control unit did not experience such high temperatures. **Table X5, Table E1** and **Fig. 15** show a time-and-temperature dependence of fogs in emulsions. In the following discussion we should emphasize that the fogging observed in the ECT plates was a small but observable effect that did not affect data retrieval to any significant degree.

The compatibility test (described below) indicated a very slow increase of fog as a function of the increasing storage period at room temperature (≈ 17°C). In the anodized aluminum box in which the ECT emulsions were flown, the fog increased from only 5% to 10% for a storage duration of 1 month to 18 months over the hermetically sealed storage emulsions (contact with Lucite plates). The ECT result implies that the observed increase of fog over the ground-storage materials was not likely to have originated from the chemical reaction with the materials in the ECT box in the space environment, but it is more likely due to the increased temperature during the periods (Jan 6 -13; Jan 26 - 30; Feb. 1 - 5, 1994) prior to the STS flight (**Fig. 17**).

Although the analysis of fog indicated with reasonable likelihood that high temperature during ground storage/transportation was responsible for an increased fog of about 30%, a further question remains: whether there was any combinatory fog increase due to other materials in the chamber, interacting at higher temperatures than that of our compatibility tests. This examination will be necessary to fully guarantee a limited fog-increase for a very long-duration space flight, and it must be addressed here as a further requirement of a ground test.

### 4.c):2 Tracing of High Energy Tracks/Showers in Emulsions

The flight emulsions provided high visibility for all individual tracks including minimum ionizing tracks. Very clear shower tracks were photographed from emulsions showing excellent quality of event recording as demonstrated in **Figs. 18 and 19**. A "normal shower development" is shown in **Fig. 18**, which is an event entered into the chamber from space in deep-space flight orientation period. An "inverse shower development" is easily identified by the unique signal of the inverse development of the lateral spread. Shown in **Fig. 19** is an example where the event produced a cascade shower from the bottom to the top of the chamber after entering and interacting with the cargo bay during the Earth-observing orientation of the STS-62.

A primary iron nucleus track and two interaction vertices in the emulsion chamber were photographed in **Figs. 20 - 22** with the highest magnification of x 100 objective lens. General (x 20) image of emulsions were compared in **Fig. 23** between an ECT emulsion and a long-duration balloon-borne emulsion, where similar excellence of track qualities are observable.

Showers were traced from the lower part of the calorimeter upward into the target and primary modules. This event tracing is expected to be subject to interference by copious background tracks at high background density. Despite the density in the order of $10^6/cm^2$ in the ECT emulsions, there were no significant difficulties in tracing events upwards even when the "jet" structure of the event becomes thin and small in the target module.

The ECT and long-duration balloon-borne emulsions (JACEE-12, 1994; JACEE-13, 1995) have the highest background level among all the past space-flight emulsion chamber experiments. It is not straightforward to assess what density of the background will prevent efficient tracing, because we do not have much experience with emulsions that have much higher background density than the ECT or JACEE-12. Nevertheless, some assessment is possible.

Emulsion is a three-dimensional micro-photographic device. The vertical focus is as sharp as 1 μm, and the lateral resolution of tracks is as good as 0.1 μm. One minimum-ionizing, relativistic track will form about 30 grains in 100 μm of track length. The visibility can be approximately defined by the average grain distance ($r_{bg}$) between different tracks versus average grain distance in a track ($r_g$):

$$r_{bg}/r_g > \lambda, \tag{12}$$

where ($\lambda \geq 1$). Sufficient track recognition with a condition of ($\lambda \sim 2$). The minimum condition to identify a track corresponds to ($\lambda \sim 1$).

A cosmic ray track has an average zenith angle of 45°, and therefore, the average lateral grain separation is 2.36 μm, while that of vertical is also 2.36 μm. This chain of grains (blobs) belonging to a single track can be recognized as a track when other grains from other tracks overwhelm and confuse the recognition of a single particular track. When one has $10^6$ /cm$^2$ track density in emulsions (ECT) the average track separation ($r_{bg}$) is in the order of 14 microns, satisfying the above ratio $r_{bg}/r_g > 1$ by a factor of about 5. If the background cosmic ray tracks (not those of trapped-belt radiation protons which will be absorbed in emulsion chamber) accumulates up to 35 times more than the ECT track density, the single ionizing track recognition becomes very hard as the $r_{bg}$ becomes as large as $r_g$. This is true for the high-sensitivity emulsions (Fuji ET-7B). Hence, our conclusion should be that the single ionizing track can be traced with increasing difficulty in high background track densities up to 3.5 x $10^7$ particles/cm$^2$, and the ECT's 14 day flights had only 1/35 of this limit. The limit may be 35 x 14 days = 490 days on orbit, provided that the emulsion chamber is large enough to absorb most of slow proton background coming from the radiation belts. The edges and the very top portion of the emulsion chamber record slow protons before their stopping, and the visibility of a single track therein will be poorer in these edge regions.

Concerning traceability in low sensitivity emulsions (Fuji ET-6B) for nuclei with charge of helium or larger; the same argument applies with different parameters. The $r_g$ of a Helium track in ET-6B is 2.53 μm. Because ET-6B records grains of background protons as few as 7 grains/100 μm, they can be completely ignored. The background tracks to be considered are those of helium and $Z/\beta \geq 2$. They are less than 30% of cosmic rays. Therefore, from the consideration of $r_{bg}$, the limit of track recognition will not be reached until exposures of 1,420 days. This limit with the low-sensitive emulsions (ET-6B) will remain close to this value even when radiation-belt protons increases in a very high orbit (500 - 1000 km), so long as the main detector part where the self-absorption of the emulsion chamber effectively works is concerned.

For heavier tracks ($Z > 2$), the average grain separation in low-sensitivity ET-6B emulsions is 1.12 μm for lithium ($Z = 3$), and 0.28 μm for Carbon ($Z = 6$). Acceptable track densities for them are very high, and the limit of exposure duration in space would exceed several years, so long as low-sensitivity emulsions are used.

### 4.c):3 Track Density in Emulsions

The track density was measured by both manual and automatic microscopes. Track by track identification was easily made by manual visual scanning as listed in **Table E1**.

The automatic microscope (CUE-2) does not identify blobs and separate grains as belonging to the same track, and gives an order of magnitude larger number of objects in a field of

view. (An advanced algorithm to connect the spatially-separated parts of a track [objects] into an identified single track is being developed, but it has not yet been used in the ECT analysis.)

The **Table E2** shows the material-thickness dependence of the object density in the ECT and JACEE-12 emulsion chambers. By the distinct identification of real tracks in the manual scanning, the number of objects in the CUE-2 auto-analysis can be calibrated as 10 times of the number of individual cosmic tracks.

**Table E2.** "Object" density dependence on vertical material thickness.

| **Object Density ($10^6$/cm$^2$)** | **P-03** at 2.29 g/cm$^2$ | **P-45** at 22.2 g/cm$^2$ | **P-69** at 33.2 g/cm$^2$ | **C-10** at 50.9 g/cm$^2$ | **C-14** at 60.9 g/cm$^2$ | **C-18** at 70.9 g/cm$^2$ | **C-22** at 80.9 g/cm$^2$ | **C-26** at 90.9 g/cm$^2$ | **C-30** at 101. g/cm$^2$ | **C-35** at 113. g/cm$^2$ |
|---|---|---|---|---|---|---|---|---|---|---|
| **ECT** | 3.59 | 4.46 | 4.70 | 4.02 | 4.08 | 3.53 | 3.71 | 1.55 | 0.99 | 0.34 |
| **JACEE-12** | 1.84 | 2.99 | 4.57 | 4.53 | - | - | 3.91 | - | - | - |

- (data not available at this time at the same vertical thickness)

### 4.c):4 Linear Energy Transfer (LET) Data

Track grains (blobs) were counted for individual particle tracks with a microscope having x 1,500 magnification. A blob is a clump of grains that are not separable with the 1,500 magnification. More grains are viewed as blobs for tracks that have higher Linear Energy Transfer (LET), and the present results on LET spectrum are lower bounds at higher LET's.
**Figs. 24 (a) - (c)** show LET spectra at the vertical thickness of 2.29 g/cm$^2$, 33.17 g/cm$^2$, and 113.4 g/cm$^2$, respectively.

The intensity of the minimum ionizing tracks does not change much with the material thickness. However, tracks that have dE/dx > 2 x minimum ionization (~ 4 MeV/g/cm$^2$) decrease substantially with increasing material thickness. While the details of the thickness dependence must wait for a full Monte Carlo simulation for quantitative analysis, it can be concluded that the observed profile should reflect absorption of slow protons of trapped belt radiation. This conclusion is also supported by comparison of the LET spectra.

At shallower depths of the ECT and JACEE-12 materials, the LET spectra are dissimilar at high LET's: Relative intensity of high LET particles at shallow material thickness are much more abundant in the ECT experiment than that of the JACEE-12, while those at deeper depths are similar, indicating that the high LET tracks of ECT materials are absorbed in the ECT materials.

For comparison, JACEE-12 data are shown at equivalent thickness (1.5 g/cm$^2$, and 70 g/cm$^2$) in **Figs. 24 (d) ~ (e)**, respectively.

### 4.d) CR-39 Analysis

CR-39 etchable plastics were separately described in this final report by the University of San Francisco co-investigators. Several independent measurements were performed at the University of Alabama in Huntsville, described below.

Owing to operational problems and increased environmental restrictions on the chemical etching facilities, the etching of the ECT CR-39 has just been completed. We have on hand now in

our lab two sets of CR-39 plates fabricated from material of the same specification (American Acrylics USF-3). One set flew in orbit for 14 days in ECT; the other for 10 days on an Antarctic balloon. A few notable differences were discovered in these two different flight experiments. An assessment of the difference of sensitivity was made by taking a temperature effect into account. Assessment of the difference in physical appearance was made in terms of scattering centers formed by small etch-pits and contaminants, nonetheless, thorough assessment requires additional material compatibility tests of CR-39 at different temperatures and at different atmospheric pressures.

### 4.d):1 CR-39 Etching, Uniformity, and Quality

Large size CR-39 plates (40 cm x 50 cm) were included in the ECT and regular balloon flight emulsion chambers. They are intended to be used for charge measurements of heavy nucleus tracks, and are also considered for the state-of-the-art coordinate measurements for future analysis of track momentum by using the multiple Coulomb scattering method.

The large-size CR-39 plates exposed in previous experiments were usually cut into smaller segments and etched (20 cm x 25 cm or smaller size) so that they fit the stage of measurement microscopes. The University of Alabama in Huntsville has developed a large stage microscope (50 cm x 50 cm) to analyze a large-size CR-39 plate for coordinate measurements. Correspondingly, the ECT CR-39's were etched in their original shape (40 cm x 50 cm) in a large etching bath at the Naval Research Laboratory. Standard etching recipe was used: 70$^0$C for 24 hours with 6.25N NaOH solution. Two large racks made from stainless-steel wire-mesh were used in a etching bath. The temperature gradient over the entire racks were monitored at various rack positions and was controlled to within ± 0.05$^o$C.

### 4.d):2 CR-39 Objects (Etch-pit hole) Data

CR-39 plates were scanned with an automated "object" analysis microscope (GALAI CUE-2 Auto-morphometer). Each plate was measured at the center (Part B) and at opposing edges (Parts A and C). Many parameters were measured automatically during the scanning operations. There were many small etch-pit holes and the measured data of the "area size", which include those of background stopping $\alpha$-particles, and contamination due to chemical instability of CR-39 surfaces. The ECT plates had a larger population of these small etch-pits relative to those of the JACEE-12 balloon flight materials, although these two experiments used the same CR-39 formulation from the same lot.

The measured "track density" strongly depends on how many of these small etch-pits are contained. Also, "average area-size" similarly depends on them, but in the opposite way: the "average size" becomes smaller when more small-sized contaminants are included. To minimize the effect of small-size contaminants, the auto-program set the minimum sampling value (60 $\mu m^2$) for the "object" area-size.

Three different sets of CR-39's were included in the ECT emulsion chambers. The group (I) are 10 sheets of CR-39 (CR1 ~ CR10), used in the emulsion chamber for regular charge measurements of high energy nuclei. The group (II) consists of 6 sheets (B2 - B7) inserted in the calorimeter section, which contained dozens of CR-39 doublets (E04 + E01, E12 + E05, ...) in cut-out slots. The dosimetry and LET spectra in the calorimeter are reported by using these materials in the separate article by the University of San Francisco group.

We measured in several places on the large CR1 - CR5 plates from group (I), and two calorimeter plates of the group (II) that held doublets of (E16-EC) and (E30-E38). The "object density" and the "average area" of objects are shown in **Figs. 25a and 25b**, respectively, as a function of increasing vertical thickness and the location (A, B and C). The central part (B) had less variation in the "object density" than those at edges (A and C). High object density at edges (A and C) indicated gradual decrease with increasing thickness. The average area size for all parts (A, B and C) did not show noticeable differences throughout all the depth for CR1 to CR6. Nonetheless, as remarked previously, these data are still subject to change due to unclear origin of contaminants of small objects. The analysis by CUE-2 auto-morphometry remains uncertain in this regard.

### 4.d):3 CR-39 Data Comparison with Balloon-borne Environments

Similar analysis was performed for CR-39 plates flown by a balloon (JACEE-12). **Figs. 26a and 26b** show the "object density" and the "average area" from the top (RRP2) to the bottom (RRC22) of the chamber. Only small variations on these data were found as a function of the increasing thickness of the chamber materials. However, the data on the top indicate higher density and average size, which quickly decreased within about 10 g/cm$^2$, suggesting absorption of slow nuclei (nearly zero cut-off energy) received near the magnetic south pole in the JACEE-12 circumpolar flight.

The most noticeable difference of etch-pit hole data between the ECT and JACEE-12 flights is the average area size. The ECT data indicates the median of ~ 250 $\mu m^2$, while the JACEE-12 balloon flight data shows that of ~ 400 $\mu m^2$. The observed difference is somewhat puzzling, because they were produced in the essentially same lot and etched at almost the same time by the same NaOH prescription. The cause of this difference is not clear. Nevertheless, we have also recognized another difference between the two samples; namely, the ECT plates were rather milky (having a lot of scattering elements ~ small etch-pits) while JACEE-12 plates were far more transparent (having less scattering centers). The number density of small etch-pits in CUE-2 auto-morphometry in fact supported this observation of the physical appearance.

The observed difference of sensitivity cannot be straightforwardly accounted for by the small difference of the charge and energy spectra of heavy nuclei in orbital flight and circumpolar balloon flight. A large difference (~ 40%) of the average area of large etch-pits is suspected as a possible environmental effect on CR-39 sensitivity during the flight.

It is well known that the sensitivity of CR-39 is strongly dependent on temperature, particularly when they are compared at low temperature ($T \leq 0°C$) and at ambient room temperature (~ 20°C) (**Fig. 27**). The former are about 50% more sensitive than the latter case, and the observed difference (~ 40%) is reasonable.

The second difference, the number of small etch-pits or contaminants, can hardly be attributed to the temperature effect only, because the ground control did not show the consistent results to support the temperature effect on this characteristic.

More importantly, these two flights had another physical difference during the flights when the cosmic tracks were recorded. The CR-39 sensitivity has been known to be low in vacuum condition. The latent image requires oxygen for track record to be fixed in polymerized molecular reactions. Because of this reason, the ECT used a pressure vessel (~ 1 atm. of air) to maintain the sensitivity of CR-39. JACEE balloon flights were always carried out with emulsion chambers

enclosed in an air-tight rubber-bag with a one-way passive valve to release interior gas out to environmental low pressure. The JACEE chamber was literally in vacuum when tracks were recorded, and did not benefit from the positive effect of oxygen for fixing the latent image of etch-pit hole. This physical difference on oxygen accompaniment with CR-39 plates can hardly account for either of the differences observed between orbital and balloon flight.

A suspicion exists for possible combinatory chemical-thermal effect on CR-39 plates. We have conducted materials compatibility tests for emulsions and X-ray films. However, no such tests were performed in the ECT experiment. Some materials in the emulsion chambers may be reactive with CR-39 surfaces and can cause irregular contaminants or quasi-etch pit holes of very small kind. Such effect, if it exists, must be activated either by moderately high temperature (~ 20°C) and/or oxygen content. Though it remains speculative, the ECT experiment alone cannot exclude such a possibility. Further material compatibility tests of CR-39 plates at high and low temperatures with and without oxygen must be performed in combination with all the emulsion chamber materials.

## 5. Conclusions: ECT Flight Data and Projected Feasibility for Long-Duration Space Flights

The ECT experiment provided sufficient materials and data to demonstrate excellent performance of an emulsion chamber for an orbital flight, and to verify the basic design approach for containment and environmental control throughout all flight operations.

The pressure chamber and active thermal control system operated normally throughout shuttle launch, orbital flight, and landing. The pressure was kept at 1 atm all the time and the ECT materials were maintained at $20 \pm 0.1$°C and 1.0 atm pressure during track registration.

The x-ray films in the emulsion calorimeter registered as many high energy cosmic ray events as expected by the pre-flight calculation using the known cosmic ray flux. The emulsion quality was found to be as good as any balloon flight experiment or ground control unit for recording cosmic ray tracks from protons to iron nuclei, including secondary mesons and cascade electrons.

The outer few cm of the dense emulsion chamber material was found to absorb efficiently the slow protons and electrons from trapped-belt radiation. The track acceptance capacity in emulsions and X-ray films and usefulness for track analyses are found to be limited more by cosmic ray intensity than the radiation dose from trapped belt particles.

The track densities of minimum ionizing tracks allowed an assessment for extrapolated long duration space flight. The ECT emulsion chamber allows track analysis of cosmic ray protons up to 1.34 years of orbital flight. Longer space flights using low-sensitivity emulsions may be useful for up to 3.9 years for helium nuclei, and even longer for carbon and larger nuclei.

The cascade recording by X-ray films was found to be useful for long-duration space exposures, with some adaptations of current method. In particular, a low-temperature under-development method was invented during the ECT experiment, allowing high-track-density exposures of the order of ~ 80 times the ECT flight for useful shower analysis, although the threshold energy will increase accordingly ($\sqrt{80}$), from $\Sigma E\gamma$~ 2 TeV for 14 day flight to > ~ 20 TeV for up to ~ 3.3 years of flight.

The CR-39 solid state track detector was useful in orbital flight, giving excellent LET spectra at various material overburdens. Some differences of the orbital flight materials in ECT chamber from those of Antarctic balloon flight were observed. The main difference, that of sensitivity, was accounted for as due to temperature effect. We should recommend a re-examination of the set-point for the thermal control system for a future flight. A lower set-point in the range of -5°C to 10°C would use less power, and provide a better operational environment for emulsions and particularly CR-39. Additional material compatibility tests of CR-39 are recommended for preparing CR-39 exposure in emulsion chamber for long-duration space flights.

## 6. References


1. T.H. Burnett et al. (JACEE Collaboration), Ap.J. **349**, 25 (1990).
2. K. Asakimori et al. (JACEE Collaboration), 23rd ICRC, **2**, 21 (1993).
3. M.L. Cherry et al. (JACEE Collaboration), 24th ICRC, Rome (1995).
4. T.A. Parnell et al. (JACEE Collaboration), Advances in Space Res. **9**, 45 (1988).
5. Walter H. Barkas, Nuclear Research Emulsions, Vol. 1, Academic Press, New York (1963).

# EMULSION CHAMBERS

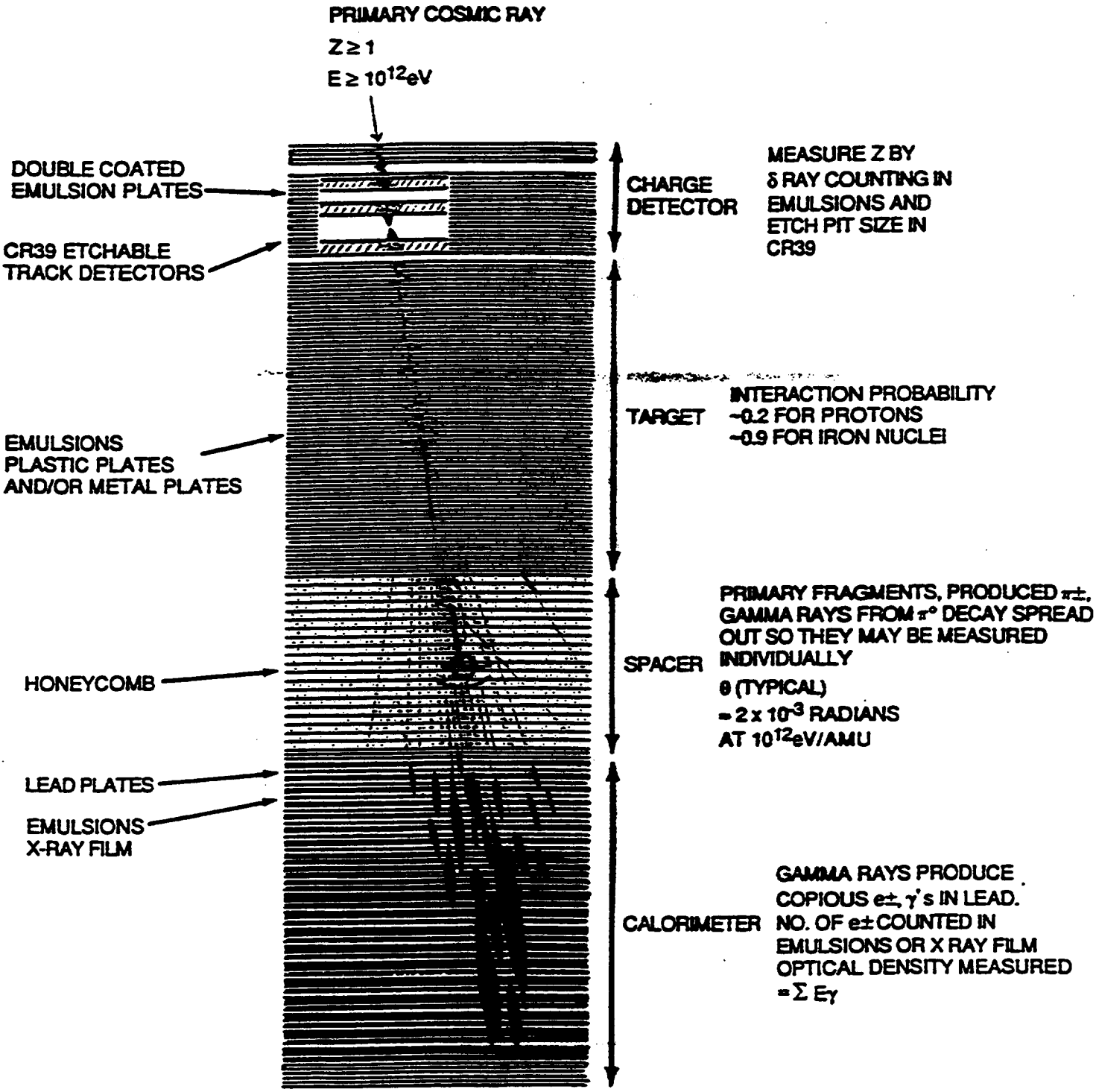


Figure 1

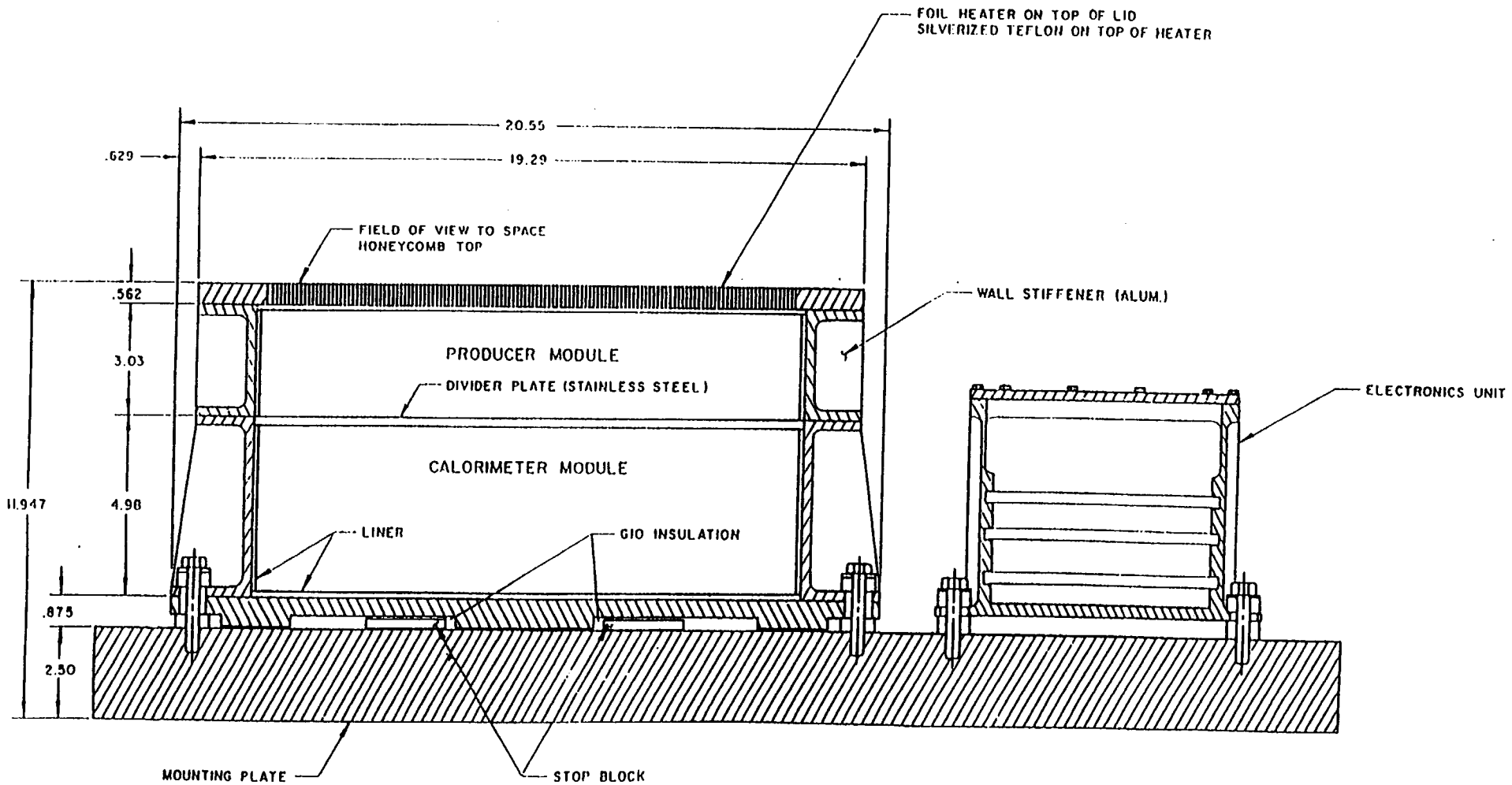
FOIL HEATER ON TOP OF LID
SILVERIZED TEFLON ON TOP OF HEATER
20.55
.629
19.29
FIELD OF VIEW TO SPACE
HONEYCOMB TOP
.562
WALL STIFFENER (ALUM.)
3.03
PRODUCER MODULE
DIVIDER PLATE (STAINLESS STEEL)
ELECTRONICS UNIT
CALORIMETER MODULE
11.947
4.98
LINER
GIO INSULATION
.875
2.50
MOUNTING PLATE
STOP BLOCK

Figure 2

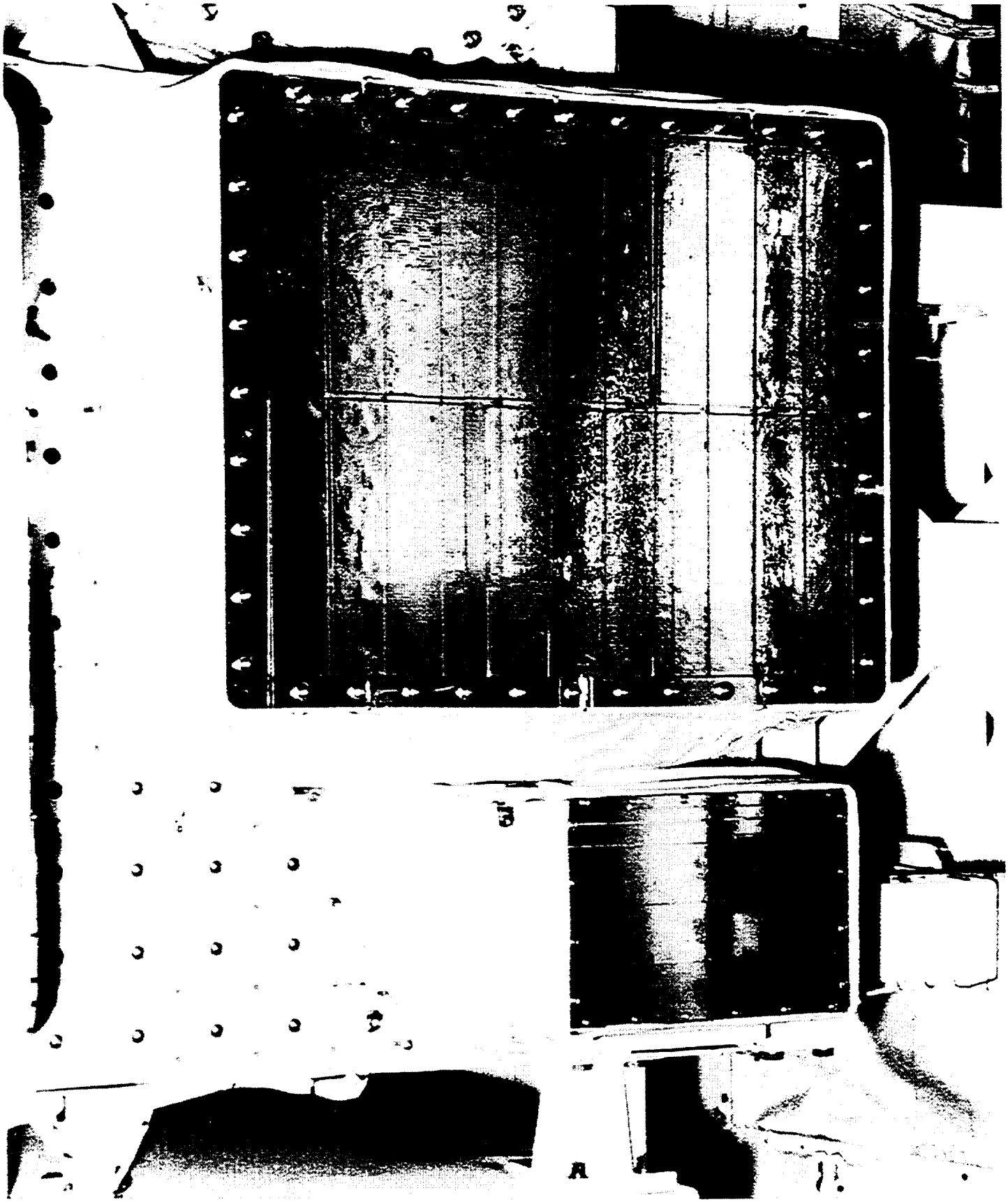

Figure 3

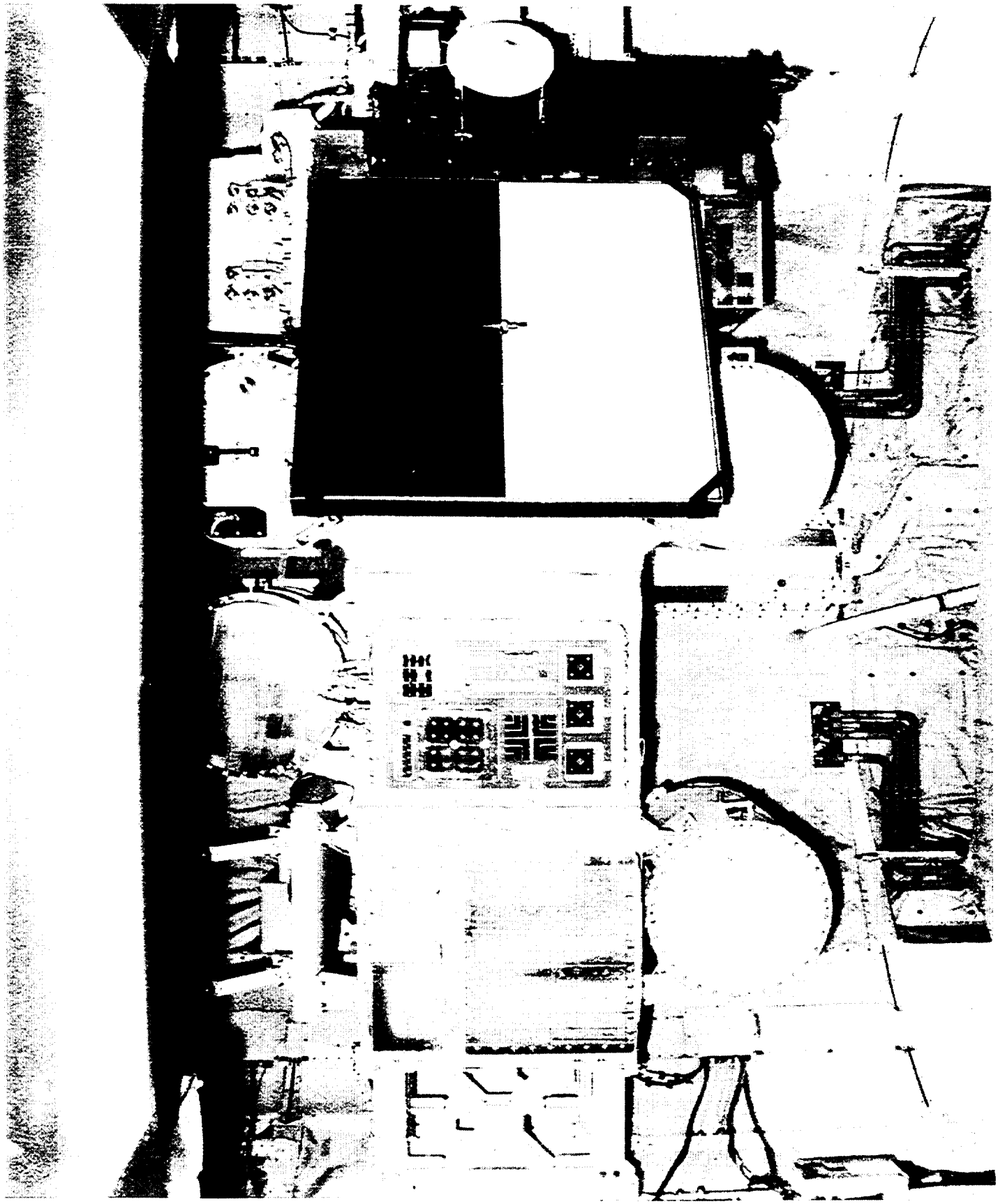

Figure 4

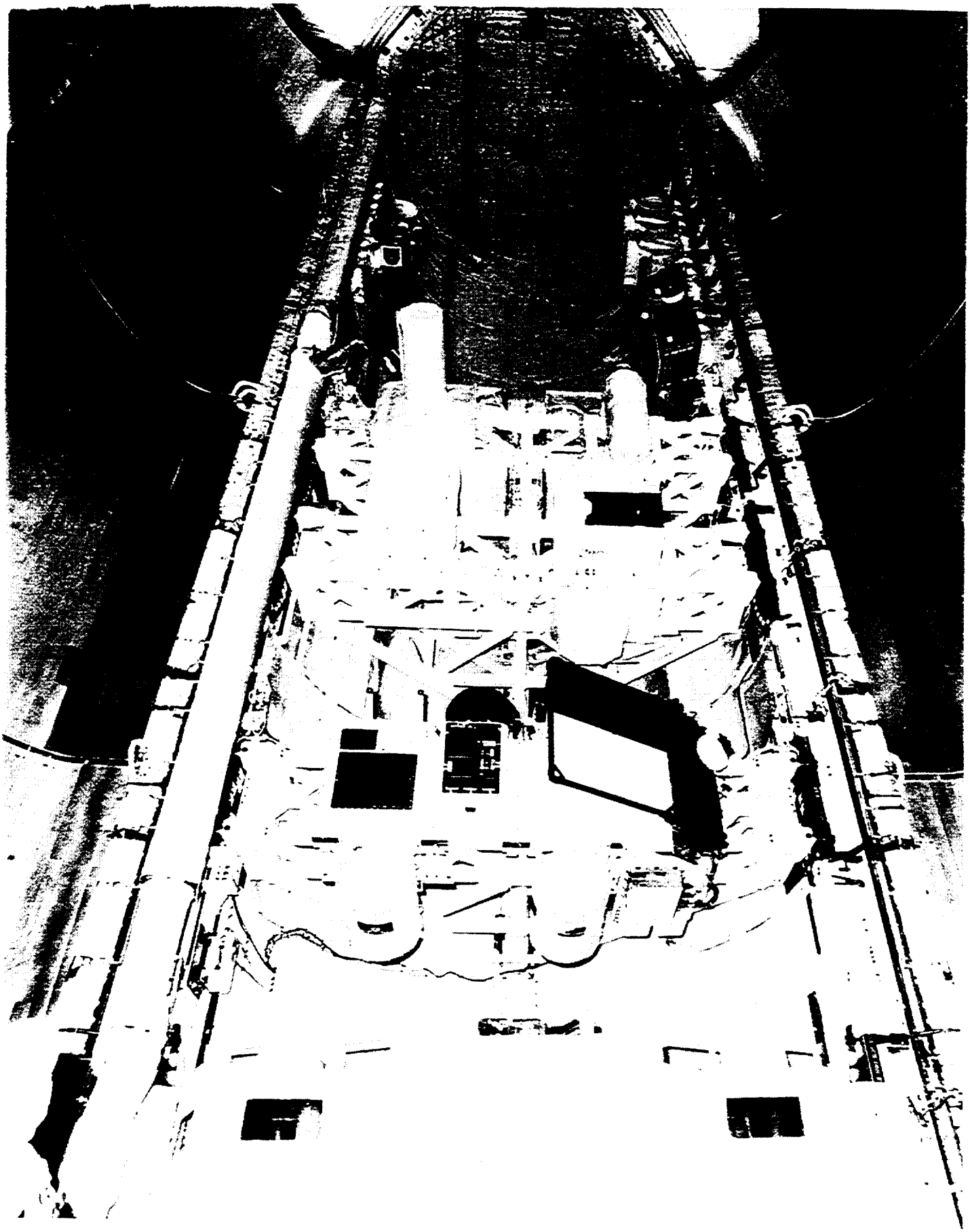

Figure 5

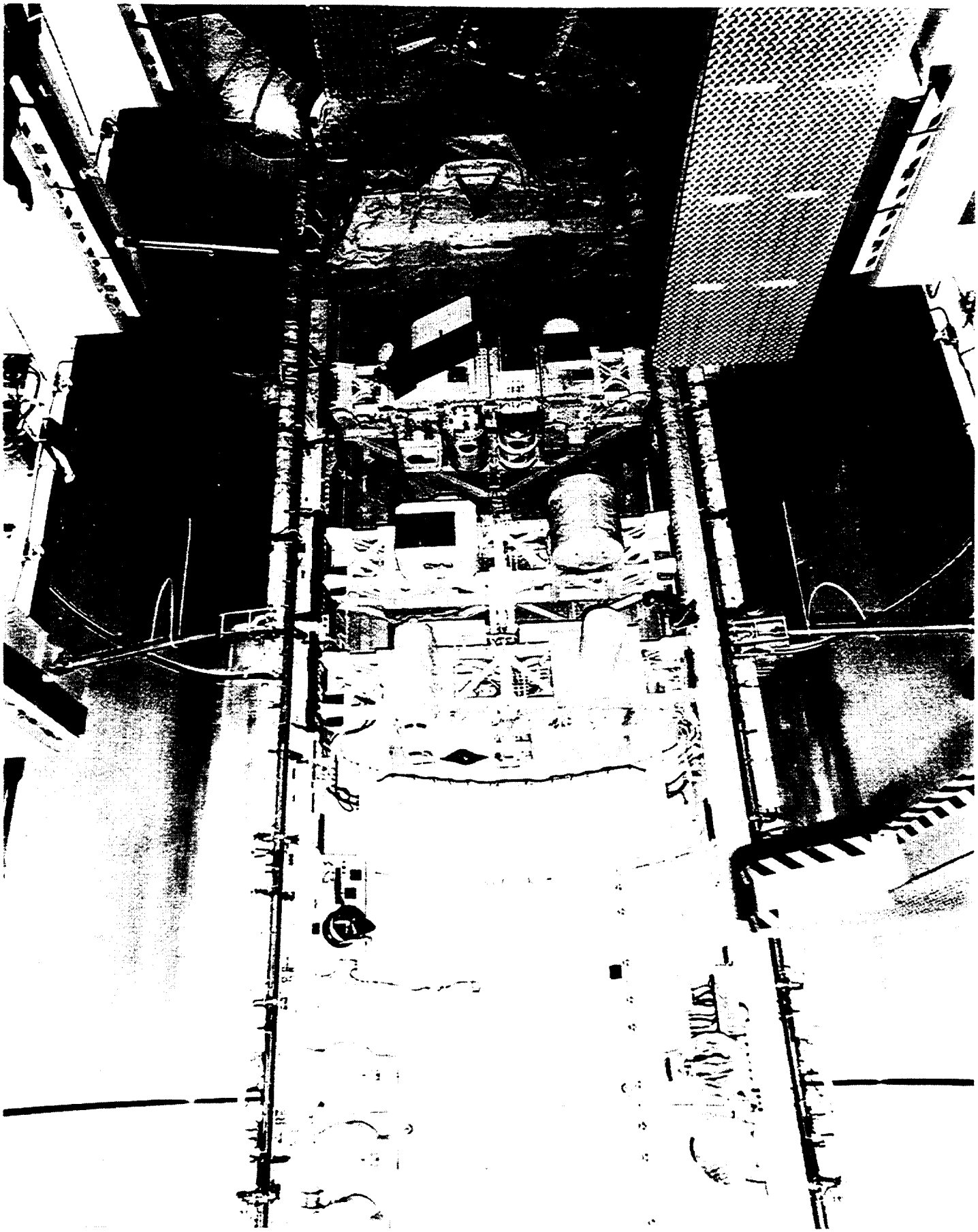

Figure 6

## Forward MPESS Configuration

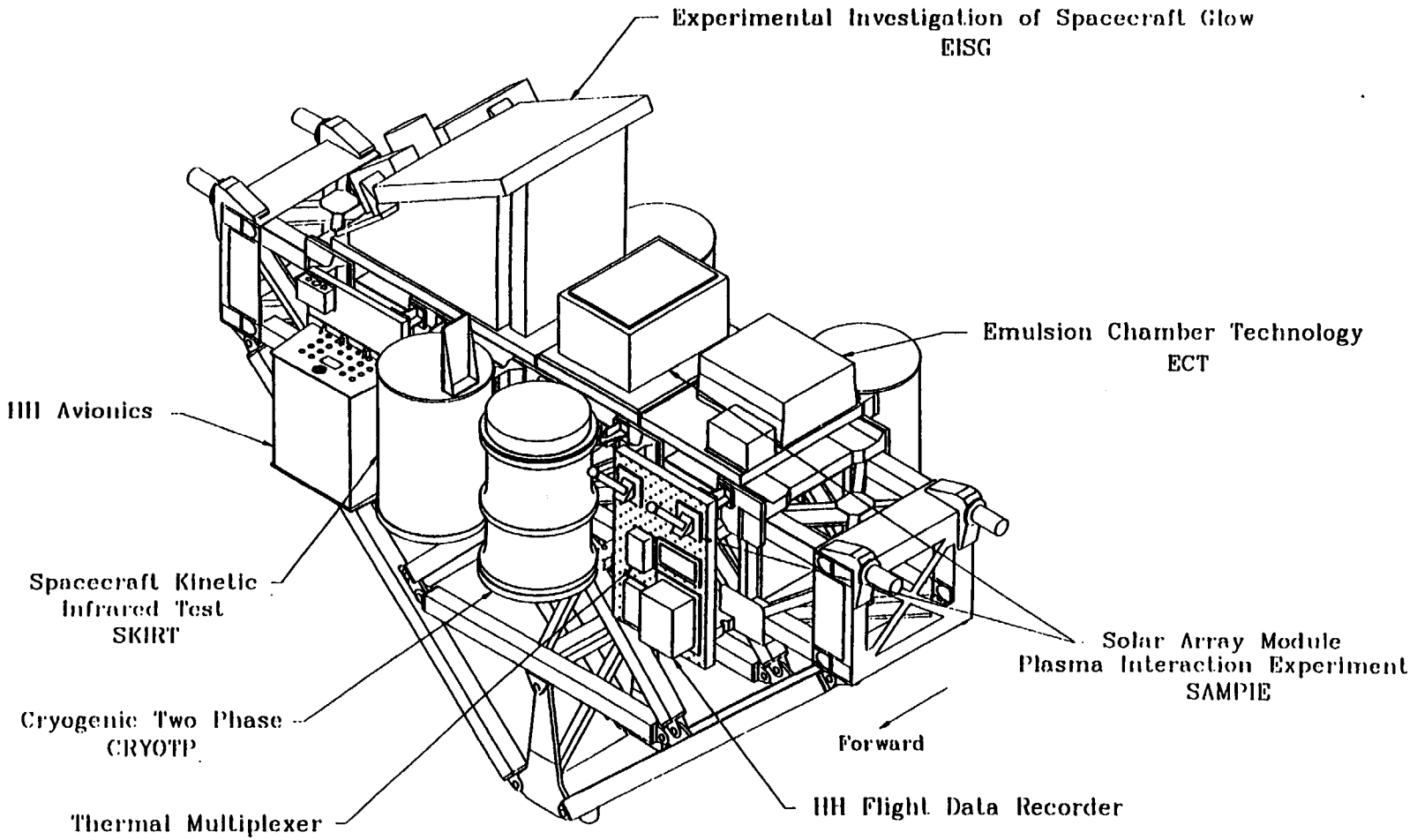




Figure 7

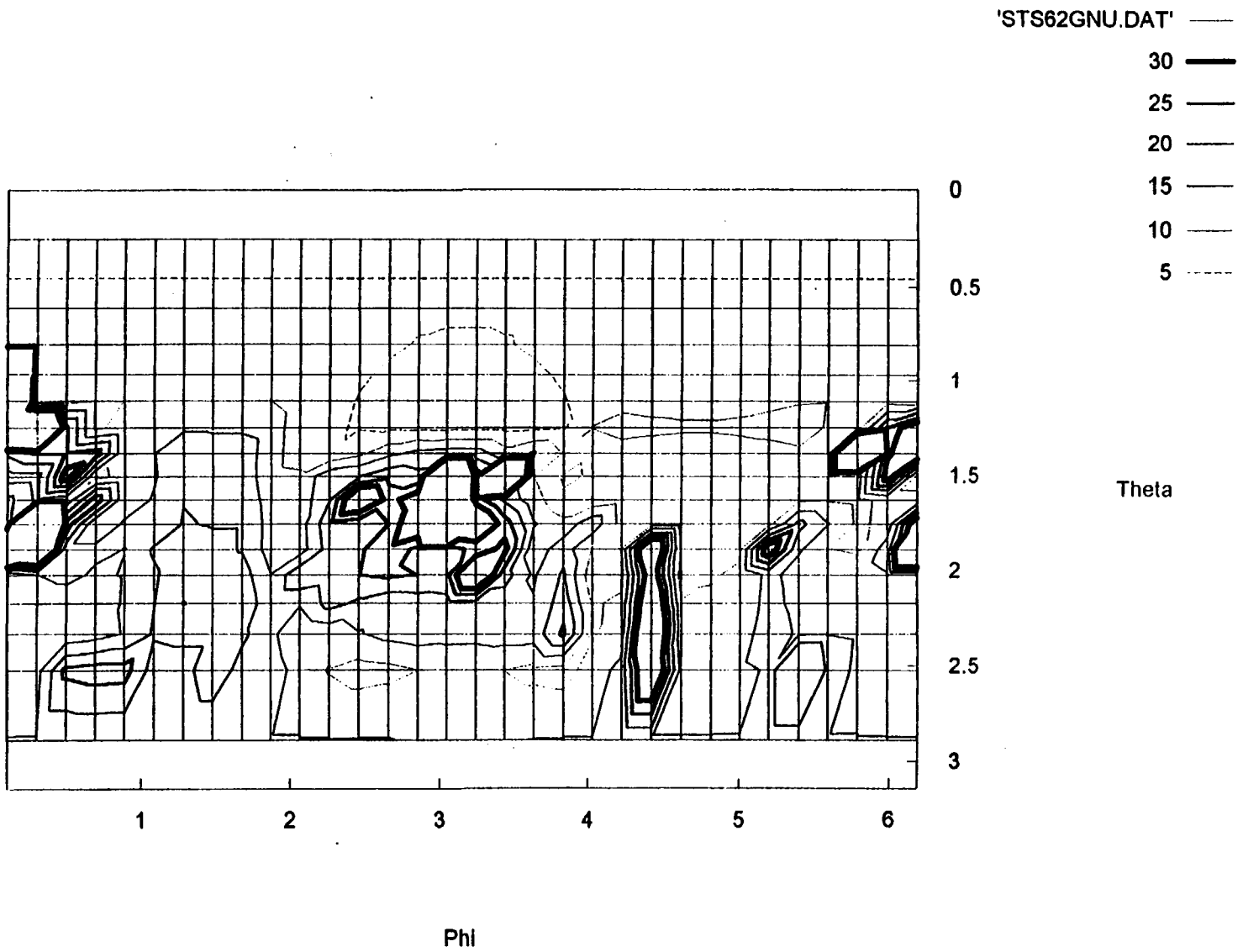


Figure 8

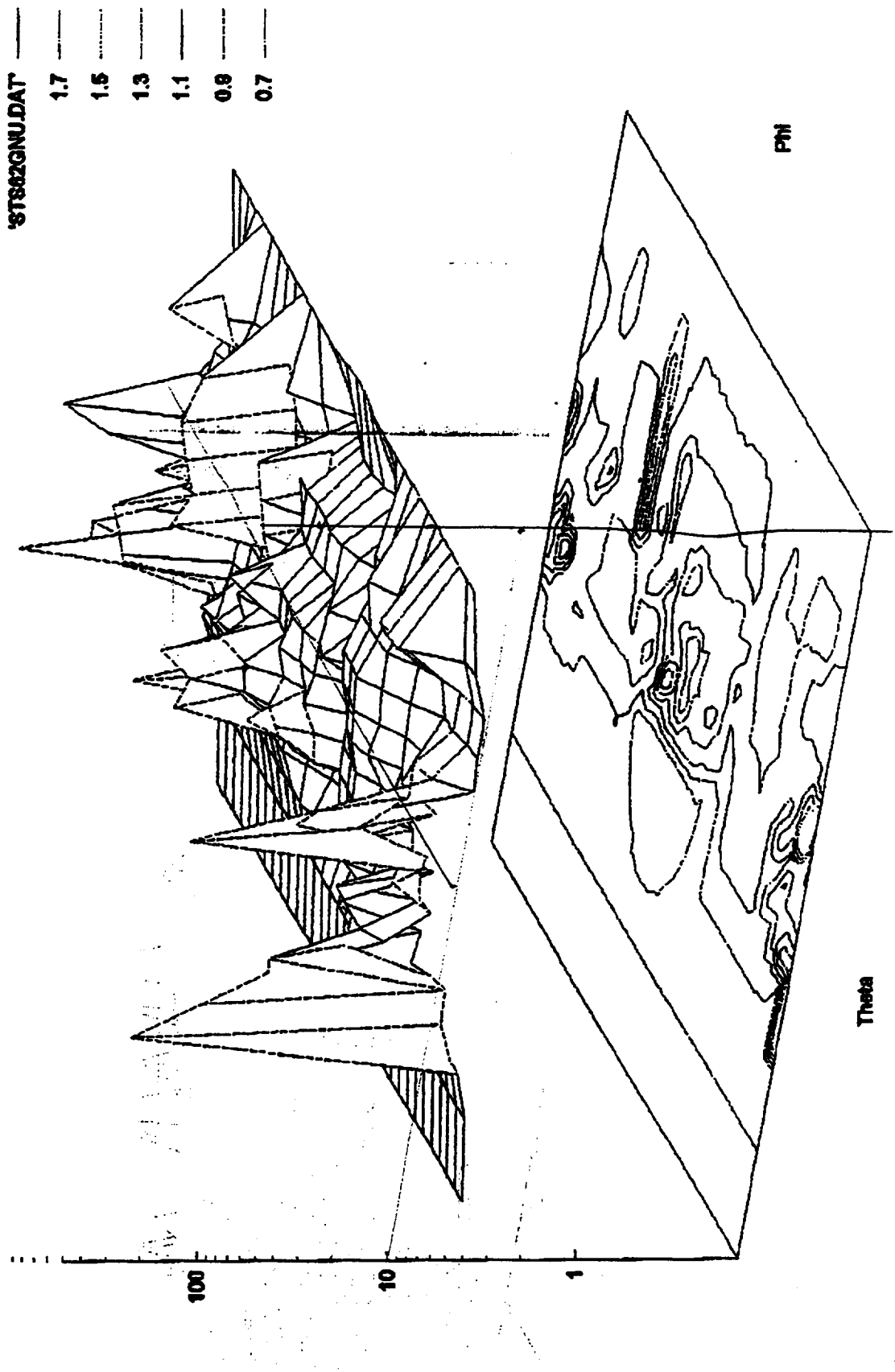


Figure 9

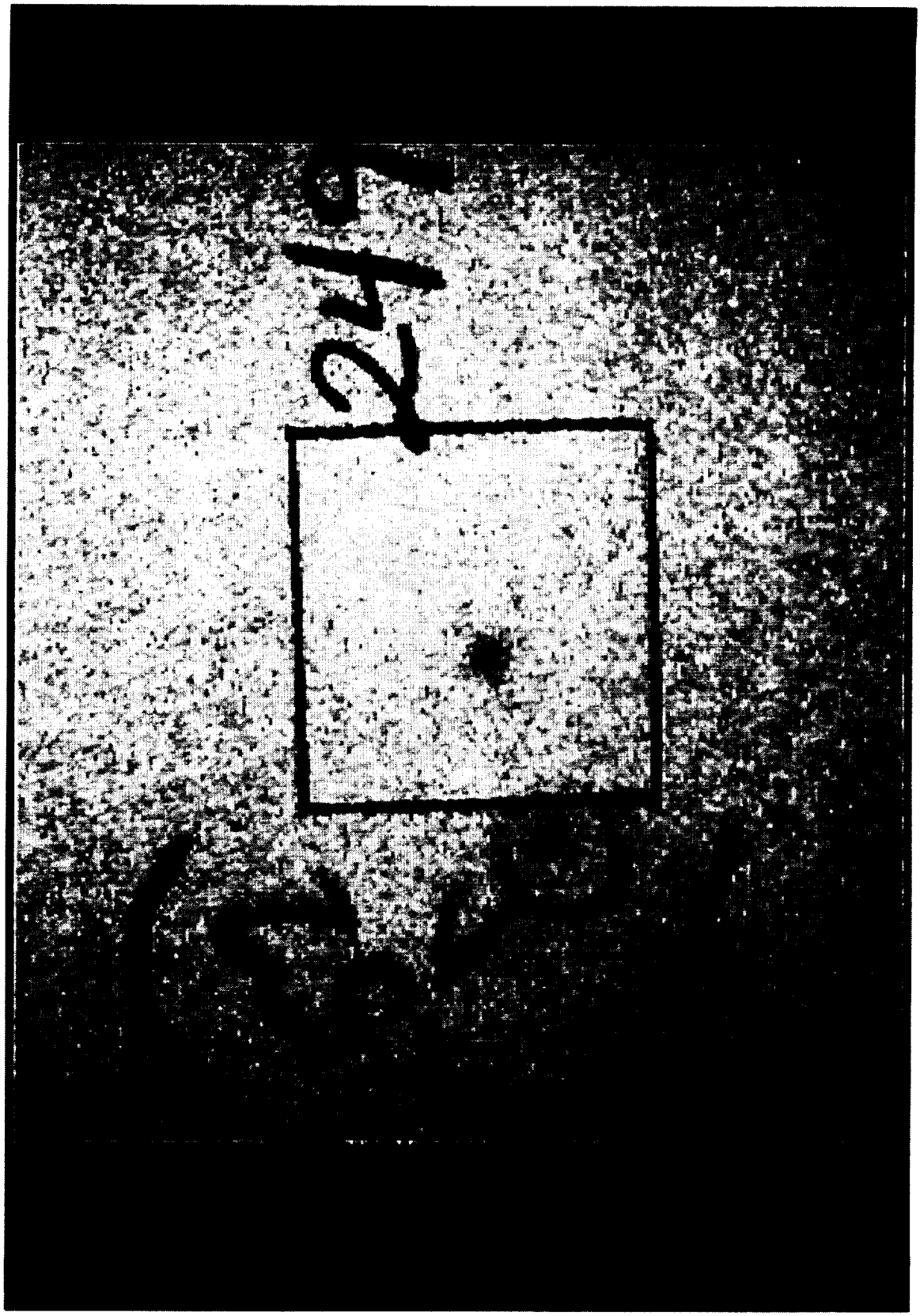

Figure 10a

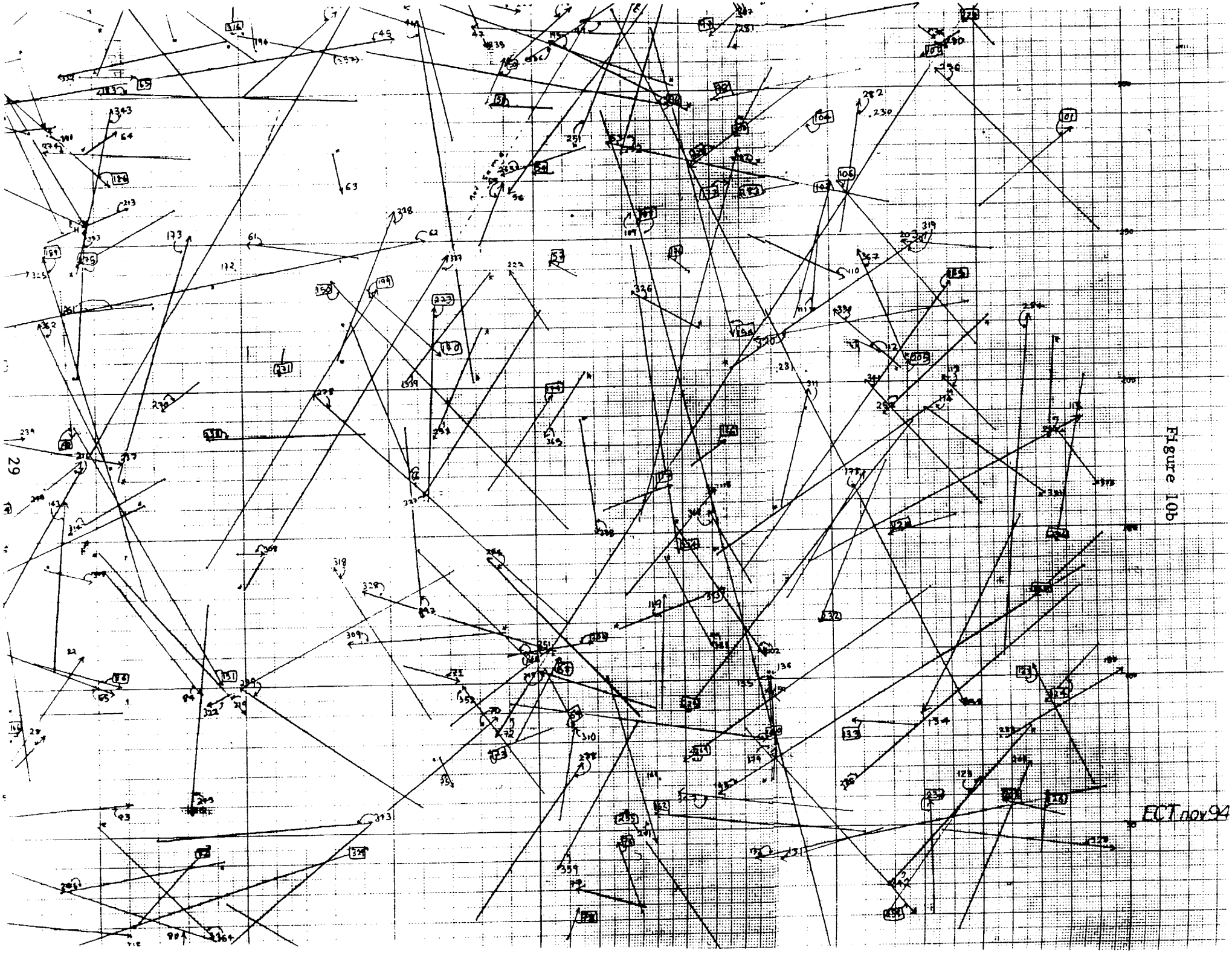

Figure 10b

ECT nov 94

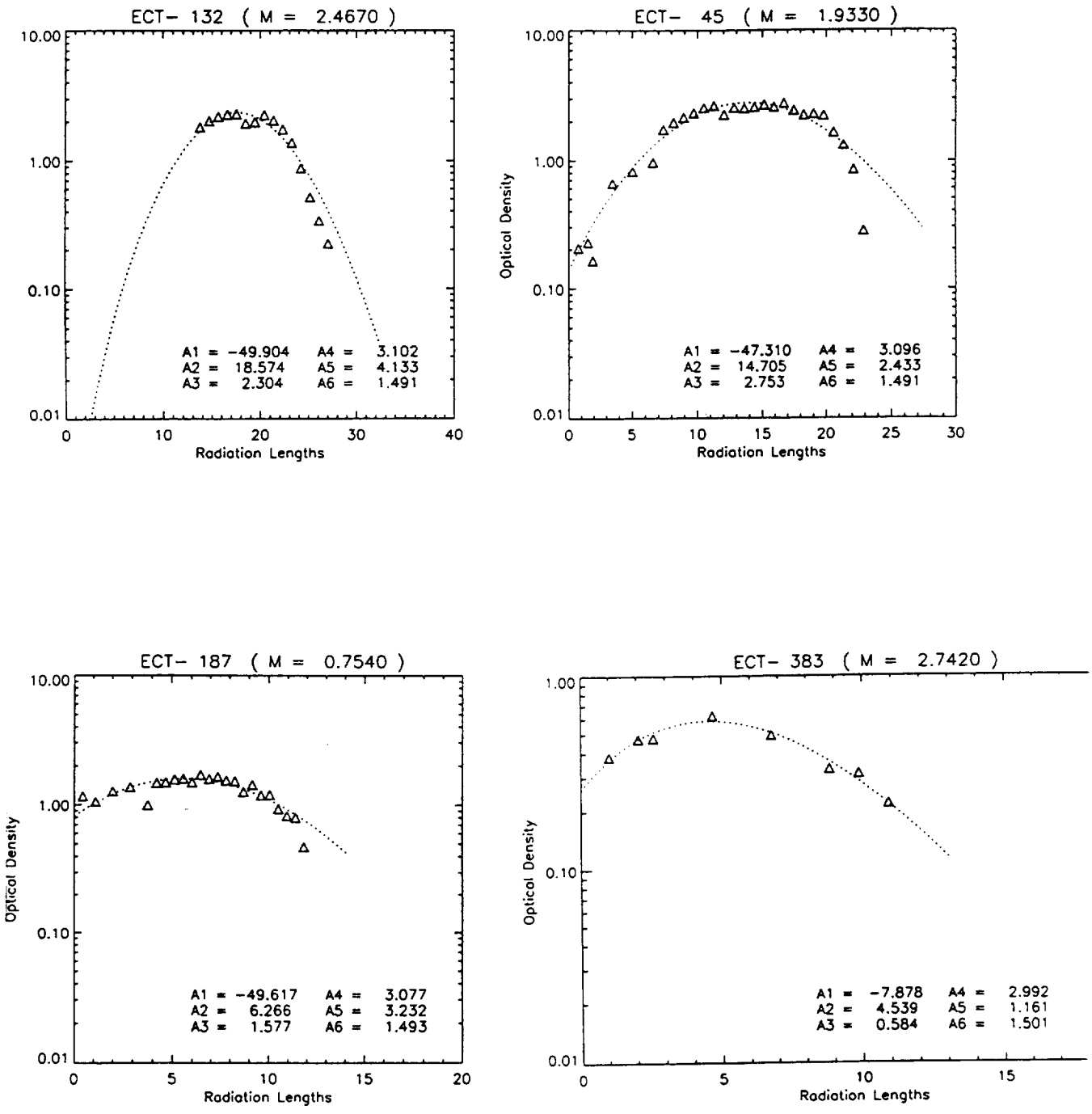
ECT- 132 ( M = 2.4670 )
A1 = -49.904 A4 = 3.102
A2 = 18.574 A5 = 4.133
A3 = 2.304 A6 = 1.491
Radiation Lengths
ECT- 45 ( M = 1.9330 )
A1 = -47.310 A4 = 3.096
A2 = 14.705 A5 = 2.433
A3 = 2.753 A6 = 1.491
Optical Density
Radiation Lengths
ECT- 187 ( M = 0.7540 )
A1 = -49.617 A4 = 3.077
A2 = 6.266 A5 = 3.232
A3 = 1.577 A6 = 1.493
Optical Density
Radiation Lengths
ECT- 383 ( M = 2.7420 )
A1 = -7.878 A4 = 2.992
A2 = 4.539 A5 = 1.161
A3 = 0.584 A6 = 1.501
Optical Density
Radiation Lengths

Figure 11

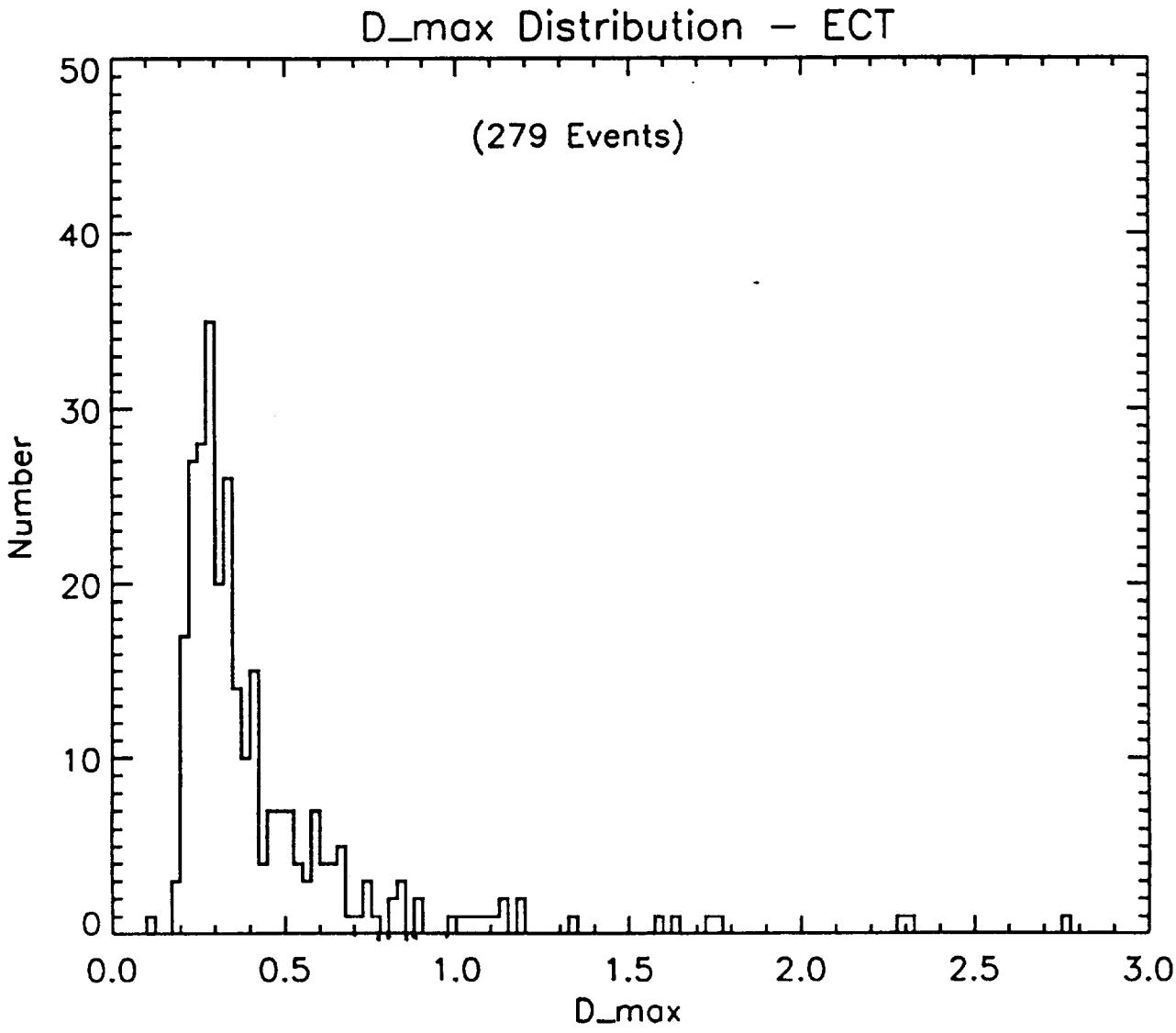
D_max Distribution – ECT
(279 Events)
Number
50
40
30
20
10
0
0.0
0.5
1.0
1.5
2.0
2.5
3.0
D_max

Figure 12a

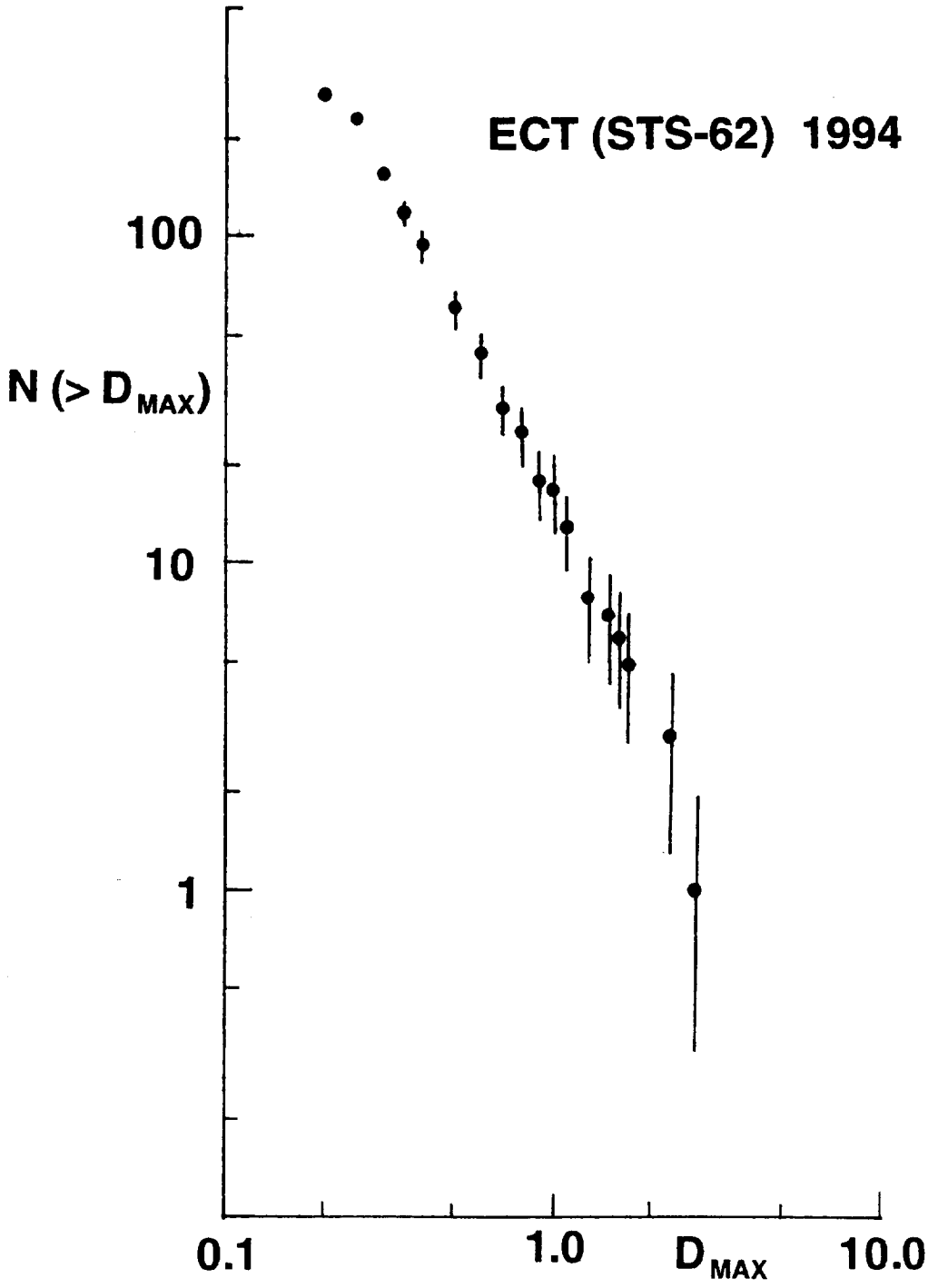


Figure 12b

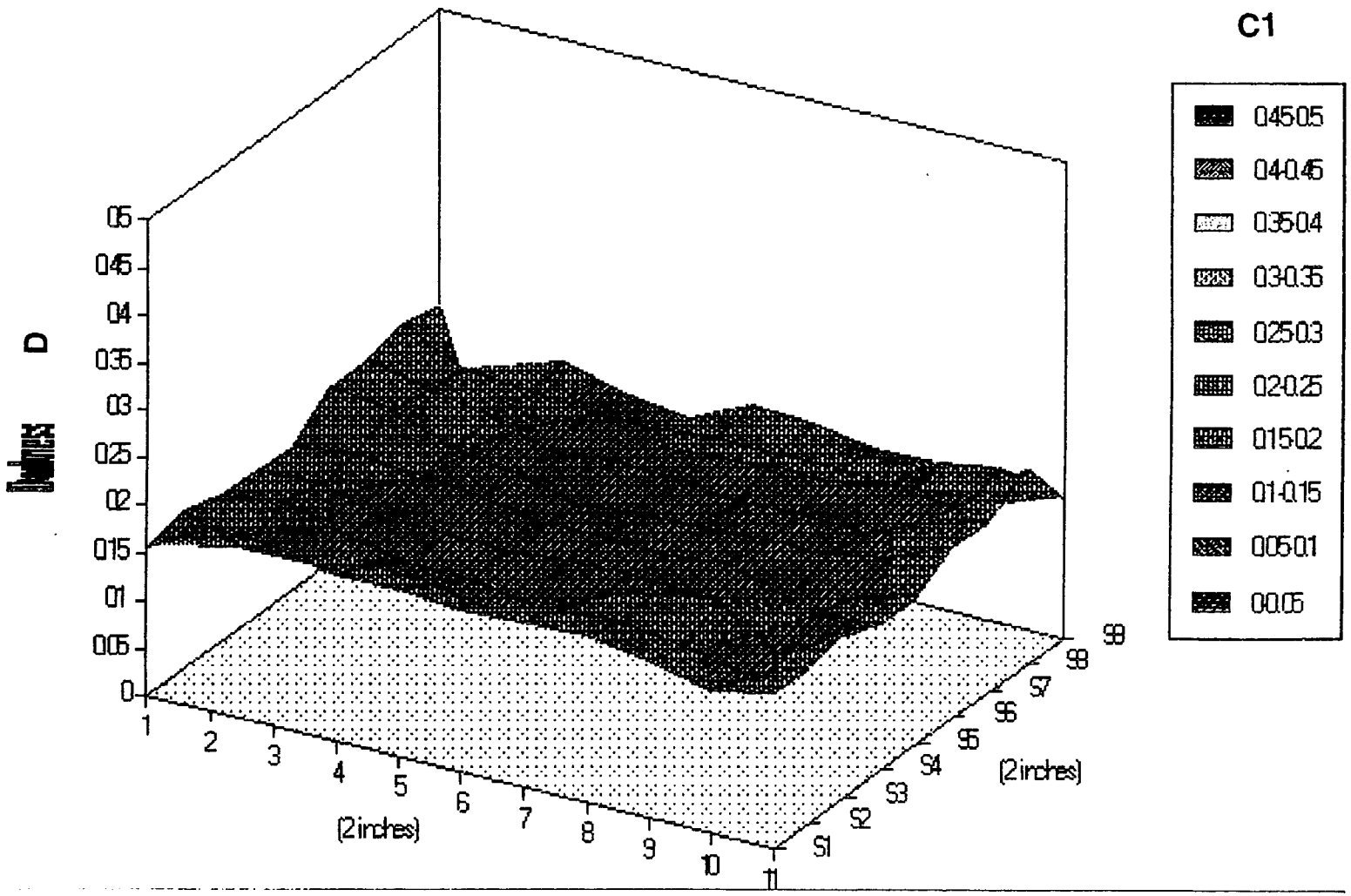
C1
0.45-0.5
0.4-0.45
0.35-0.4
0.3-0.35
0.25-0.3
0.2-0.25
0.15-0.2
0.1-0.15
0.05-0.1
0-0.05
D
0.5
0.45
0.4
0.35
0.3
0.25
0.2
0.15
0.1
0.05
0
1
2
3
4
5
6
7
8
9
10
11
(2 inches)
S1
S2
S3
S4
S5
S6
S7
S8
S9
(2 inches)

Figure 13-1

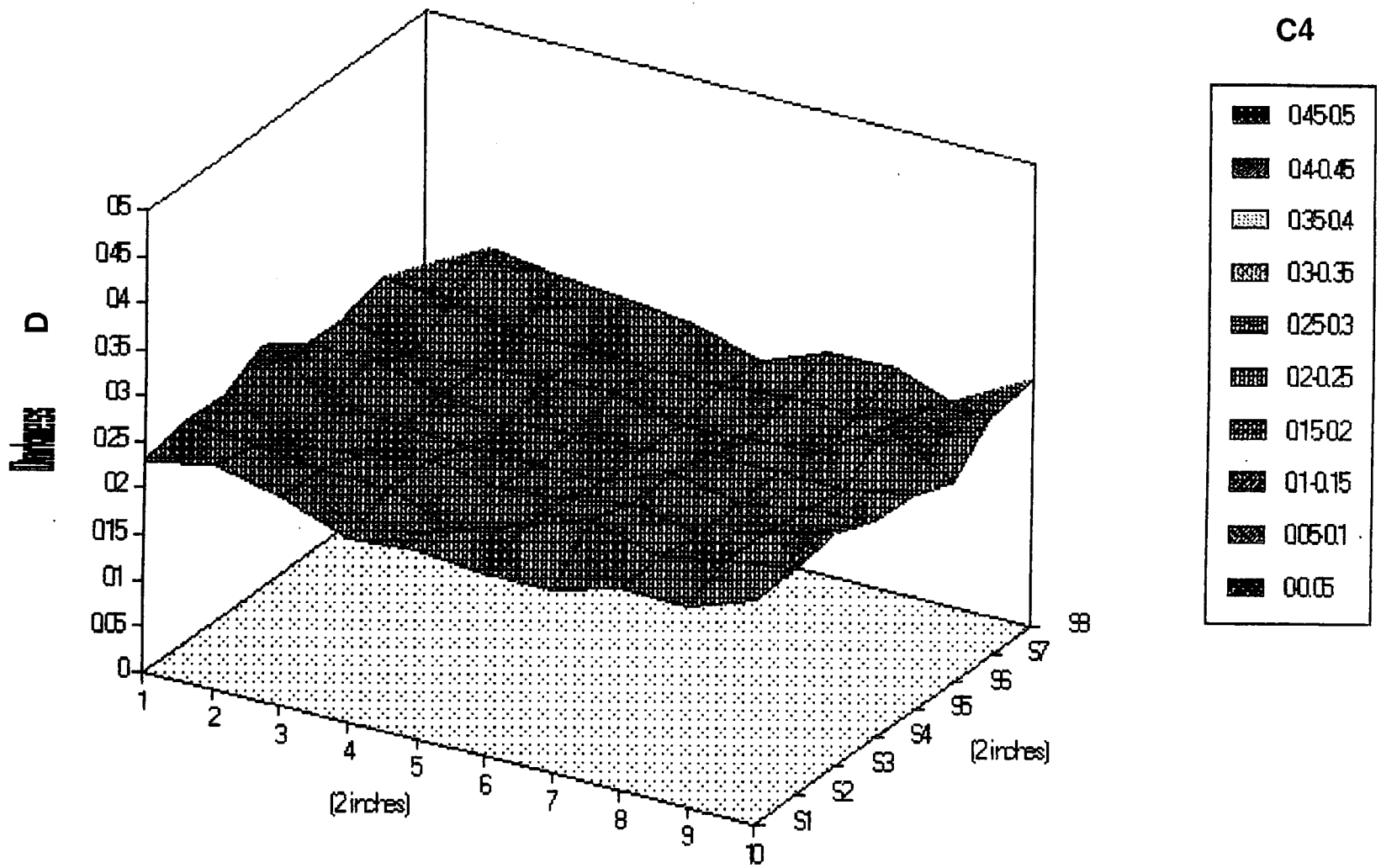
C4
0.45-0.5
0.4-0.45
0.35-0.4
0.3-0.35
0.25-0.3
0.2-0.25
0.15-0.2
0.1-0.15
0.05-0.1
0-0.05
D
0.5
0.45
0.4
0.35
0.3
0.25
0.2
0.15
0.1
0.05
0
1
2
3
4
5
6
7
8
9
10
(2 inches)
S1
S2
S3
S4
S5
S6
S7
S8
(2 inches)

Figure 13-2

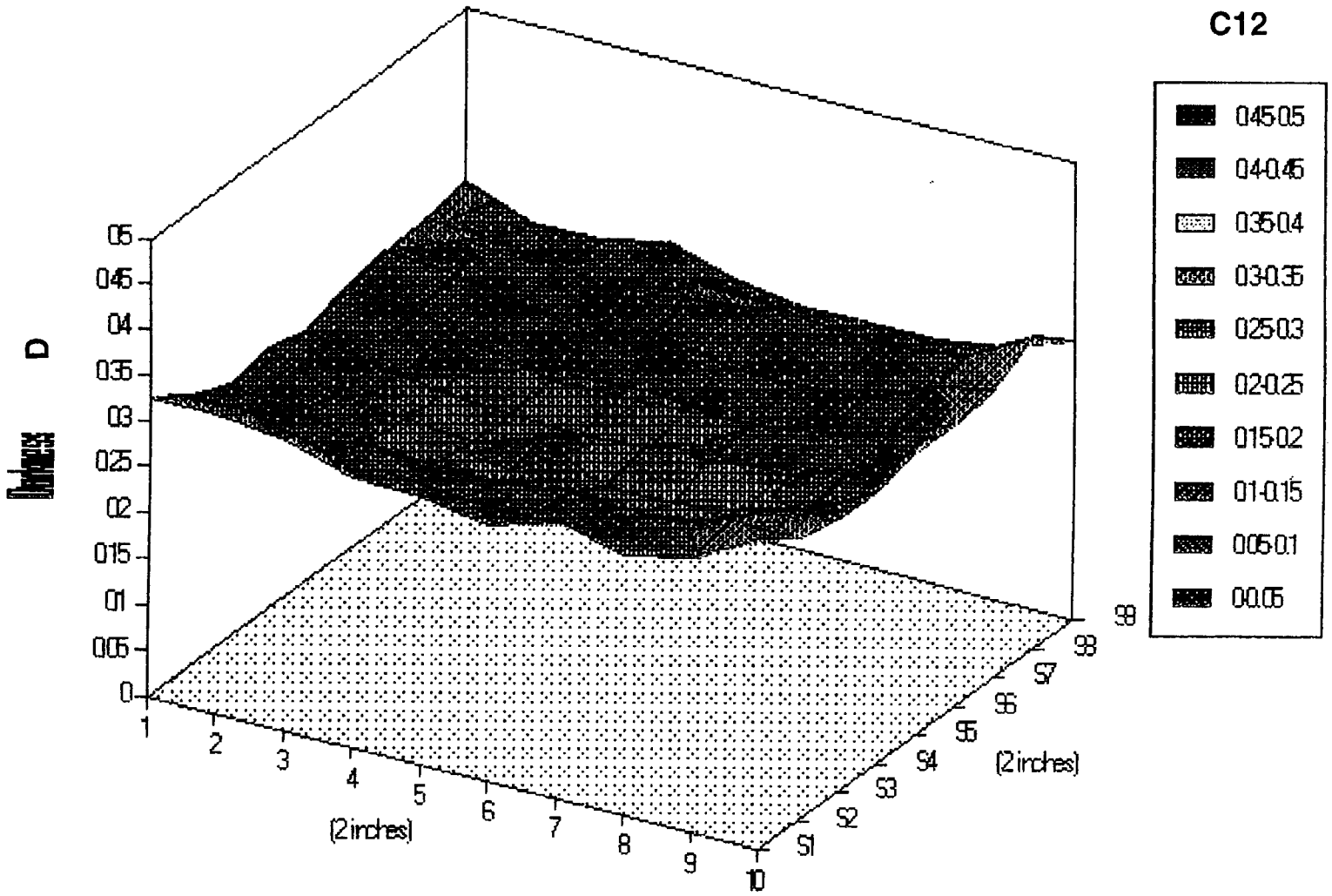
C12
0.45-0.5
0.4-0.45
0.35-0.4
0.3-0.35
0.25-0.3
0.2-0.25
0.15-0.2
0.1-0.15
0.05-0.1
0-0.05
D
0.5
0.45
0.4
0.35
0.3
0.25
0.2
0.15
0.1
0.05
0
1
2
3
4
5
6
7
8
9
10
(2 inches)
S1
S2
S3
S4
S5
S6
S7
S8
(2 inches)

Figure 13-3

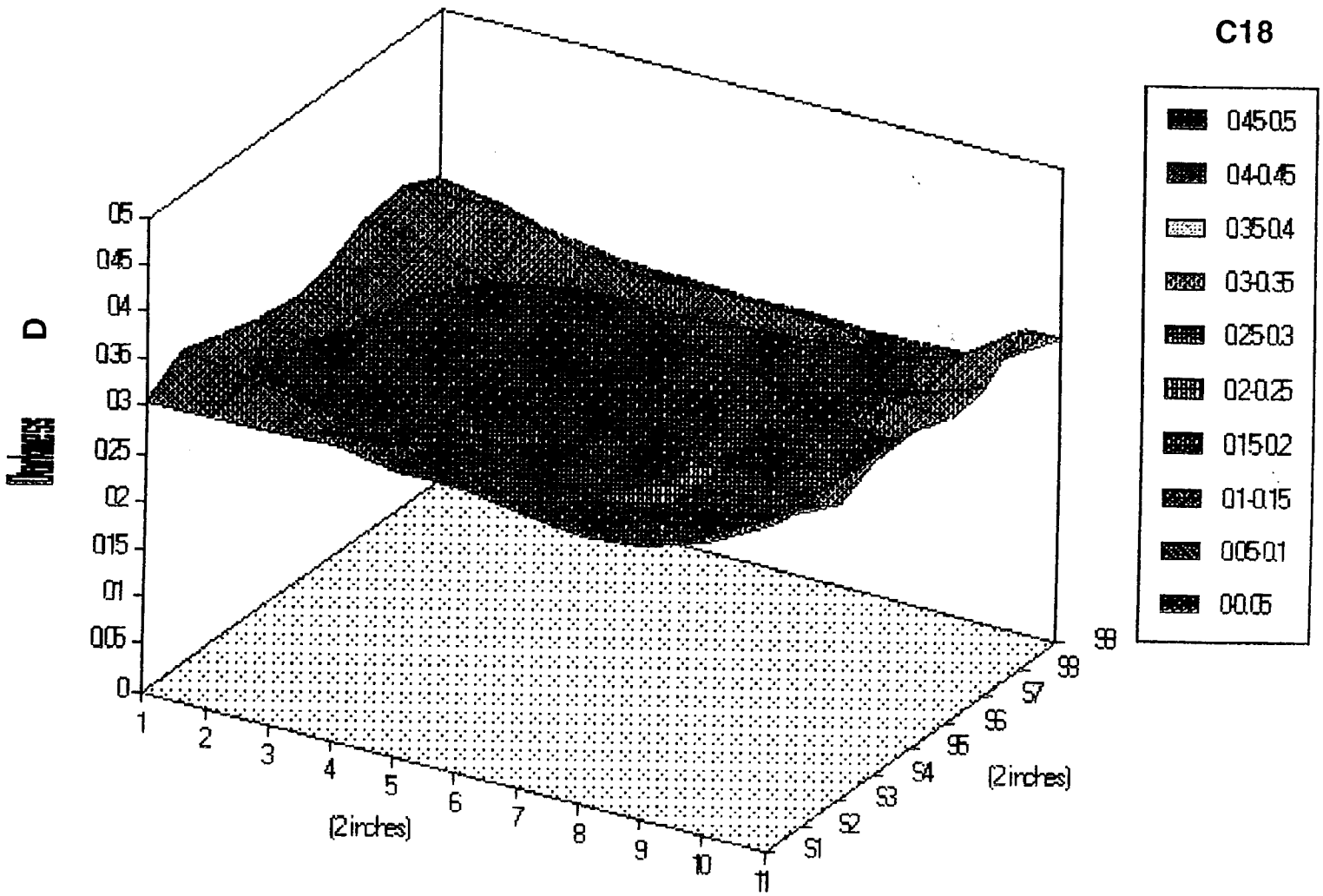
C18
0.45-0.5
0.4-0.45
0.35-0.4
0.3-0.35
0.25-0.3
0.2-0.25
0.15-0.2
0.1-0.15
0.05-0.1
0-0.05
D
0.5
0.45
0.4
0.35
0.3
0.25
0.2
0.15
0.1
0.05
0
1
2
3
4
5
6
7
8
9
10
11
(2inches)
S1
S2
S3
S4
S5
S6
S7
S8
(2inches)

Figure 13-4

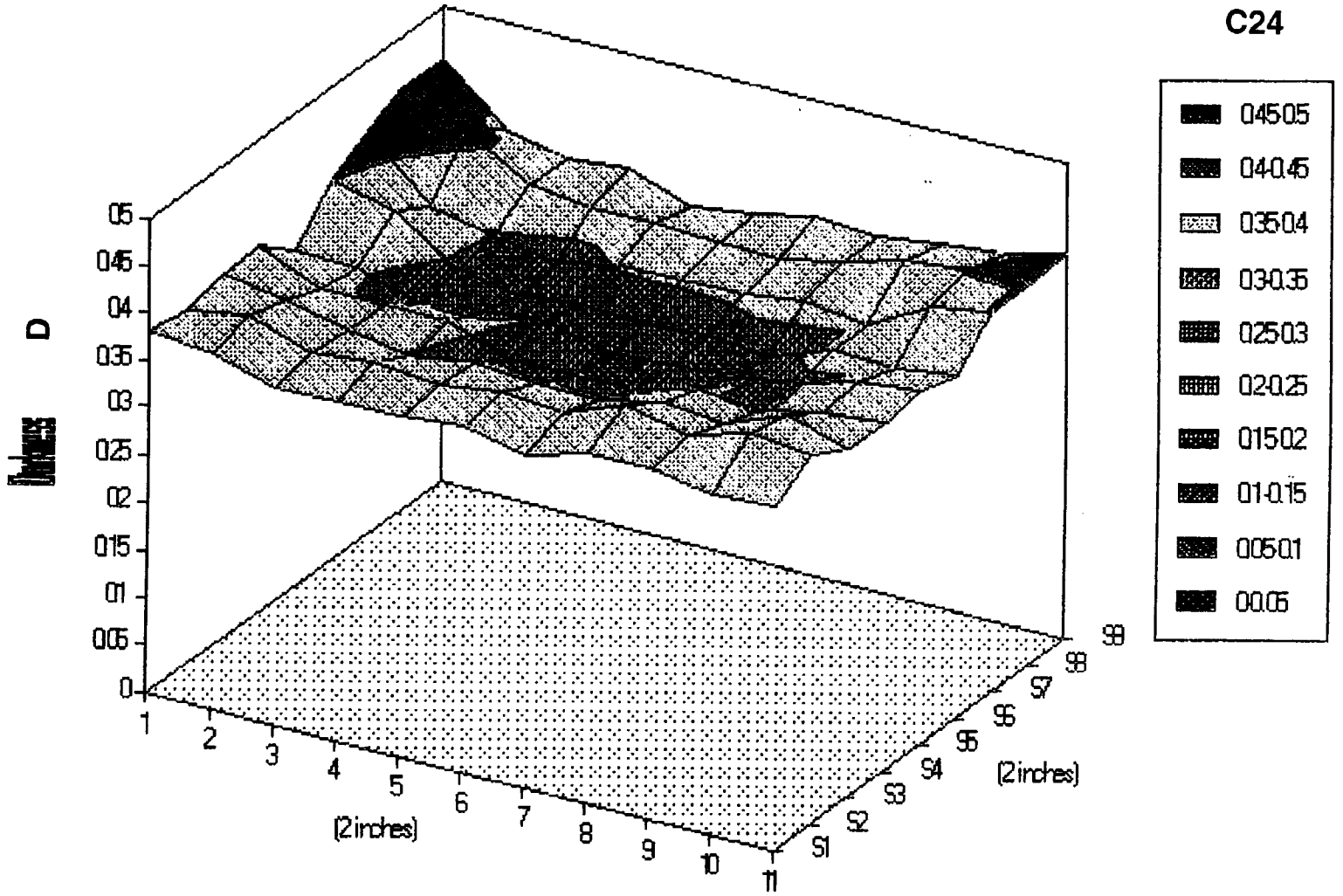
C24
0.45-0.5
0.4-0.45
0.35-0.4
0.3-0.35
0.25-0.3
0.2-0.25
0.15-0.2
0.1-0.15
0.05-0.1
0-0.05
D
0.5
0.45
0.4
0.35
0.3
0.25
0.2
0.15
0.1
0.05
0
1
2
3
4
5
6
7
8
9
10
11
(2 inches)
S1
S2
S3
S4
S5
S6
S7
S8
S9
(2 inches)

Figure 13-5

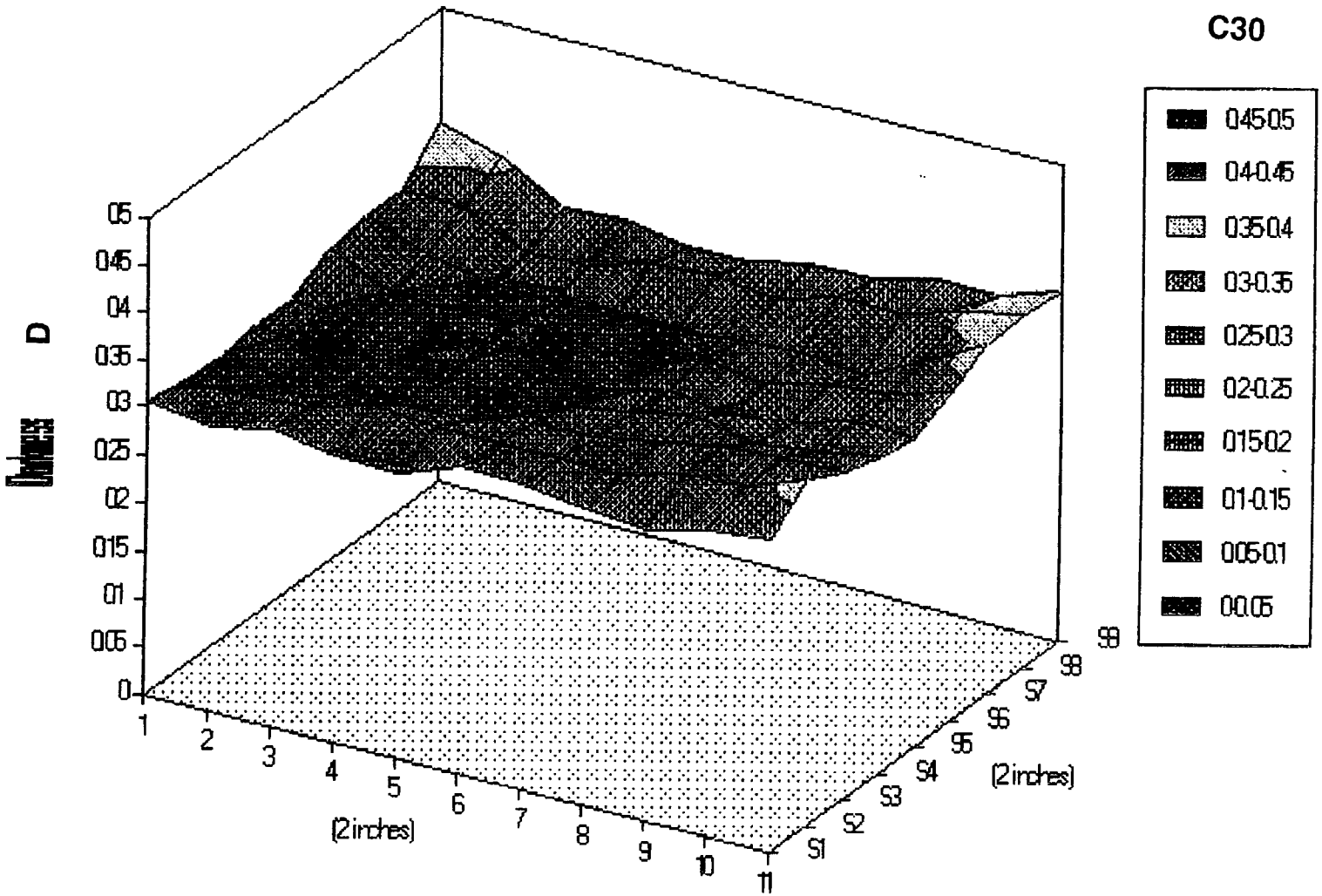
C30
0.45-0.5
0.4-0.45
0.35-0.4
0.3-0.35
0.25-0.3
0.2-0.25
0.15-0.2
0.1-0.15
0.05-0.1
0-0.05
D
0.5
0.45
0.4
0.35
0.3
0.25
0.2
0.15
0.1
0.05
0
1
2
3
4
5
6
7
8
9
10
11
(2 inches)
S1
S2
S3
S4
S5
S6
S7
S8
S9
(2 inches)

Figure 13-6

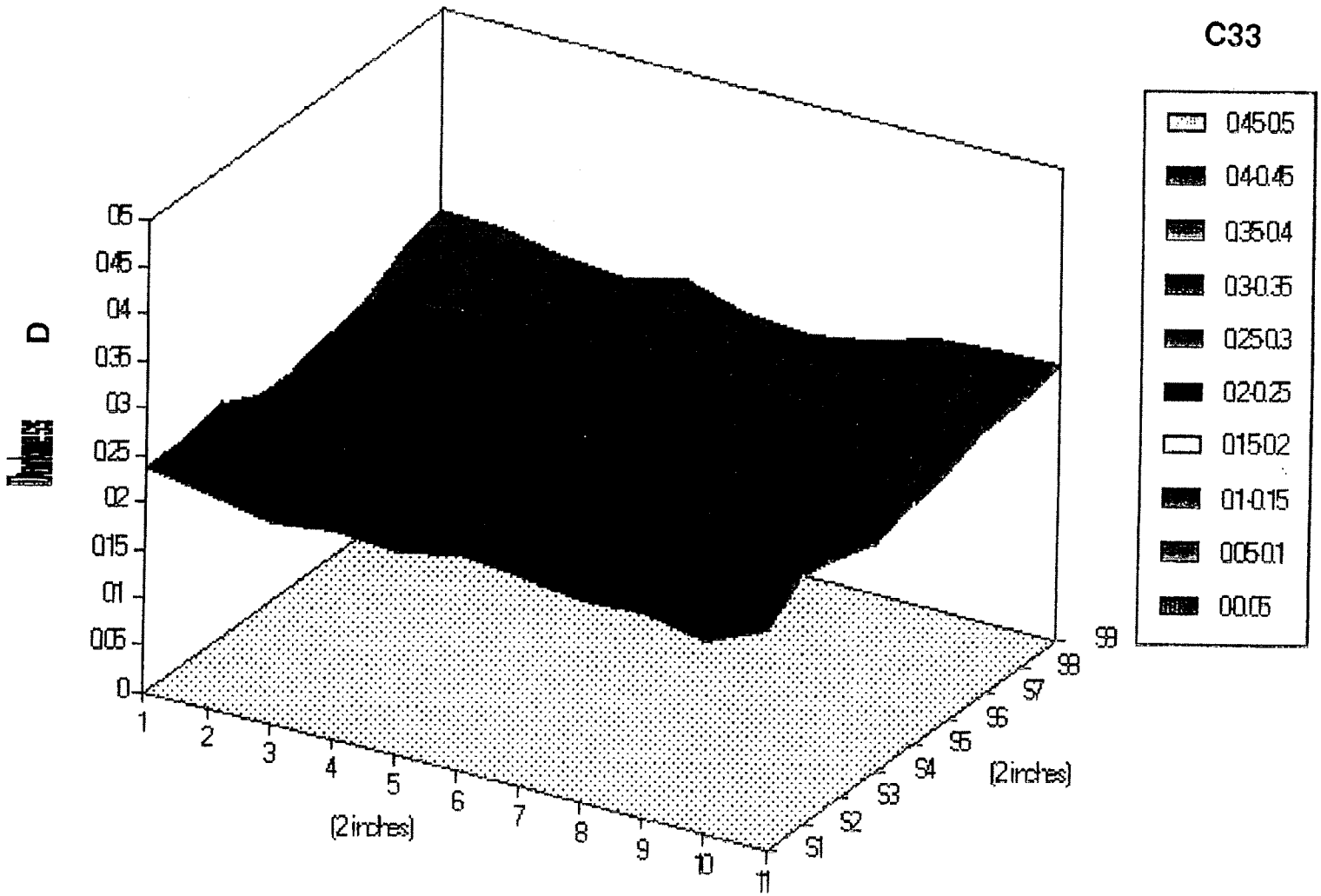
C33
0.45-0.5
0.4-0.45
0.35-0.4
0.3-0.35
0.25-0.3
0.2-0.25
0.15-0.2
0.1-0.15
0.05-0.1
0-0.05
D
0.5
0.45
0.4
0.35
0.3
0.25
0.2
0.15
0.1
0.05
0
1
2
3
4
5
6
7
8
9
10
11
(2 inches)
S1
S2
S3
S4
S5
S6
S7
S8
S9
(2 inches)

Figure 13-7

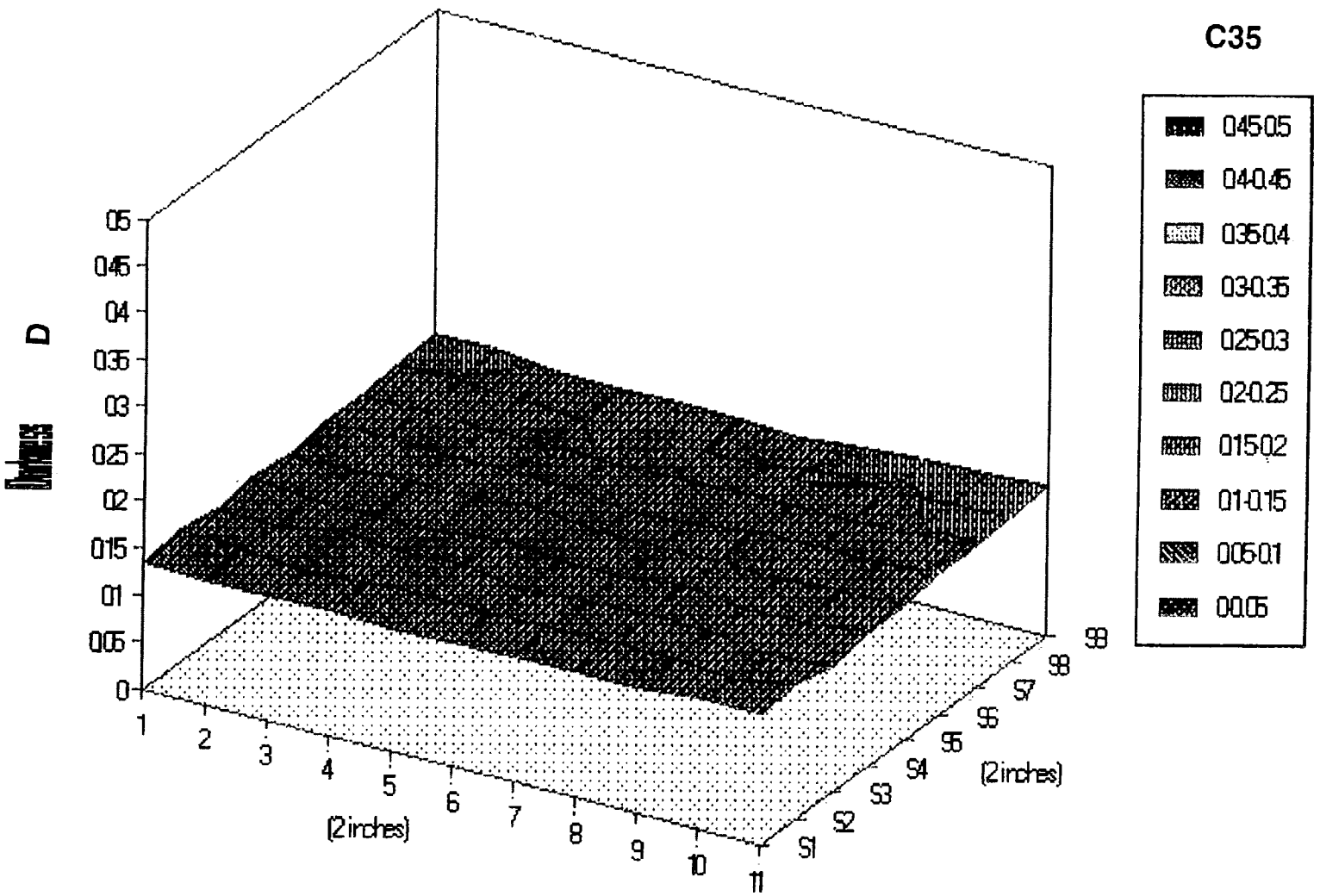
C35
0.45-0.5
0.4-0.45
0.35-0.4
0.3-0.35
0.25-0.3
0.2-0.25
0.15-0.2
0.1-0.15
0.05-0.1
0-0.05
D
0.5
0.45
0.4
0.35
0.3
0.25
0.2
0.15
0.1
0.05
0
1
2
3
4
5
6
7
8
9
10
11
(2 inches)
S1
S2
S3
S4
S5
S6
S7
S8
S9
(2 inches)

Figure 13-8

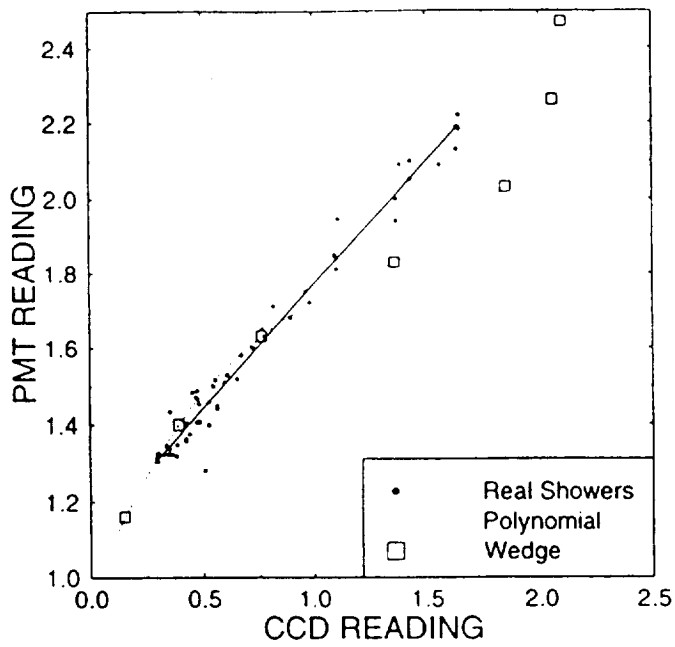


Raw CCD density calibration. Slit size is 250$\mu$m for both systems. Note the distinct difference between sterile (wedge) and dirty (real data) calibration.

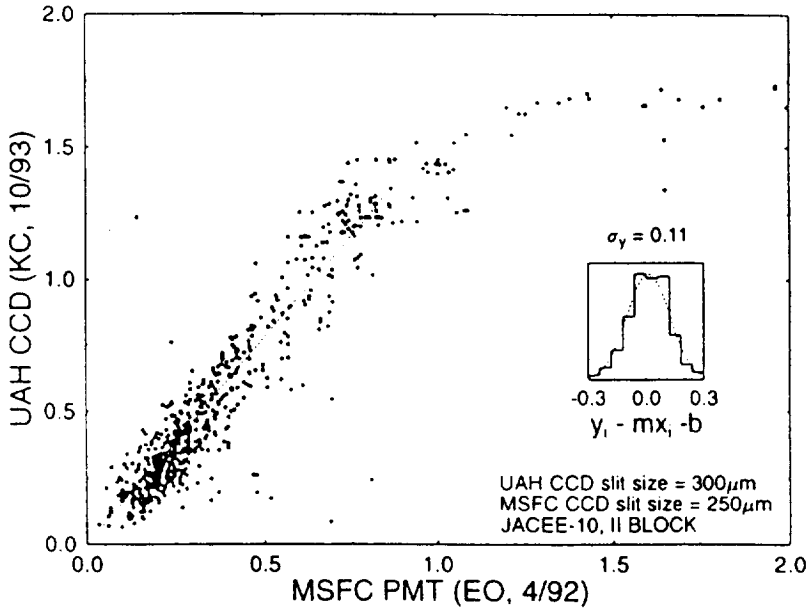


Net CCD density calibration. Several hundred real shower spots are used. Measurements fit well within a line of $D_{CCD} = 1.55 D_{PMT}$ for $D_{PMT} < 1.0$

Figs. 14a & 14b

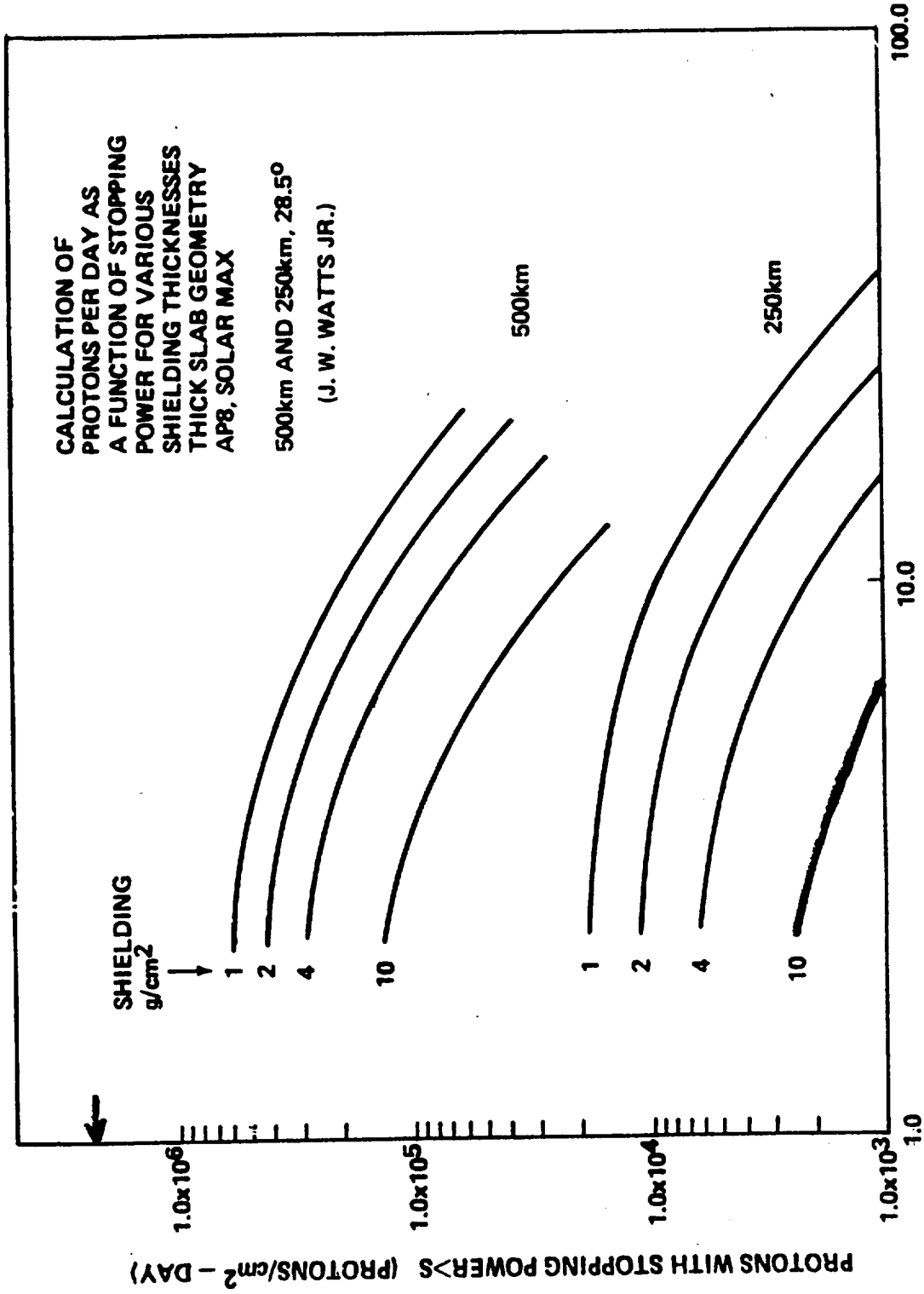
CALCULATION OF
PROTONS PER DAY AS
A FUNCTION OF STOPPING
POWER FOR VARIOUS
SHIELDING THICKNESSES
THICK SLAB GEOMETRY
AP8, SOLAR MAX
500km AND 250km, 28.5°
(J. W. WATTS JR.)
500km
250km
SHIELDING
g/cm²
1
2
4
10
1
2
4
10
1.0x10⁶
1.0x10⁵
1.0x10⁴
1.0x10³
1.0
10.0
100.0
STOPPING POWER (MEV—cm/g)
PROTONS WITH STOPPING POWER>S (PROTONS/cm² – DAY)

Figure 14c

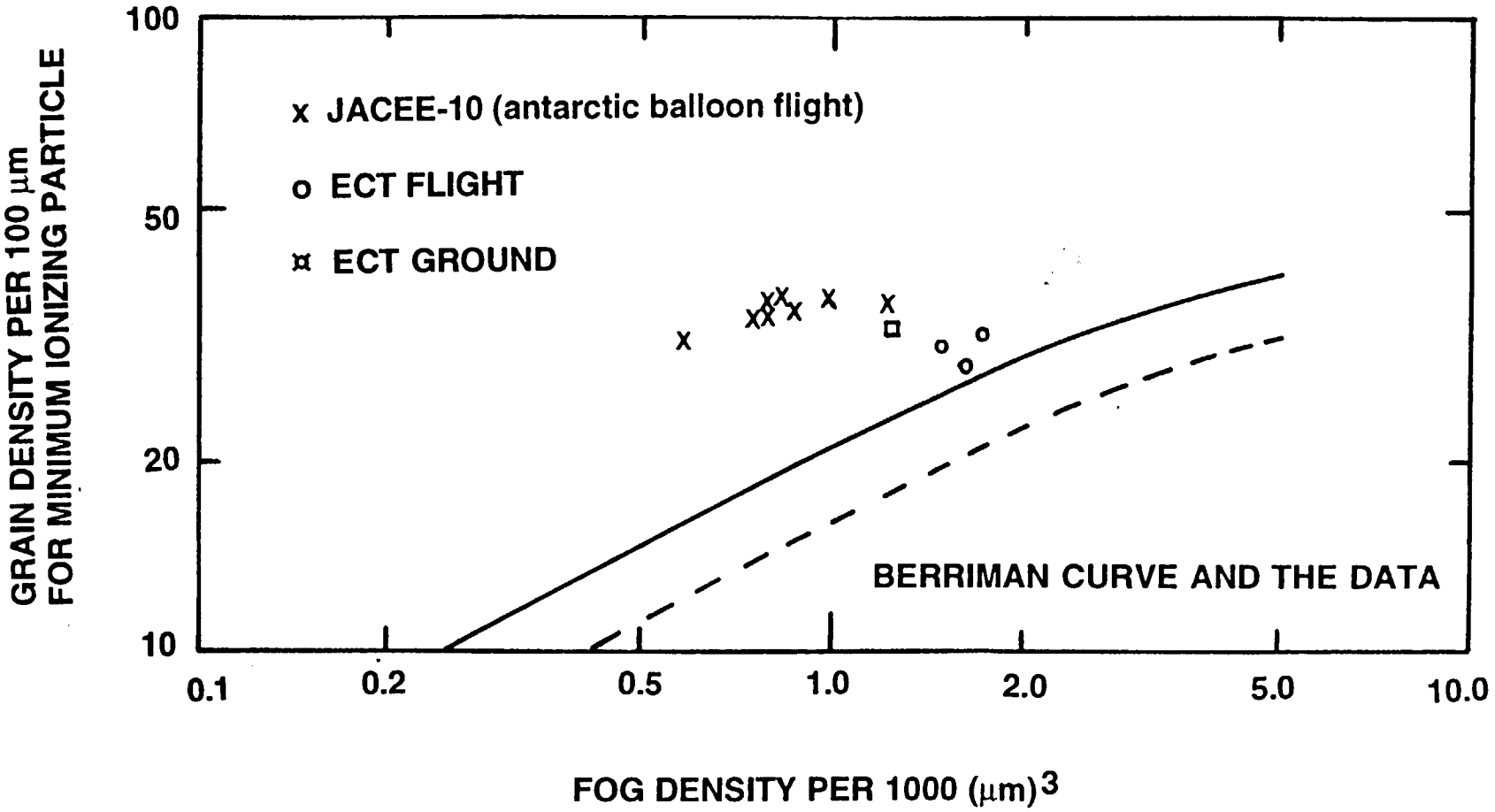
GRAIN DENSITY PER 100 μm
FOR MINIMUM IONIZING PARTICLE
100
50
20
10
x JACEE-10 (antarctic balloon flight)
o ECT FLIGHT
¤ ECT GROUND
BERRIMAN CURVE AND THE DATA
0.1
0.2
0.5
1.0
2.0
5.0
10.0
FOG DENSITY PER 1000 (μm)3

Figure 15

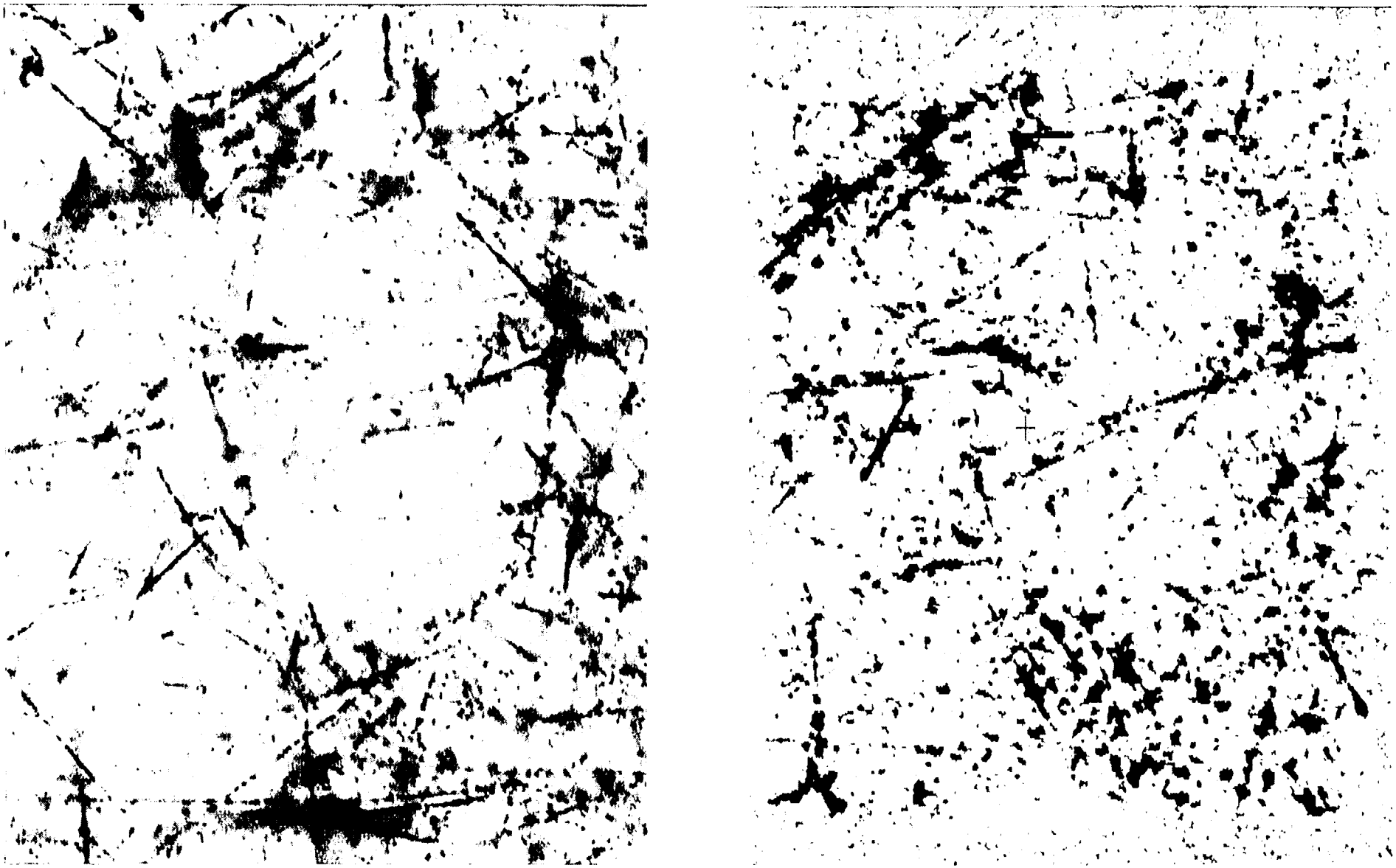

Figure 16

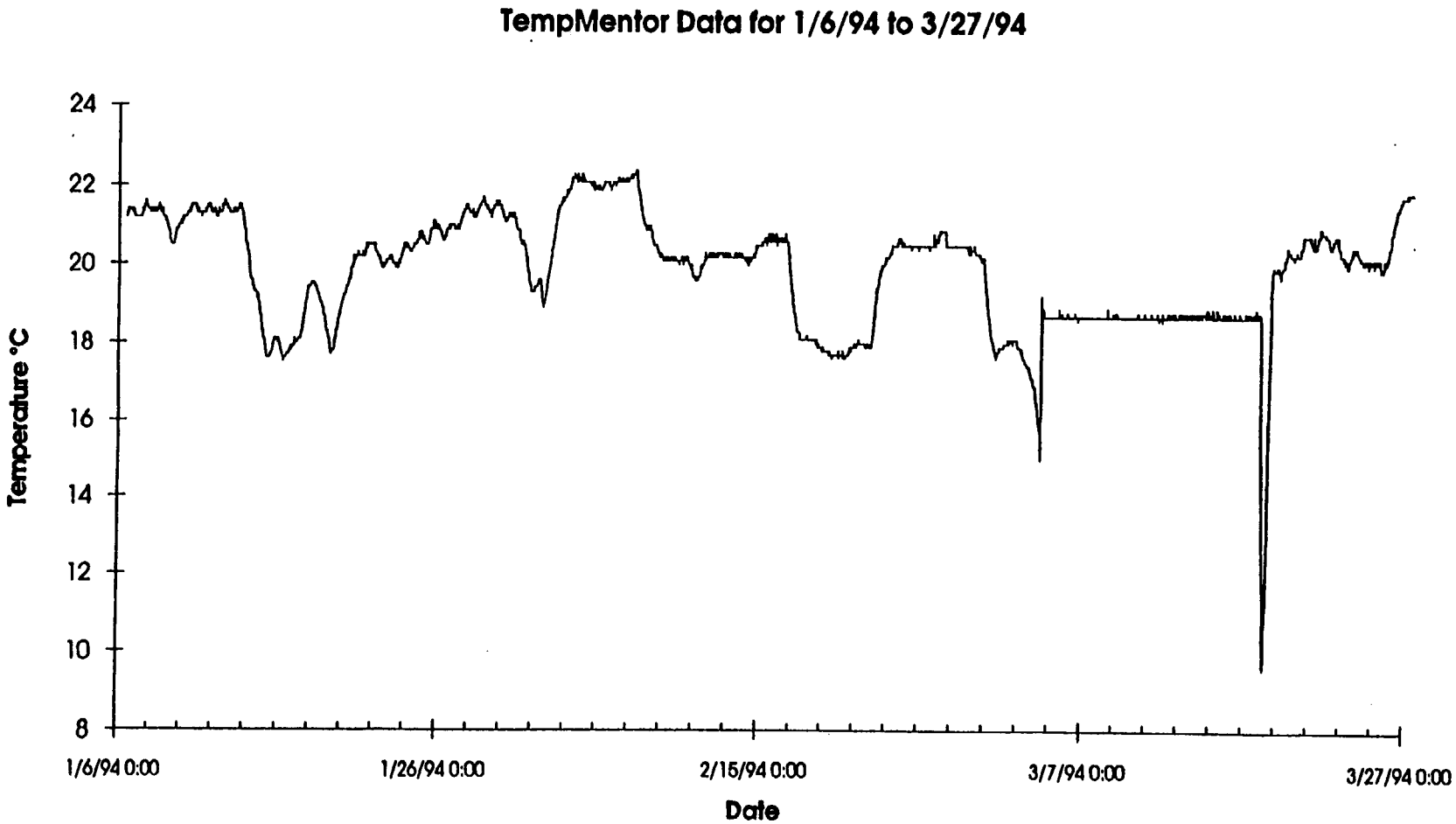
TempMentor Data for 1/6/94 to 3/27/94
Temperature °C
24
22
20
18
16
14
12
10
8
1/6/94 0:00
1/26/94 0:00
2/15/94 0:00
3/7/94 0:00
3/27/94 0:00
Date

Figure 17

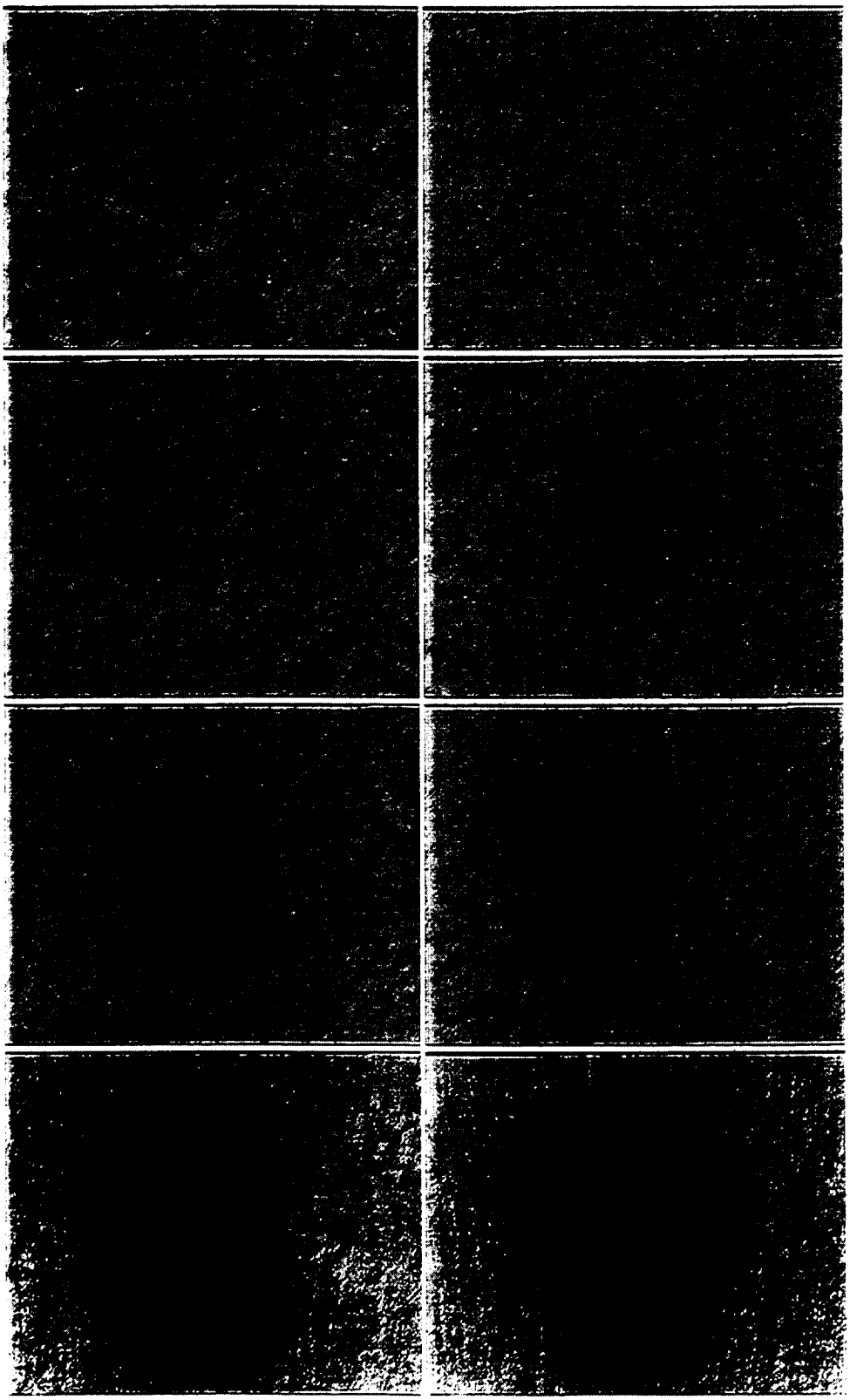


Figure 18

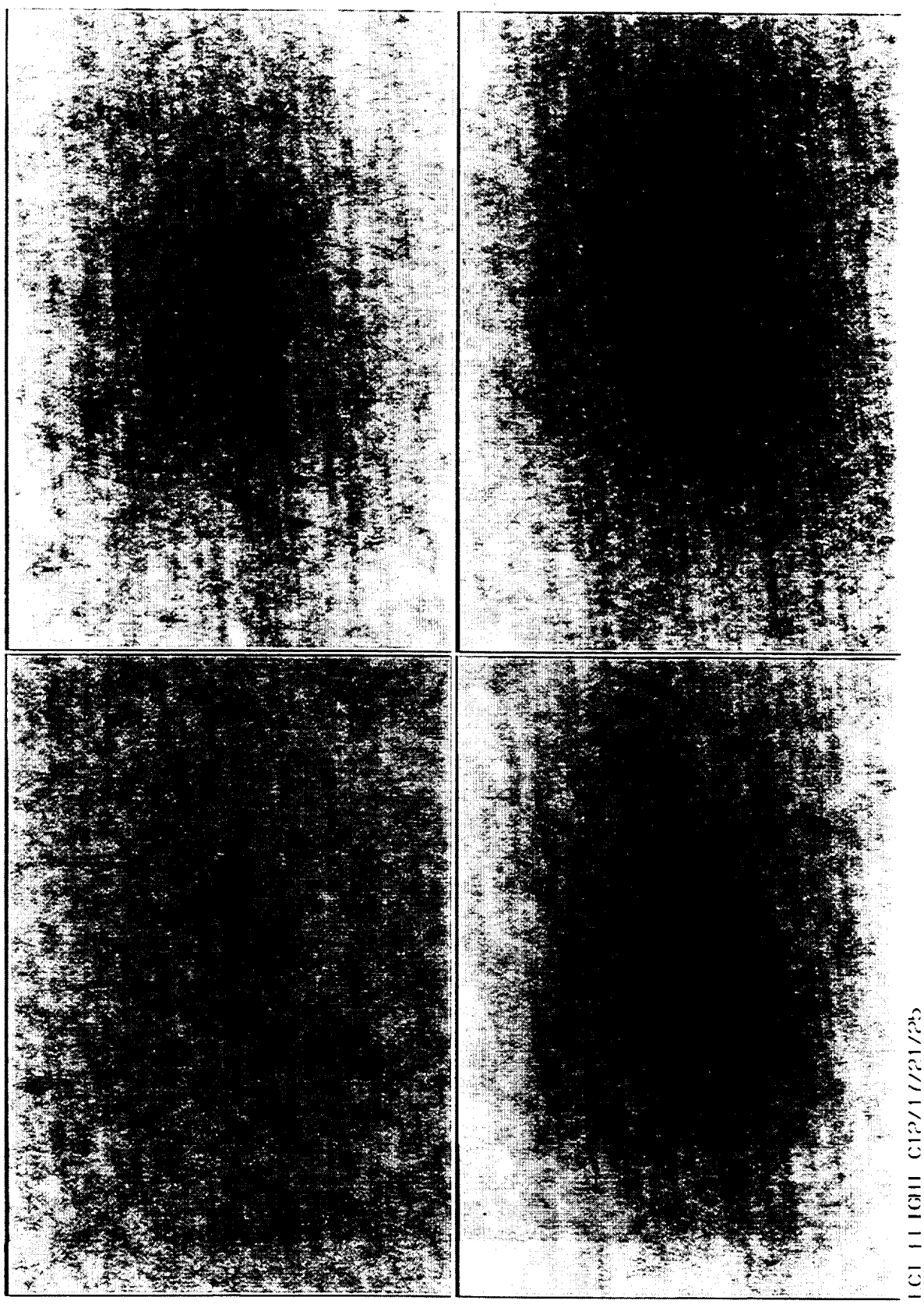

Figure 19


Figure 20

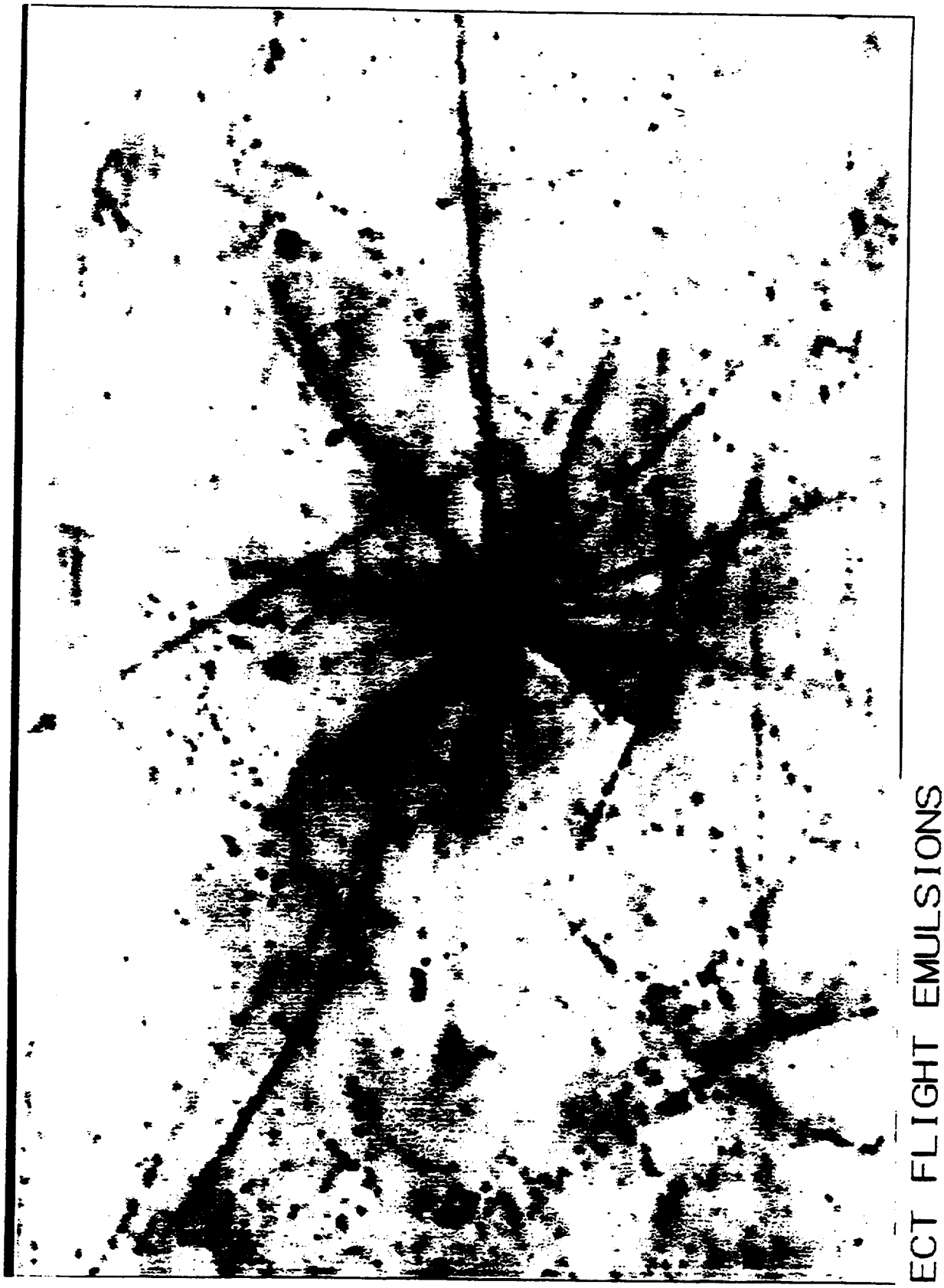


Figure 21

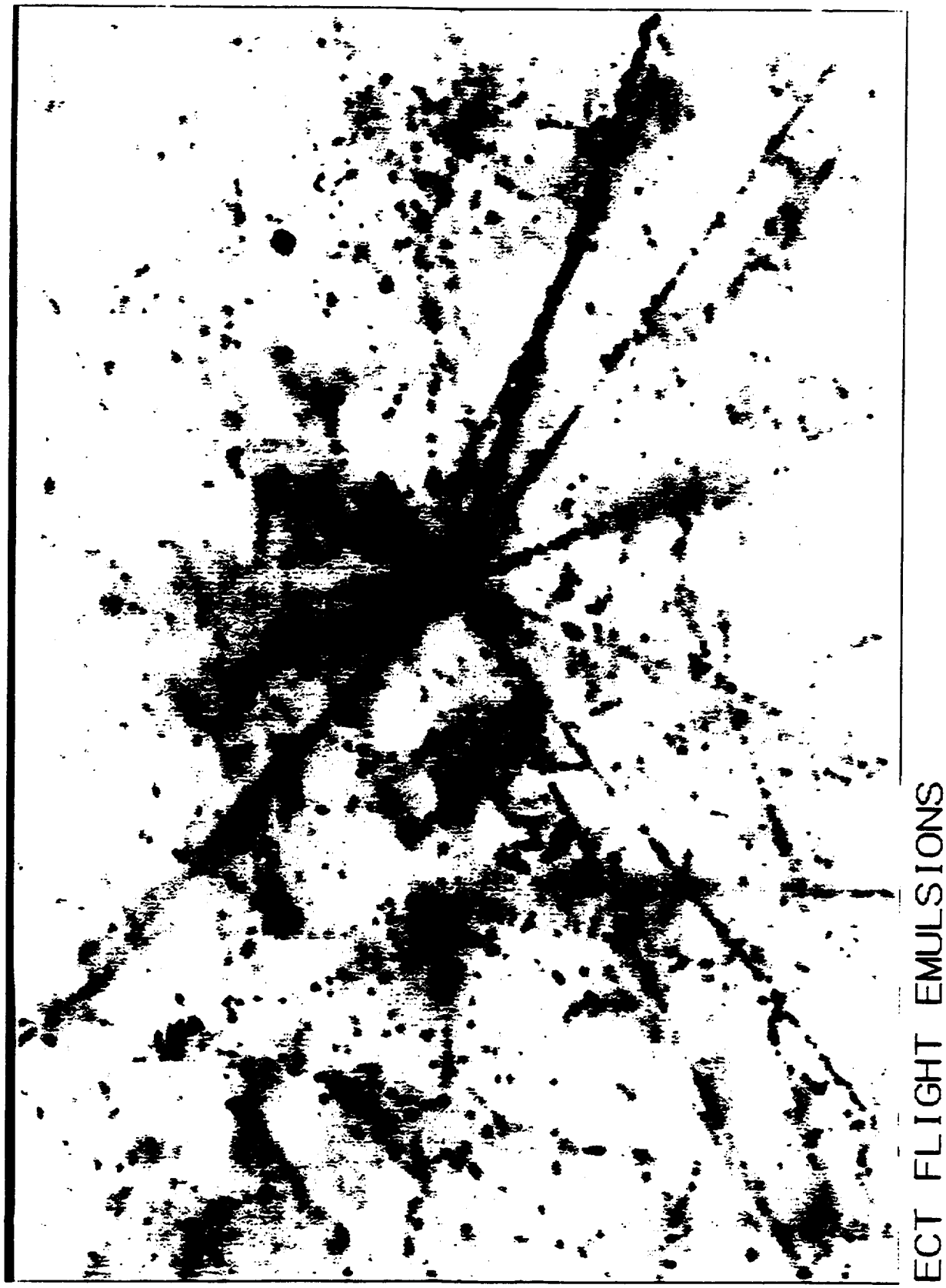


Figure 22

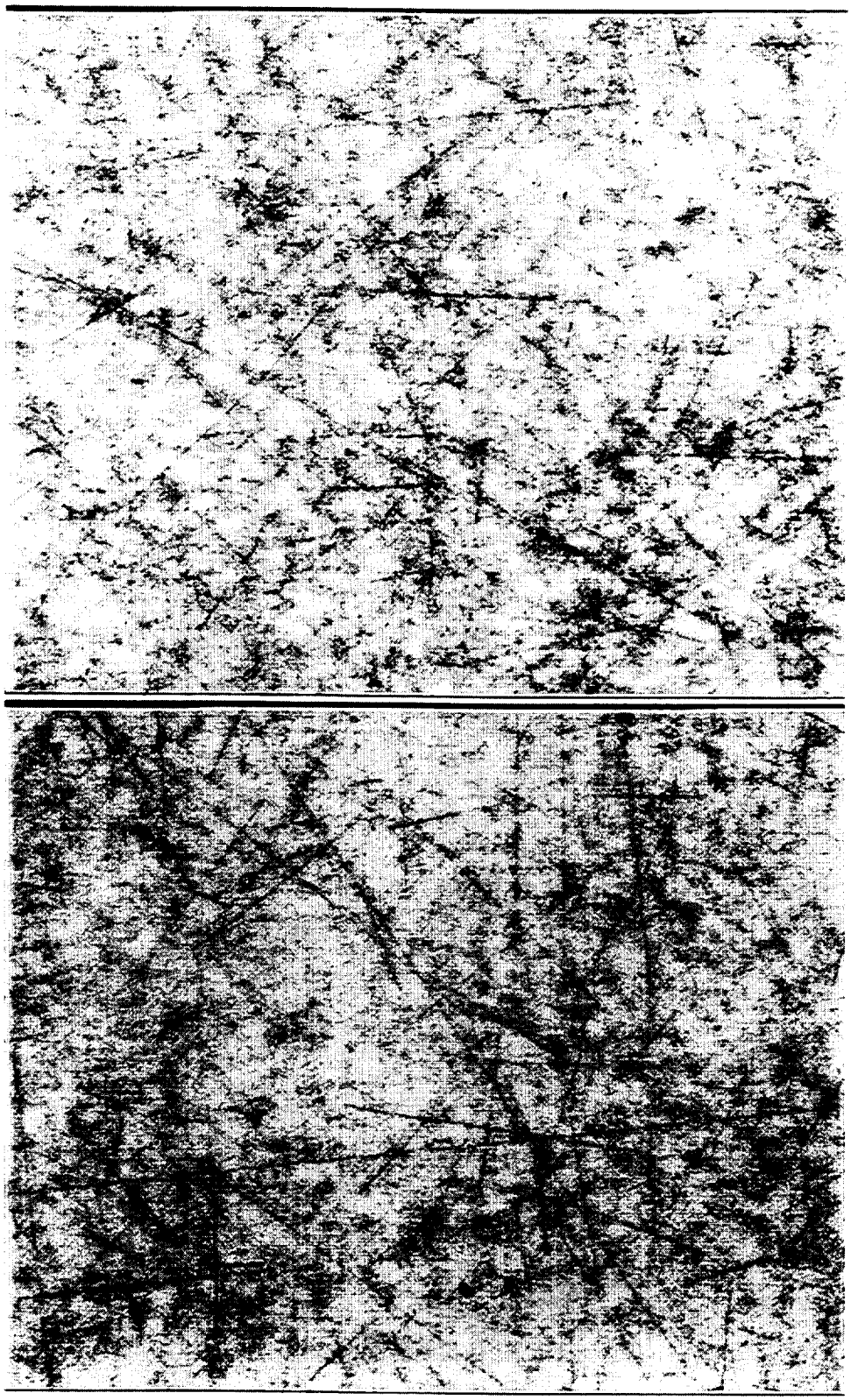

ECT FLIGHT(TOP)  LDBF(BOTTOM)

Figure 23

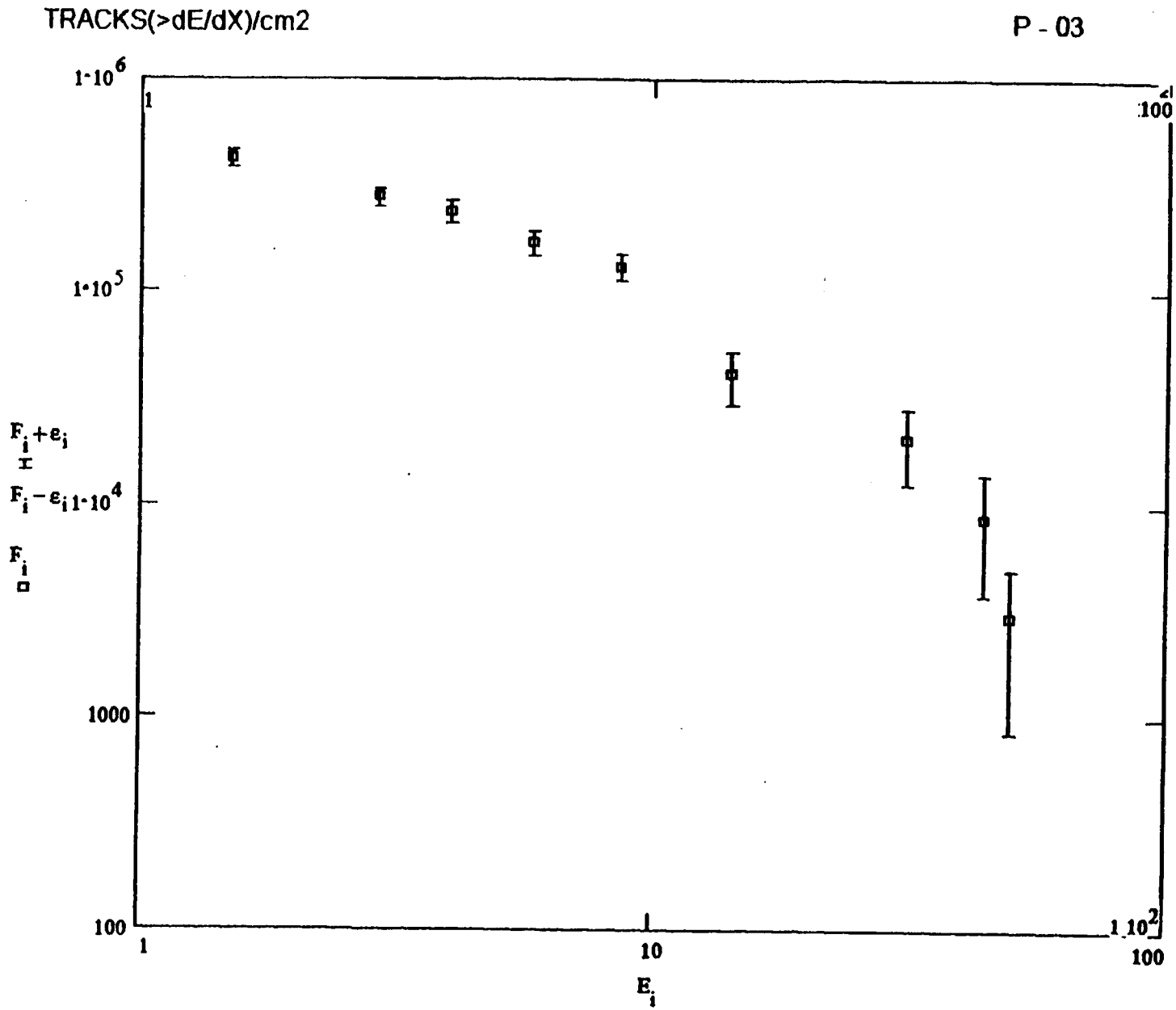


Figure 24a Integral Linear Energy Transfer Spectrum in the emulsion plate located 1.4 g/cm2 from the top of ECT chamber

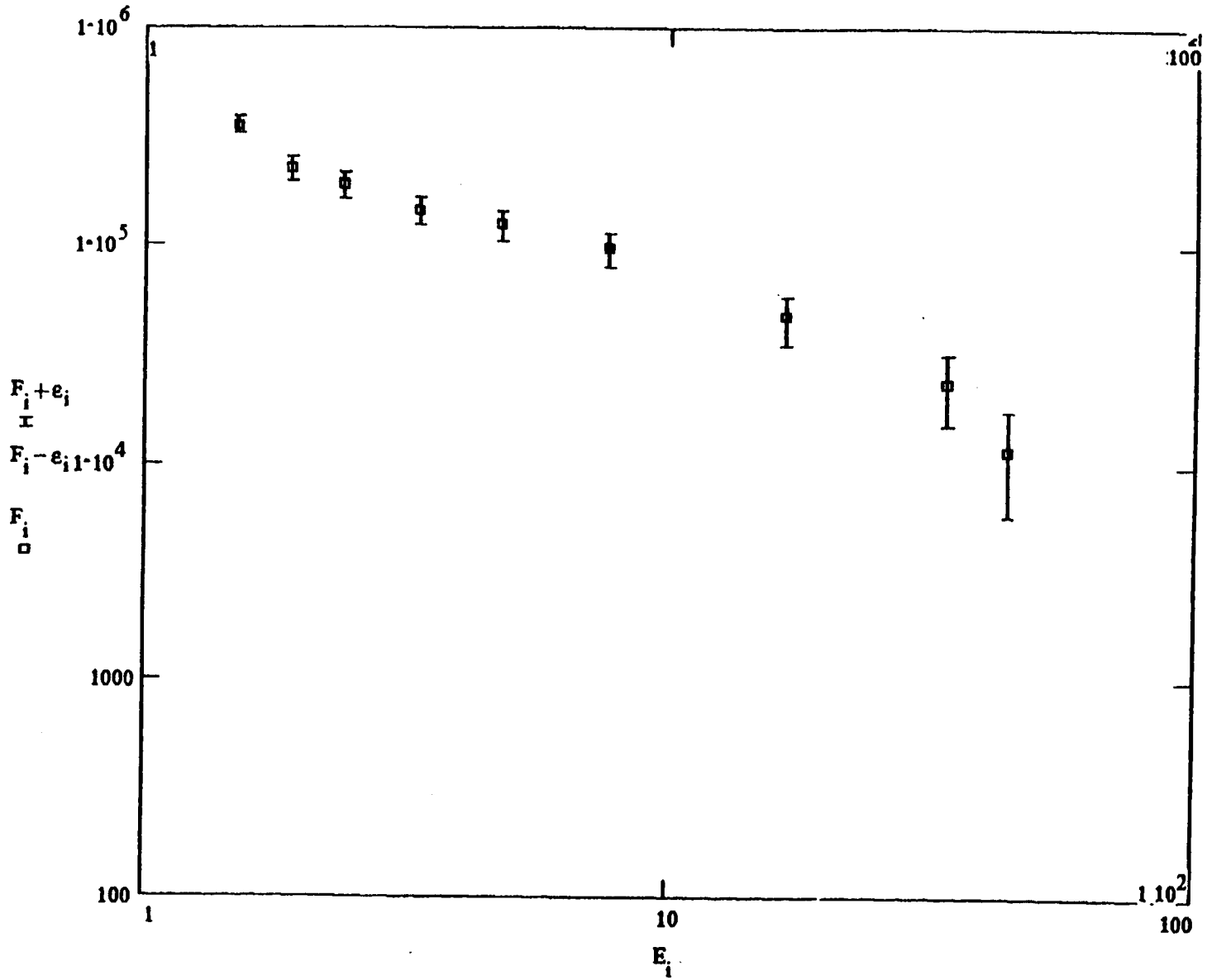


Figure 24-b

Integral Linear Energy Transfer Spectrum in the emulsion plate located 16.7 g/cm2 from the top of ECT chamber

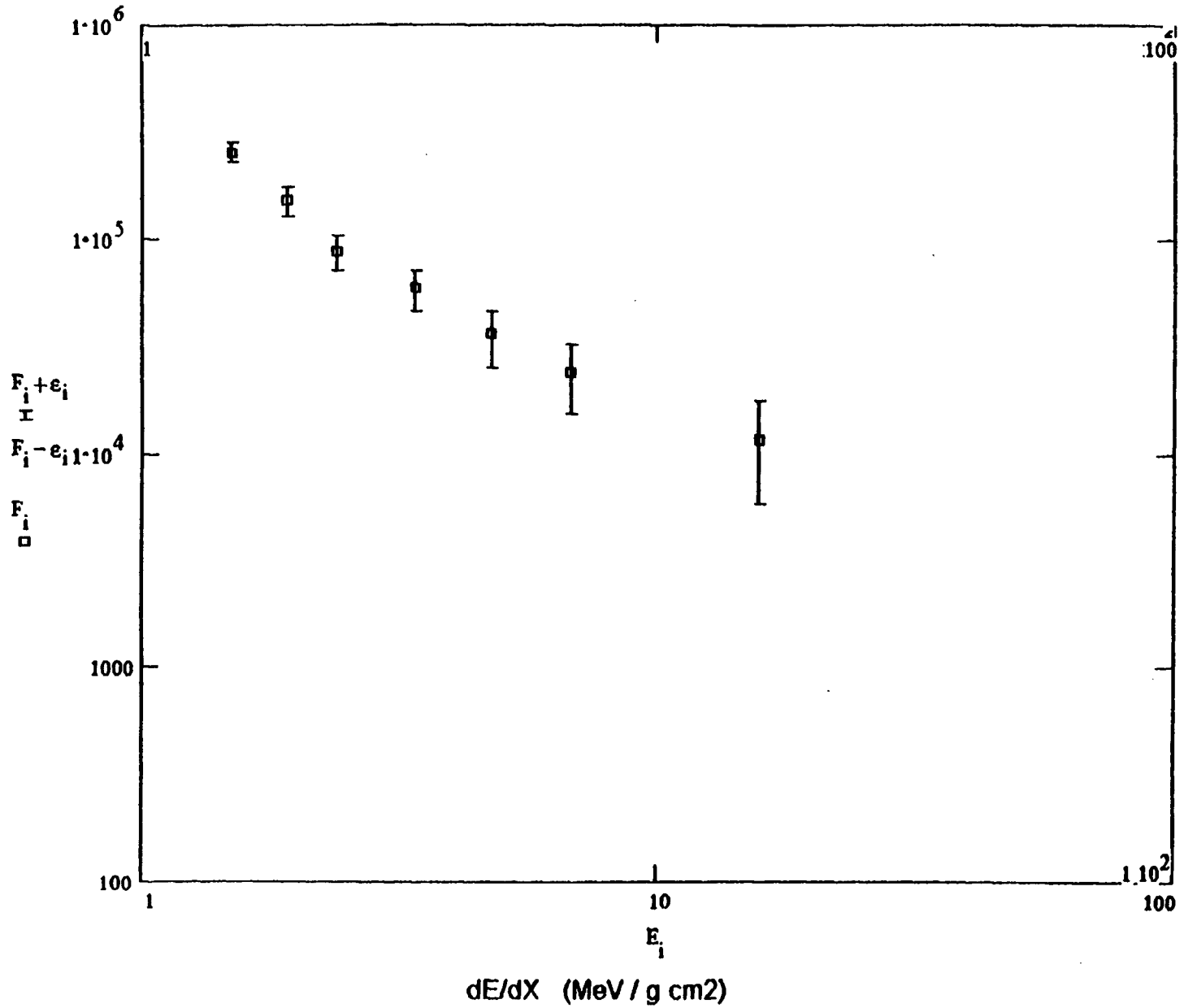


Figure 24-c Integral Linear Energy Transfer Spectrum in the emulsion plate located 94.5 g/cm2 from the top of ECT chamber

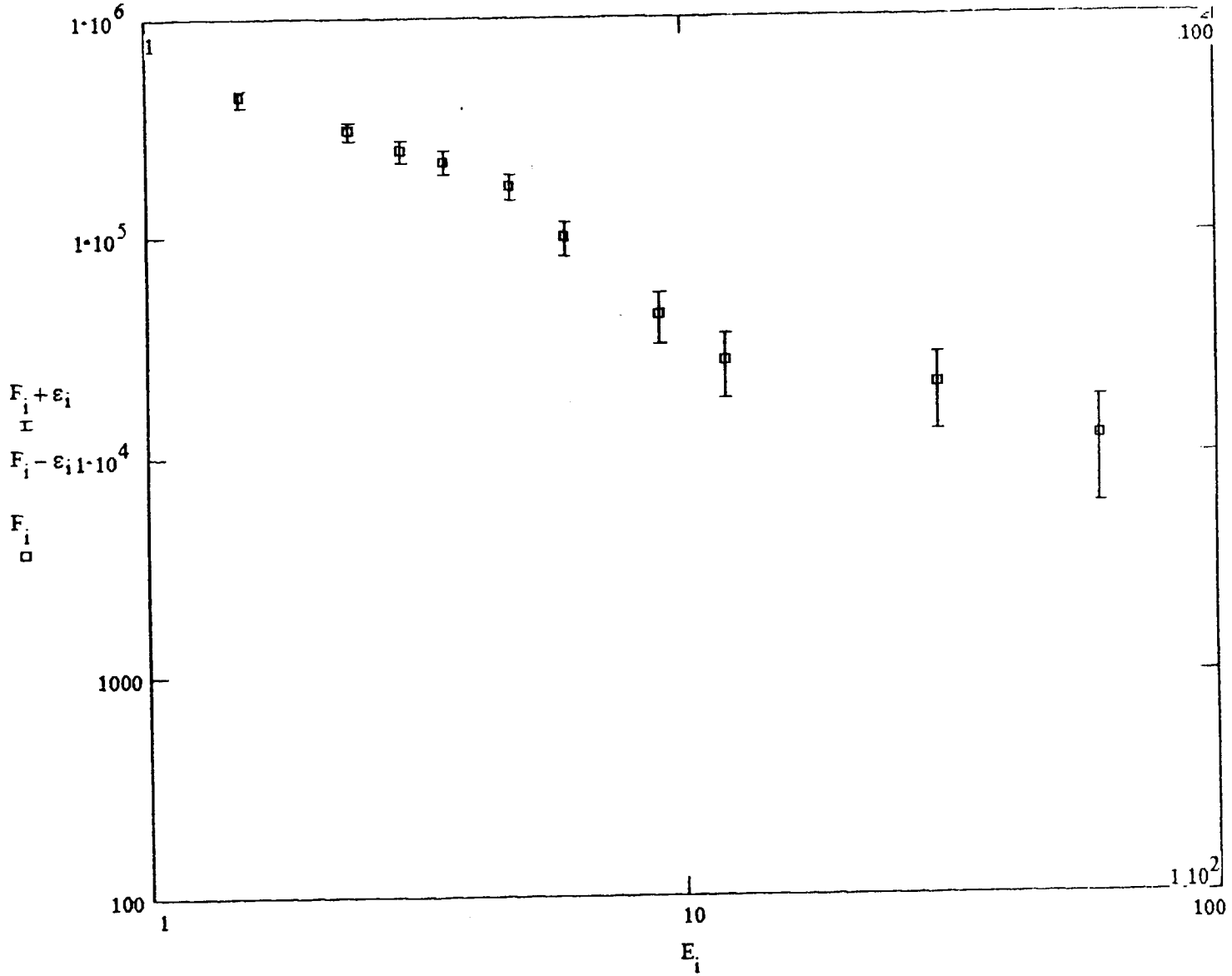


Figure 24d Integral Linear Energy Transfer Spectrum in the emulsion plate located about 1.5 g/cm2 from the top of JACEE chamber

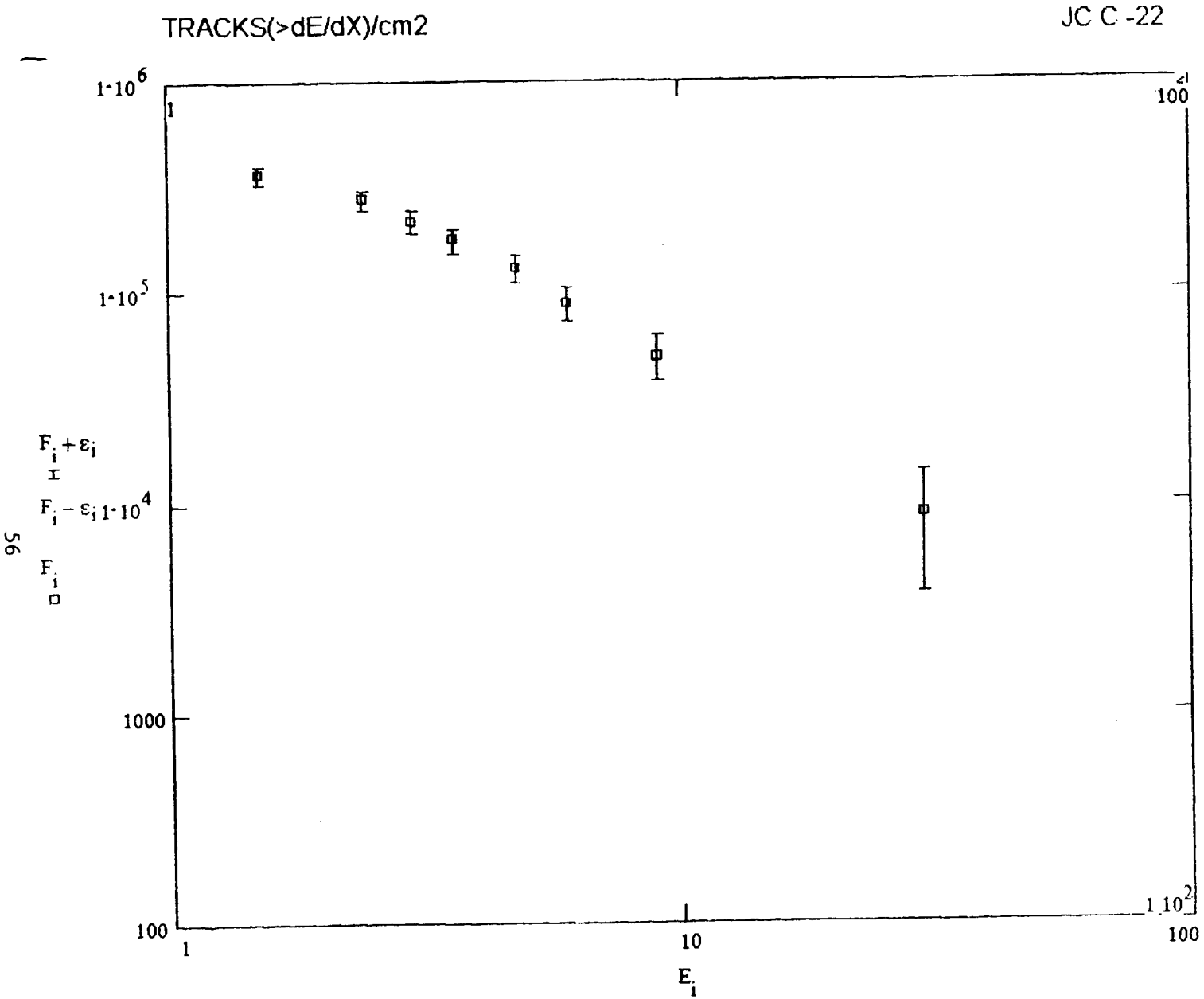


Figure 24e

Integral Linear Energy Transfer Spectrum
in the emulsion plate located about 70 g/cm2
from the top of JACEE chamber

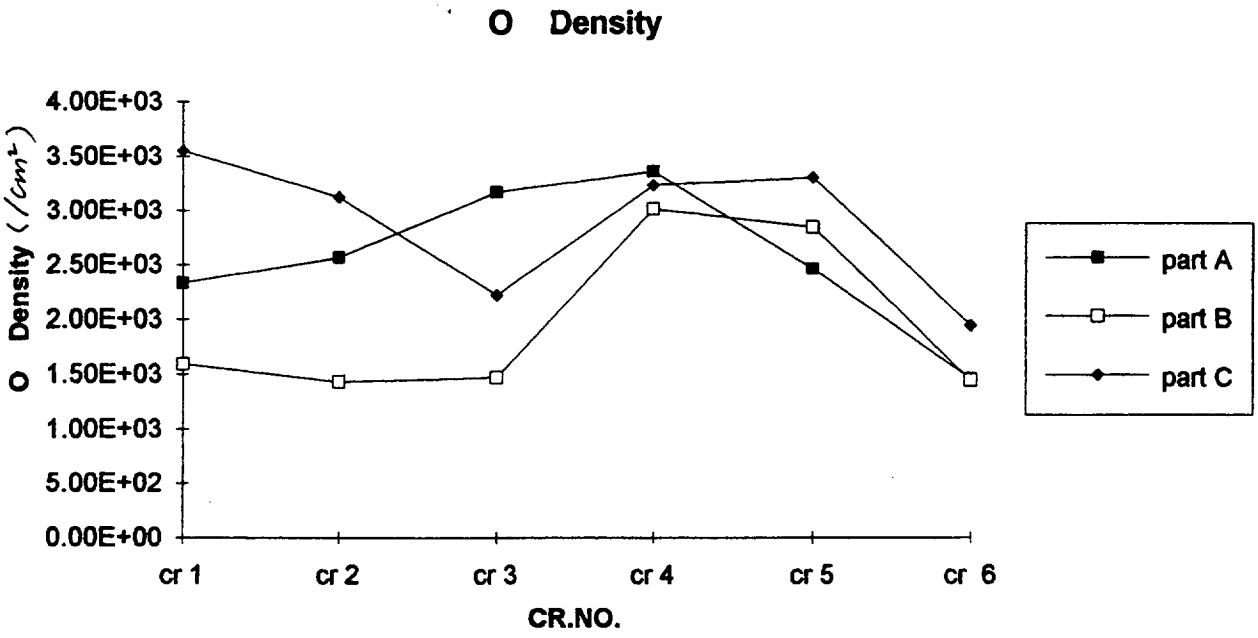
O Density
4.00E+03
3.50E+03
3.00E+03
2.50E+03
2.00E+03
1.50E+03
1.00E+03
5.00E+02
0.00E+00
O Density (/cm²)
cr 1
cr 2
cr 3
cr 4
cr 5
cr 6
CR.NO.
part A
part B
part C

Figure 25a

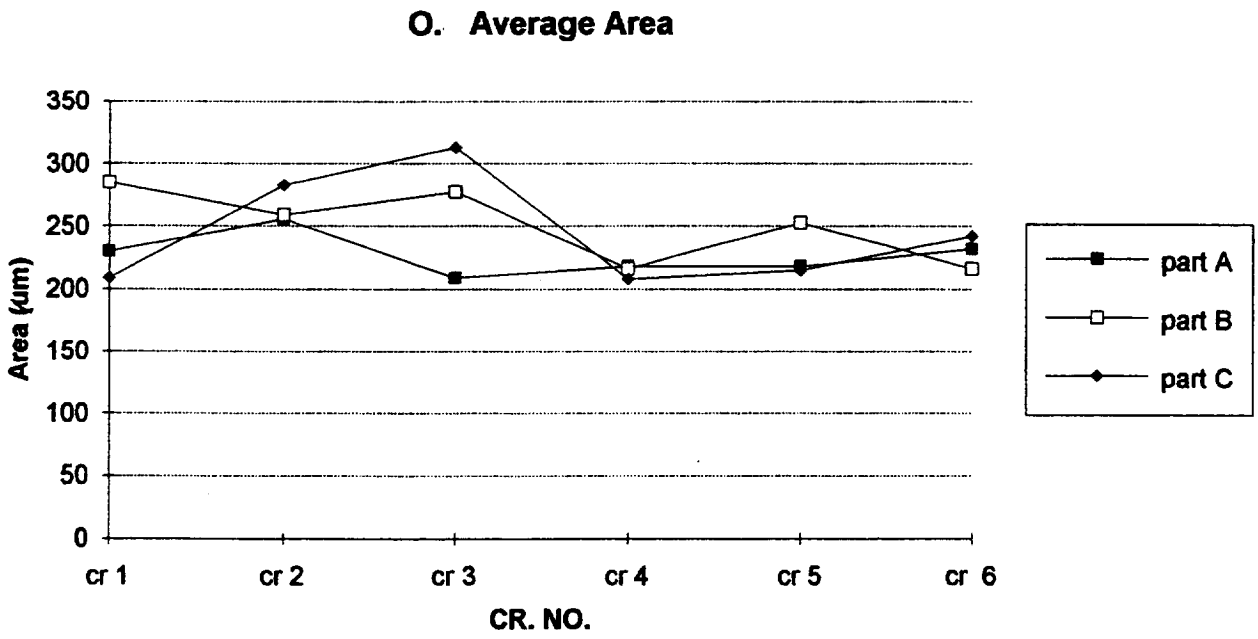
O. Average Area
350
300
250
200
150
100
50
0
Area (µm)
cr 1
cr 2
cr 3
cr 4
cr 5
cr 6
CR. NO.
part A
part B
part C

Figure 25b

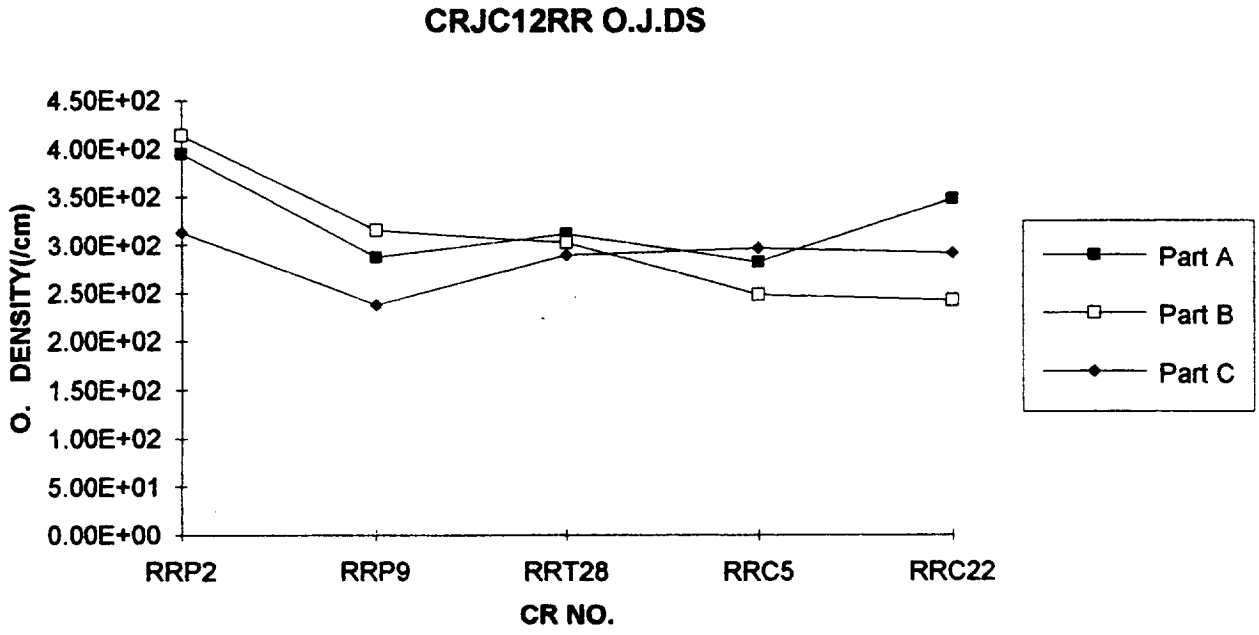
CRJC12RR O.J.DS
4.50E+02
4.00E+02
3.50E+02
3.00E+02
2.50E+02
2.00E+02
1.50E+02
1.00E+02
5.00E+01
0.00E+00
O. DENSITY(/cm)
RRP2
RRP9
RRT28
RRC5
RRC22
CR NO.
Part A
Part B
Part C

Figure 26a

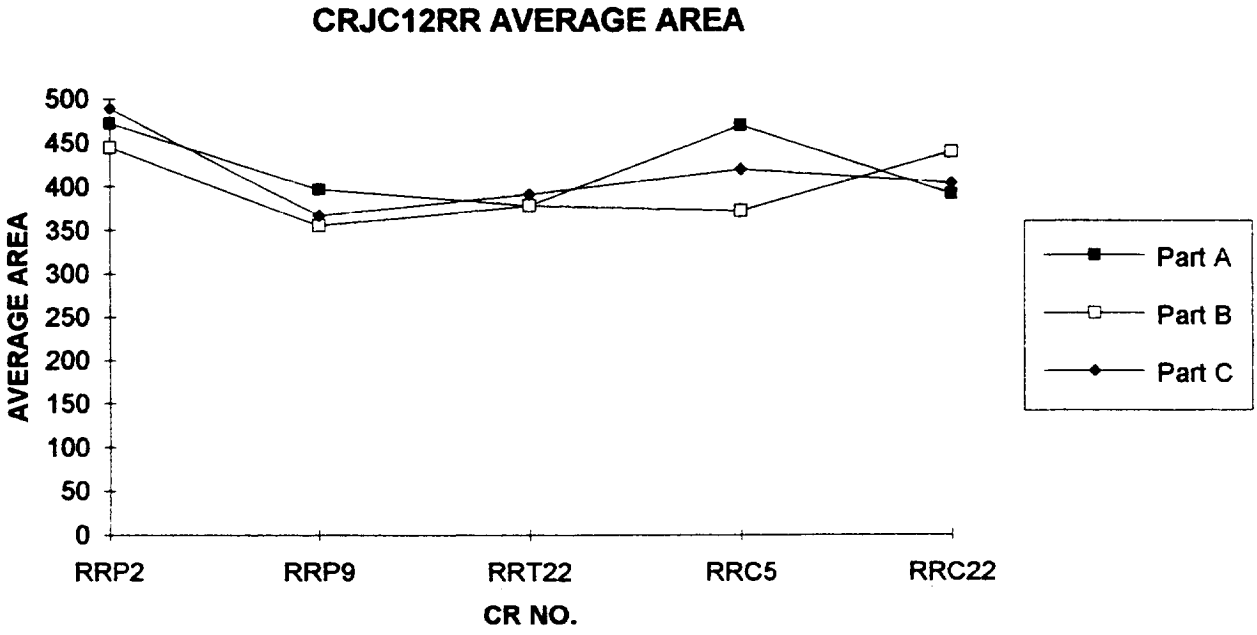
CRJC12RR AVERAGE AREA
AVERAGE AREA
500
450
400
350
300
250
200
150
100
50
0
RRP2
RRP9
RRT22
RRC5
RRC22
CR NO.
Part A
Part B
Part C

Figure 26b

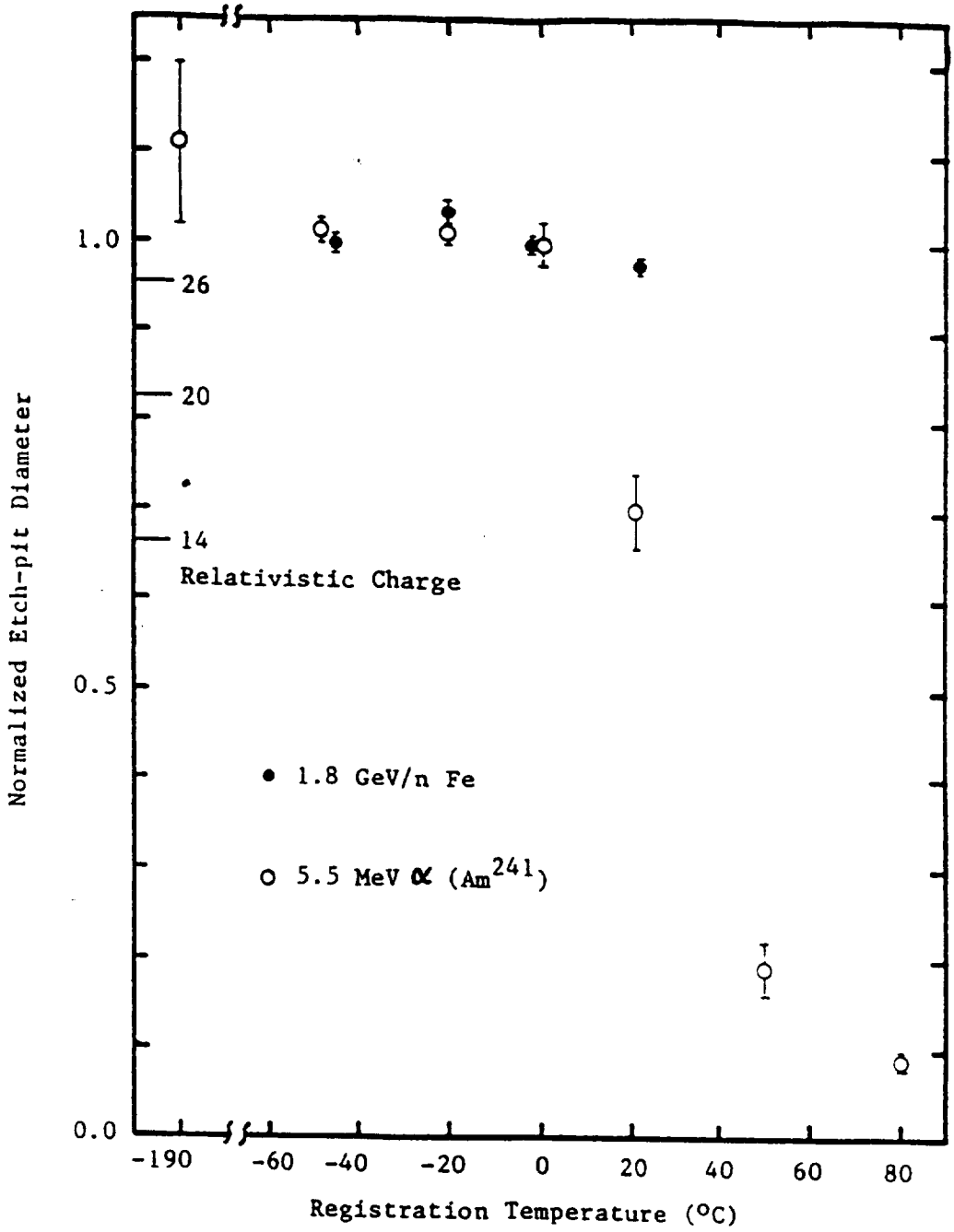
Normalized Etch-pit Diameter
1.0
0.5
0.0
26
20
14
Relativistic Charge
• 1.8 GeV/n Fe
o 5.5 MeV α (Am241)
-190
-60
-40
-20
0
20
40
60
80
Registration Temperature (°C)

Figure 27

# APPENDIX A

ECT Dosimetery Report: LET Spectra,
Absorbed Doses and Neutron Dose Equivalents

# Measurement of LET Spectra, Absorbed Doses and Low Energy Neutron Dose Equivalents in the Emulsion Chamber Technology Experiment

## Final Report

E. V. Benton, A. L. Frank,
E. R. Benton, and L. A. Frigo

Subcontract No. SUB92-162-A4
University of Alabama in Huntsville
Huntsville, AL 35899

28 August 1995

ERIL RESEARCH, INC.
P.O. BOX 150788 - SAN RAFAEL, CA 94915-0788

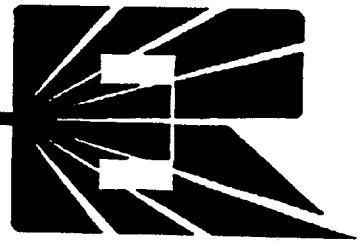

# Measurement of LET Spectra, Absorbed Doses and Low Energy Neutron Dose Equivalents in the Emulsion Chamber Technology Experiment


## Abstract

LET spectra, total absorbed dose and low energy neutron fluence and dose equivalent measurements were made at various locations throughout the Emulsion Chamber Technology (ECT) experiment. LET spectra were measured under seven different shielding depths in the vertical center of the experiment stack. The low LET (<10 keV/$\mu$m) region of the spectrum appeared to be dominated by stopping primary protons and was attenuated by the experiment shielding as measured from the lid to the base of the experiment stack. The mid (>10 keV/$\mu$m) and high (>100 keV/$\mu$m) LET regions of the spectrum appeared to be dominated by short range, high LET secondary particles produced in interactions between high energy protons and the nuclei of the experiment components. Only 20% of the high LET particles were long range (>600 $\mu$m) and thus considered to be galactic cosmic rays (GCR). Of this long range particles, ~80% were seen to be arriving from the direction of space (opposite Earth) and were stopping, illustrating the effect of the large amount of shielding in the ECT experiment on the GCR component. Little difference was seen in the overall integral LET flux spectra as a function of shielding.

Total absorbed dose was measured in TLDs at nine locations across the surface of each of the seven CR-39 PNTD pairs. Dose was seen to decrease as a function of shielding as measured from the top of the experiment stack. A mean dose of 238 $\pm$ 3 mrad was measured under 1.19 g/cm$^2$, while a mean dose of 142 $\pm$ 1 mrad was measured under 94.91 g/cm$^2$. There was little variation in dose amongst the different TLD locations across a given PNTD pair with the exception of PNTD Position 5. Dose through the experiment stack at Position 5 was substantially greater than that measured in other TLD positions, most likely due to the shielding environment surrounding the experiment and the orientation of the spacecraft relative to the South Atlantic Anomaly (SAA) during much of the mission.

Thermal (<0.2 eV) and Resonance (0.2 eV–1 MeV) neutron dose equivalents were measured at three locations within the experiment stack. A thermal dose equivalent of 0.30 $\pm$ 0.0 mrem and resonance dose equivalent of 11.3 $\pm$ 5.6 mrem were measured under the maximum shielding of 94.91 g/cm$^2$. Maximum thermal and resonance neutron dose equivalents of 0.79 $\pm$ 0.16 and 39 $\pm$ 19 mrem, respectively, were measured in the middle of the stack under 41.84 g/cm$^2$. This was substantially higher than similar measurements made under lower shielding in previous STS missions, demonstrating the effect of shielding as a neutron moderator and thermalizer.

# Contents

# 1 Introduction

The Emulsion Chamber Technology (ECT) experiment consisted of a thick stack of radiation sensitive materials including nuclear emulsion, x-ray film, and CR-39 plastic nuclear track detector (PNTD). Interspersed within the experiment stack were seven doublets of CR-39 to measure the LET spectra above ~5 keV/$\mu$m. Arrayed inside each CR-39 doublet were Thermoluminescent Detectors (TLDs) to measure total absorbed dose. Also included in three locations within the experiment were neutron detectors to measure thermal (<0.2 eV) and resonance (0.2 eV–1 MeV) neutron fluences and dose equivalents.

The ECT experiment flew in the cargo bay of the Space Shuttle on the STS-62 mission. STS-62 was launched on 4 March 1994 at 7:53 A.M. Central Standard Time. The mission lasted a total of 335.27 hours or 13.969 days. STS-62 had a mean altitude of 296 km and an orbital inclination of 39.0°. STS-62 was an Earth observation mission and the cargo bay was open toward the Earth, placing the bulk of the orbiter between the ECT experiment and space.

Exposure to ionizing radiation can be analyzed in terms of energy spectra or Linear Energy Transfer (LET) spectra. The LET of a particle is a measure of the change in the energy of the particle per unit path length and varies inversely with the energy of the particle. A particle's LET is believed to be of greater relevance than its energy in terms of significance to radiation sensitive materials and components and to radiobiology since LET is a measure of energy transferred to the surrounding medium through which the particle is traveling. CR-39 PNTDs measure the fluence (particle density per unit area, solid angle) and the LET of ionizing radiation of $LET_{\infty}$·$H_2O$ $\geq$5 keV/$\mu$m. Fluence and LET measurements can be combined to produce integral fluence and dose LET spectra. The fluence or dose from particles greater than a given LET on the $y$-axis is plotted as a function of LET on the $x$-axis. TLDs measure total absorbed dose directly and measurements are presented in units of mrad. Since TLDs are not capable of recording LET, it is not possible to convert the dose to dose equivalent.

The altitude and inclination of the spacecraft orbit affects the relative contribution of the different radiation components to the total dose. For low inclination orbits (28.5°) above

~300 km, the major source of dose will be from trapped protons in the South Atlantic Anomaly (SAA). A low altitude, higher inclination space shuttle mission, (~300 km) at 39.0° inclination, such as STS-62 will receive a lower dose from trapped protons in the SAA than will lower inclination (28.5°) missions. Exposure to trapped protons can be seen in LET spectra measurements as stopping primary protons in the low (<10 keV/$\mu$m) LET region and as short range, high LET secondary particles in the mid (>10 keV/$\mu$m) and high (>100 keV/$\mu$m) regions. Relative and absolute contributions from GCR are functions of orbital inclination with polar orbits receiving the greatest GCR contribution and equatorial orbits receiving a smaller GCR contribution. High inclination, lower altitude orbits for the space shuttle (57°) receive the major contribution to total dose from GCR. However, the orbital inclination of STS-62 (39.0°) is high enough to allow GCR to make a significant contribution to dose and LET spectra.

# 2 Experiment

## 2.1 Assembly of Experiment

The CR-39 layers to be included in the ECT experiment were cut to dimensions of 49.8 × 39.8 cm$^2$. Thirteen (13) detector squares of 3×3 cm$^2$ were cut into the larger sheets. These squares were used to measure LET spectra following the experiment. A portion of one edge of each of the squares was left uncut so that the square detector would remain attached to the larger sheet during the experiment. Twenty-seven (27) circles of 0.5 cm diameter were also cut into the detector sheets to accommodate TLDs. Figure 1 shows the location of the LET spectra squares and the TLDs. Each square was numbered as to location in the larger sheet. The three TLDs nearest each numbered square share that number. A unique identifying detector number, of the form ESS-NN, was scribed into each square in the lower right-hand corner opposite the uncut edge. Figure 2 shows the numbering convention for each PNTD square. E stands for ECT, SS denotes the number of the CR-39 sheet in the batch, and NN denotes the position of the PNTD square on the sheet. A number of the form ESS was scribed in the lower right hand corner of the large CR-39 sheet in order to identify it after the PNTD squares had been removed. The scribed side of each layer is the

Table 1: Composition and type of each CR-39 pair assembled for the ECT experiment.

| Top Layer Number | Bottom Layer Number | TLD |
|---|---|---|
| E04 | E01 | √ |
| E12 | E05 | √ |
| E15 | E14 | √ |
| E19 | E20 | √ |
| E21 | E24 | √ |
| E33 | E25 | √ |
| E35 | E39 | √ |
| E16 | E-C | |
| E30 | E38 | |

top side.

The CR-39 sheets were assembled into pairs. The polyethylene protective layers were removed from each CR-39 surface. A layer of 8 $\mu$m kimfoil (polycarbonate) was placed between the two CR-39 layers of the pair as a separator. The layers were carefully aligned so that the PNTD squares would line up with each other in the two CR-39 sheets. The layers were secured together around the edges of the CR-39 sheets with 6 mil Teflon (3M) tape. Additional Teflon tape was placed around the perimeter of the TLD holes in order to keep the two sheets from buckling. A TLD-700 ($^7$LiF) chip was placed in each of the TLD holes. The TLD chips were covered with Whatman filter paper and taped into place with Teflon tape. The finished detector assembly was then covered in a protective layer of 25 $\mu$m thick polycarbonate foil. Nine (9) CR-39 pairs were assembled, seven (7) with TLDs and two (2) without TLDs. Table 1 lists the sheet number and assembly type of each of the CR-39 pairs.

Thermal and Resonance Neutron Detectors (TRNDs) consisting of layers of CR-39 PNTD and $^6$LiF were assembled for inclusion in the ECT experiment. The TRNDs are roughly 1/2"×1/2" and are ~3 mm in thickness. TRNDs were assembled in pairs with one being covered with a layer of Gd foil neutron absorber. The TRND pairs are covered on both sides by a layer of Whatman filter paper and are labeled. Three (3) flight and one (1) ground control TRND were assembled. Table 2 shows the contents and label of each TRND pair.

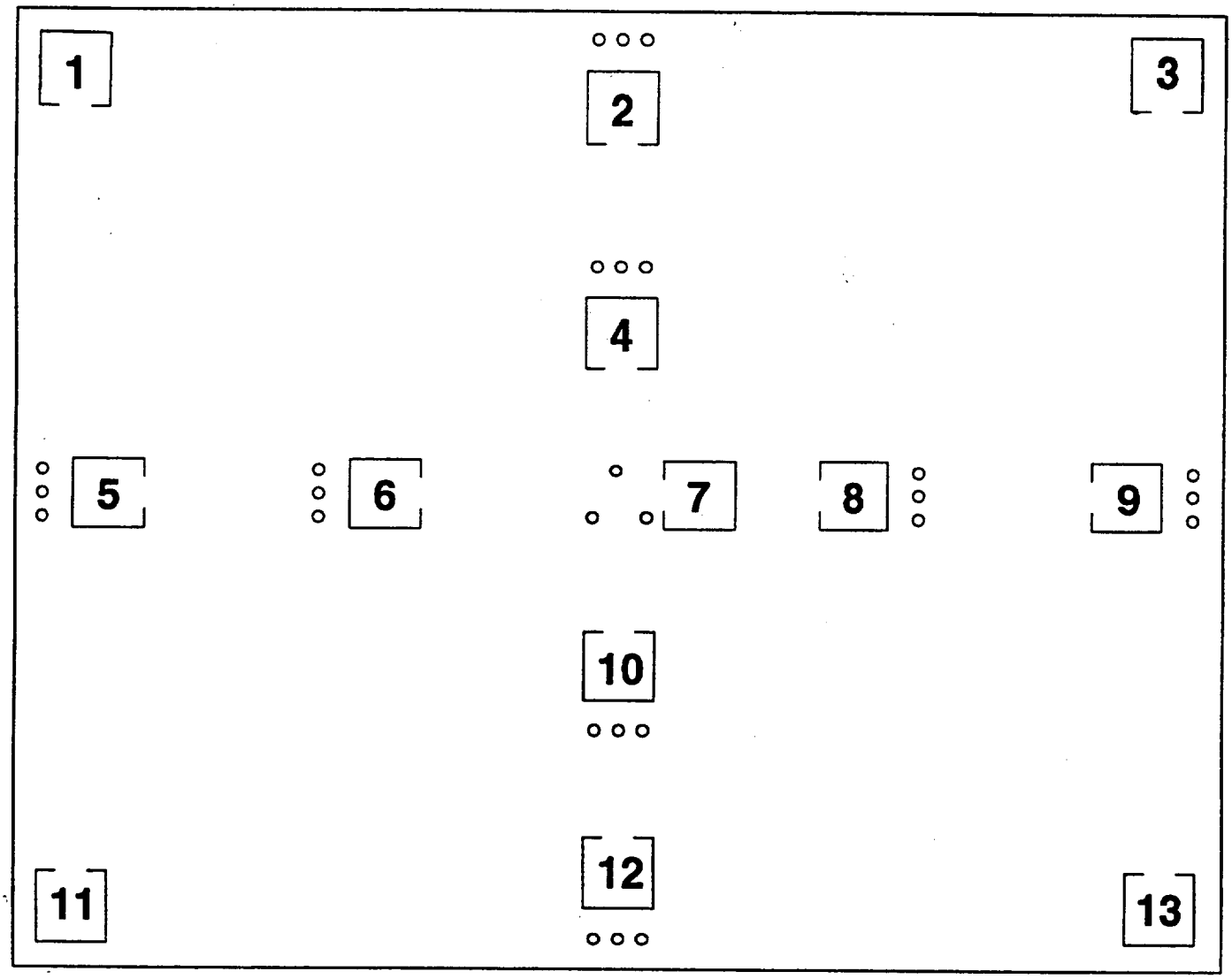


Figure 1: Positions of the CR-39 cut-outs and TLDs on the surface of the large CR-39 detector pairs.

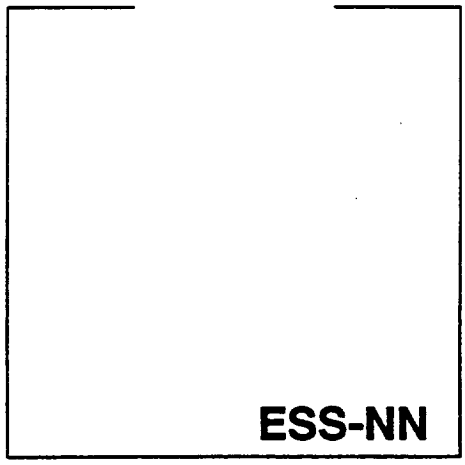


Figure 2: Numbering convention for CR-39 PNTD cut-outs. E stands for ECT, SS is the number of the CR-39 sheet, and NN is the position of the detector in the sheet.

Table 2: Thermal and Resonance Neutron Detectors (TRNDs) to be included in the ECT experiment.

| Pair | Type | Gd foil |
|---|---|---|
| A1,A2 | flight | A1 |
| B1,B2 | flight | B1 |
| C1,C2 | flight | C1 |
| D1,D2 | ground | D1 |

Table 3: Shielding of CR-39 and TLD layers relative to the normal of the detector stack. Shielding is measured relative to both the top and the bottom of the experiment.

| Doublet No. | Top to Bottom Shielding ($g/cm^2$) | Bottom to Top Shielding ($g/cm^2$) |
|---|---|---|
| E33/E25 | 1.19 | 93.87 |
| E21/E24 | 8.36 | 86.70 |
| E15/E14 | 26.71 | 68.35 |
| E19/E20 | 41.84 | 53.22 |
| E34/E39 | 69.45 | 25.61 |
| E12/E05 | 87.07 | 7.99 |
| E04/E01 | 94.91 | 0.15 |

The assembled CR-39 pairs and TRNDs were then shipped to University of Alabama, Huntsville for integration into the ECT experiment. A set of 16 ground control TLDs of the same manufactured batch as those included in the CR-39 assemblies were included for control purposes along with four CR-39 pieces.

## 2.2 Shielding of the ECT Experiment

The ECT experiment consisted of a thick stack of radiation sensitive materials inside an aluminum canister and placed inside the Shuttle cargo bay. The orientation of the CR-39 sheets was normal to the orbiter vertical. Table 3 gives the shielding values of the CR-39 detectors and TLDs measured normal to the detector stack. During most of the mission, the orbiter was oriented upside-down relative to the Earth, that is the open cargo bay faced the Earth's surface. The shielding of the experiment can be measured from two origins, the top of the experiment closes to the Earth and the bottom of the experiment, closest to space. The first set of shielding values, top to bottom, are relevant in trying to understand the exposure of the experiment to low LET radiation including primary protons. The second set of shielding values, bottom to top, are of relevance in understanding the exposure of the experiment to GCR, since most of the GCR arrived in the experiment stack from the space side.

# 3 LET Spectra Measurements from CR-39 PNTDs

## 3.1 Calibration of CR-39 PNTDs

The CR-39 batch manufactured for the ECT experiment needed to be calibrated in order to transform measured track data from the experimental detectors into LET information. Samples of the ECT batch of CR-39 were exposed to heavy-ion beams of known energy and LET at the Lawrence Berkeley Laboratory Bevalac accelerator and to protons and $\alpha$-particles at the University of Tokyo cyclotron. Samples of detector material were cut out of the ECT CR-39 sheets and machined into 4×4 $cm^2$ squares. These detectors were then exposed to a fluence of $\sim 2.5 \times 10^3$ particles/$cm^2$. The detectors were exposed in ambient pressure and temperature. Beam direction was normal to the detector surface.

Following exposure, the detectors were divided into two groups, one etched in a solution of 6.25 $N$ NaOH at 50°C for 168 hours and the other etched in a solution of 6.25 $N$ NaOH at 50°C for 36 hours. Bulk etch measurements were made by the loss-of-mass method. The detectors were read out using the Automated Track Analysis System. Track diameters were automatically measured in a 4 $cm^2$ region in the center of the detector. The reduced etch rate for each ion/energy pair was then calculated using the following formula:

$$V_R - 1 = \frac{1 + (d/2B)^2}{1 - (d/2B)^2} - 1, \tag{1}$$

where $d$ is the mean track diameter and $B$ is the bulk etch of the detector. A curve of the form:

$$x = a_0 + a_1 y + a_2 y^2 + a_3 y^3 + a_4 y^4, \tag{2}$$

was fitted to the calibration data points, where

$$x = \log_{10}(\mathrm{LET}_{200} \cdot \mathrm{CR} - 39) \tag{3}$$

and

$$y = \log_{10}(V_R - 1). \tag{4}$$

Separate calibration functions were determined for the 36 hour and 168 hour detectors. These calibration functions were later used to convert the measured track parameters from the flight detectors into values of LET.

## 3.2 Chemical Processing of CR-39

LET spectra was measured in CR-39 PNTDs at seven shielding depths within the ECT stack. Doublets were removed from the thirteen locations on the large CR-39 sheets. The upper sheet of each doublet was etched for 36 hours in a solution of 6.25 $N$ NaOH at 50°C. The lower sheet in each doublet was etch for 168 hours in 6.25 $N$ NaOH at 50°C. The two etching regimes were used in order to enhance tracks from two different components of the LET spectra. The values of bulk etch (thickness of material removed from each surface of the CR-39 detector by chemical processing) of detectors processed for 168 hours and 36 hours were ~40 $\mu$m and ~8 $\mu$m, respectively.

## 3.3 Analysis of Processed Detectors

LET spectra was measured in each of the two layers from the doublet in position 7 on the large CR-39 sheet. A three pass, semi-automated track analysis system was used to scan the detector surface and measure the particle tracks. During the first pass, an etched CR-39 layer was placed on the microscope stage and all the objects on the detector surface (both tracks and noise) were automatically located. During the second pass, a human operator reviewed all the detected objects, separating particle tracks from spurious noise events. Finally, during the third pass, the operator measured semi-major and semi-minor axes of each elliptical track opening. The measured track parameters were converted to the unitless reduced etch rate ratio, $V_R$, by:

$$V_R = \sqrt{1 + \frac{4(a/B)^2}{[1-(b/B)^2]^2}}, \tag{5}$$

where $a$ and $b$ are the semi-major and semi-minor axes of the track surface openings and $B$ is the bulk etch of the detector. Values of $V_R$ were converted to LET using the calibration functions determined for the specific manufactured batch of CR-39 employed in the ECT experiment. Separate calibration functions were used for the 168 and 36 hour etches.

## 3.4 Generation of LET Spectra

Two etching regimes were used in order to enhance tracks produced by particles belonging to different components of the LET spectra. The 168 hour etch allows low LET tracks to become sufficiently large to be easily located and measured. However, the long etch period over-etches tracks produced by short-range, high-LET secondaries. The 36 hour etch permits short-range, high-LET secondary particle tracks to be measured since these tracks are not over-etched during the short etch period. Low LET tracks are too small to be easily measured using such a short etch time.

The LET spectra for each layer of the doublet was determined separately. The spectra for the two etch durations were then combined to create a total LET spectrum. Figure 3 shows the integral LET flux spectra measured in the two detectors of the E04/E01 doublet for the 36 hour etch, the 168 hour etch and the combined spectra. At low LETs, there is little difference between the 168 hour spectrum and the combined spectra, while at high LETs, the 36 hour spectrum is identical to the combined spectra. The 168 hour spectrum falls off more rapidly than does the 36 hour spectrum at high LETs, illustrating that the longer etch period causes some of the high LET data to be lost. This data mostly takes the form of tracks from short-range, high-LET secondary particles. These particles have ranges less than the $\sim$40 $\mu$m bulk etch produced by the 168 hour etch, and the resulting tracks are over-etched and unmeasurable after this thickness of detector is removed. The 36 hour etch only extends down to $\sim$30 keV/$\mu$m, while the 168 hour spectra extends down to $\sim$5 keV/$\mu$m, the minimum LET registration threshold in CR-39. The shorter etching regime does not provide enough time for the low LET tracks to become large enough to be readily located and measured. By combining the LET spectra for the two etch regimes, an LET spectrum covering both LET regions is obtained.

The values of uncertainty in the LET spectra have been estimated. Figure 4 shows the combined integral LET flux spectrum for detectors E04/E01 with error bars. In the low LET region ($LET_\infty \cdot H_2O \approx 10$ keV/$\mu$m) the uncertainty in the integral flux spectrum is $\sim$6%. For $LET_\infty \cdot H_2O \approx 100$ keV/$\mu$m, the integral LET flux spectrum uncertainty is $\sim$8%. At high LET ($LET_\infty \cdot H_2O \approx 500$ keV/$\mu$m), the uncertainty in integral flux spectrum is $\sim$40%. The

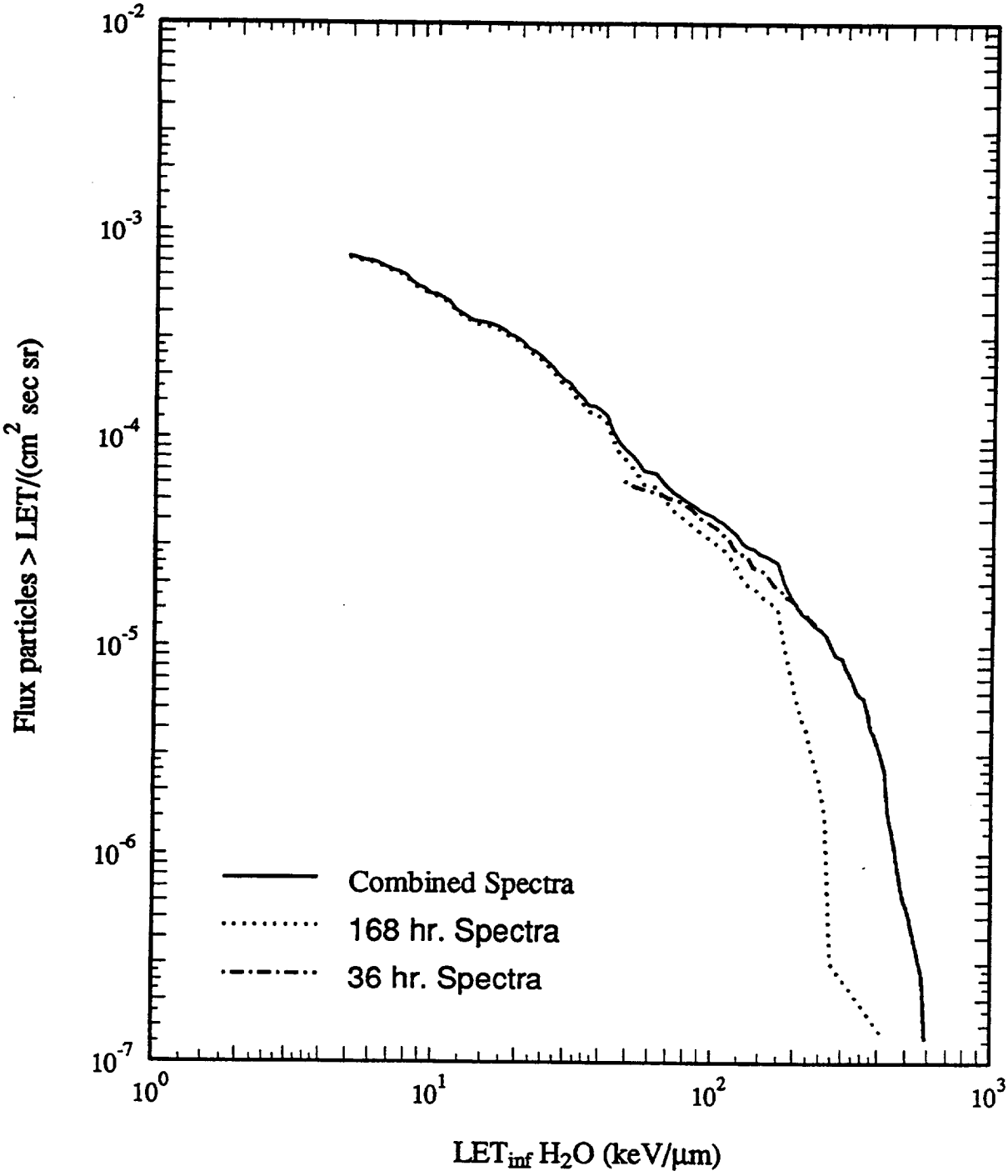


Figure 3: LET spectra measured in detector layer E01 etched for 36 hours, E04 etched for 168 hours, and E01 and E04 combined.

sizable increase in uncertainty at high LET is due to poor statistics since there are only a small number of tracks in this LET region. Values of uncertainty in integral LET flux spectra were similar for the other six measured LET spectra.

## 3.5 Results and Discussion of LET Spectra Measurements

Figure 5 shows the combined integral LET flux spectra for the seven CR-39 doublets measured for the ECT experiment. Figures 6 to 12 show separately the combined integral LET spectra for each doublet. Over most of the LET range, there is close agreement between all seven spectra within the limits of uncertainty. At low LET, the highest flux values were seen in detectors E33/E25 (Figure 6). This detector pair was closest to the lid of the experiment and was the least shielded pair from low LET particles arriving from the Earth direction. Since the cargo bay was opened toward the Earth and the layers E33/E25 were the most heavily shielded pair from particles arriving from the space (anti-Earth) direction, this detector pair had one of the lowest flux spectra in the high LET region ($LET_{\infty}$·$H_2O$>100 keV/$\mu$m). A significant fraction of the particles in the high LET region are GCR and the largest flux of GCR is expected from the space direction.

Detector pair E04/E01 (Figure 12) was at the bottom of the ECT experiment stack, closest to the floor of the cargo bay. It was the most heavily shielded detector pair from particles arriving from the Earth direction and the least shielded from particles arriving from the space direction. E04/E01 had amongst the lowest flux values in both the low and high LET regions showing the complexity of shielding effects. In addition to the shielding from the experiment stack, there is also significant shielding from the orbiter itself, especially from the floor of the cargo bay which was parallel to the experiment stack.

The highest values for LET flux spectra in the mid and high LET regions ($LET_{\infty}$·$H_2O \gtrsim 20$ keV/$\mu$m) were measured in detector pairs E15/E14 and E19/E20 (Figures 8 and 9, respectively). These detector pairs were in the middle of the experiment stack. Given the shielding of these detector pairs from the experiment stack as measured from the space-end of the experiment, plus the shielding of the orbiter, these two detector pairs were probably the most heavily shielded of the experiment. This relatively large amount of shielding probably led

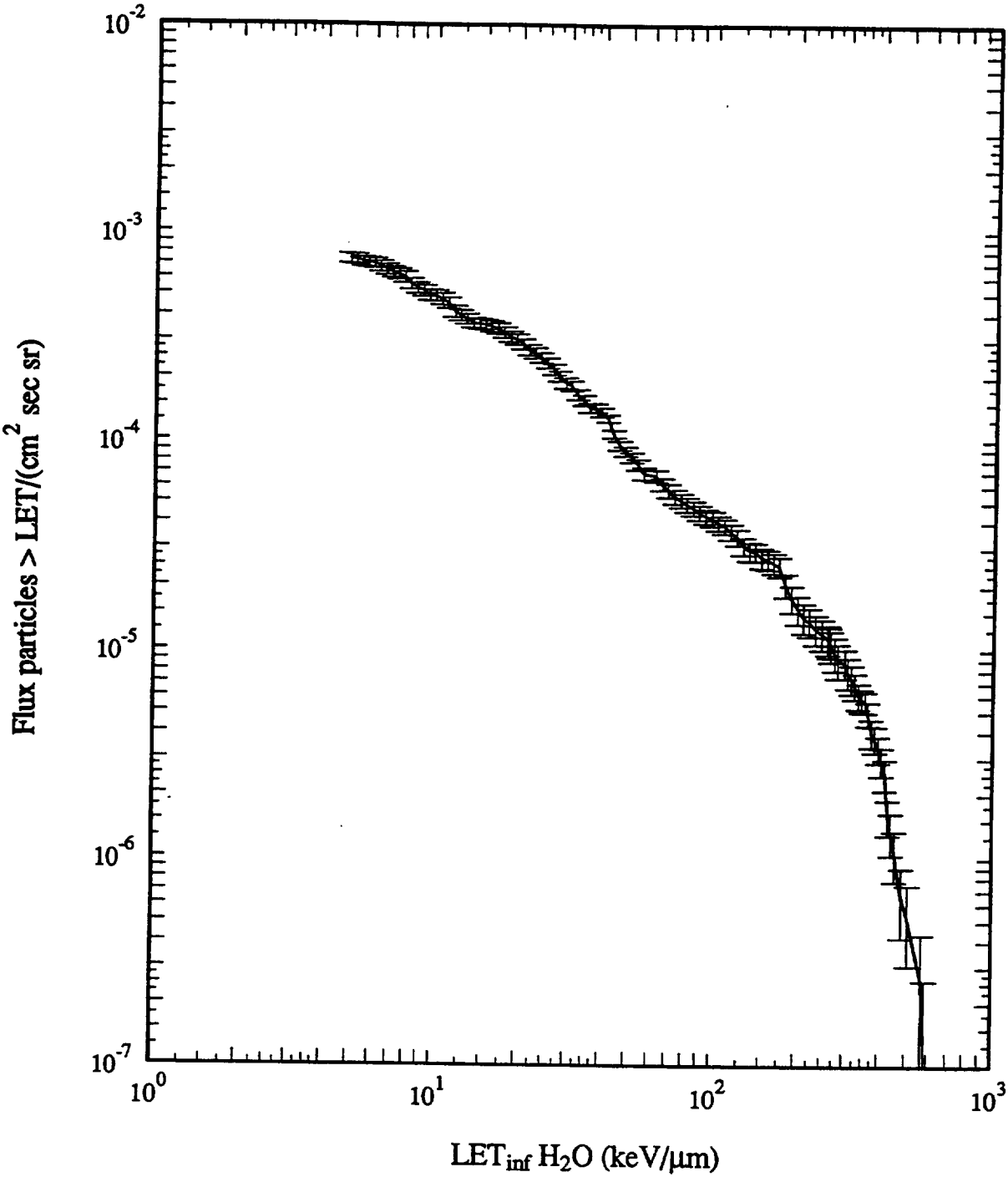


Figure 4: Combined integral LET flux spectra from detectors E04 and E01 with error bars illustrating uncertainty in the measurement. Uncertainty in the other six measured LET spectra was similar.

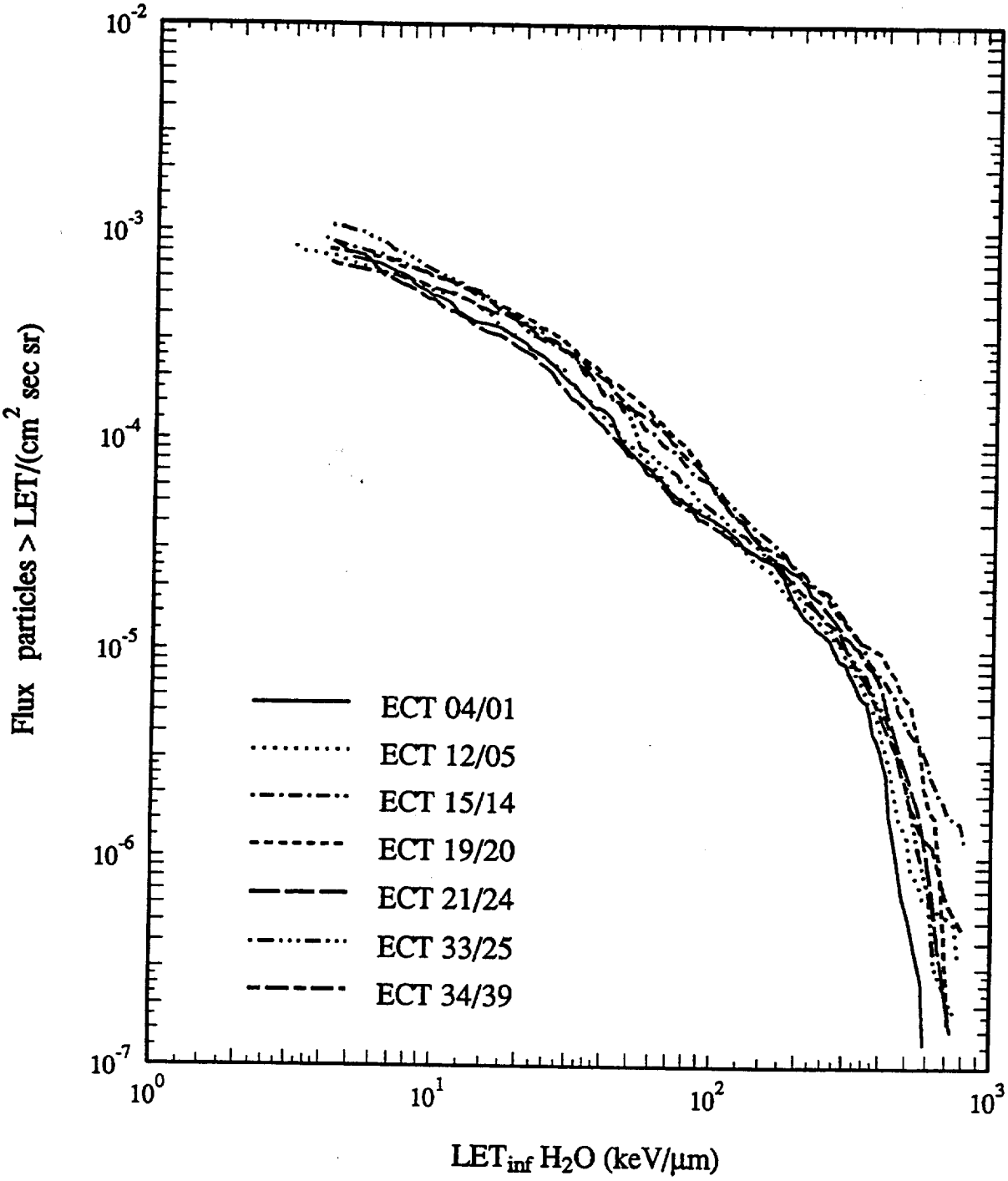


Figure 5: Combined Integral LET flux spectra for the seven CR-39 detector pairs measured in the ECT experiment.

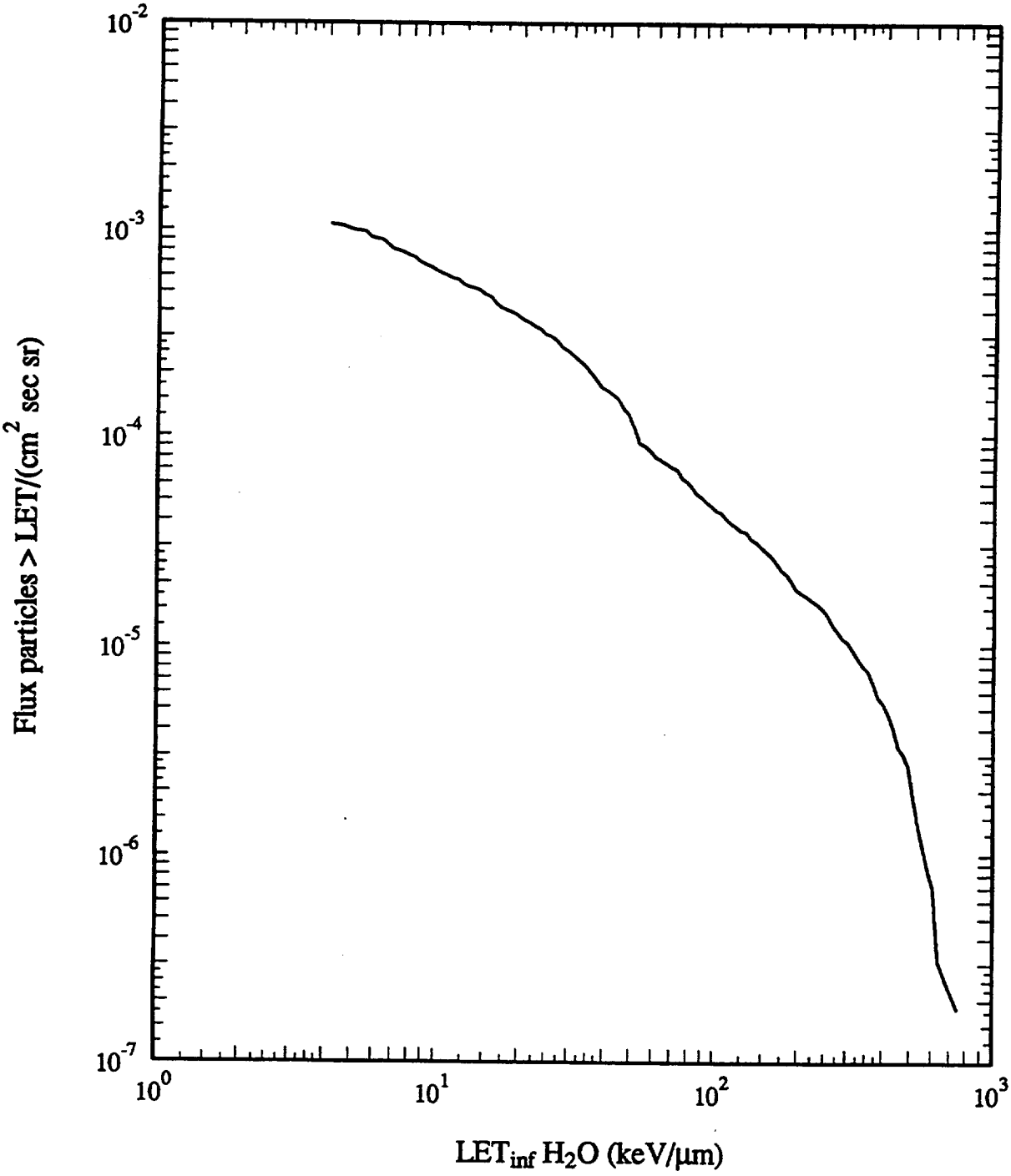


Figure 6: Combined Integral LET flux spectra for CR-39 detector pair E33/E25, under 1.19 g/cm$^2$ shielding, measured from the lid of the experiment container.

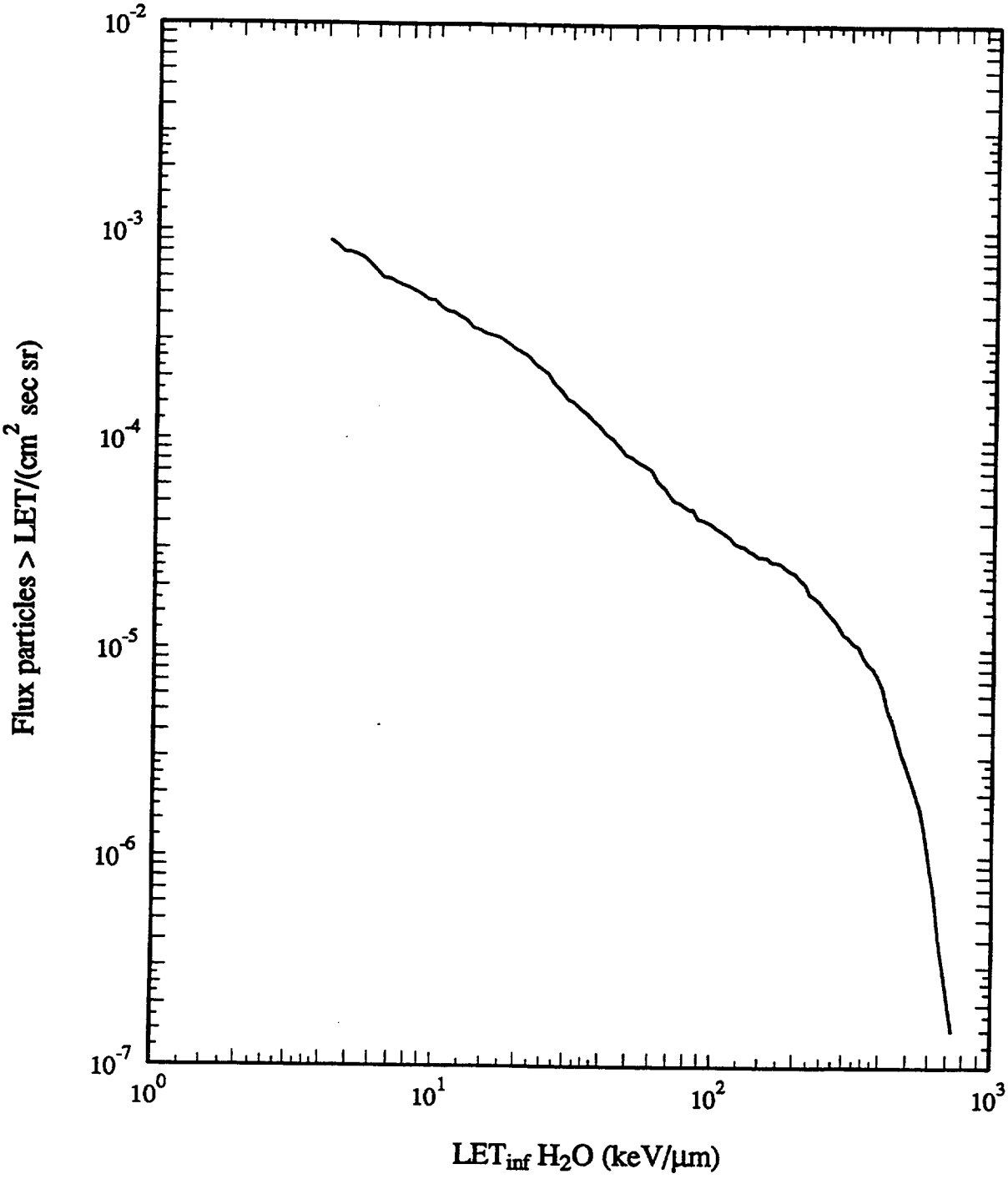


Figure 7: Combined Integral LET flux spectra for CR-39 detector pair E21/E24, under 8.36 g/cm$^2$ shielding, measured from the lid of the experiment container.

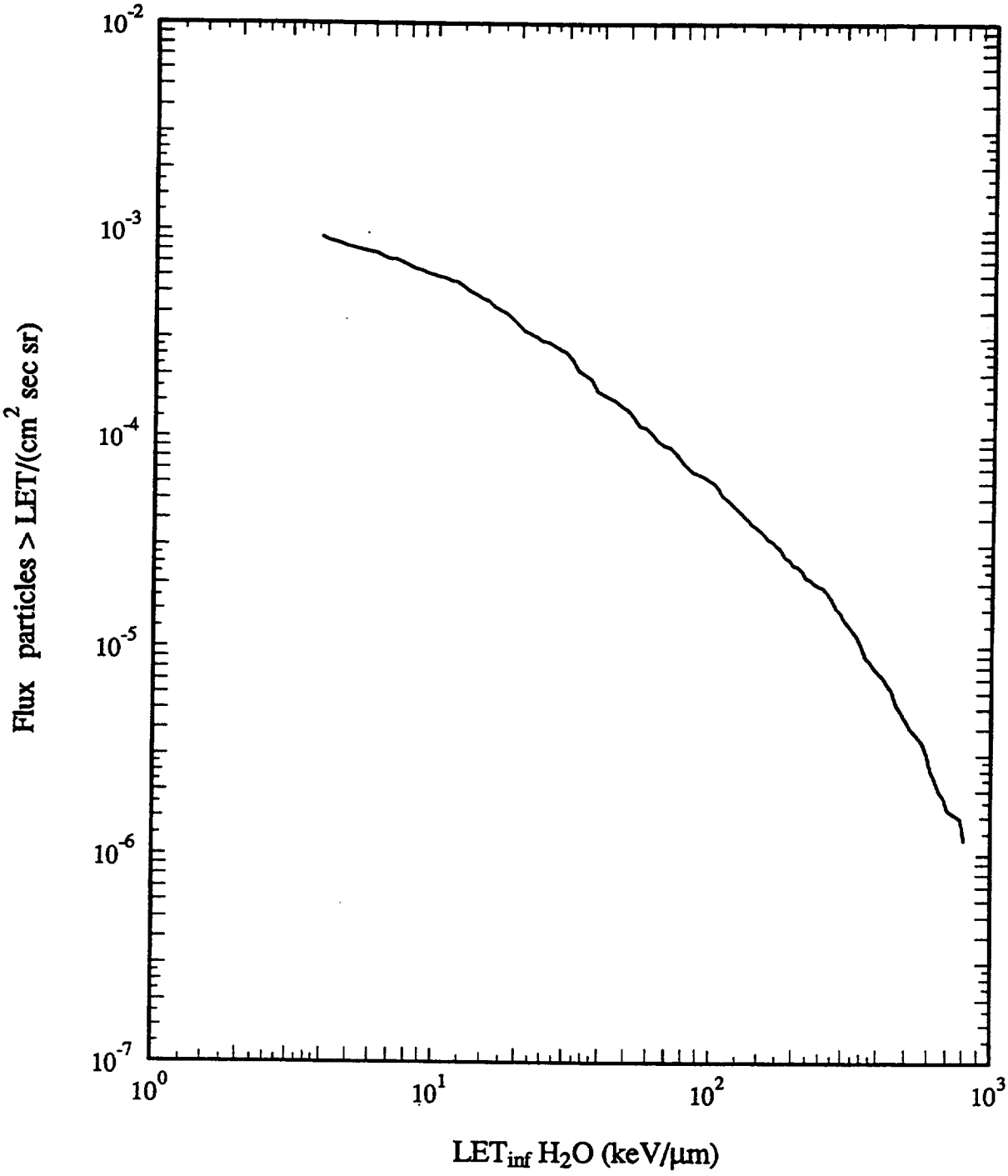


Figure 8: Combined Integral LET flux spectra for CR-39 detector pair E15/E14, under 26.71 g/cm$^2$ shielding, measured from the lid of the experiment container.

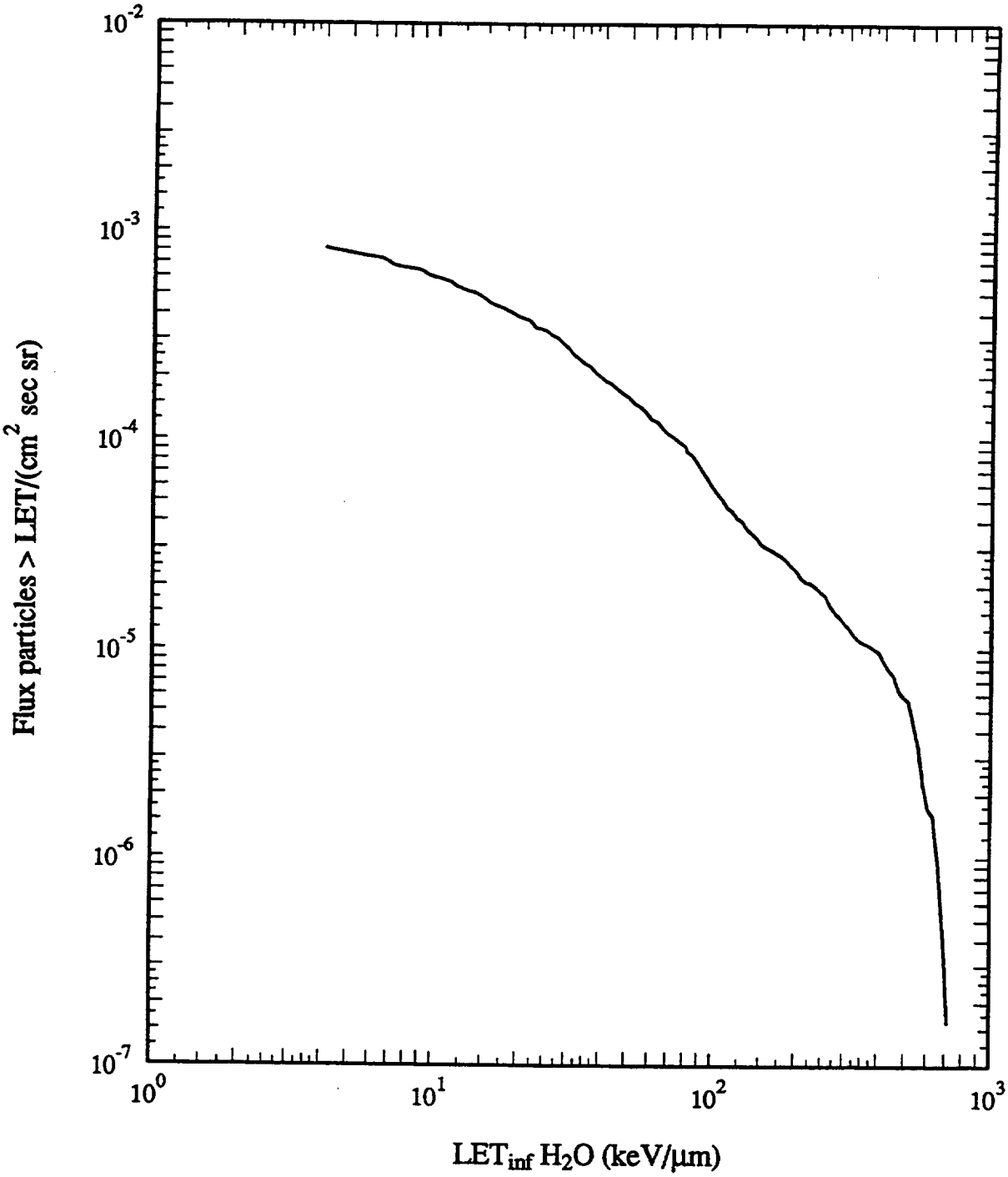


Figure 9: Combined Integral LET flux spectra for CR-39 detector pair E19/E20, under 41.84 g/cm$^2$ shielding, measured from the lid of the experiment container.

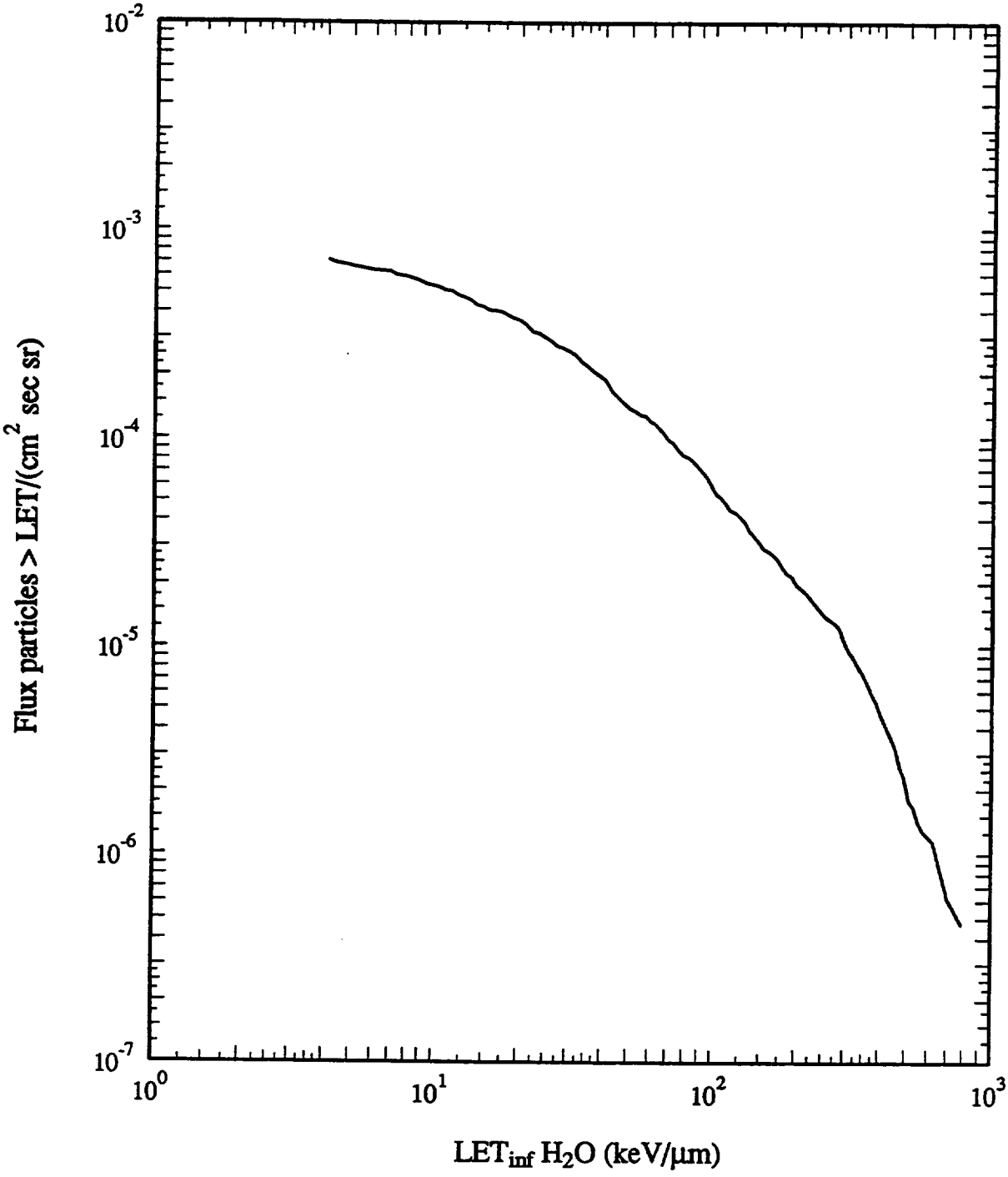


Figure 10: Combined Integral LET flux spectra for CR-39 detector pair E34/E39, under 69.45 g/cm$^2$ shielding, measured from the lid of the experiment container.

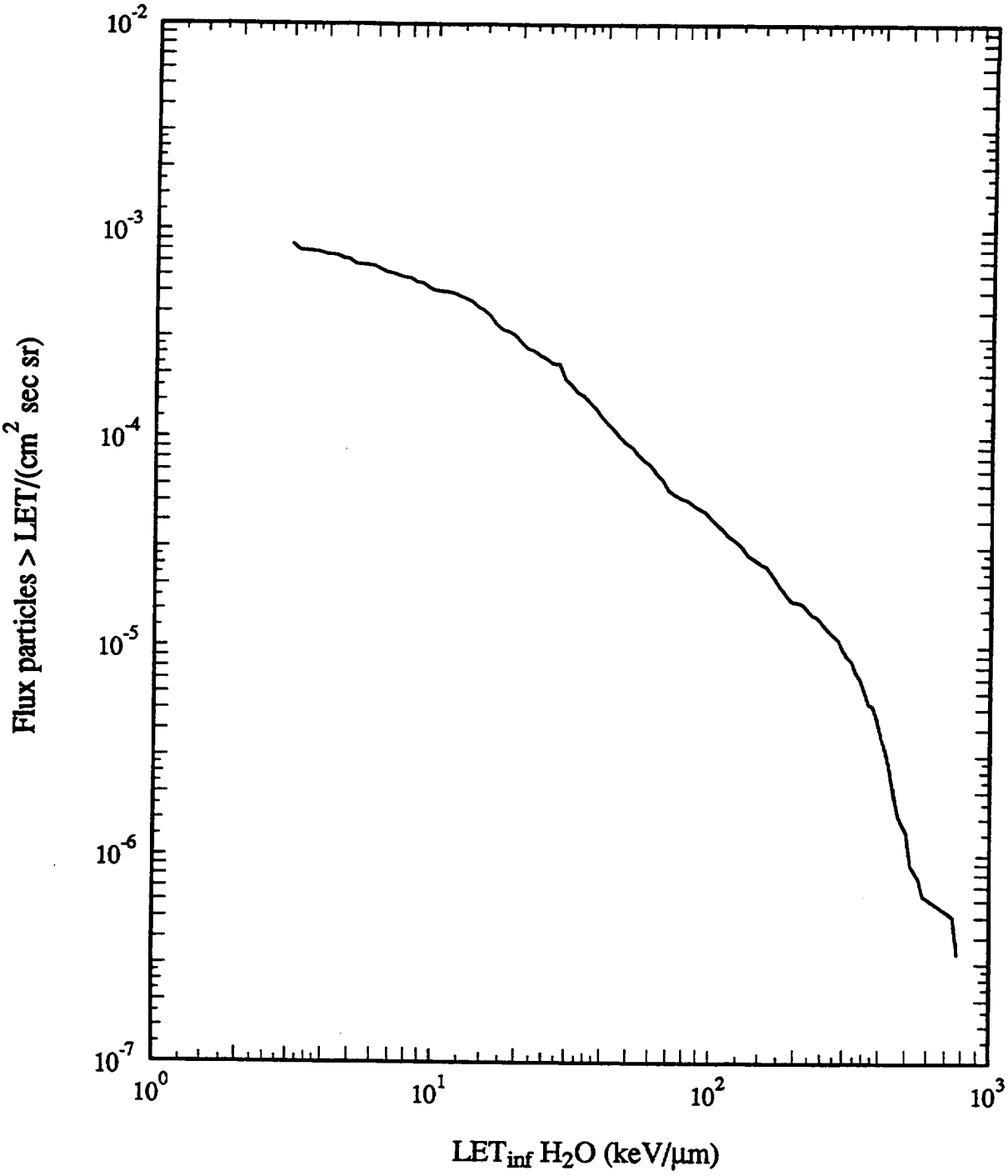


Figure 11: Combined Integral LET flux spectra for CR-39 detector pair E12/E04, under 87.07 g/cm$^2$ shielding, measured from the lid of the experiment container.

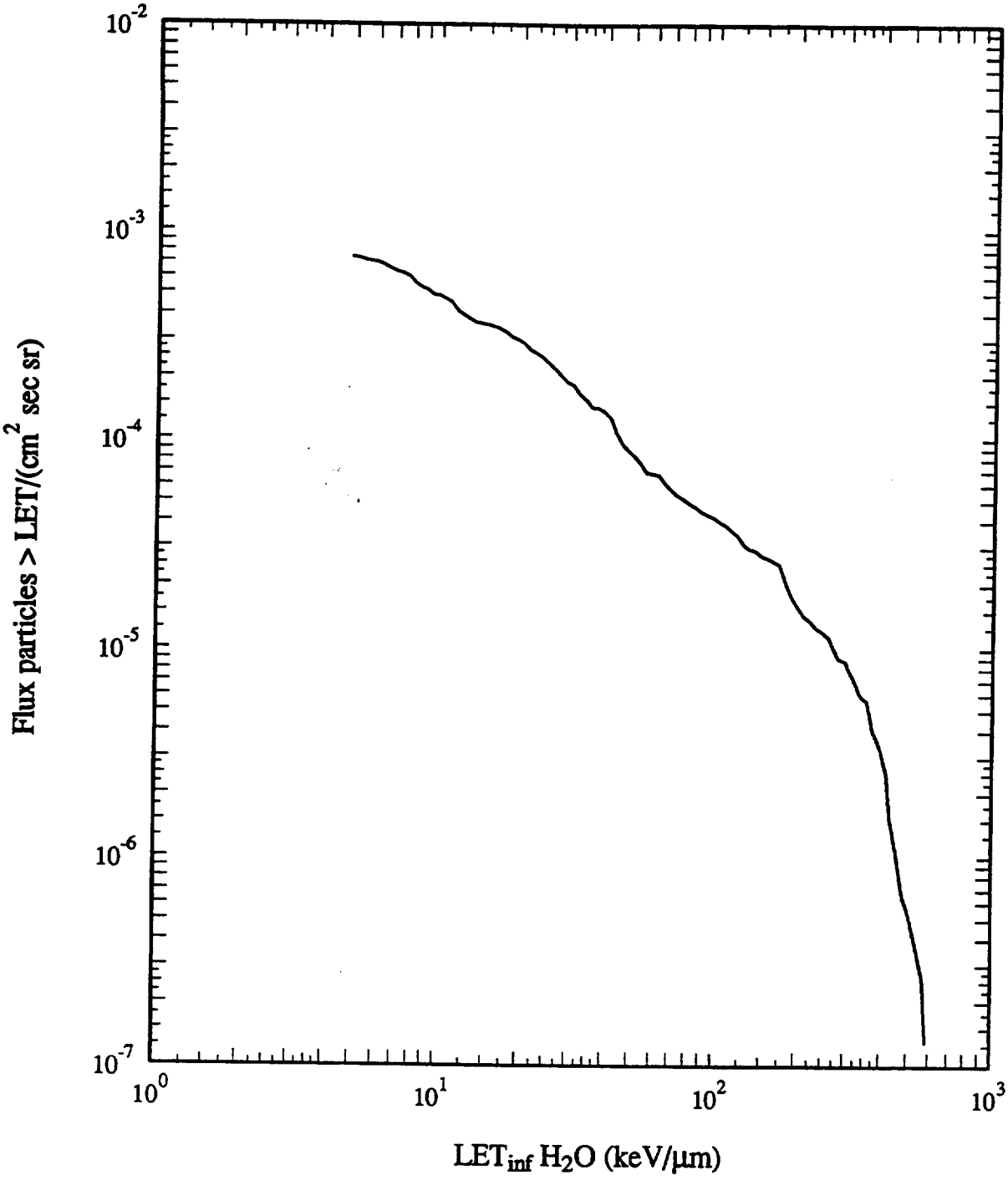


Figure 12: Combined Integral LET flux spectra for CR-39 detector pair E04/E01, under 94.91 g/cm$^2$ shielding, measured from the lid of the experiment container.

to a large production of short-range, high-LET secondary particles in these layers. Particls passing through the experiment were reduced in energy and increased in cross sections from nucleon interactions. They subsequently underwent inelastic collisions with the heavier nuclei (C and O) of the CR-39 and surrounding materials, producing the relatively high signal measured in the mid to high LET region.

Particle events were divided into two categories, long range events (>600 $\mu$m) consisting mostly of GCR, and short range events (<600 $\mu$m). Long range particle events were identified when two tracks, one of each surface of the detector layer, were found to have been made by the same particle. Since the pre-etch thickness of the CR-39 layers was ~600 $\mu$m, the minimum range of two surface particles events was on the order of this thickness. The remaining particle events took the form of single tracks on only one surface of the CR-39 detector. At low LETs, (<10 keV/$\mu$m), most of these events are made up of stopping primary protons. At higher LETs, a significant fraction of these events are caused by short-range, high-LET secondary particles. The minimum range of a particle observed in CR-39 as a track following a 36 hour etch is ~8 $\mu$m.

For all seven detector pairs measured, ~20% of the particle events were long range. In CR-39 detectors flown in less heavily shielded configurations (i.e. inside a Shuttle mid-deck locker), long range events show little change in LET through the thickness of the detector. Tracks on each of the two detector surfaces are roughly of equal size, indicating that the particle's LET is changing only slowly. For a majority of the long range particle events measured in the ECT CR-39 layers, the track on the surface of the detector facing space was often smaller than the track on the surface facing Earth. This was seen in ~80% of the long range particle events and indicates that the particles were arriving from the direction of space and that they were near the end of their ranges (i.e. the change in track size indicates the rapid change in LET seen near the particle's Bragg peak). That fact that so many of the long range particle events were near their stopping points illustrates the effect of heavy shielding of the ECT experiment on the GCR component.

# 4 Dose Measurements with TLDs

Sets of three TLDs were positioned in nine locations across the plane of each of the seven CR-39 detector pairs (see Figure 1). Following disassembly of the detectors after flight, all the TLDs were read out along with background detectors. Measured dose values from each of the three TLDs within a given set were averaged together to obtain a mean dose for that particular position on a given CR-39 detector layer. Mean measured doses from TLDs are listed in Table 4, along with the uncertainty in each measurement, in terms of CR-39 pair and TLD position. Also listed in Table 4 is the mean dose and its uncertainty for all TLD positions on each CR-39 doublet. Figure 13 shows the measured TLD doses for each of the nine positions as a function of shielding depth measured from the bottom to the top of the experiment stack. Figure 14 shows a similar plot of dose as a function of shielding measured from the top of the stack to the bottom. Figure 15 shows the mean dose for each detector layer as a function of shielding depth measured from top to bottom.

As can be seen in Figures 14 and 15, dose dropped rapidly as a function of shielding between the first two layers, E33/E25 and E21/E24, from 248 $\pm$ 3 to 197 $\pm$ 2 mrad within $\sim$7 g/cm$^2$. Dose remained relatively constant between layers E21/E24 and E12/E05, dropping from 197 $\pm$ 2 to 181 $\pm$ 2 mrad through $\sim$79 g/cm$^2$. The dose again fell off rapidly between layers E12/E05 and E04/E01, dropping from 181 $\pm$ 2 to 142 $\pm$ 1 mrad in $\sim$8 g/cm$^2$.

Measured doses in each of the nine TLD positions were relatively similar across a given detector layer. Only TLD Position 5 differed significantly from this pattern. The initial decrease in dose between layers E33/E25 and E21/E24 is not as great as that measured in the other TLD locations and dose can be seen to rise between layers E21/E24 and E19/E20 at Position 5, while it remains relatively constant for the other locations. Between E19/E20 and E04/E01, dose at Position 5 falls off gently. The reason for this difference in dose as a function of shielding between TLD Position 5 and the other eight TLD locations is most likely due to a combination in differences in shielding and in the orientation of the spacecraft during most of the mission. TLD Position 5 was on the right-most side of the detector sheet as can be seen in Figure 1. Thus it was close to the vertical side of the experiment

Table 4: Tissue absorbed doses and uncertainties (mrad) for the nine TLD positions on each layer and for the seven CR-39 PNTD layers. Also included are average dose values for each layer.

| CR-39 Doublet Number | Total Absorbed Dose (mrad) | | | | | | | | | |
|---|---|---|---|---|---|---|---|---|---|---|
| | *TLD Position* | | | | | | | | | |
| | *2* | *4* | *5* | *6* | *7* | *8* | *9* | *10* | *12* | *Mean* |
| E33/E25 | 248 ± 7 | 250 ± 8 | 235 ± 7 | 258 ± 8 | 251 ± 8 | 275 ± 8 | 235 ± 7 | 266 ± 8 | 212 ± 6 | 248 ± 3 |
| E21/E24 | 195 ± 6 | 199 ± 6 | 223 ± 7 | 191 ± 6 | 191 ± 6 | 203 ± 6 | 188 ± 6 | 194 ± 6 | 188 ± 6 | 197 ± 2 |
| E14/E14 | 203 ± 6 | 198 ± 6 | 237 ± 7 | 198 ± 6 | 197 ± 6 | 197 ± 6 | 184 ± 6 | 176 ± 5 | 186 ± 6 | 197 ± 2 |
| E19/E20 | 177 ± 5 | 175 ± 5 | 242 ± 7 | 180 ± 5 | 175 ± 5 | 167 ± 5 | 176 ± 5 | 171 ± 5 | 182 ± 5 | 193 ± 2 |
| E34/E39 | 185 ± 6 | 183 ± 5 | 230 ± 7 | 186 ± 6 | 171 ± 5 | 166 ± 5 | 179 ± 5 | 176 ± 5 | 195 ± 6 | 186 ± 2 |
| E12/E05 | 177 ± 5 | 174 ± 5 | 207 ± 6 | 177 ± 5 | 169 ± 5 | 180 ± 5 | 173 ± 5 | 175 ± 5 | 195 ± 6 | 181 ± 2 |
| E04/E01 | 143 ± 4 | 144 ± 4 | 175 ± 5 | 138 ± 4 | 135 ± 4 | 125 ± 4 | 124 ± 4 | 136 ± 4 | 154 ± 5 | 142 ± 1 |

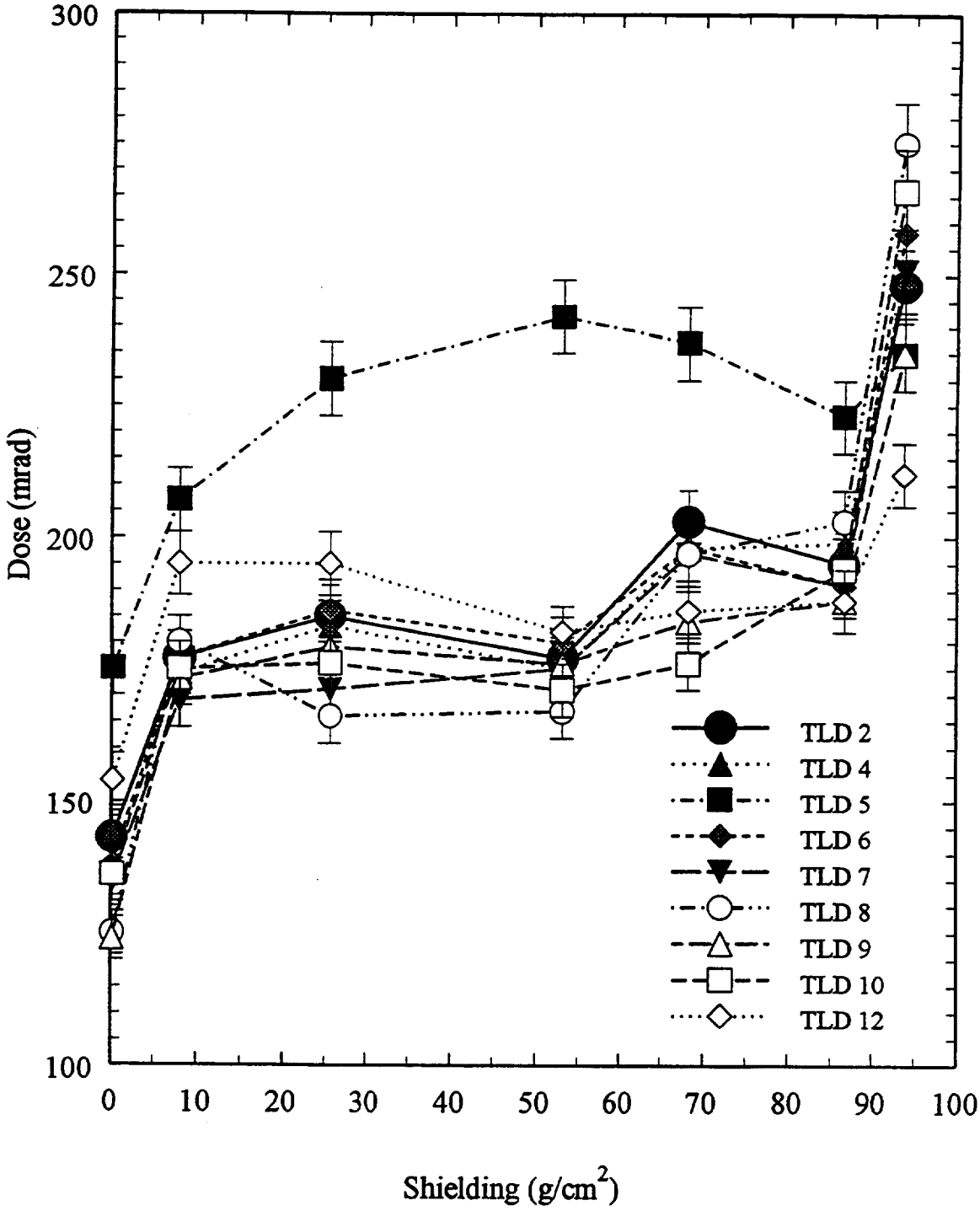


Figure 13: Dose in TLDs as a function of shielding depth as measured from the bottom to the top of the experiment stack for each of the nine TLD positions.

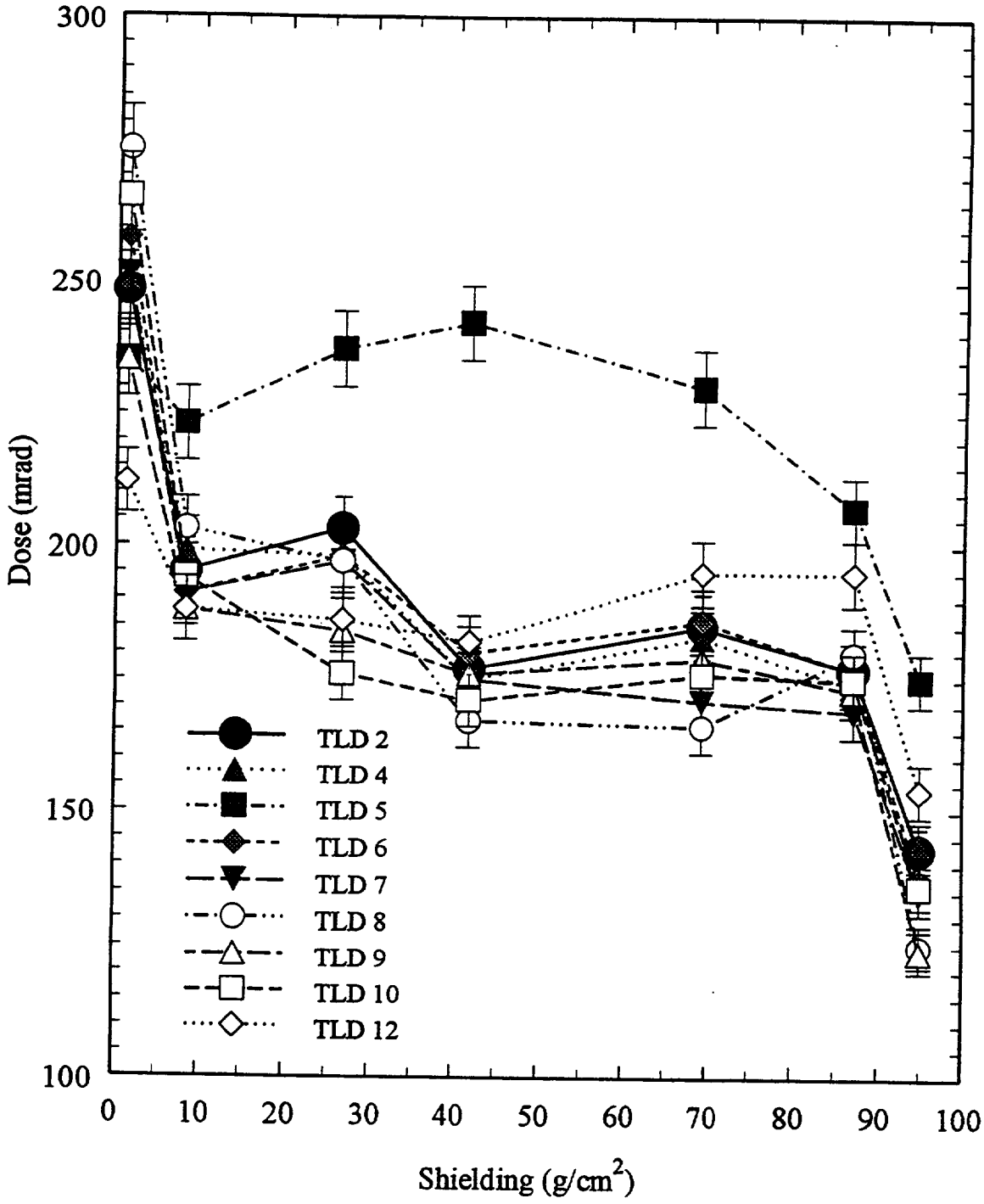


Figure 14: Dose in TLDs as a function of shielding depth in the experiment stack as measured from top to bottom for each of the nine TLD positions.

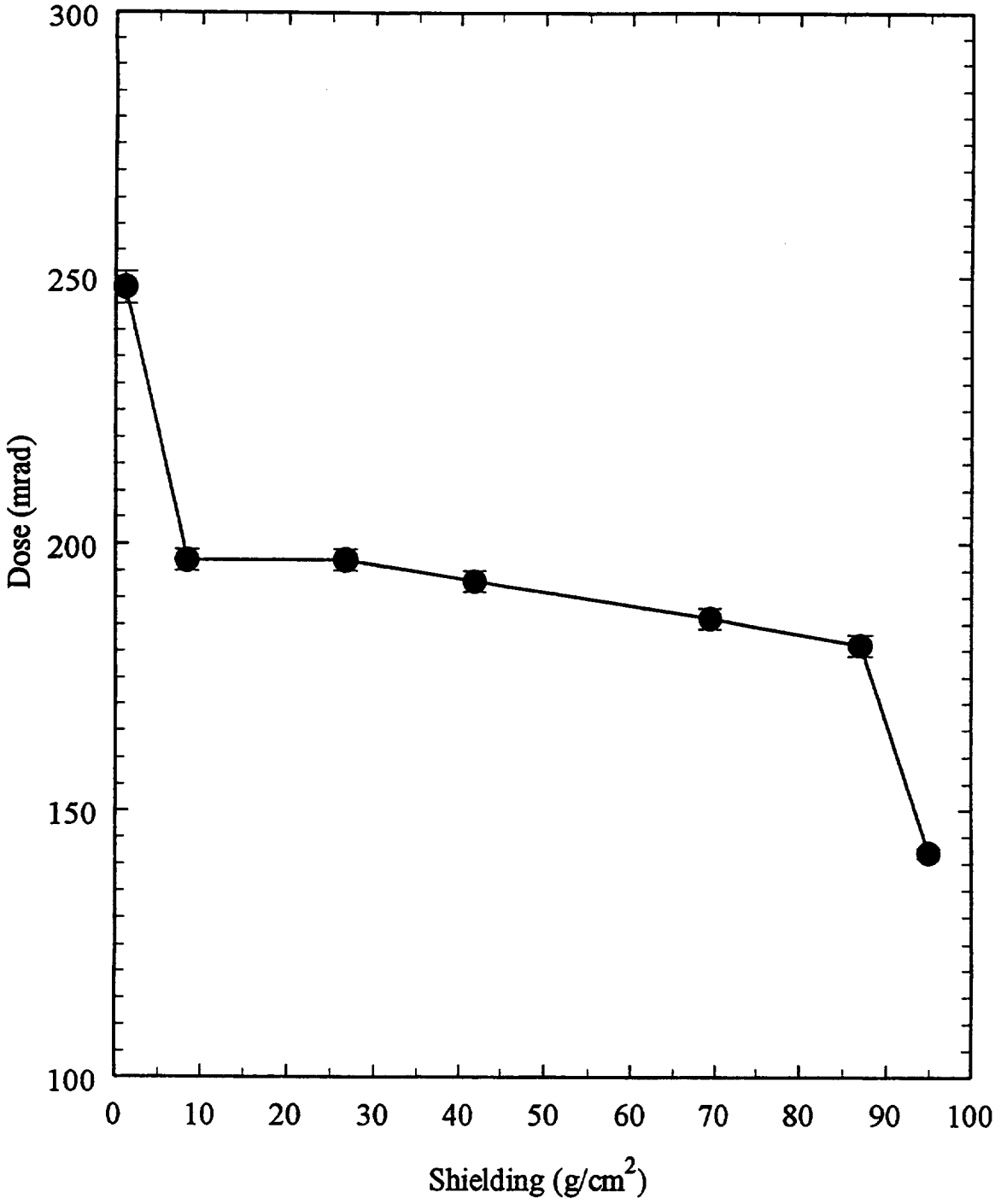


Figure 15: Mean TLD dose as a function of shielding depth from top to bottom in the ECT experiment stack.

container. Given the higher doses at mid-level values of shielding in TLD 5 versus the other locations, this location may be have been under the minimum of shielding from surrounding experiments and from the orbiter itself. TLD Position 12 also shows an increase in dose between layers E19/E20 and E12/E05, illustrating a similar minimum of vertical shielding.

It is also possible that TLD Position 5 was facing toward the West, the direction of greatest trapped proton flux, while the spacecraft traversed the SAA, during the majority of the mission, leading to a higher dose from trapped protons in this particular TLD position. Since the spacecraft was oriented upside down with the open cargo bay facing the Earth, the vertical sides of the experiment were perpendicular to the Earth's surface during most of the mission. Trapped protons, travelling in a helical motion around the lines of the geomagnetic field tend to encounter the spacecraft parallel to the Earth's surface. Due to the East/West trapped proton anisotropy, the greatest flux of trapped protons impinges on the spacecraft from the West. STS-62 was an Earth observation mission and it is likely that the orientation of the orbiter remained fixed relative to the Earth during much of the mission. This would permit the East/West effect to be seen in the relative doses of TLDs positioned across the detector surface and may explain the substantially larger doses seen in TLD position 5 and, to a lesser degree, TLD position 12 as compared to doses measured in the other TLD positions.

# 5 Low Energy Neutron Fluences and Dose Equivalents

The thermal (<0.2 eV) and resonance (0.2 eV–1 MeV) neutron fluences and dose equivalents were measured in the ECT assembly on STS-62 with Thermal/Resonance Neutron Detectors (TRNDs). The TRNDs are composed of $^{6}$LiF films between CR-39 PNTD layers. Each detector contains a pair of $^{6}$LiF/CR-39 sandwiches with one of the pair covered by Gd foil (25 $\mu$m) thermal neutron absorbers. When irradiated with neutrons, the $^{6}$Li(n,$\alpha$)T reaction takes place and the CR-39 layers are irradiated in turn by lower energy $\alpha$-particles. In the half of the detector covered by Gd, the thermal neutrons are eliminated from the reactions, allowing a separation between thermal- and resonance-induced track densities on the CR-39. By assuming energy spectra for the incident neutrons (a well-thermalized spectrum below 0.2 eV; a $E_n^{-1}$ moderated spectrum between 0.2 eV and 1 MeV) calibrations in neutrons/track

have been determined for the TRND.

The ECT experiment contained three TRNDs: Detector C (1 and 2) were placed at corners of the assembly below the chamber lid (under 0.306 g/cm$^2$), Detector B was centered in the lower calorimeter (under 44.34 and 50.57 g/cm$^2$ to top and bottom, respectively), Dectector A was centered in the lower calorimeter (under 89.57 and 5.34 g/cm$^2$). A fourth detector (D) was shipped with the flight detectors in a Ground Control unit and provided background measurements.

After postflight return of the dosimeters, the TRNDs were disassembled and the CR-39 layers were processed for 4.5 hour in 6.25 $N$ NaOH solution at 70°C. The $\alpha$-particle track densities on the CR-39 were counted under 200 $\times$. The measured track densities are given in Table 5. Each track density is an average from the CR-39 layers above and below the $^6$LiF/CR-39 film and is a measure of $4\pi$ neutron incidence (an average is used because TRNDs have been calibrated for a single CR-39 layer in contact with the $^6$LiF film.

There is a large variation in track densities in Table 5 with Detector C only about 3 times greater than the Ground Control (D). The most centered position (B) has track densities $\sim$10 times greater than Detector C and 3 times greater than Detector A. Not shown is the fact that in Detector A (near the bottom of the assembly) the track densities from the top CR-39 layer were $\sim$3 times larger than those on the bottom CR-39 layer. Low energy neutron densities clearly fall off sharply near the edges of he ECT assembly. The same difference was not seen between top and bottom CR-39 layers in Dectector C (near the top corners of the assembly) where all track densities were low.

Track densities are converted to neutron fluences and dose equivalents in Table 6. Detector calibration has been described by Benton et al.[1]. Dose equivalent conversion factors from NCRP (1971) were used which incorporated QF values of 2 for thermal neutrons and 6.4 for resonance neutrons. The low energy neutron dose equivalents of 11.6, 39, and 3.1 mrem (of 1.03, 3.5 and 0.28 mrem/d) can be compared with previous Shuttle measurements. The average of 11 flight measurements (from a variety of altitudes and inclinations) is 0.26 mrem/d with a $\sigma$ of 0.12 mrem/d. The dose equivalent in the interior of the ECT assembly is much higher than previous measurements and demonstrates that substantial neutron moderation and thermalization takes place within a hydrogenous mass. The TLD

Table 5: Track Densities from the ECT TRNDs

| Detector | Total Track Density ($cm^{-2}$) | Background Subtracted Track Density ($cm^{-2}$) |
|---|---|---|
| A | 1311 ± 42 | 1223 ± 43 |
| A-Gd | 439 ± 18 | 394 ± 19 |
| B | 3597 ± 87 | 3509 ± 87 |
| B-Gd | 1370 ± 40 | 1325 ± 40 |
| C | 235 ± 12 | 147 ± 14 |
| C-Gd | 152 ± 10 | 107 ± 12 |
| D | 88 ± 7 | |
| D-Gd | 45 ± 6 | |

Gd designates detectors with Gadolinium covers.
Detector D was a Ground Control unit and the track densities represent background for the flight detectors.
Positions of the A, B, and C detectors were at the top, middle and bottom, respectively, of the ECT assembly.

absorbed dose near Detector B was about 170 mrad and lower energy neutron dose equivalent represents less than 23% of the total.

# 6 Conclusion

Measurements of LET spectra were fairly typical for a STS mission of this altitude and inclination. STS-62 was in a 39°, 296 km orbit, falling between the minimum and maximum orbital inclinations for the Space Shuttle of 28.5° and 57°, respectively. Thus STS-62 received significant fractions of its radiation exposure from the ionizing radiation components that dominate these two extremes: stopping primary protons and short range, high LET secondaries from trapped protons in the SAA for low inclination orbits and GCR for high inclination orbits. Little difference was seen amongst the seven measured integral LET flux spectra as a function of shielding. The largest flux in the low LET region (<10 keV/$\mu$m)

Table 6: Neutron fluence and Dose Equivalent from ECT TRNDs

| Detector | Energy Range | Neutron Fluence ($cm^{-2}$) | Dose Equivalent (mrem) | Dose Equivalent ($\mu$Sv) |
|---|---|---|---|---|
| A | <0.2 eV | $3.0 \pm 0.6 \times 10^5$ | $0.30 \pm 0.06$ | $3.0 \pm 0.6$ |
| | 0.2 eV–1 MeV | $2.3 \pm 1.1 \times 10^6$ | $11.3 \pm 5.6$ | $113 \pm 56$ |
| B | <0.2 eV | $7.8 \pm 1.6 \times 10^5$ | $0.79 \pm 0.16$ | $7.9 \pm 1.6$ |
| | 0.2 eV–1 MeV | $7.7 \pm 3.8 \times 10^6$ | $38 \pm 19$ | $380 \pm 190$ |
| C | <0.2 eV | $1.4 \pm 0.7 \times 10^4$ | $0.015 \pm 0.007$ | $0.15 \pm 0.07$ |
| | 0.2 eV–1 MeV | $6.2 \pm 3.1 \times 10^5$ | $3.1 \pm 1.5$ | $31 \pm 15$ |

was seen in detector pair E33/E25 under 1.19 g/cm$^2$ (Figure 6) and most likely took the form of stopping primary protons encountered in the SAA. The largest fluxes in the mid (>10 keV/$\mu$m) and high (>100 keV/$\mu$m) regions were seen in detector pairs E15/E14 (Figure 8) and E19/E20 (Figure 9), and were probably mainly secondaries produced by trapped protons in the SAA. Previous work on the Long Duration Exposure Facility (LDEF) demonstrated that the production of proton-induced secondaries increases with shielding[2]. While E15/E14 and E19/E20 were in the middle range of shielding in the experiment (26.71 and 41.84 g/cm$^2$, respectively) they may have been the most heavily shielded layers when the additional shielding of the spacecraft and surrounding experiments is taken into account and it is this total shielding that is responsible for the large number of proton-induced secondary particle tracks seen in these detectors.

Approximately 20% of the mid to high LET particle events were long range (>600 $\mu$m) and thus can be considered to have been produced by GCR. Of the long range particles, 80% were slowing; that is a noticeable difference in size could be seen between tracks on each of the two detector surfaces. This permitted the direction of these particles to be determined and it was found that the large majority of long range particles arrived in the experiment stack from the direction opposite the Earth and passed through the stack towards the Earth. This illustrates the effect of the large amount of shielding (~100 g/cm$^2$) of the ECT experiment

on GCR.

Total absorbed dose as measured by TLDs was seen to be attenuated by shielding in the experiment stack. The least shielded layer (1.19 g/cm$^2$) had a mean dose of 248 $\pm$ 3 mrad. Dose decreased rapidly in the first $\sim$7 g/cm$^2$ of shielding and then plateaued at $\sim$190 mrad in the middle of the experiment stack. At the bottom of the stack, under the greatest shielding of 94.91 g/cm$^2$, mean dose dropped to 142 $\pm$ 1 mrad. Little difference in dose could be seen for the nine TLD locations across a given detector layer, except for TLD Position 5. This position measured a significantly higher dose in the middle levels of the experiment stack and was on the left-most edge of the detector stack. This difference in measured dose as a function of TLD position was probably due to a combination of shielding and experiment orientation. Previous work on LDEF[3] demonstrated the differences in dose across a spacecraft orbiting in a fixed orientation relative to the Earth due to the East/West trapped proton anisotropy in the SAA. Since STS-62 was an Earth observation mission, it is reasonable to assume that the orbiter remained in a fixed orientation for a significant portion of the mission. It is possible that TLD Position 5 was oriented toward the West and under comparatively low shielding, leading to a disproportionately large dose from trapped protons at this position as compared to other TLD positions across the detector surface.

Thermal and resonance neutron dose equivalents were found to vary substantially with shielding. In this case shielding can be considered a neutron thermalizing and moderating medium, since in was largely hydrogenous in composition. A low energy dose equivalent of 3.5 mrem/d was measured in Detector B under 41.84 g/cm$^2$. This is substantially greater than the 0.26 mrem/d mean dose equivalent measured on previous STS missions, demonstrating the effect of the hydrogenous mass of the experiment in neutron moderation and thermalization.

Since the ECT experiment was included on an Earth observation STS mission and thus orbited upside down during most of the flight, the primary objectives of the experiment could not be met. However, the fact that a large percentage (80%) of long range particle events were found to be traversing the experiment from space towards the Earth and were seen to be slowing down validates the general design of the experiment. LET spectra measurements showed that a substantial fraction (80%) of mid to high LET particles took the form of short

range, high LET secondaries produced by trapped protons and indicates that this component is significant in orbits of this inclination (39°) as well as lower inclination orbits and must be adequately taken into account during the data reduction and analysis process.

# References

[1] E. V. Benton, R. P. Henke, A. L. Frank, C. S. Johnson, R. M. Cassou, M. T. Tran, and E. Etter. Space radiation dosimetry aboard Cosmos 1129: U. S. portion of experiment K-309. In M. A. Heinrich and K. A. Souza, editors, *Final Reports of U. S. Plant and Radiation Experiments Flown on the Soviet Satellite Cosmos 1129*, T. M. 81288. NASA, Ames Research Center, 1981.

[2] E. R. Benton, I. Csige, E. V. Benton, and L. A. Frigo. Contribution of proton-induced short range secondaries to the LET spectra on LDEF. In *LDEF–69 Months in Space: Third Post-Retrieval Symposium*, NASA-CP 3275, pages 167–178, Washington DC, 1995.

[3] E. V. Benton, I. Csige, A. L. Frank, E. R. Benton, L. A. Frigo, T. A. Parnell, J. Watts, and A. Harmon. Absorbed dose and LET spectra measurements on LDEF. In *LDEF–69 Months in Space: Third Post-Retrieval Symposium*, NASA-CP 3275, pages 125–148, Washington DC, 1995.

# APPENDIX B

## ECT Mechanical, Thermal, and Electrical Systems Report

Orbital Sciences Corporation
Space & Electronics Systems Group
Huntsville Technical Support Center
1525 Perimeter Parkway, Suite 200
Huntsville, ALabama 35806

# Table of Contents

## 1.0 Summary

This report documents the preparation and performance of the Emulsion Chamber Technology Experiment (ECT) hardware and software for the OAST-2/STS-62 mission aboard the Orbiter Columbia. Also discussed are lessons learned, current status and issues for future flights of ECT.

ECT flew as one of several experiments comprising the OAST-2 payload on STS-62, beginning with launch at KSC on 4 March 1994 and ending with touchdown at KSC on 18 March 1994. The ECT flight hardware was located on the upper surface of the Hitchhiker-M bridge structure in the aft end of the payload bay, next to the portside payload bay sill. The hardware was facing out of the payload bay in the +Z direction, affording an acceptable view. The effective exposure time accrued was seventy-five (75) hours. Columbia's flight performance was nominal and impacts on experiment operations were minimal.

Excellent thermal control of the ECT Emulsion Chamber was maintained during flight and no significant power interruptions occurred. Telemetry and recovered on-board data confirm that the temperature of the Emulsion Chamber was controlled to 20 ± 1 °C throughout the entire flight. The flight hardware arrived back at MSFC after the OAST-2/STS-62 mission in good condition. The emulsion stack showed no apparent thermal, mechanical, light or radiation damage and contained returned data. All stored electronic data was recovered.

The mechanical interference problem identified during system-level integration and testing at GSFC involving the pressure transducer and the adjacent mounting bolt was eliminated by correct positioning of the pressure transducer during final assembly of the Emulsion Chamber. No interference problems were encountered during pre-launch integration at KSC. None of the thermal switches de-bonded during shipment, ground handling or flight.

## 2.0 Current Status

The flight hardware, quality-sensitive spares and quality-sensitive ground support equipment (GSE) are packed for storage in the ECT Shipping Container. All AA alkaline cells have been removed from the Electronics Unit and the Temp Mentor. Quality Assurance documentation and the Hardware Activity Log are packed with the hardware.

Quality Assurance coverage has been maintained by NASA since hardware delivery and acceptance. MSFC Quality Assurance personnel have indicated that QA coverage will be continuous and that ECT will be ready for re-flight provided that all quality-sensitive items are placed in appropriate storage at MSFC. As of the time of this report, the flight

hardware, quality-sensitive spares, quality-sensitive GSE and non-quality-sensitive items have been placed in bonded storage at MSFC.

Emulsion stack materials, including the lead sheets and processed plates, are in the custody of the Cosmic Ray Emulsion Laboratory (MSFC/ES62). Development hardware and other non-quality-sensitive or non-flight items are currently stored at UAH Materials Science Building. Post flight data products provided by NASA will also be found at UAH Materials Science Building.

## 3.0 Assembly, Integration and Flight

### 3.1 Assembly for Flight

Previous reports have described the system-level integration and testing at GSFC. The Temp Mentor's RS-232 power loop-back feature caused the Temp Mentor on-board power depletion while at GSFC. Thus, no temperature record for the period 10/26/93 through 11/23/93 exists. A mechanical interference problem was identified involving the pressure transducer and the adjacent mounting bolt. The bolt was omitted for GSFC testing. The ECT hardware was de-integrated and shipped back to MSFC from GSFC after completion of the required integration and testing activities, arriving on 11/23/93. The test emulsion stack arrived with no apparent damage. The ECT hardware also arrived in excellent condition. The materials for the flight emulsion stack had been made ready by this time at the Cosmic Ray Emulsion Laboratory (MSFC/ES62).

#### 3.1.1 Emulsion Chamber Assembly

The Emulsion Chamber was cleaned thoroughly before final assembly for flight. The loading of the flight emulsion stack went extremely well once again. The assembly of the Emulsion Chamber with emulsion stack has now been sucessfully completed three times, once with the development hardware and twice with the flight hardware. The use of alignment fixtures during assembly was abandoned early on and the standard procedure is to assemble the Bottom Plate and Lower Chamber before loading. The Emulsion Chamber assembly procedure is included in Appendix A. The flight emulsion stack configuration record was provided by the Cosmic Ray Emulsion Laboratory (MSFC/ES62) and is included in Appendix B.

The pressure transducer was rotated to the extreme counter-clockwise or (nearly) vertical position when installed on the Emulsion Chamber, in order to alleviate the interference problem involving the pressure transducer and the adjacent mounting bolt. As a result, no mechanical interference was encountered during integration of the ECT flight hardware at KSC. This step of the Emulsion Chamber assembly must be performed with

the ECT Flight Wiring Harness connected to the Emulsion Chamber in order to ensure proper positioning of the pressure transducer while preventing interference with the adjacent feedthrough connector.

The O-rings used in the assembly of the Emulsion Chamber were coated with a minimum amount of vacuum grease. Leak testing followed assembly, with Helium detection and pressure decay tests. In keeping with the ECT mission approach, no extraordinary methods were used. It was noted during testing that considerable amounts of Helium had been absorbed by the stack materials, evidenced by unexpected pressure increases during pressure decay tests. The Emulsion Chamber was left pressurized with air to approximately 30 psia for shipment to KSC.

### 3.1.2 Electronics Unit Assembly

The Electronics Unit was cleaned thoroughly before final assembly for flight. Fresh AA alkaline cells were installed in the Electronics Unit and the Temp Mentor. A flight-qualified PROM hosting the 7/93 version of the ECT flight software was installed in the Electronics Unit. This version of the flight software was verified by over 150 hours of test operation before installation in the Electronics Unit.

The power loop-back feature was disabled on the Temp Mentor's RS-232 port and instead built into the Electronics Unit's RS-232 port, feedthrough connector J7. Power is now conserved because GSE cables are connected to the Electronics Unit's RS-232 port for only a relatively short time, during ground operations.

## 3.2 Final Preparations for Shipment

Two bimetallic thermal switches were re-bonded to the Emulsion Chamber with flight epoxy. Flight velcro was installed on both assemblies, lockwires were installed, lockwire ends were encapsulated with flight epoxy, and touch-ups were made on heater wire insulation and silverized Teflon tape. After some assurances were given by GSFC concerning ferry temperature control, the decision was made to omit the Solimide TA-301 polyimide foam insulation, due to its tendency to shed particulates. It is likely that a method could be developed using adhesive tape or a hot surface to seal the surfaces and make the foam acceptable for flight. The concerns raised last summer by GSFC's QA contractor and others were addressed with these actions.

All exposed connectors on the Emulsion Chamber and Electronics Unit were covered with Teflon dust covers before shipment. The Temp Mentor was deployed and the ECT Shipping Container was sealed for shipment on 12/29/93. Shipment to KSC occurred on 1/3/94.

## 3.3 Integration for Flight

The ECT team arrived at KSC on 1/4/94. OAST-2 integration and testing activities took place in Hangar AM. The hardware was unpacked, checked out and installed on the Small Top Pallet. The Emulsion Chamber was vented to atmosphere. The Temp Mentor data was recovered and the Temp Mentor was deployed for flight. The Small Top Pallet with the ECT flight hardware was then installed on the HH-M structure. Power and data cables were integrated, followed by installation of the MLI and ground wires. The Emulsion Chamber was again vented to atmosphere just before the MLI was closed. GSFC provided some grounding lugs, lockwires and cable ties, cleaning of the radiator surfaces and some stitching on the MLI. Integration and testing activities were completed on 1/6/94. OAST-2 was integrated with the Orbiter Columbia some weeks later.

## 3.4 The OAST-2 Mission

ECT flew as one of several experiments comprising the OAST-2 payload on STS-62, beginning with launch at KSC on 4 March 1994 and ending with touchdown at KSC on 18 March 1994. The ECT flight hardware was located on the upper surface of the Hitchhiker-M bridge structure in the aft end of the payload bay, next to the portside payload bay sill. The hardware was facing out of the payload bay in the +Z direction, affording an acceptable view. The effective exposure time accrued was seventy-five (75) hours. Columbia's flight performance was nominal and impacts on experiment operations were minimal.

The ECT team staffed the GSFC Payload Operations Control Center (POCC) around the clock during the OAST-2/STS-62 flight. Training sessions and mission simulations were also supported in the weeks prior to the mission.

## 3.5 De-integration

The ECT flight hardware was de-integrated from OAST-2 and packed for shipment to MSFC on 5 April 1994 at KSC. The ECT Shipping Container, along with spares and materials arrived at MSFC early on 6 April 1994. Disassembly, processing of emulsion stack materials and packing for storage followed. The Hardware Activity Log is included in Appendix C.

## 4.0 Engineering Performance

### 4.1 Thermal Performance

The performance of the ECT thermal control system was excellent. The OAST-2 payload experienced a cold soak period after reaching orbit, due to Orbiter operations before OAST-2 power-up. Early telemetry indicated that the temperature of the emulsion stack ranged from approximately 9 °C (after correction) at the top of the stack (near the space radiator) to approximately 16 °C at the middle and bottom locations. Power was applied to OAST-2 and its experiments, including ECT, at MET 00:02:39 (Mission Elapsed Time, dd:hh:mm), or two hours, thirty-nine minutes after launch. Upon power-up the ECT thermal control system began operation and Emulsion Chamber temperatures began to recover. At no time did the emulsion stack temperature fall below 5 °C. Figures 1 and 2 provide the internal temperatures and power consumption for ECT following power-up. From the data contained in Figure 1, the thermal time constant of the emulsion stack is estimated to be approximately five (5) hours.

After recovery from the cold soak, the temperature of the ECT Emulsion Chamber was maintained at 20 ± 1 °C in all spacecraft attitudes throughout the entire flight. Orbiter performance was nominal and no significant interruptions of experiment power occurred. Telemetry and recovered on-board data confirm that the temperature of the Emulsion Chamber was controlled to 20 ± 1 °C. Correction of the readings for the emulsion stack top thermistor (Appendix E) is required as described in the thermistor calibration report contained in Appendix D. After correction, these values do indeed fall within the specified range of 20 ± 1 °C.

The temperature of the Small Top Pallet remained within the range of 0 - 40 °C in all spacecraft attitudes throughout the entire flight, as promised by GSFC. It was reported that the Small Top Pallet heater was never needed during the flight.

All of the telemetry data relevant to ECT flight operations is presented in Appendices E - I. These include the three emulsion stack temperatures, ECT power and the Small Top Pallet temperature, recorded at thirty-minute intervals at the POCC at GSFC.

Previous reports have presented analytical predictions and thermal test results. Predictions, test results and flight results are shown in Table 1. In all analyses and tests Emulsion Chamber temperatures were controlled to within the range of 20 ± 1 °C unless the analysis or test reports indicated otherwise.

ECT power consumption varies considerably with Orbiter attitude. Generally, predictions and test environments were conservative as compared to the flight data.

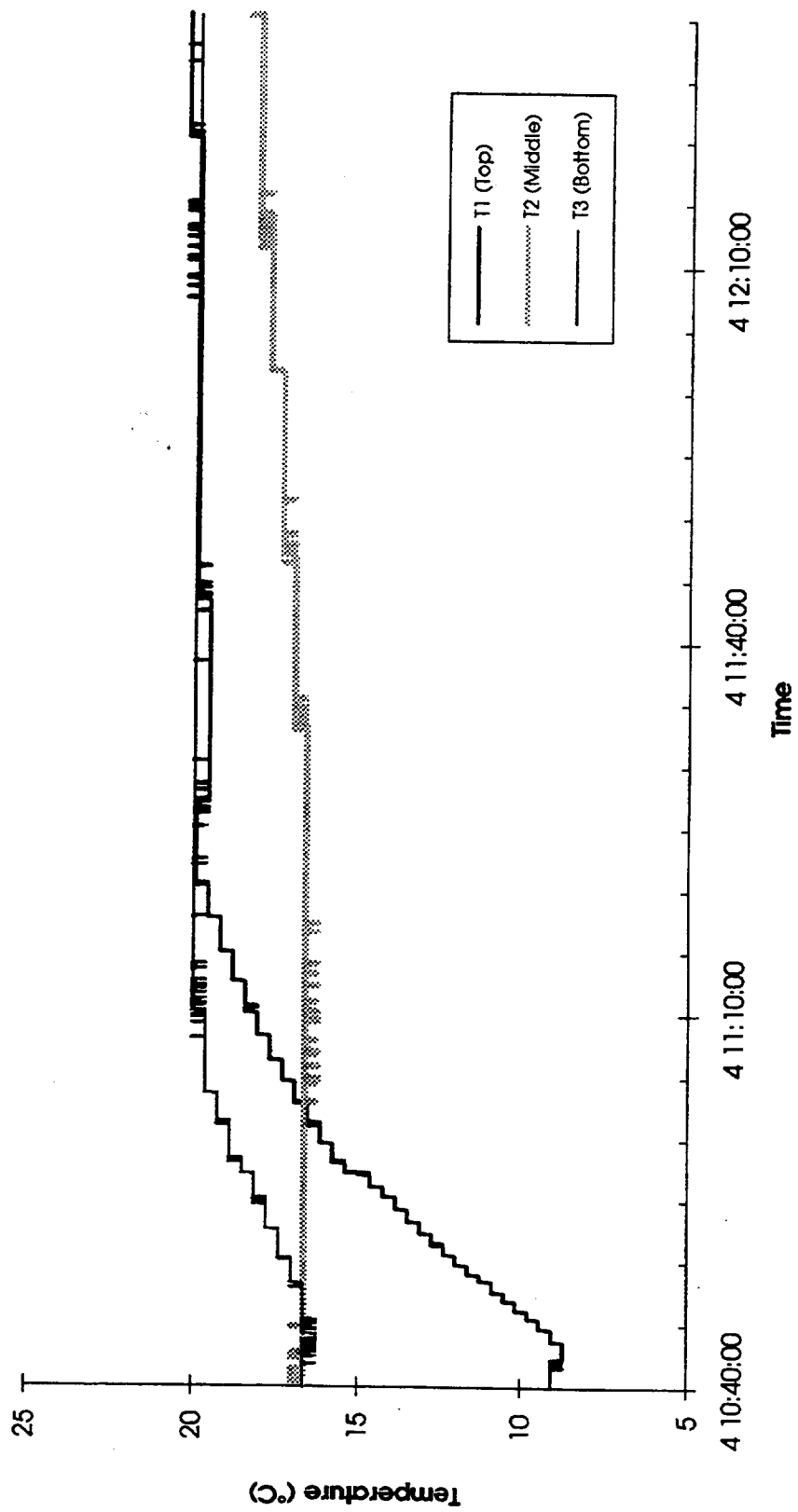
ECT Internal Thermistors, MET 0/02:40:00 - MET 0/04:10:00, Power-up
Temperature (°C)
25
20
15
10
5
4 10:40:00
4 11:10:00
4 11:40:00
4 12:10:00
Time
T1 (Top)
T2 (Middle)
T3 (Bottom)

Figure 1.

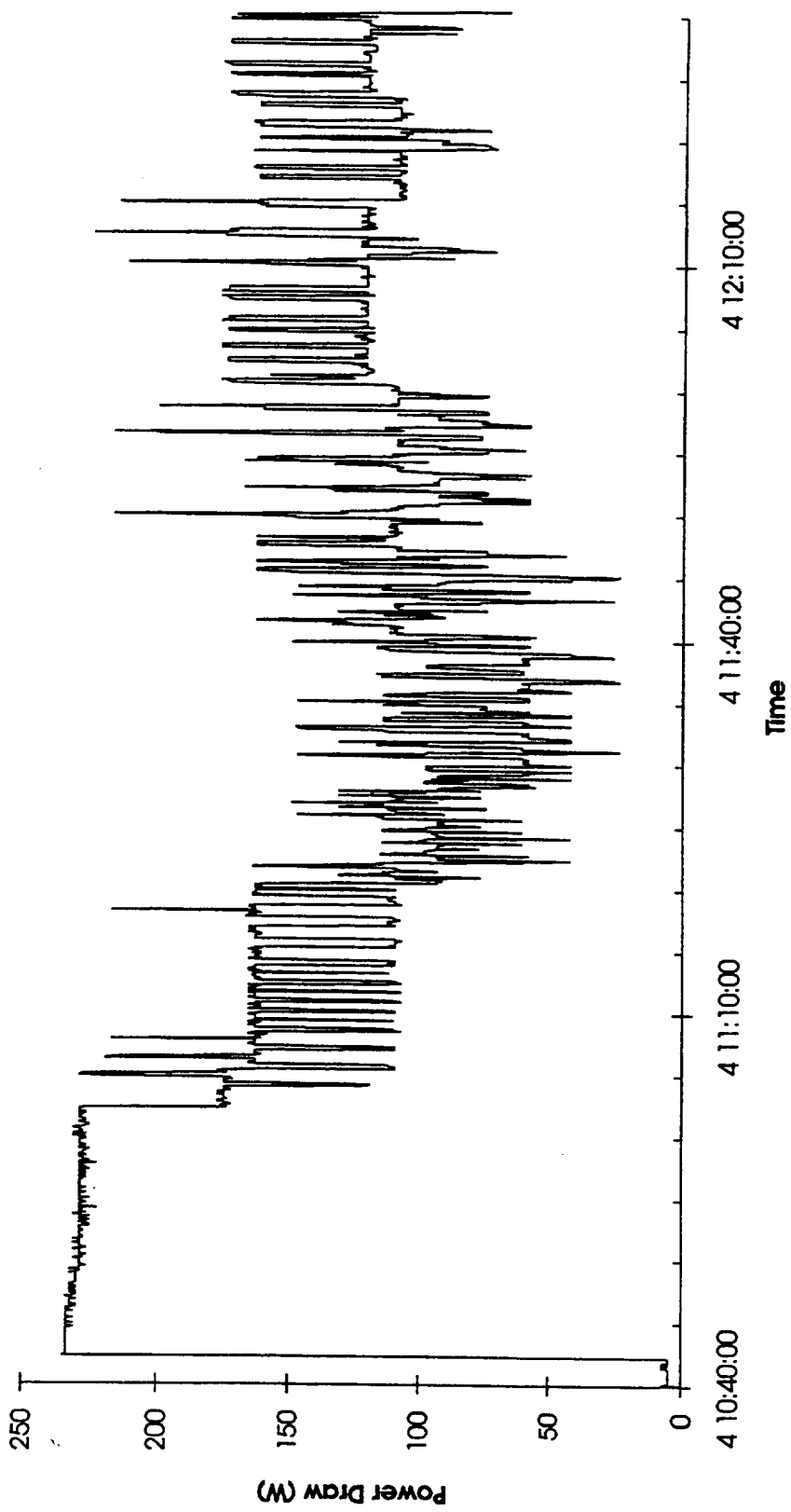
ECT Power Draw, MET 0/02:40:00 - MET 0/04:10:00, Power-up
Power Draw (W)
250
200
150
100
50
0
4 10:40:00
4 11:10:00
4 11:40:00
4 12:10:00
Time

Figure 2.

Table 1. Comparison of Predictions, Test Results and Flight Results

| Orbiter Attitude | Predicted Avg. Power (W) | Tested Avg. Power (W) | Flight Avg. Power (W) |
|---|---|---|---|
| Bay-to-Sun | 38 | 76 | 61 |
| Tail-to-Earth | not predicted | not tested | 95 |
| Bay-to Earth | 78 | 76 | 54 |
| Bay-to-Space | 112 | 131 | 109 |

4.1.1 Bay-to-Sun Attitude

The predicted power value was expected to be rather low compared to test and flight results. This is due to the fact that the bay-to-sun thermal environment was supplied by the GSFC thermal contractor for OAST-2's first flight assignment and was not updated (because it was such a conservative environment) until after the UAH thermal analysis was completed, but before thermal testing was conducted.

This attitude was used a few times for thermal conditioning of the payload bay before extended periods in cold attitudes. The period MET 09:18:08 - MET 09:19:08 is the best and longest example. Temperature and power data for the period MET 09:18:08 - MET 09:19:08 are shown in Figures 3 and 4.

4.1.2 Tail-to-Earth Attitude

This attitude was flown to accommodate OAST-2. The period MET 09:19:08 - MET 09:20:28 is one example. Temperature and power data for the period MET 09:19:08 - MET 09:20:28 are shown in Figures 3 and 5. No thermal environment was provided before the mission.

4.1.3 Bay-to Earth Attitude

This attitude was flown for the bulk of the mission to accommodate the primary payload. Temperature and power data for the period MET 03:03:21 - MET 03:05:02 are shown in Figures 6 and 7.

4.1.4 Bay-to-Space Attitude

This attitude was flown a few times to accommodate OAST-2 and certain Orbiter operations. The period MET 10:06:51 - MET 10:08:36 is one example. Temperature and power data for the period MET 10:06:51 - MET 10:08:36 are shown in Figures 8 and 9.

Figure 3. **ECT Internal Thermistors, MET 9/18:08 - MET 9/20:28, Bay-to-Sun & Tail-to-Earth**

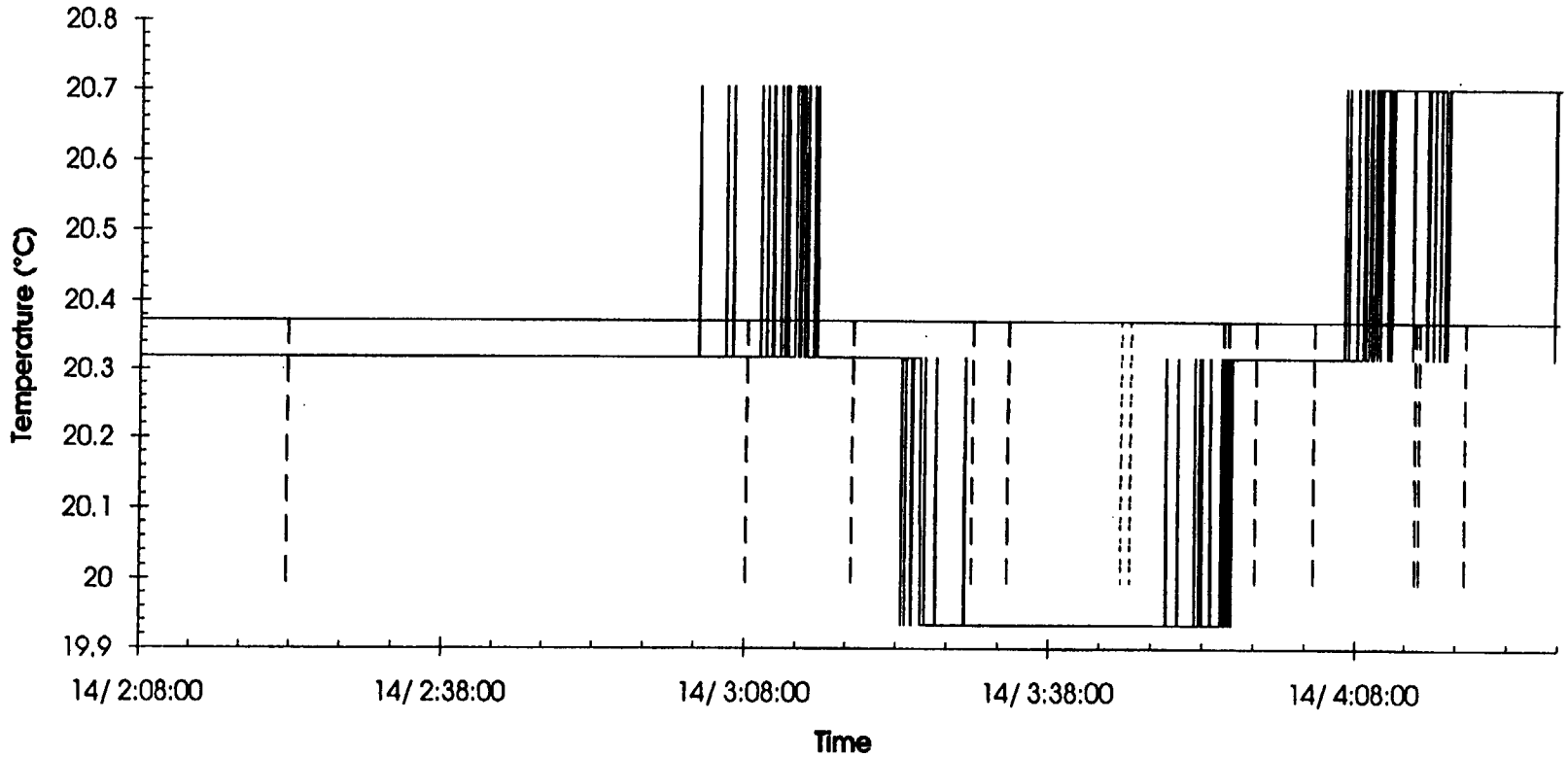

Figure 4. **ECT Power Draw, MET 9:18:08 - MET 9:19:08, Bay-to-Sun**

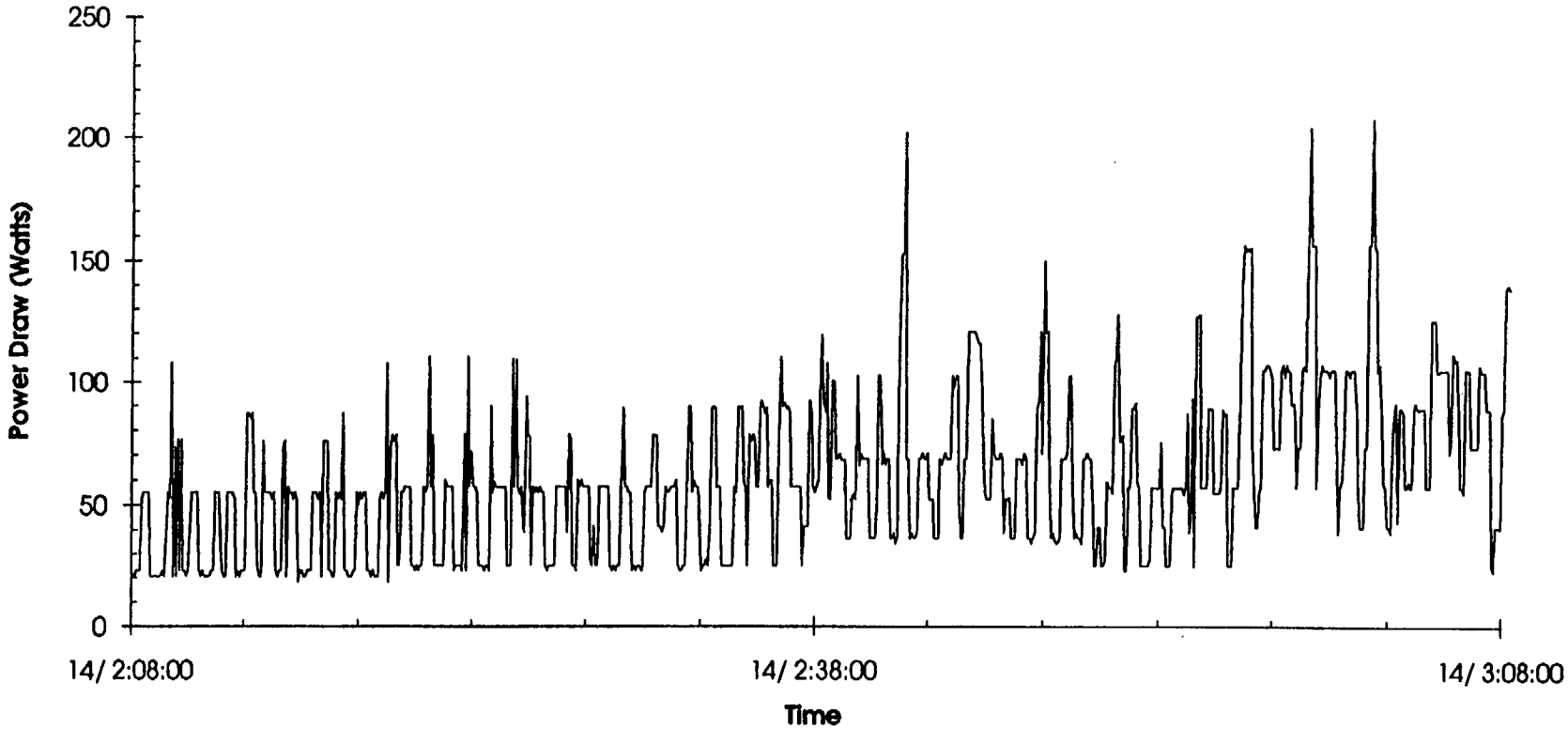


**Bay-to-Sun Avg. Pwr. 61W**

Figure 5. **ECT Power Draw, MET 9:19:08 - MET 9:20:28, Tail-to-Earth**

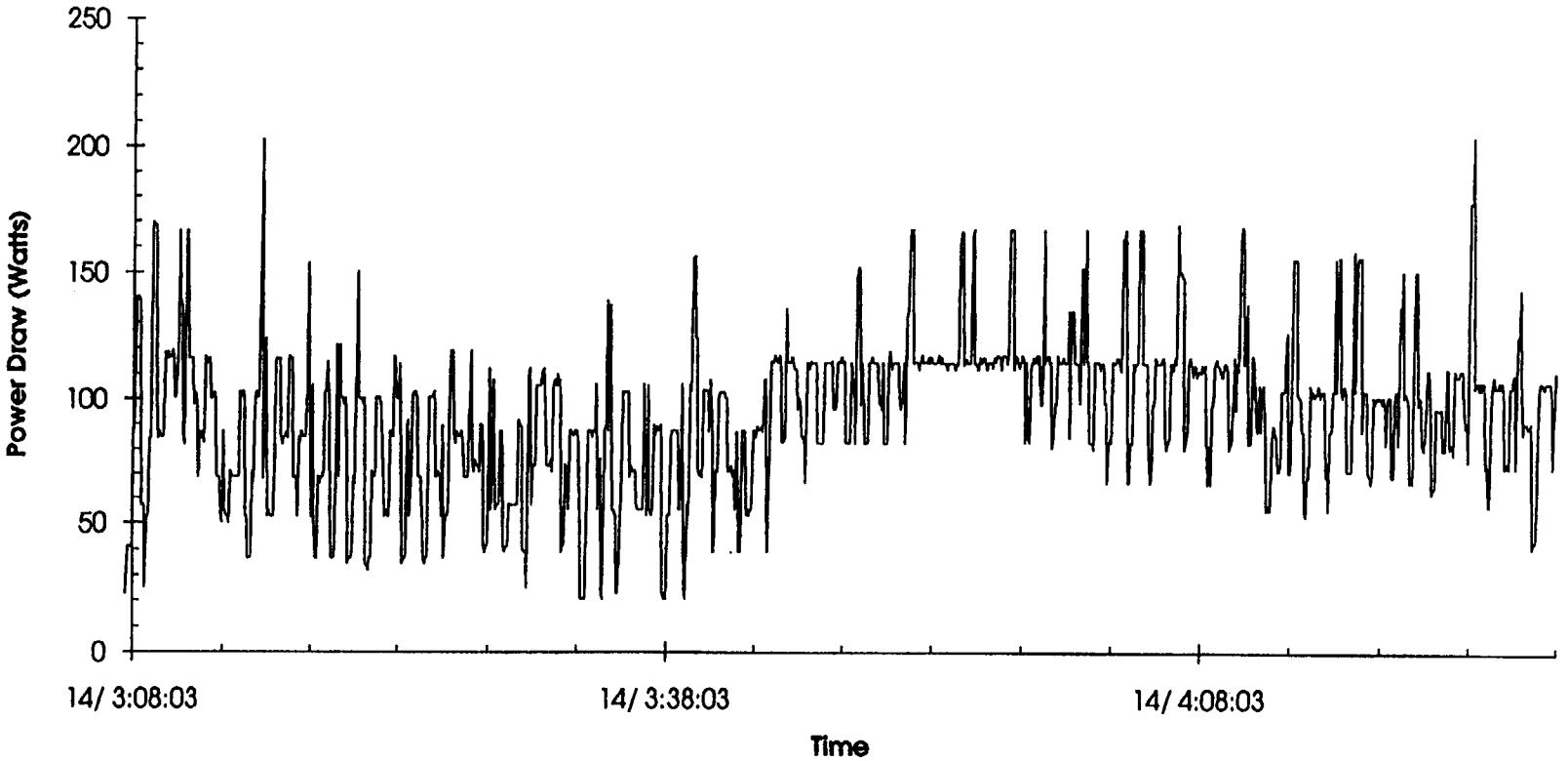


**Tail-to-Earth Avg. Pwr. 95W**

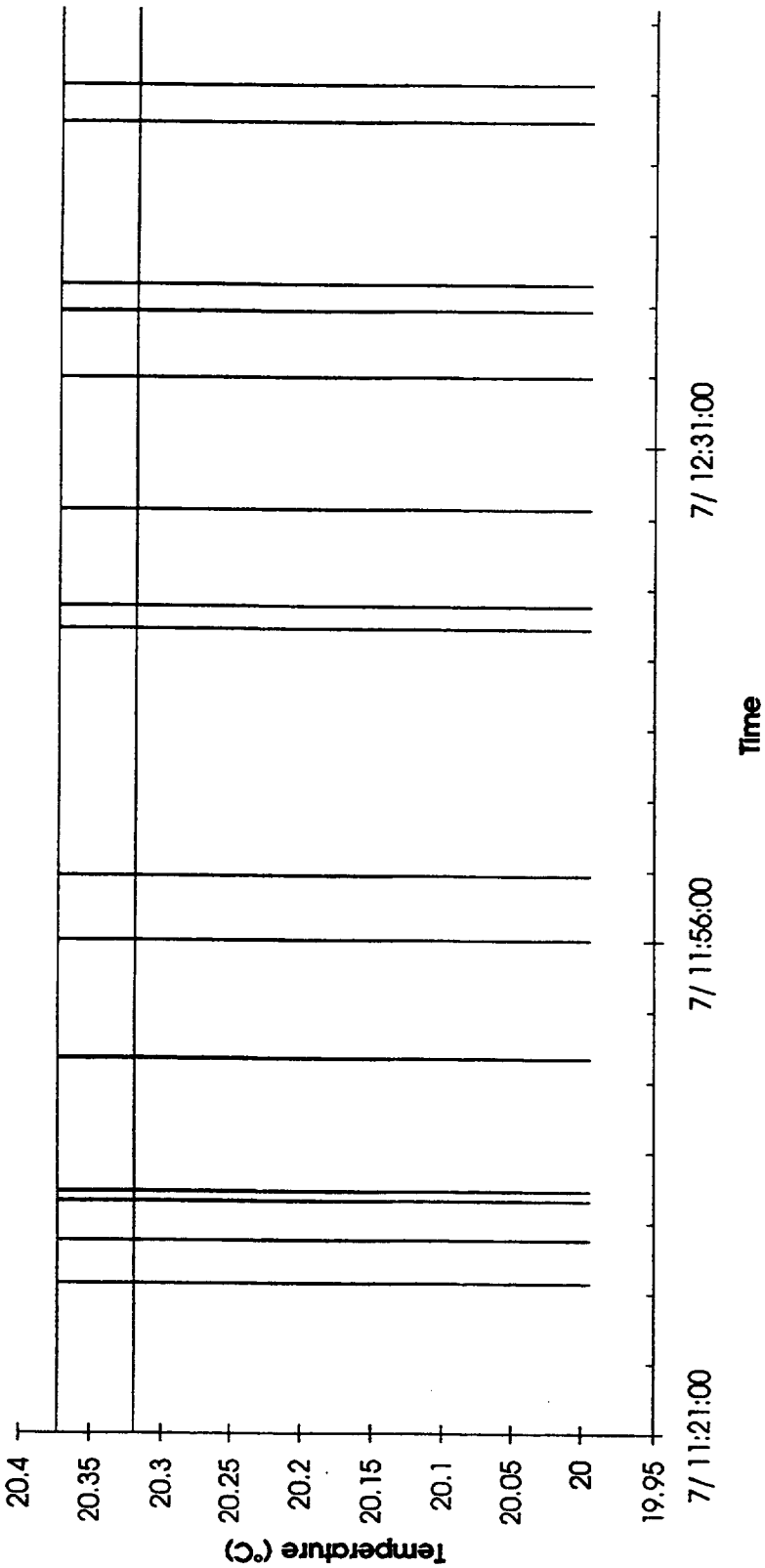
ECT Internal Thermistors, MET 3/03:21 - MET 3/05:02, Bay-to-Earth
Temperature (°C)
20.4
20.35
20.3
20.25
20.2
20.15
20.1
20.05
20
19.95
7/ 11:21:00
7/ 11:56:00
7/ 12:31:00
Time

Figure 6.

Figure 7. **ECT Power Draw, MET 3/03:21 - MET 3/05:02, Bay-to-Earth**

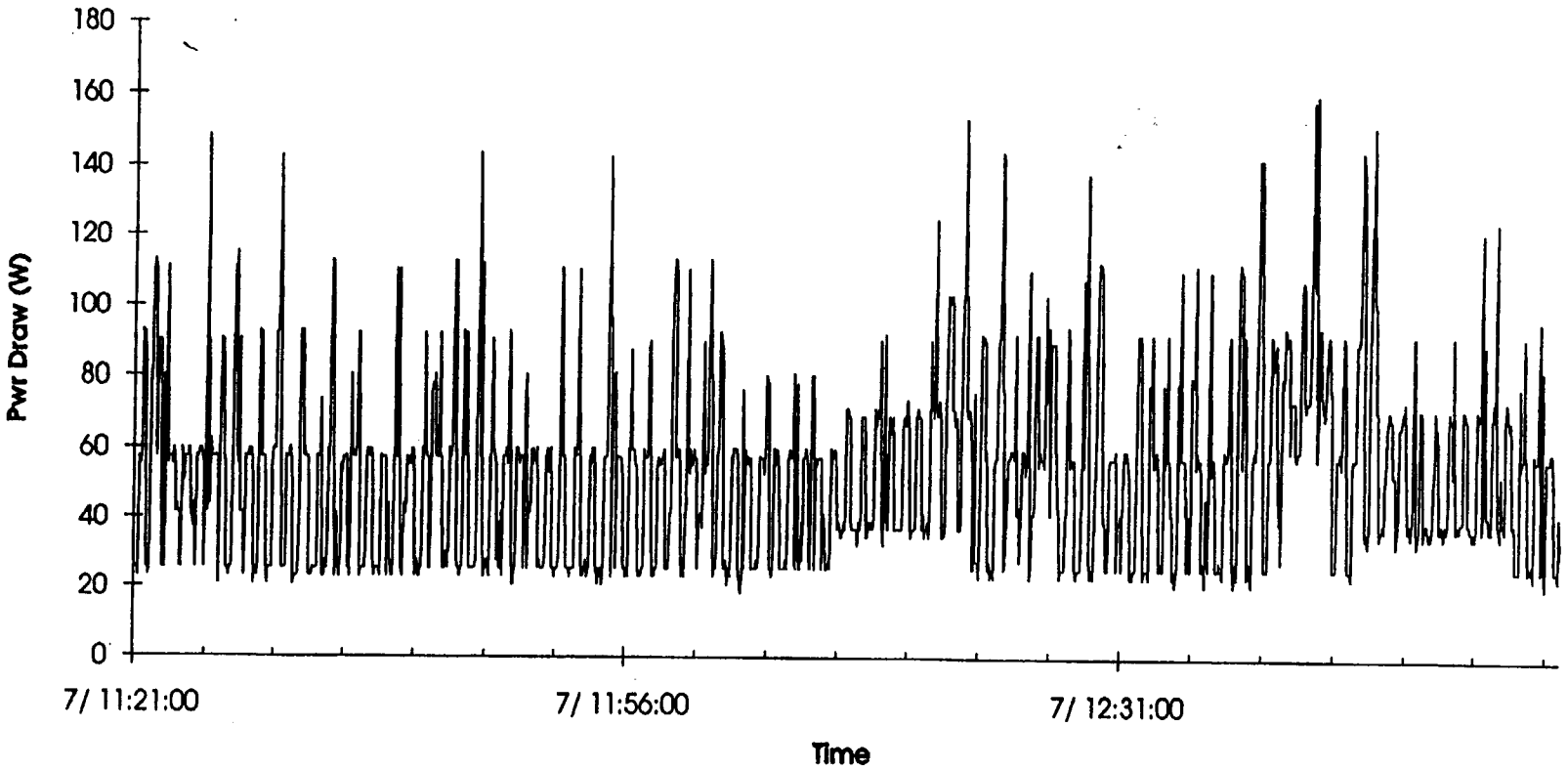


**Bay-to-Earth Avg. Pwr. 54W**

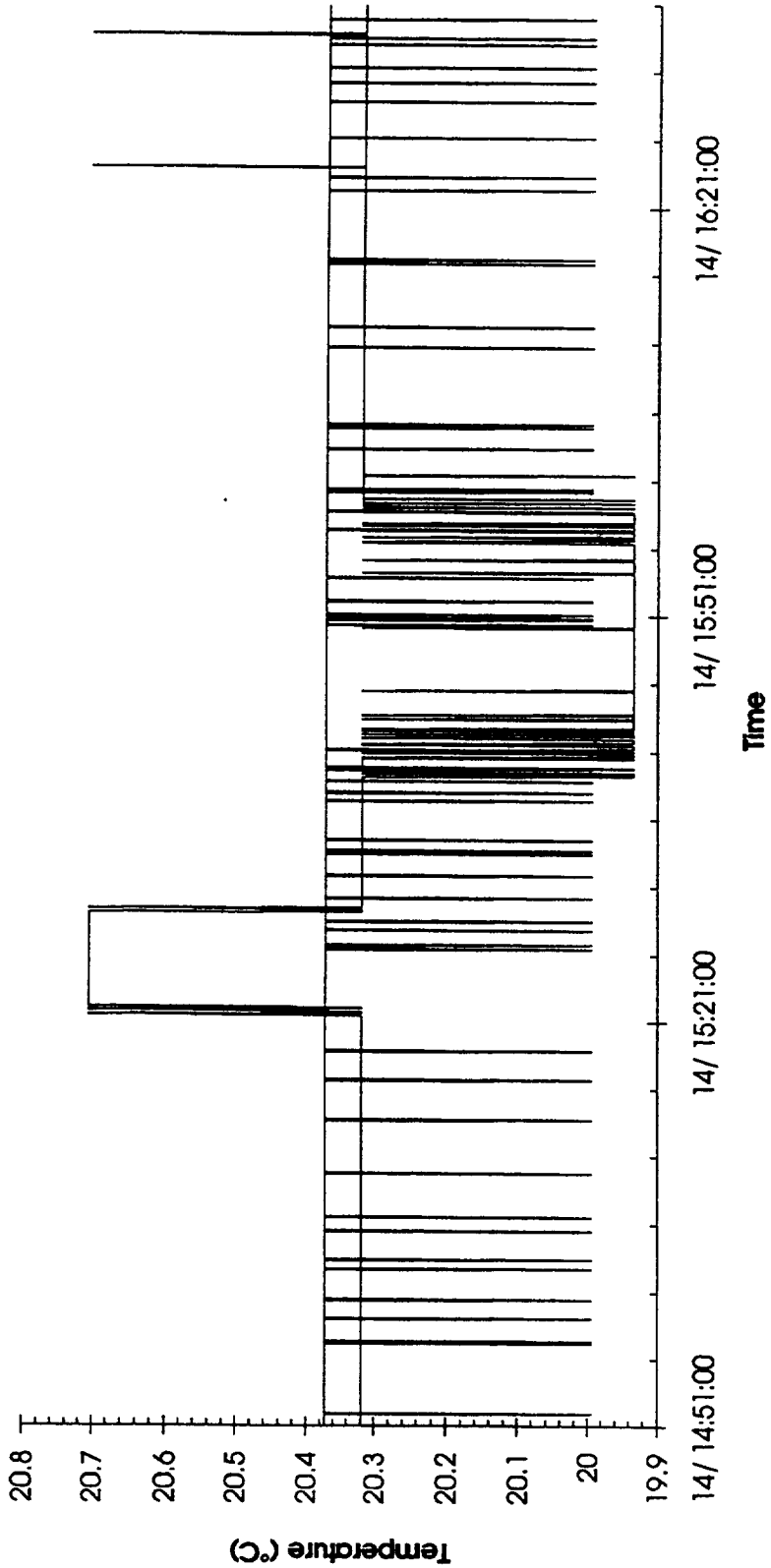
ECT Internal Thermistors, MET 10/06:51 - MET 10/08:36, Bay-to-Space
Temperature (°C)
20.8
20.7
20.6
20.5
20.4
20.3
20.2
20.1
20
19.9
14/ 14:51:00
14/ 15:21:00
14/ 15:51:00
14/ 16:21:00
Time

Figure 8.

Figure 9. **ECT Power Draw, MET 10/06:51 - MET 10/08:36, Bay-to-Space**

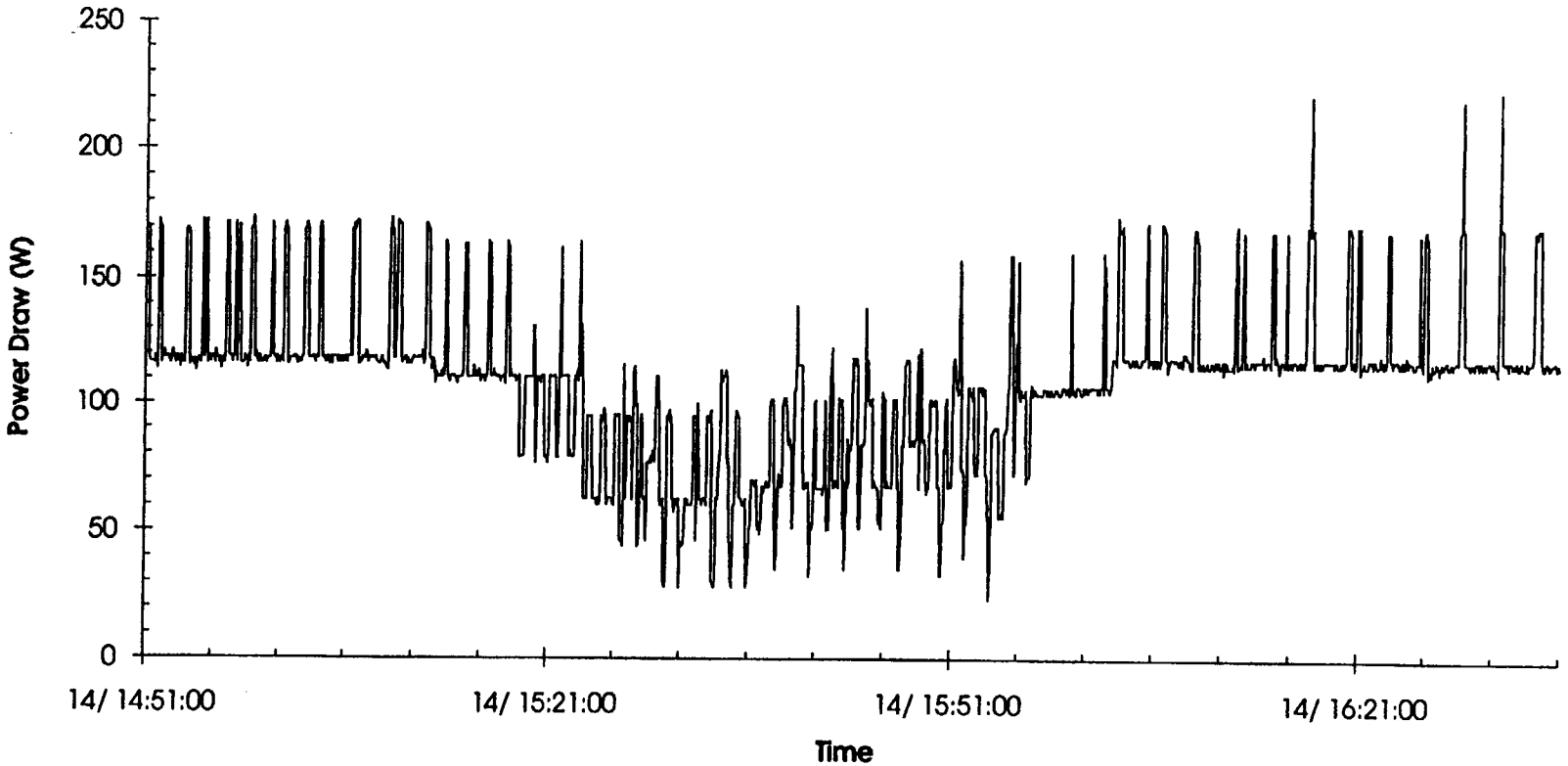


**Bay-to-Space Avg. Pwr. 109W**

## 4.2 Mechanical Performance

The ECT flight hardware and GSE mechanical performance was nominal. No damage or unusual wear was noted and all flight parts, including fasteners, were recovered after de-integration and disassembly. No mechanical spares were required for the OAST-2/STS-62 mission. No mechanical damage to the flight emulsion stack or evidence of light leakage has been reported to date.

### 4.2.1 Mechanical Interference

A mechanical interference problem was identified during GSFC integration and testing involving the pressure transducer and the adjacent mounting bolt. Gerard Durback (GSFC) elected to omit the mounting bolt during GSFC integration and testing. Upon final assembly, the pressure transducer was rotated to the extreme counter-clockwise or (nearly) vertical position when installed on the Emulsion Chamber, in order to alleviate this interference problem. No mechanical interference was encountered during integration of the ECT flight hardware at KSC and all mounting hardware was installed for flight.

### 4.2.2 Mechanical Installation

Installation of the Emulsion Chamber onto the Small Top Pallet for flight was performed by GSFC personnel with assistance from the ECT team and mounting hardware torques and gaps were set according to the procedure agreed to by Gerard Durback (GSFC) and Dr. Fran Wessling (UAH). All thermal insulation hardware was installed. During installation it was determined that some mounting hardware gaps were present on the upper side of the Emulsion Chamber mounting flange and some were present on the lower side. Gerard Durback (GSFC) elected to employ shims in either or both positions such that the total of the two gaps would be within specification. Gerard Durback (GSFC) also elected to omit all shims on the Electronics Unit mounting hardware. Final mounting bolt torque values were 160 - 170 inch-pounds for both the Emulsion Chamber and the Electronics Unit. The GSFC installation procedure is included in Appendix J.

### 4.2.3 Emulsion Chamber Internal Pressure

As shown in Figure 10, the Emulsion Chamber maintained a steady internal pressure after some initial transients. In keeping with the ECT mission approach, no extraordinary methods were used in the fabrication or assembly of the Emulsion Chamber to ensure that internal pressure is maintained during orbital flight. The O-rings used in the assembly of the Emulsion Chamber were coated with a minimum amount of vacuum grease. Leak testing followed assembly, with Helium detection and pressure decay tests. It was noted during testing that considerable amounts of Helium had been absorbed by

the stack materials, evidenced by unexpected pressure increases during pressure decay tests. The Emulsion Chamber was left pressurized with air to approximately 30 psia for shipment to KSC.

### 4.2.4 Epoxy Adhesive Bonding of Thermal Switches

An effective procedure for bonding thermal switches to the flight hardware with epoxy adhesive was developed. The ECT epoxy adhesive bonding procedure is included in Appendix K. Surface preparation and cleanliness were found to be of the utmost importance. Extra washing of the bonding site with acetone seemed to be helpful and was usually included after the last cleaning step. Our recommendation for any future use of thermal switches is that the stud-mounted variety be employed if possible, preventing the need for bonding the parts.

## 4.3 Electrical & Data Performance

The Electronics Unit system operated nominally. Thermal control of the flight hardware was uninterrupted. The AA alkaline cells for the Electronics Unit on-board memory back-up power performed nominally and the stored record from the Electronics Unit on-board memory was recovered intact, if incomplete (refer to Section 4.3.2), after the flight hardware was returned to MSFC. See Figures 10 - 13.

Temp Mentor operation was nominal. The Temp Mentor on-board memory was more than adequate, the AA alkaline cells performed nominally and the stored record from the Temp Mentor on-board memory was recovered intact after the flight hardware was returned to MSFC. See Figures 14 and 15.

### 4.3.1 Temp Mentor

The Temp Mentor RS-232 port power loop-back feature energizes the Temp Mentor RS-232 interface whenever the Temp Mentor interface cable is plugged into the Temp Mentor RS-232 port, as it is when carried aboard the Electronics Unit. (This was the cause of the Temp Mentor power depletion while at GSFC. Thus, no temperature record for the period 10/26/93 through 11/23/93 exists.) This power loop-back was disabled on the Temp Mentor's RS-232 port and instead built into the Electronics Unit's RS-232 port, feedthrough connector J7, before delivery to KSC. Temp Mentor power is now conserved because GSE cables are connected to the Electronics Unit's RS-232 port, feedthrough connector J7, for only a relatively short time, during ground operations.

If a different Temp Mentor unit is intended for flight aboard the Electronics Unit in subsequent missions the same RS-232 port power loop-back must be disabled on that Temp Mentor's RS-232 port.

Figure 10. **Emulsion Chamber Pressure**

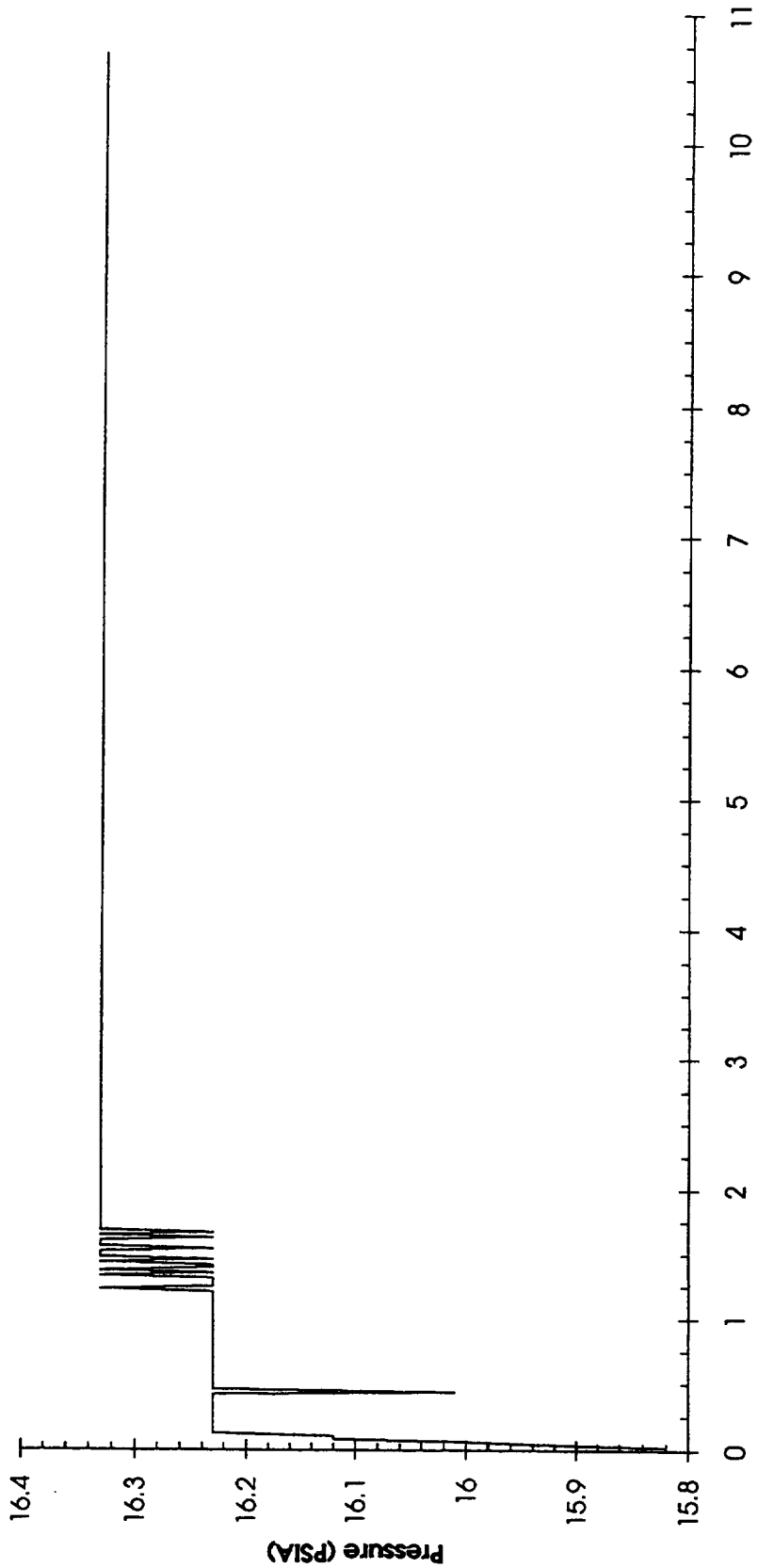

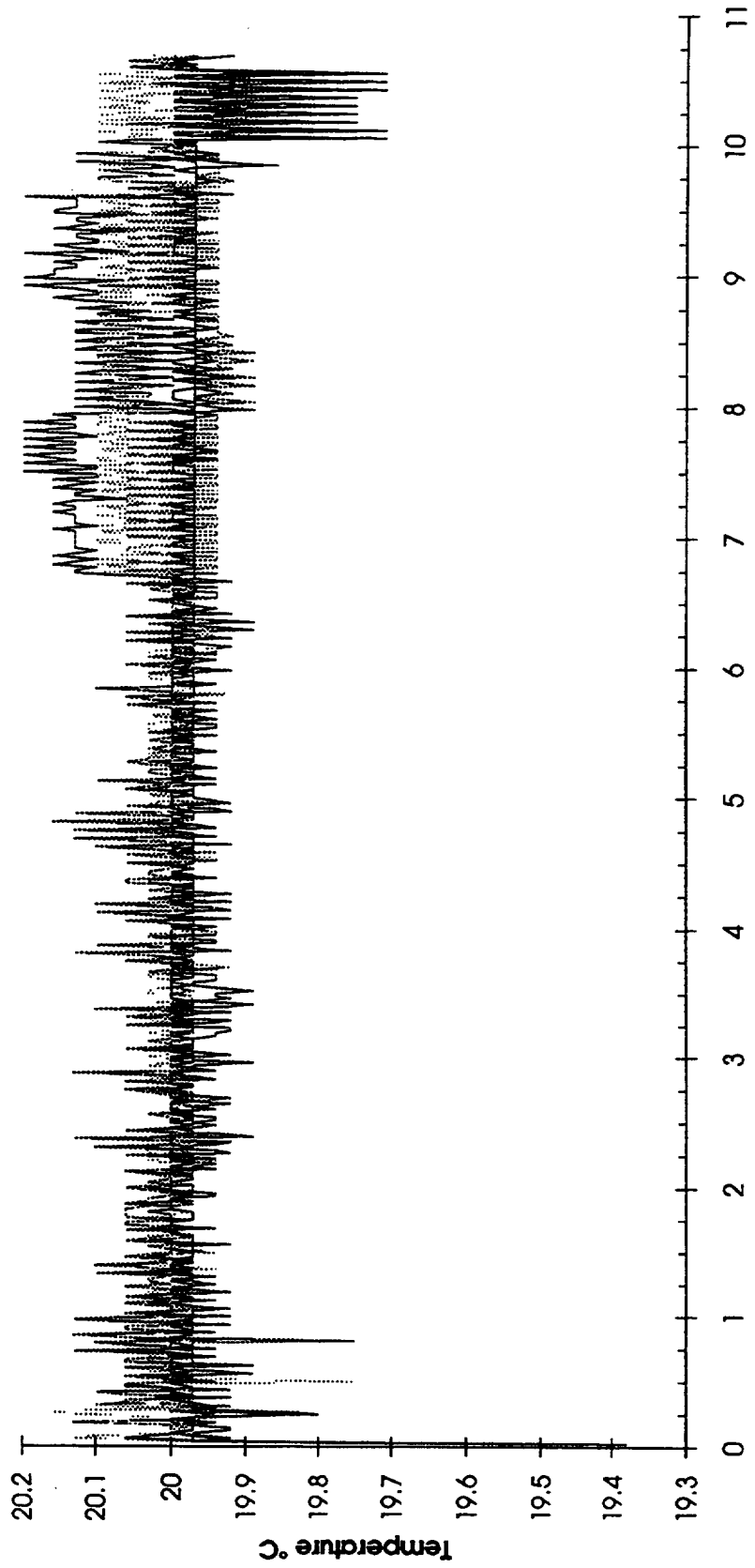
Chamber Top Thermistor Temperatures (Fine Channels 1-6)
Temperature °C
20.2
20.1
20
19.9
19.8
19.7
19.6
19.5
19.4
19.3
0
1
2
3
4
5
6
7
8
9
10
11
Power On Time (Days)

Figure 11.

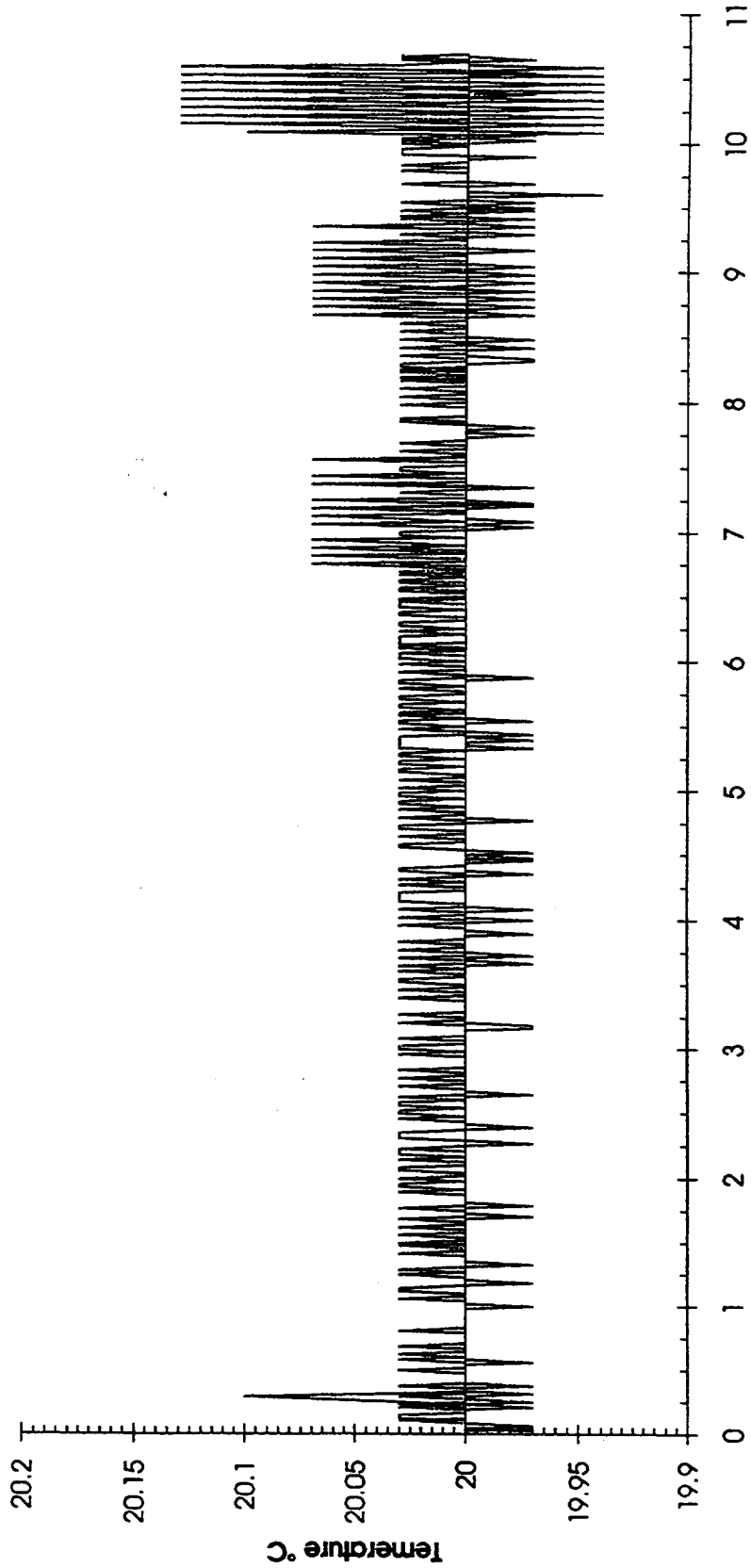
Chamber Bottom Thermistor Temperatures (Fine Channels 7-10)
Temperature °C
20.2
20.15
20.1
20.05
20
19.95
19.9
0
1
2
3
4
5
6
7
8
9
10
11
Power On Time (Days)

Figure 12.

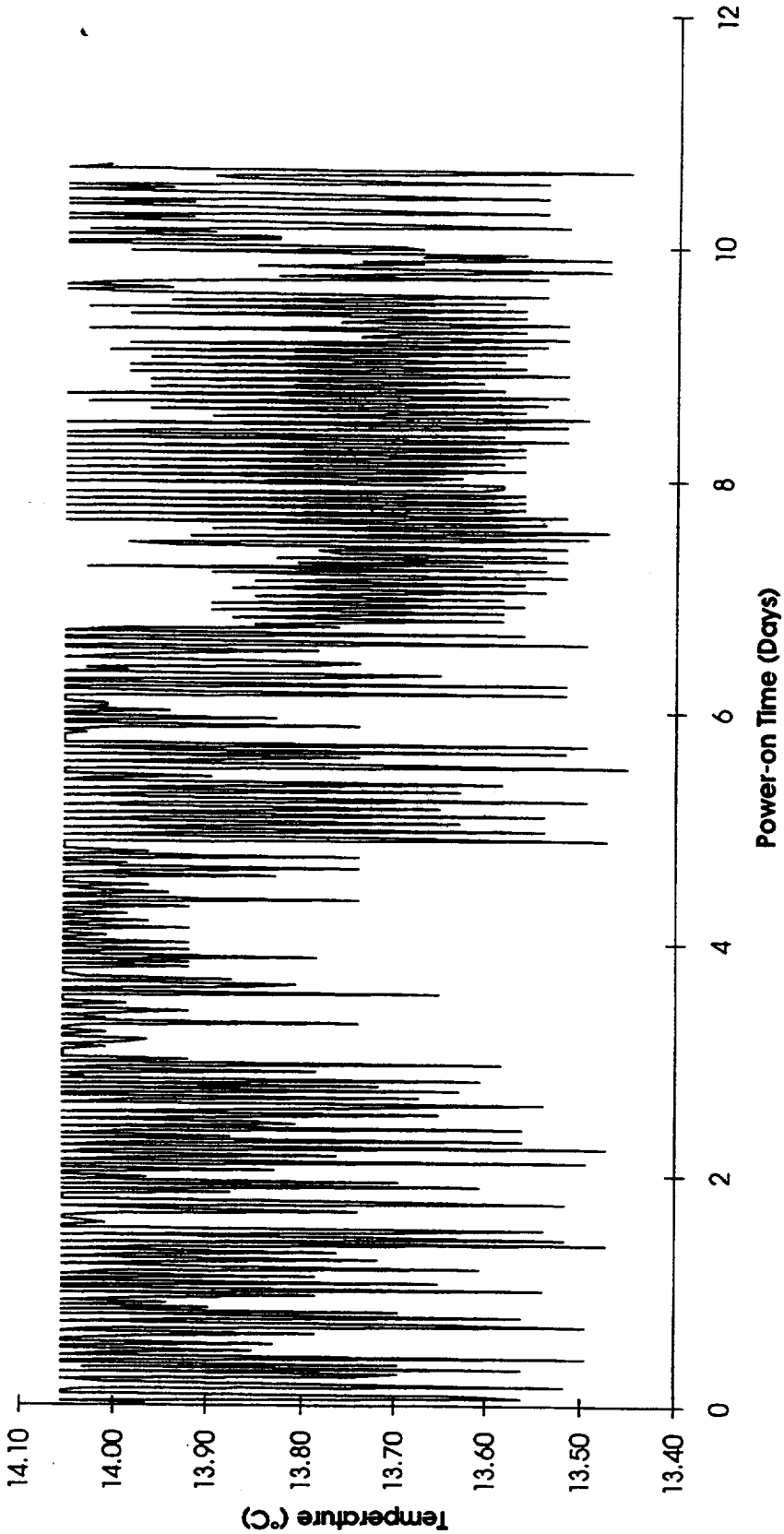
Electronics Unit Thermistor Temperature (Fine Channel 11)
Temperature (°C)
14.10
14.00
13.90
13.80
13.70
13.60
13.50
13.40
0
2
4
6
8
10
12
Power-on Time (Days)

Figure 13.

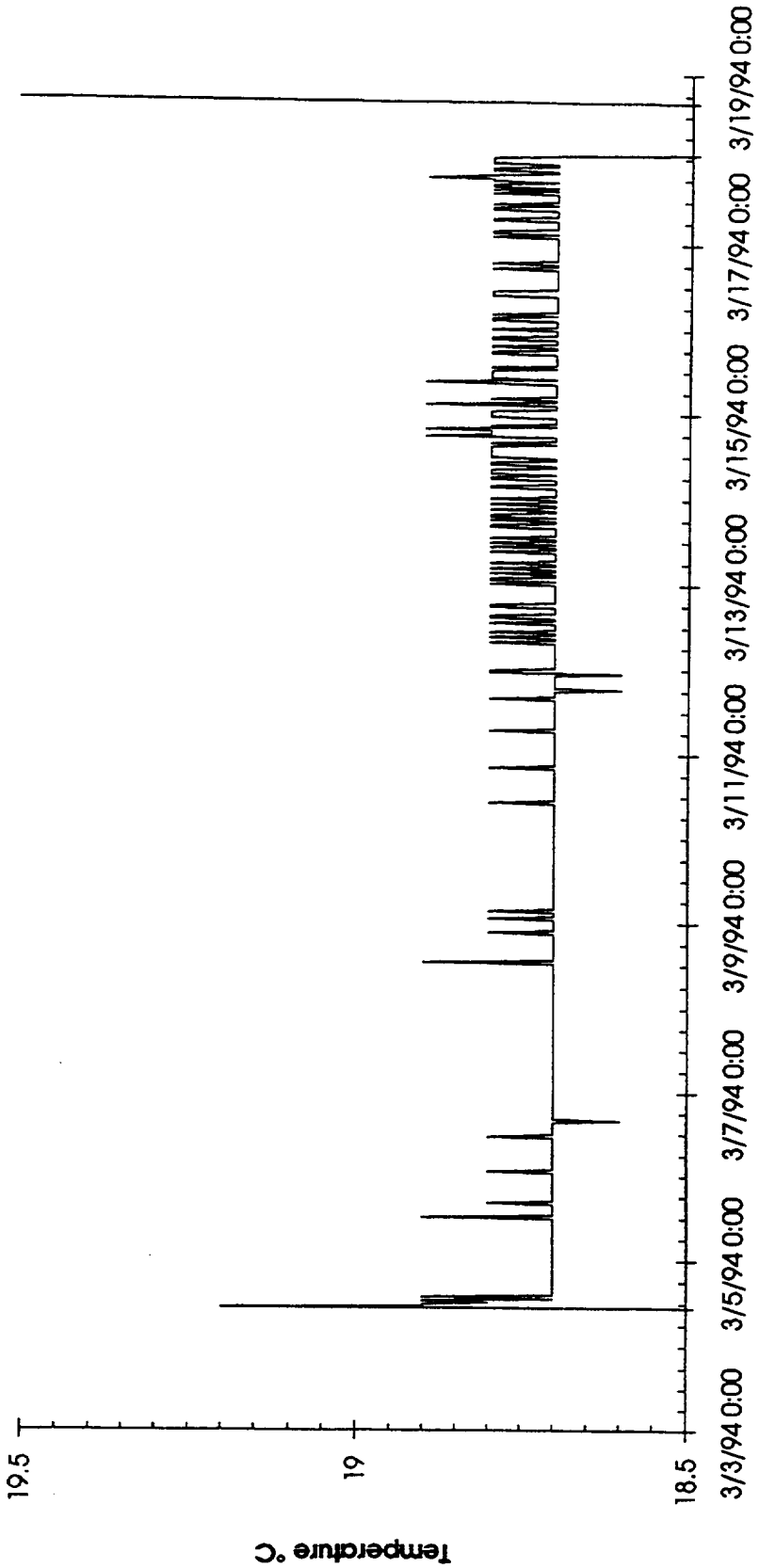
TempMentor Data for 3/3/94 to 3/19/94
Temperature °C
19.5
19
18.5
3/3/94 0:00
3/5/94 0:00
3/7/94 0:00
3/9/94 0:00
3/11/94 0:00
3/13/94 0:00
3/15/94 0:00
3/17/94 0:00
3/19/94 0:00
Date

Figure 14.

Figure 15. TempMentor Data for 1/6/94 to 3/27/94

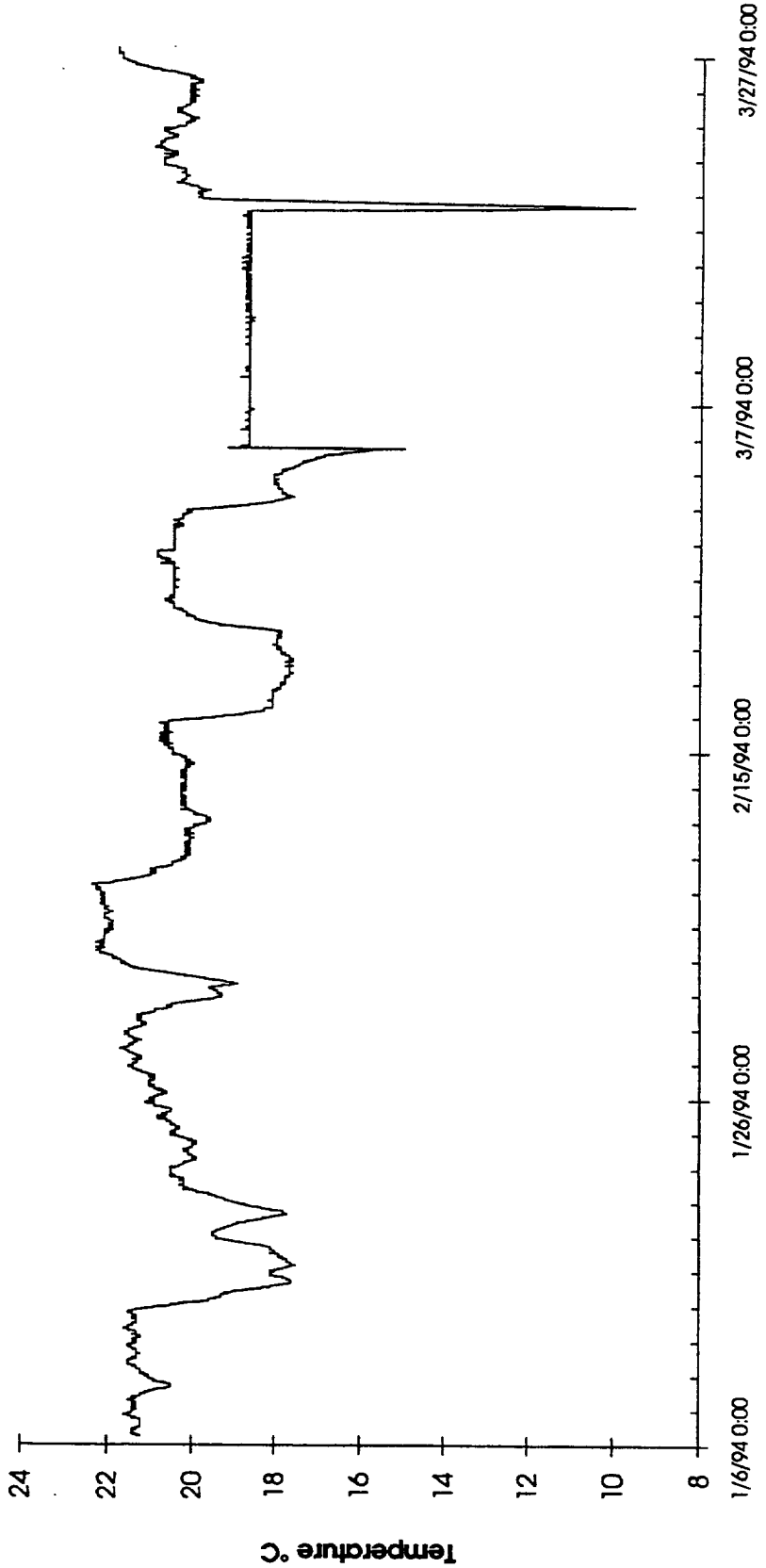

### 4.3.2 Electronics Unit

The 7/93 version of the ECT flight software was used for the OAST-2/STS-62 mission. It was loaded into the pedigreed flight PROMs for the final assembly of the Electronics Unit. The flight software was verified by more than 150 hours of test operation before final assembly of the Electronics Unit. The 7/93 version of the software prevents data overwriting so that no stored data is lost after all available on-board memory is used. However, data storage was not optimized in the 7/93 version and all available on-board memory was used by Flight Day 11. (The STS-62 flight lasted fourteen days.) Nonetheless, nominal temperature measurement and heater power control continued without interruption and the recorded data was recovered. The Temp Mentor data (Figures 14 and 15) and the telemetry data (Appendices E - I) confirm that thermal control was uninterrupted.

Data storage can be and should be made more efficient for use in subsequent missions.

### 4.3.3 Ground Software

The LabView application was used by John Weber (FS) to create software to display and capture telemetry data on spacecraft pointing, experiment power and three temperatures in real time. Due to late changes in mission planning for telemetry by JSC spacecraft pointing data was not received. The power and temperature data parameters were successfully displayed on screen and captured on hard disk.

### 4.3.4 Data Products

Utilization of the telemetry data captured by the ECT ground system turned out to be rather difficult, requiring a great amount of manual file manipulation. Snapshots of the telemetry data were printed at the POCC every thirty minutes. Plots of this data were provided by GSFC's thermal contractor and are included in Appendices E - I.

Utilization of the stored data recovered from the Electronics Unit and the Temp Mentor was straightforward. This data is shown in Figures 10 - 15. Averaging of power values did require some post-processing of the Electronics Unit data.

The primary NASA data product for telemetry is essentially a copy of the entire mission telemetry stream, accompanied by a index. This contains all telemetry data from the Orbiter and from the Hitchhiker Avionics. The necessary post-processing task was not attempted. This data has been supplied on nine-track magnetic tape and on CD-ROM.

## 5.0 Issues for Future Flights

The next flight for ECT will likely be of much longer duration than the fourteen-day flight of OAST-2/STS-62. With minor modifications, the hardware and software can be made ready for such a mission. Five issues must be addressed: (1) limited carrier spacecraft electrical power for thermal control; (2) limited electrical power for Temp Mentor power and Electronics Unit memory back-up power from ECT on-board power sources; (3) limited Temp Mentor and Electronics Unit memory for data storage; (4) the availability and compatibility of telemetry data; and (5) the availability and compatibility of electrical connectors.

### 5.1 Limited Carrier Spacecraft Power

With regard to thermal control, limitations on available carrier spacecraft electrical power will necessitate modifications to the ECT thermal control design, such as covering a portion of the radiator surface with MLI or thermal louvers. A different temperature set point for the Emulsion Chamber may also be needed, with possible impacts on flight software and thermal switches. A lower set point will affect the length of power interruption which may be tolerated without damage to the emulsion stack.

### 5.2 Limited ECT On-board Power

Back-up power for Electronics Unit memory was provided by two AA alkaline cells. The Temp Mentor power was provided by four AA alkaline cells. The adequacy of these power sources must be evaluated against missions of longer duration. The present number and/or type of cells may be inadequate.

Once again, if a new Temp Mentor is to be carried aboard the Electronics Unit, then the power loop-back must be disabled on the Temp Mentor's RS-232 port. This is intended to prevent power depletion.

### 5.3 Limited Memory

Data storage in Electronics Unit memory should be optimized. This was known before the OAST-2/STS-62 flight, but Chris Watson (UAH) was not able to complete the task in time for delivery to KSC. With the efficient use of available Electronics Unit memory, the frequency of data storage and perhaps the number of parameters stored might be adjusted such that the available Electronics Unit memory is sufficient for a mission of longer duration. The Electronics Unit design allows adding memory to the system, but a memory upgrade will result in more expense and probably more testing. The appropriate sample rate for the Temp Mentor must also be selected, based on the Temp Mentor available memory and longer mission durations.

## 5.4 Telemetry Data

During the flight of OAST-2/STS-62, data was provided to ground personnel via telemetry for experiment power and three temperatures. However, this data was handled and formatted by the Hitchhiker Avionics system prior to transmission. To enable the use of telemetry data during another flight, similar arrangements must be provided by the carrier spacecraft and compatible hardware/software resources must be made ready for ground monitoring. Close coordination between the ECT team and the appropriate authorities will be vital to the availability of telemetry data during any subsequent mission.

## 5.5 Electrical Connectors

The lack of available and compatible electrical connectors may present significant difficulties, especially if schedules are short. It is recommended that at least a flight-qualified mating connector for the Electronics Unit power feedthrough connector, J1, be located and made available as soon as possible.

## 5.6 Mechanical Interfaces

ECT is designed to be compatible with GSFC's Small Top Pallet. This interface consists of a grid of 3/8"-24 inserts on 7.000 cm centers to accept primary structural fasteners and a staggered grid of #10-32 lockplates for tie-down fasteners. For the OAST-2 mission, GSFC supplied all mounting fasteners. ECT supplied thermal standoff hardware and special parts designed to transmit shear loads.

For a future mission, a new mounting plate might be developed, if no suitable existing structure is available. Only a portion of the 3/8"-24 hole pattern and a small number of #10-32 holes for tie-downs would be required.

# 6.0 MSFC Contacts

| | |
|---|---|
| Rickey Clements, Quality Assurance | 544-7394 |
| Lou Ann Fikes, Chief Engineer's Office | 544-6495 |
| John Owens, Program Manager | 544-1969 |
| Dr. Tom Parnell, Project Scientist | 544-7690 |
| David Siersma, Payload Integration & Testing | 544-1325 |

# APPENDIX C

## Emulsion Stack Assembly Procedure

# EMULSION CHAMBER ASSEMBLY PROCEDURE
# ECT FLIGHT ARTICLE

1/28/93

CAUTION: DARKROOM CONDITIONS REQUIRED!

1. Clean the internal surfaces of the major flight structural elements of the Emulsion Chamber with alcohol. These parts are: Upper Chamber (P/N 4005), Lower Chamber (P/N 4006), Top (P/N 4012) and Bottom Plate (P/N 4013).

2. Mask and paint the internal surfaces of the major flight structural elements of the Emulsion Chamber with Krylon, Clear, No. 1303. Steps 17 and 18 of this procedure may be performed at this point.

3. Install Lower Chamber (with O-ring) on Bottom Plate. Align the Lower Chamber with the Bottom Plate and install mechanical fasteners. Install vacuum hardware. Install Lucite shims in Lower Chamber at two adjoining wall locations.

4. Build up calorimeter module emulsion stack on top of Bottom Plate inside Lower Chamber. Install the internal thermistor(s) with Eccobond 285/11. Placement will be as directed by the PI. Cut grooves in shims and plates for thermistor leads, if required. Install feedthrough connectors.

5. Install remaining Lucite shims in Lower Chamber, between the calorimeter module emulsion stack and the Lower Chamber wall at the two remaining locations opposite those shims previously installed. Insert additional Lucite or stainless steel shims until the desired fit is obtained.

6. Install window frame and mylar sheet on Lower Chamber. Connect vacuum source to Lower Chamber vacuum port.

7. Evacuate Lower Chamber and check calorimeter module emulsion stack height and flatness. Remove window frame and mylar sheet and adjust calorimeter module emulsion stack as needed.

8. Repeat Steps 6 and 7 of this procedure as necessary to obtain desired stable calorimeter module emulsion stack height and flatness.

9. Install steel divider plate on Lower Chamber.

10. Install Upper Chamber (with O-ring) on Lower Chamber. Align the Upper Chamber with the Lower Chamber and install mechanical fasteners. Install vacuum hardware. Install Lucite shims in Lower Chamber at two adjoining wall locations.

11. Build up producer module emulsion stack on top of steel divider plate inside Upper Chamber. Install the internal thermistor(s) with Eccobond 285/11. Placement will be as directed by the PI. Cut grooves in shims and plates for thermistor leads, if required. Install feedthrough connectors.

12. Install remaining Lucite shims in Upper Chamber, between the calorimeter module emulsion stack and the Upper Chamber wall at the two remaining locations opposite those shims previously installed. Insert additional Lucite or stainless steel shims until the desired fit is obtained.

13. Install window frame and mylar sheet on Upper Chamber. Connect vacuum source to Upper Chamber vacuum port.

14. Evacuate Upper Chamber and check producer module emulsion stack height and flatness. Remove window frame and mylar sheet and adjust producer module emulsion stack as needed.

15. Repeat Steps 13 and 14 of this procedure as necessary to obtain desired stable producer module emulsion stack height and flatness.

16. Install Top (with O-ring) on Upper Chamber. Align the Top with the Upper Chamber and install mechanical fasteners.

17. Clean the external surfaces of the major flight structural elements of the Emulsion Chamber with alcohol. These parts are: Upper Chamber (P/N 4005), Lower Chamber (P/N 4006), Top (P/N 4012) and Bottom Plate (P/N 4013).

18. Install Emulsion Chamber external thermal and electrical hardware on the major flight structural elements of the Emulsion Chamber.

# APPENDIX D

## Flight Emulsion Stack Configuration

# ECT MATERIALS COMPOSITION

| *NAME* | MATERIAL NAME | THICKNESS µm | MASS g/cm2 | HEIGHT µm | mfp % | r.l. % | Sum mfp % | Sum r.l. % | Sum g/cm2 |
|---|---|---|---|---|---|---|---|---|---|
| ********** | APPENDICES | | | 200,000 | | | 0.000 | 0.000 | 0.000 |
| RUBBER | SHIM | 4,890.000 | 1.298 | 200,000 | 0.148 | 0.865 | 0.148 | 0.865 | 1.298 |
| PLASTIC #1 | NEUTRON MON | 600.000 | 0.085 | 195,110 | 0.102 | 0.210 | 0.249 | 1.076 | 1.383 |
| PLASTIC #2 | NEUTRON MON | 600.000 | 0.085 | 194,510 | 0.102 | 0.210 | 0.351 | 1.286 | 1.468 |
| PLASTIC #3 | NEUTRON MON | 600.000 | 0.085 | 193,910 | 0.102 | 0.210 | 0.453 | 1.496 | 1.554 |
| PLASTIC #4 | THERMISTA | 600.000 | 0.085 | 193,310 | 0.102 | 0.210 | 0.555 | 1.706 | 1.639 |
| PLASTIC #5 | NEUTRON MON | 600.000 | 0.085 | 192,040 | 0.102 | 0.210 | 0.657 | 1.916 | 1.724 |
| PLASTIC #6 | NEUTRON MON | 600.000 | 0.085 | 191,440 | 0.102 | 0.210 | 0.759 | 2.127 | 1.809 |
| PLASTIC #7 | TLD'S | 600.000 | 0.085 | 190,840 | 0.102 | 0.210 | 0.861 | 2.337 | 1.894 |
| ********** | END OF APP. | | | 190,240 | | | 0.861 | 2.337 | 1.894 |
| | | | | 190,240 | | | 0.861 | 2.337 | 1.894 |
| | | | | 190,240 | | | 0.861 | 2.337 | 1.894 |
| ********** | ******** | | | 190,240 | | | 0.861 | 2.337 | 1.894 |
| PRIMARY | MODULE | | | 190,240 | | | 0.861 | 2.337 | 1.894 |
| ********** | ******** | | | 190,240 | | | 0.861 | 2.337 | 1.894 |
| | | | | 190,240 | | | 0.861 | 2.337 | 1.894 |
| | | | | 190,240 | | | 0.861 | 2.337 | 1.894 |
| HRH-HR8 #1 | SCREEN FILM | 3,500.000 | 0.081 | 190,240 | 0.920 | 5.466 | 1.781 | 7.803 | 1.976 |
| P1 (E33-25) | CR-39 | 600.000 | 0.087 | 186,740 | 0.102 | 0.210 | 1.883 | 8.013 | 2.063 |
| G01 | GLASSINE | 25.000 | 0.005 | 186,140 | 0.005 | 0.004 | 1.888 | 8.017 | 2.068 |
| P02 (P1) ——* | EMULSION 7B | 200.000 | 0.077 | 186,115 | 0.058 | 0.702 | 1.946 | 8.719 | 2.145 |
| * | LUCITE 300 | 300.000 | 0.035 | 185,915 | 0.051 | 0.105 | 1.997 | 8.824 | 2.180 |
| * | EMULSION 6B | 200.000 | 0.077 | 185,615 | 0.058 | 0.702 | 2.054 | 9.525 | 2.257 |
| G03 — | GLASSINE | 25.000 | 0.005 | 185,415 | 0.005 | 0.004 | 2.059 | 9.529 | 2.262 |
| P03————* | EMULSION 7B | 75.000 | 0.029 | 185,390 | 0.022 | 0.263 | 2.081 | 9.792 | 2.291 |
| * | LUCITE 500 | 800.000 | 0.059 | 185,315 | 0.136 | 0.280 | 2.217 | 10.073 | 2.350 |
| * | EMULSION 6B | 75.000 | 0.029 | 184,515 | 0.022 | 0.263 | 2.239 | 10.336 | 2.379 |
| G04 — | GLASSINE | 25.000 | 0.005 | 184,440 | 0.005 | 0.004 | 2.244 | 10.340 | 2.384 |
| P04————* | EMULSION 7B | 200.000 | 0.772 | 184,415 | 0.058 | 0.702 | 2.301 | 11.041 | 3.156 |
| * | LUCITE BASE | 300.000 | 0.035 | 184,215 | 0.051 | 0.105 | 2.352 | 11.147 | 3.191 |
| * | EMULSION 6B | 200.000 | 0.772 | 183,915 | 0.058 | 0.702 | 2.410 | 11.848 | 3.963 |
| G05 — | GLASSINE | 25.000 | 0.005 | 183,715 | 0.005 | 0.004 | 2.415 | 11.852 | 3.968 |
| P06————* | EMULSION 7B | 75.000 | 0.029 | 183,690 | 0.022 | 0.263 | 2.437 | 12.115 | 3.997 |
| * | LUCITE BASE | 800.000 | 0.059 | 183,615 | 0.136 | 0.280 | 2.573 | 12.396 | 4.056 |
| * | EMULSION 7B | 75.000 | 0.029 | 182,815 | 0.022 | 0.263 | 2.594 | 12.659 | 4.085 |
| G07 — | GLASSINE | 25.000 | 0.005 | 182,740 | 0.005 | 0.004 | 2.599 | 12.663 | 4.090 |
| P07————* | EMULSION 7B | 200.000 | 0.772 | 182,715 | 0.058 | 0.702 | 2.657 | 13.364 | 4.862 |
| * | LUCITE BASE | 300.000 | 0.035 | 182,515 | 0.051 | 0.105 | 2.708 | 13.469 | 4.897 |
| * | EMULSION 6B | 200.000 | 0.772 | 182,215 | 0.058 | 0.702 | 2.765 | 14.171 | 5.669 |
| G08 — | GLASSINE | 25.000 | 0.005 | 182,015 | 0.022 | 0.263 | 2.787 | 14.434 | 5.674 |
| P09————* | EMULSION 7B | 75.000 | 0.029 | 181,990 | 0.022 | 0.263 | 2.809 | 14.697 | 5.703 |
| * | LUCITE BASE | 800.000 | 0.059 | 181,915 | 0.136 | 0.280 | 2.945 | 14.978 | 5.762 |
| * | EMULSION 7B | 75.000 | 0.029 | 181,115 | 0.022 | 0.263 | 2.966 | 15.241 | 5.791 |
| | | | | 181,040 | | | 2.966 | 15.241 | 5.791 |
| ********** | ******** | | | 181,040 | | | 2.966 | 15.241 | 5.791 |
| PRODUCER | MODULE | | | 181,040 | | | 2.966 | 15.241 | 5.791 |
| ********** | ******** | | | 181,040 | | | 2.966 | 15.241 | 5.791 |
| | | | | 181,040 | | | 2.966 | 15.241 | 5.791 |
| | ********** | | | 181,040 | | | 2.966 | 15.241 | 5.791 |
| | PRODUCER | | | 181,040 | | | 2.966 | 15.241 | 5.791 |
| | 1ST CYCLE | | | 181,040 | | | 2.966 | 15.241 | 5.791 |
| | ********** | | | 181,040 | | | 2.966 | 15.241 | 5.791 |
| | | | | 181,040 | | | 2.966 | 15.241 | 5.791 |
| G10 — | GLASSINE | 25.000 | 0.005 | 181,040 | 0.022 | 0.263 | 2.988 | 15.504 | 5.796 |
| P10————* | EMULSION 7B | 200.000 | 0.772 | 181,015 | 0.058 | 0.702 | 3.045 | 16.205 | 6.568 |

# ECT MATERIALS COMPOSITION

| NAME | MATERIAL NAME | THICKNESS µm | MASS g/cm2 | HEIGHT µm | mfp % | r.l. % | Sum mfp % | Sum r.l. % | Sum g/cm2 |
|---|---|---|---|---|---|---|---|---|---|
| | | | | | | | | | |
| * | LUCITE BASE | 300.000 | 0.035 | 180,815 | 0.051 | 0.105 | 3.096 | 16.311 | 6.604 |
| * | EMULSION 7B | 200.000 | 0.772 | 180,515 | 0.058 | 0.702 | 3.154 | 17.012 | 7.376 |
| G11 — | GLASSINE | 25.000 | 0.005 | 180,315 | 0.022 | 0.263 | 3.176 | 17.275 | 7.381 |
| P11———* | EMULSION 7B | 75.000 | 0.029 | 180,290 | 0.022 | 0.263 | 3.197 | 17.538 | 7.410 |
| * | LUCITE BASE | 800.000 | 0.059 | 180,215 | 0.136 | 0.280 | 3.333 | 17.819 | 7.469 |
| * | EMULSION 7B | 75.000 | 0.029 | 179,415 | 0.022 | 0.263 | 3.355 | 18.082 | 7.498 |
| G12 — | GLASSINE | 25.000 | 0.005 | 179,340 | 0.005 | 0.004 | 3.360 | 18.086 | 7.503 |
| P12———* | EMULSION 7B | 75.000 | 0.029 | 179,315 | 0.022 | 0.263 | 3.381 | 18.349 | 7.532 |
| * | LUCITE BASE | 800.000 | 0.059 | 179,240 | 0.136 | 0.280 | 3.517 | 18.629 | 7.591 |
| * | EMULSION 7B | 75.000 | 0.029 | 178,440 | 0.022 | 0.263 | 3.539 | 18.892 | 7.620 |
| G13 — | GLASSINE | 25.000 | 0.005 | 178,365 | 0.005 | 0.004 | 3.544 | 18.896 | 7.625 |
| L1 | LEAD | 500.000 | 0.568 | 178,340 | 0.292 | 8.910 | 3.836 | 27.806 | 8.192 |
| G14 — | GLASSINE | 25.000 | 0.005 | 177,840 | 0.022 | 0.263 | 3.858 | 28.069 | 8.197 |
| P13———* | EMULSION 7B | 75.000 | 0.029 | 177,815 | 0.022 | 0.263 | 3.879 | 28.332 | 8.226 |
| * | LUCITE BASE | 800.000 | 0.059 | 177,740 | 0.136 | 0.280 | 4.015 | 28.613 | 8.285 |
| * | EMULSION 7B | 75.000 | 0.029 | 176,940 | 0.022 | 0.263 | 4.037 | 28.876 | 8.314 |
| G15 — | GLASSINE | 25.000 | 0.005 | 176,865 | 0.005 | 0.004 | 4.042 | 28.880 | 8.319 |
| CR1 (P14) | CR-39 | 600.000 | 0.087 | 176,840 | 0.104 | 0.215 | 4.146 | 29.094 | 8.406 |
| G16 — | GLASSINE | 25.000 | 0.005 | 176,240 | 0.005 | 0.004 | 4.151 | 29.098 | 8.411 |
| P15———* | EMULSION 7B | 75.000 | 0.029 | 176,215 | 0.022 | 0.263 | 4.173 | 29.361 | 8.440 |
| * | LUCITE BASE | 800.000 | 0.059 | 176,140 | 0.136 | 0.280 | 4.309 | 29.641 | 8.499 |
| * | EMULSION 7B | 75.000 | 0.029 | 175,340 | 0.022 | 0.263 | 4.330 | 29.905 | 8.528 |
| | | | | 175,265 | | | 4.330 | 29.905 | 8.528 |
| | ********** | | | 175,265 | | | 4.330 | 29.905 | 8.528 |
| | PRODUCER | | | 175,265 | | | 4.330 | 29.905 | 8.528 |
| | 2ND CYCLE | | | 175,265 | | | 4.330 | 29.905 | 8.528 |
| | ********** | | | 175,265 | | | 4.330 | 29.905 | 8.528 |
| | | | | 175,265 | | | 4.330 | 29.905 | 8.528 |
| G17 — | GLASSINE | 25.000 | 0.005 | 175,265 | 0.022 | 0.263 | 4.352 | 30.168 | 8.533 |
| P16———* | EMULSION 7B | 200.000 | 0.772 | 175,240 | 0.058 | 0.702 | 4.410 | 30.869 | 9.305 |
| * | LUCITE BASE | 300.000 | 0.035 | 175,040 | 0.051 | 0.105 | 4.461 | 30.974 | 9.341 |
| * | EMULSION 6B | 200.000 | 0.772 | 174,740 | 0.058 | 0.702 | 4.518 | 31.676 | 10.113 |
| G18 — | GLASSINE | 25.000 | 0.005 | 174,540 | 0.022 | 0.263 | 4.540 | 31.939 | 10.118 |
| P17———* | EMULSION 7B | 75.000 | 0.029 | 174,515 | 0.022 | 0.263 | 4.561 | 32.202 | 10.147 |
| * | LUCITE BASE | 800.000 | 0.059 | 174,440 | 0.136 | 0.280 | 4.697 | 32.483 | 10.206 |
| * | EMULSION 7B | 75.000 | 0.029 | 173,640 | 0.022 | 0.263 | 4.719 | 32.746 | 10.235 |
| G19 — | GLASSINE | 25.000 | 0.005 | 173,565 | 0.005 | 0.004 | 4.724 | 32.750 | 10.240 |
| P18———* | EMULSION 7B | 75.000 | 0.029 | 173,540 | 0.022 | 0.263 | 4.746 | 33.013 | 10.269 |
| * | LUCITE BASE | 800.000 | 0.059 | 173,465 | 0.136 | 0.280 | 4.882 | 33.293 | 10.328 |
| * | EMULSION 7B | 75.000 | 0.029 | 172,665 | 0.022 | 0.263 | 4.903 | 33.556 | 10.357 |
| G20 — | GLASSINE | 25.000 | 0.005 | 172,590 | 0.005 | 0.004 | 4.908 | 33.560 | 10.362 |
| L2 | LEAD | 500.000 | 0.568 | 172,565 | 0.292 | 8.910 | 5.201 | 42.470 | 10.929 |
| G21 — | GLASSINE | 25.000 | 0.005 | 172,065 | 0.022 | 0.263 | 5.222 | 42.733 | 10.934 |
| P19———* | EMULSION 7B | 75.000 | 0.029 | 172,040 | 0.022 | 0.263 | 5.244 | 42.996 | 10.963 |
| * | LUCITE BASE | 800.000 | 0.059 | 171,965 | 0.136 | 0.280 | 5.380 | 43.276 | 11.022 |
| * | EMULSION 7B | 75.000 | 0.029 | 171,165 | 0.022 | 0.263 | 5.401 | 43.540 | 11.051 |
| G22 — | GLASSINE 25 | 25.000 | 0.005 | 171,090 | 0.005 | 0.004 | 5.406 | 43.543 | 11.056 |
| CR2 (P20) | CR-39 | 600.000 | 0.087 | 171,065 | 0.104 | 0.215 | 5.510 | 43.758 | 11.143 |
| G23 — | GLASSINE | 25.000 | 0.005 | 170,465 | 0.005 | 0.004 | 5.516 | 43.762 | 11.148 |
| P21———* | EMULSION 7B | 75.000 | 0.029 | 170,440 | 0.022 | 0.263 | 5.537 | 44.025 | 11.177 |
| * | LUCITE BASE | 800.000 | 0.059 | 170,365 | 0.136 | 0.280 | 5.673 | 44.305 | 11.236 |
| * | EMULSION 7B | 75.000 | 0.029 | 169,565 | 0.022 | 0.263 | 5.695 | 44.568 | 11.265 |
| | | | | 169,490 | | | 5.695 | 44.568 | 11.265 |
| | ********** | | | 169,490 | | | 5.695 | 44.568 | 11.265 |
| | PRODUCER | | | 169,490 | | | 5.695 | 44.568 | 11.265 |

# ECT MATERIALS COMPOSITION

| NAME | MATERIAL NAME | THICKNESS µm | MASS g/cm2 | HEIGHT µm | mfp % | r.l. % | Sum mfp % | Sum r.l. % | Sum g/cm2 |
|---|---|---|---|---|---|---|---|---|---|
| | | | | | | | | | |
| | 3RD CYCLE | | | 169,490 | | | 5.695 | 44.568 | 11.265 |
| | ********** | | | 169,490 | | | 5.695 | 44.568 | 11.265 |
| | | | | 169,490 | | | 5.695 | 44.568 | 11.265 |
| G24 — | GLASSINE | 25.000 | 0.005 | 169,490 | 0.005 | 0.004 | 5.700 | 44.572 | 11.270 |
| P22———* | EMULSION 7B | 200.000 | 0.772 | 169,465 | 0.058 | 0.702 | 5.757 | 45.274 | 12.042 |
| * | LUCITE BASE | 300.000 | 0.035 | 169,265 | 0.051 | 0.105 | 5.808 | 45.379 | 12.078 |
| * | EMULSION 7B | 200.000 | 0.772 | 168,965 | 0.058 | 0.702 | 5.866 | 46.081 | 12.850 |
| G25 — | GLASSINE | 25.000 | 0.005 | 168,765 | 0.005 | 0.004 | 5.871 | 46.085 | 12.855 |
| P23———* | EMULSION 7B | 75.000 | 0.029 | 168,740 | 0.022 | 0.263 | 5.893 | 46.348 | 12.884 |
| * | LUCITE BASE | 800.000 | 0.059 | 168,665 | 0.136 | 0.280 | 6.029 | 46.628 | 12.943 |
| * | EMULSION 7B | 75.000 | 0.029 | 167,865 | 0.022 | 0.263 | 6.050 | 46.891 | 12.972 |
| G26 — | GLASSINE | 25.000 | 0.005 | 167,790 | 0.005 | 0.004 | 6.055 | 46.895 | 12.977 |
| P24———* | EMULSION 7B | 75.000 | 0.029 | 167,765 | 0.022 | 0.263 | 6.077 | 47.158 | 13.006 |
| * | LUCITE BASE | 800.000 | 0.059 | 167,690 | 0.136 | 0.280 | 6.213 | 47.439 | 13.065 |
| * | EMULSION 7B | 75.000 | 0.029 | 166,890 | 0.022 | 0.263 | 6.234 | 47.702 | 13.094 |
| G27 — | GLASSINE | 25.000 | 0.005 | 166,815 | 0.005 | 0.004 | 6.240 | 47.706 | 13.099 |
| L3 | LEAD | 500.000 | 0.568 | 166,790 | 0.292 | 8.910 | 6.532 | 56.615 | 13.666 |
| G28 — | GLASSINE | 25.000 | 0.005 | 166,290 | 0.022 | 0.263 | 6.553 | 56.879 | 13.671 |
| P25———* | EMULSION 7B | 75.000 | 0.029 | 166,265 | 0.022 | 0.263 | 6.575 | 57.142 | 13.700 |
| * | LUCITE BASE | 800.000 | 0.059 | 166,190 | 0.136 | 0.280 | 6.711 | 57.422 | 13.759 |
| * | EMULSION 7B | 75.000 | 0.029 | 165,390 | 0.022 | 0.263 | 6.733 | 57.685 | 13.788 |
| G29 — | GLASSINE | 25.000 | 0.005 | 165,315 | 0.005 | 0.004 | 6.738 | 57.689 | 13.793 |
| CR3 (P26) | CR-39 | 600.000 | 0.087 | 165,290 | 0.104 | 0.215 | 6.842 | 57.904 | 13.880 |
| G30 — | GLASSINE | 25.000 | 0.005 | 164,690 | 0.005 | 0.004 | 6.847 | 57.908 | 13.885 |
| P27———* | EMULSION 7B | 75.000 | 0.029 | 164,665 | 0.022 | 0.263 | 6.869 | 58.171 | 13.914 |
| * | LUCITE BASE | 800.000 | 0.059 | 164,590 | 0.136 | 0.280 | 7.004 | 58.451 | 13.973 |
| * | EMULSION 7B | 75.000 | 0.029 | 163,790 | 0.022 | 0.263 | 7.026 | 58.714 | 14.002 |
| | | | | 163,715 | | | 7.026 | 58.714 | 14.002 |
| | ********** | | | 163,715 | | | 7.026 | 58.714 | 14.002 |
| | PRODUCER | | | 163,715 | | | 7.026 | 58.714 | 14.002 |
| | 4TH CYCLE | | | 163,715 | | | 7.026 | 58.714 | 14.002 |
| | ********** | | | 163,715 | | | 7.026 | 58.714 | 14.002 |
| | | | | 163,715 | | | 7.026 | 58.714 | 14.002 |
| G31 — | GLASSINE | 25.000 | 0.005 | 163,715 | 0.005 | 0.004 | 7.031 | 58.718 | 14.007 |
| P28———* | EMULSION 7B | 200.000 | 0.772 | 163,690 | 0.058 | 0.702 | 7.089 | 59.420 | 14.779 |
| * | LUCITE BASE | 300.000 | 0.035 | 163,490 | 0.051 | 0.105 | 7.140 | 59.525 | 14.815 |
| * | EMULSION 6B | 200.000 | 0.772 | 163,190 | 0.058 | 0.702 | 7.197 | 60.226 | 15.587 |
| G32 — | GLASSINE | 25.000 | 0.005 | 162,990 | 0.005 | 0.004 | 7.202 | 60.230 | 15.592 |
| P29———* | EMULSION 7B | 75.000 | 0.029 | 162,965 | 0.022 | 0.263 | 7.224 | 60.494 | 15.621 |
| * | LUCITE BASE | 800.000 | 0.059 | 162,890 | 0.136 | 0.280 | 7.360 | 60.774 | 15.680 |
| * | EMULSION 7B | 75.000 | 0.029 | 162,090 | 0.022 | 0.263 | 7.382 | 61.037 | 15.709 |
| G33 — | GLASSINE | 25.000 | 0.005 | 162,015 | 0.005 | 0.004 | 7.387 | 61.041 | 15.714 |
| P30———* | EMULSION 7B | 75.000 | 0.029 | 161,990 | 0.022 | 0.263 | 7.408 | 61.304 | 15.743 |
| * | LUCITE BASE | 800.000 | 0.059 | 161,915 | 0.136 | 0.280 | 7.544 | 61.584 | 15.802 |
| * | EMULSION 7B | 75.000 | 0.029 | 161,115 | 0.022 | 0.263 | 7.566 | 61.847 | 15.831 |
| G34 — | GLASSINE | 25.000 | 0.005 | 161,040 | 0.005 | 0.004 | 7.571 | 61.851 | 15.836 |
| L4 | LEAD | 500.000 | 0.568 | 161,015 | 0.292 | 8.910 | 7.863 | 70.761 | 16.403 |
| G35 — | GLASSINE | 25.000 | 0.005 | 160,515 | 0.022 | 0.263 | 7.885 | 71.024 | 16.408 |
| P31———* | EMULSION 7B | 75.000 | 0.029 | 160,490 | 0.022 | 0.263 | 7.906 | 71.287 | 16.437 |
| * | LUCITE BASE | 800.000 | 0.059 | 160,415 | 0.136 | 0.280 | 8.042 | 71.568 | 16.496 |
| * | EMULSION 7B | 75.000 | 0.029 | 159,615 | 0.022 | 0.263 | 8.064 | 71.831 | 16.525 |
| G36 — | GLASSINE | 25.000 | 0.005 | 159,540 | 0.005 | 0.004 | 8.069 | 71.835 | 16.530 |
| CR4 (P32) | CR-39 | 600.000 | 0.087 | 159,515 | 0.104 | 0.215 | 8.173 | 72.049 | 16.617 |
| G37 — | GLASSINE | 25.000 | 0.005 | 158,915 | 0.005 | 0.004 | 8.178 | 72.053 | 16.622 |
| P33———* | EMULSION 7B | 75.000 | 0.029 | 158,890 | 0.022 | 0.263 | 8.200 | 72.316 | 16.651 |

# ECT MATERIALS COMPOSITION

| NAME | MATERIAL NAME | THICKNESS µm | MASS g/cm2 | HEIGHT µm | mfp % | r.l. % | Sum mfp % | Sum r.l. % | Sum g/cm2 |
|---|---|---|---|---|---|---|---|---|---|
| | | | | | | | | | |
| * | LUCITE BASE | 800.000 | 0.059 | 158,815 | 0.136 | 0.280 | 8.336 | 72.597 | 16.710 |
| * | EMULSION 7B | 75.000 | 0.029 | 158,015 | 0.022 | 0.263 | 8.357 | 72.860 | 16.739 |
| G37A | GLASSINE | 25.000 | 0.005 | 157,940 | 0.005 | 0.004 | 8.362 | 72.864 | 16.744 |
| E21-24 | CR-39 | 600.000 | 0.087 | 157,915 | 0.104 | 0.215 | 8.467 | 73.078 | 16.831 |
| G37B | GLASSINE | 25.000 | 0.005 | 157,315 | 0.005 | 0.004 | 8.472 | 73.082 | 16.836 |
| | | | | 157,290 | | | 8.472 | 73.082 | 16.836 |
| | ********** | | | 157,290 | | | 8.472 | 73.082 | 16.836 |
| | PRODUCER | | | 157,290 | | | 8.472 | 73.082 | 16.836 |
| | 5TH CYCLE | | | 157,290 | | | 8.472 | 73.082 | 16.836 |
| | ********** | | | 157,290 | | | 8.472 | 73.082 | 16.836 |
| | | | | 157,290 | | | 8.472 | 73.082 | 16.836 |
| G38 — | GLASSINE | 25.000 | 0.005 | 157,290 | 0.005 | 0.004 | 8.477 | 73.086 | 16.841 |
| P34———* | EMULSION 7B | 200.000 | 0.772 | 157,265 | 0.058 | 0.702 | 8.534 | 73.788 | 17.613 |
| * | LUCITE BASE | 300.000 | 0.035 | 157,065 | 0.051 | 0.105 | 8.585 | 73.893 | 17.648 |
| * | EMULSION 7B | 200.000 | 0.772 | 156,765 | 0.058 | 0.702 | 8.643 | 74.595 | 18.420 |
| G39 — | GLASSINE | 25.000 | 0.005 | 156,565 | 0.005 | 0.004 | 8.648 | 74.598 | 18.425 |
| P35———* | EMULSION 7B | 75.000 | 0.029 | 156,540 | 0.022 | 0.263 | 8.670 | 74.862 | 18.454 |
| * | LUCITE BASE | 800.000 | 0.059 | 156,465 | 0.136 | 0.280 | 8.806 | 75.142 | 18.513 |
| * | EMULSION 7B | 75.000 | 0.029 | 155,665 | 0.022 | 0.263 | 8.827 | 75.405 | 18.542 |
| G40 — | GLASSINE | 25.000 | 0.005 | 155,590 | 0.005 | 0.004 | 8.832 | 75.409 | 18.547 |
| P36———* | EMULSION 7B | 75.000 | 0.029 | 155,565 | 0.022 | 0.263 | 8.854 | 75.672 | 18.576 |
| * | LUCITE BASE | 800.000 | 0.059 | 155,490 | 0.136 | 0.280 | 8.990 | 75.952 | 18.635 |
| * | EMULSION 7B | 75.000 | 0.029 | 154,690 | 0.022 | 0.263 | 9.012 | 76.215 | 18.664 |
| G41 — | GLASSINE | 25.000 | 0.005 | 154,615 | 0.005 | 0.004 | 9.017 | 76.219 | 18.669 |
| L5 | LEAD | 500.000 | 0.568 | 154,590 | 0.292 | 8.910 | 9.309 | 85.129 | 19.237 |
| G42 — | GLASSINE | 25.000 | 0.005 | 154,090 | 0.022 | 0.263 | 9.330 | 85.392 | 19.242 |
| P37———* | EMULSION 7B | 75.000 | 0.029 | 154,065 | 0.022 | 0.263 | 9.352 | 85.655 | 19.271 |
| * | LUCITE BASE | 800.000 | 0.059 | 153,990 | 0.136 | 0.280 | 9.488 | 85.936 | 19.330 |
| * | EMULSION 7B | 75.000 | 0.029 | 153,190 | 0.022 | 0.263 | 9.510 | 86.199 | 19.359 |
| G43 — | GLASSINE | 25.000 | 0.005 | 153,115 | 0.005 | 0.004 | 9.515 | 86.203 | 19.364 |
| CR5 (P38) | CR-39 | 600.000 | 0.087 | 153,090 | 0.104 | 0.215 | 9.619 | 86.417 | 19.451 |
| G44 — | GLASSINE | 25.000 | 0.005 | 152,490 | 0.005 | 0.004 | 9.624 | 86.421 | 19.456 |
| P39———* | EMULSION 7B | 75.000 | 0.029 | 152,465 | 0.022 | 0.263 | 9.646 | 86.684 | 19.485 |
| * | LUCITE BASE | 800.000 | 0.059 | 152,390 | 0.136 | 0.280 | 9.781 | 86.965 | 19.544 |
| * | EMULSION 7B | 75.000 | 0.029 | 151,590 | 0.022 | 0.263 | 9.803 | 87.228 | 19.573 |
| | | | | 151,515 | | | 9.803 | 87.228 | 19.573 |
| | ********** | | | 151,515 | | | 9.803 | 87.228 | 19.573 |
| | PRODUCER | | | 151,515 | | | 9.803 | 87.228 | 19.573 |
| | 6TH CYCLE | | | 151,515 | | | 9.803 | 87.228 | 19.573 |
| | ********** | | | 151,515 | | | 9.803 | 87.228 | 19.573 |
| | | | | 151,515 | | | 9.803 | 87.228 | 19.573 |
| G45 — | GLASSINE | 25.000 | 0.005 | 151,515 | 0.005 | 0.004 | 9.808 | 87.232 | 19.578 |
| P40———* | EMULSION 7B | 200.000 | 0.772 | 151,490 | 0.058 | 0.702 | 9.866 | 87.933 | 20.350 |
| * | LUCITE BASE | 300.000 | 0.035 | 151,290 | 0.051 | 0.105 | 9.917 | 88.038 | 20.385 |
| * | EMULSION 6B | 200.000 | 0.772 | 150,990 | 0.058 | 0.702 | 9.974 | 88.740 | 21.157 |
| G46 — | GLASSINE | 25.000 | 0.005 | 150,790 | 0.005 | 0.004 | 9.980 | 88.744 | 21.162 |
| P41———* | EMULSION 7B | 75.000 | 0.029 | 150,765 | 0.022 | 0.263 | 10.001 | 89.007 | 21.191 |
| * | LUCITE BASE | 800.000 | 0.059 | 150,690 | 0.136 | 0.280 | 10.137 | 89.287 | 21.250 |
| * | EMULSION 7B | 75.000 | 0.029 | 149,890 | 0.022 | 0.263 | 10.159 | 89.551 | 21.279 |
| G47 — | GLASSINE | 25.000 | 0.005 | 149,815 | 0.005 | 0.004 | 10.164 | 89.554 | 21.284 |
| P42———* | EMULSION 7B | 75.000 | 0.029 | 149,790 | 0.022 | 0.263 | 10.185 | 89.818 | 21.313 |
| * | LUCITE BASE | 800.000 | 0.059 | 149,715 | 0.136 | 0.280 | 10.321 | 90.098 | 21.372 |
| * | EMULSION 7B | 75.000 | 0.029 | 149,640 | 0.022 | 0.263 | 10.343 | 90.361 | 21.401 |
| G48 — | GLASSINE | 25.000 | 0.005 | 149,565 | 0.005 | 0.004 | 10.348 | 90.365 | 21.406 |
| L6 | LEAD | 500.000 | 0.568 | 149,540 | 0.292 | 8.910 | 10.640 | 99.275 | 21.974 |

# ECT MATERIALS COMPOSITION

| *NAME* | MATERIAL NAME | THICKNESS μm | MASS g/cm2 | HEIGHT μm | mfp % | r.l. % | Sum mfp % | Sum r.l. % | Sum g/cm2 |
|---|---|---|---|---|---|---|---|---|---|
| | | | | | | | | | |
| G49 — | GLASSINE | 25.000 | 0.005 | 149,040 | 0.022 | 0.263 | 10.662 | 99.538 | 21.979 |
| P43———* | EMULSION 7B | 75.000 | 0.029 | 149,015 | 0.022 | 0.263 | 10.683 | 99.801 | 22.008 |
| * | LUCITE BASE | 800.000 | 0.059 | 148,940 | 0.136 | 0.280 | 10.819 | 100.081 | 22.067 |
| * | EMULSION 7B | 75.000 | 0.029 | 148,140 | 0.022 | 0.263 | 10.841 | 100.344 | 22.096 |
| G50 — | GLASSINE | 25.000 | 0.005 | 148,065 | 0.005 | 0.004 | 10.846 | 100.348 | 22.101 |
| CR6(P50) | CR-39 | 600.000 | 0.087 | 148,040 | 0.104 | 0.215 | 10.950 | 100.563 | 22.188 |
| G51 — | GLASSINE | 25.000 | 0.005 | 147,440 | 0.005 | 0.004 | 10.955 | 100.567 | 22.193 |
| P45———* | EMULSION 7B | 75.000 | 0.029 | 147,415 | 0.022 | 0.263 | 10.977 | 100.830 | 22.222 |
| * | LUCITE BASE | 800.000 | 0.059 | 147,340 | 0.136 | 0.280 | 11.113 | 101.110 | 22.281 |
| * | EMULSION 7B | 75.000 | 0.029 | 146,540 | 0.022 | 0.263 | 11.134 | 101.373 | 22.310 |
| | | | | 146,465 | | | 11.134 | 101.373 | 22.310 |
| | ********** | | | 146,465 | | | 11.134 | 101.373 | 22.310 |
| | PRODUCER | | | 146,465 | | | 11.134 | 101.373 | 22.310 |
| | 7TH CYCLE | | | 146,465 | | | 11.134 | 101.373 | 22.310 |
| | ********** | | | 146,465 | | | 11.134 | 101.373 | 22.310 |
| | | | | 146,465 | | | 11.134 | 101.373 | 22.310 |
| G52 — | GLASSINE | 25.000 | 0.005 | 146,465 | 0.005 | 0.004 | 11.140 | 101.377 | 22.315 |
| P46———* | EMULSION 7B | 200.000 | 0.772 | 146,440 | 0.058 | 0.702 | 11.197 | 102.079 | 23.087 |
| * | LUCITE BASE | 300.000 | 0.035 | 146,240 | 0.051 | 0.105 | 11.248 | 102.184 | 23.122 |
| * | EMULSION 7B | 200.000 | 0.772 | 145,940 | 0.058 | 0.702 | 11.306 | 102.886 | 23.894 |
| G53 — | GLASSINE | 25.000 | 0.005 | 145,740 | 0.005 | 0.004 | 11.311 | 102.890 | 23.899 |
| P47———* | EMULSION 7B | 75.000 | 0.029 | 145,715 | 0.022 | 0.263 | 11.332 | 103.153 | 23.928 |
| * | LUCITE BASE | 800.000 | 0.059 | 145,640 | 0.136 | 0.280 | 11.468 | 103.433 | 23.987 |
| * | EMULSION 7B | 75.000 | 0.029 | 144,840 | 0.022 | 0.263 | 11.490 | 103.696 | 24.016 |
| G54 — | GLASSINE | 25.000 | 0.005 | 144,765 | 0.005 | 0.004 | 11.495 | 103.700 | 24.021 |
| P48———* | EMULSION 7B | 75.000 | 0.029 | 144,740 | 0.022 | 0.263 | 11.517 | 103.963 | 24.050 |
| * | LUCITE BASE | 800.000 | 0.059 | 144,665 | 0.136 | 0.280 | 11.653 | 104.243 | 24.109 |
| * | EMULSION 7B | 75.000 | 0.029 | 143,865 | 0.022 | 0.263 | 11.674 | 104.507 | 24.138 |
| G55 — | GLASSINE | 25.000 | 0.005 | 143,790 | 0.005 | 0.004 | 11.679 | 104.510 | 24.143 |
| L7 | LEAD | 500.000 | 0.568 | 143,765 | 0.292 | 8.910 | 11.972 | 113.420 | 24.711 |
| G56 — | GLASSINE | 25.000 | 0.005 | 143,265 | 0.022 | 0.263 | 11.993 | 113.683 | 24.716 |
| P49———* | EMULSION 7B | 75.000 | 0.029 | 143,240 | 0.022 | 0.263 | 12.015 | 113.946 | 24.745 |
| * | LUCITE BASE | 800.000 | 0.059 | 143,165 | 0.136 | 0.280 | 12.151 | 114.227 | 24.804 |
| * | EMULSION 7B | 75.000 | 0.029 | 142,365 | 0.022 | 0.263 | 12.172 | 114.490 | 24.833 |
| G57 — | GLASSINE | 25.000 | 0.005 | 142,290 | 0.005 | 0.004 | 12.177 | 114.494 | 24.838 |
| CR7(P50)E38 | CR-39 | 600.000 | 0.087 | 142,265 | 0.104 | 0.215 | 12.281 | 114.708 | 24.925 |
| G58 — | GLASSINE | 25.000 | 0.005 | 141,665 | 0.005 | 0.004 | 12.287 | 114.712 | 24.930 |
| P51———* | EMULSION 7B | 75.000 | 0.029 | 141,640 | 0.022 | 0.263 | 12.308 | 114.975 | 24.959 |
| * | LUCITE BASE | 800.000 | 0.059 | 141,565 | 0.136 | 0.280 | 12.444 | 115.256 | 25.018 |
| * | EMULSION 7B | 75.000 | 0.029 | 140,765 | 0.022 | 0.263 | 12.466 | 115.519 | 25.047 |
| | | | | 140,690 | | | 12.466 | 115.519 | 25.047 |
| | ********** | | | 140,690 | | | 12.466 | 115.519 | 25.047 |
| | PRODUCER | | | 140,690 | | | 12.466 | 115.519 | 25.047 |
| | 8TH CYCLE | | | 140,690 | | | 12.466 | 115.519 | 25.047 |
| | ********** | | | 140,690 | | | 12.466 | 115.519 | 25.047 |
| | | | | 140,690 | | | 12.466 | 115.519 | 25.047 |
| G59 — | GLASSINE | 25.000 | 0.005 | 140,690 | 0.005 | 0.004 | 12.471 | 115.523 | 25.052 |
| P52———* | EMULSION 7B | 200.000 | 0.772 | 140,665 | 0.058 | 0.702 | 12.528 | 116.224 | 25.824 |
| * | LUCITE BASE | 300.000 | 0.035 | 140,465 | 0.051 | 0.105 | 12.579 | 116.330 | 25.859 |
| * | EMULSION 6B | 200.000 | 0.772 | 140,165 | 0.058 | 0.702 | 12.637 | 117.031 | 26.631 |
| G60 — | GLASSINE | 25.000 | 0.005 | 139,965 | 0.005 | 0.004 | 12.642 | 117.035 | 26.636 |
| P53———* | EMULSION 7B | 75.000 | 0.029 | 139,940 | 0.022 | 0.263 | 12.664 | 117.298 | 26.665 |
| * | LUCITE BASE | 800.000 | 0.059 | 139,865 | 0.136 | 0.280 | 12.800 | 117.579 | 26.724 |
| * | EMULSION 7B | 75.000 | 0.029 | 139,065 | 0.022 | 0.263 | 12.821 | 117.842 | 26.753 |
| G61 — | GLASSINE | 25.000 | 0.005 | 138,990 | 0.005 | 0.004 | 12.826 | 117.846 | 26.758 |

| NAME | MATERIAL NAME | THICKNESS µm | MASS g/cm2 | HEIGHT µm | mfp % | r.l. % | Sum mfp % | Sum r.l. % | Sum g/cm2 |
|---|---|---|---|---|---|---|---|---|---|
| | | | | | | | | | |
| P54————* | EMULSION 7B | 75.000 | 0.029 | 138,965 | 0.022 | 0.263 | 12.848 | 118.109 | 26.787 |
| * | LUCITE BASE | 800.000 | 0.059 | 138,890 | 0.136 | 0.280 | 12.984 | 118.389 | 26.846 |
| * | EMULSION 7B | 75.000 | 0.029 | 138,090 | 0.022 | 0.263 | 13.005 | 118.652 | 26.875 |
| G62 — | GLASSINE | 25.000 | 0.005 | 138,015 | 0.005 | 0.004 | 13.011 | 118.656 | 26.880 |
| L8 | LEAD | 500.000 | 0.568 | 137,990 | 0.292 | 8.910 | 13.303 | 127.566 | 27.448 |
| G63— | GLASSINE | 25.000 | 0.005 | 137,490 | 0.022 | 0.263 | 13.324 | 127.829 | 27.453 |
| P55————* | EMULSION 7B | 75.000 | 0.029 | 137,465 | 0.022 | 0.263 | 13.346 | 128.092 | 27.482 |
| * | LUCITE BASE | 800.000 | 0.059 | 137,390 | 0.136 | 0.280 | 13.482 | 128.372 | 27.541 |
| * | EMULSION 7B | 75.000 | 0.029 | 136,590 | 0.022 | 0.263 | 13.504 | 128.635 | 27.570 |
| G64 — | GLASSINE | 25.000 | 0.005 | 136,515 | 0.005 | 0.004 | 13.509 | 128.639 | 27.575 |
| CR8(P56)E30 | CR-39 | 600.000 | 0.087 | 136,490 | 0.104 | 0.215 | 13.613 | 128.854 | 27.662 |
| G65— | GLASSINE | 25.000 | 0.005 | 135,890 | 0.005 | 0.004 | 13.618 | 128.858 | 27.667 |
| P57————* | EMULSION 7B | 75.000 | 0.029 | 135,865 | 0.022 | 0.263 | 13.640 | 129.121 | 27.696 |
| * | LUCITE BASE | 800.000 | 0.059 | 135,790 | 0.136 | 0.280 | 13.775 | 129.401 | 27.755 |
| * | EMULSION 7B | 75.000 | 0.029 | 134,990 | 0.022 | 0.263 | 13.797 | 129.664 | 27.784 |
| | | | | 134,915 | | | 13.797 | 129.664 | 27.784 |
| | ********** | | | 134,915 | | | 13.797 | 129.664 | 27.784 |
| | PRODUCER | | | 134,915 | | | 13.797 | 129.664 | 27.784 |
| | 9TH CYCLE | | | 134,915 | | | 13.797 | 129.664 | 27.784 |
| | ********** | | | 134,915 | | | 13.797 | 129.664 | 27.784 |
| | | | | 134,915 | | | 13.797 | 129.664 | 27.784 |
| G66 — | GLASSINE | 25.000 | 0.005 | 134,915 | 0.005 | 0.004 | 13.802 | 129.668 | 27.789 |
| P58————* | EMULSION 7B | 200.000 | 0.772 | 134,890 | 0.058 | 0.702 | 13.860 | 130.370 | 28.561 |
| * | LUCITE BASE | 300.000 | 0.035 | 134,690 | 0.051 | 0.105 | 13.911 | 130.475 | 28.596 |
| * | EMULSION 7B | 200.000 | 0.772 | 134,390 | 0.058 | 0.702 | 13.968 | 131.177 | 29.368 |
| G67 — | GLASSINE | 25.000 | 0.005 | 134,190 | 0.005 | 0.004 | 13.973 | 131.181 | 29.373 |
| P59————* | EMULSION 7B | 75.000 | 0.029 | 134,165 | 0.022 | 0.263 | 13.995 | 131.444 | 29.402 |
| * | LUCITE BASE | 800.000 | 0.059 | 134,090 | 0.136 | 0.280 | 14.131 | 131.724 | 29.461 |
| * | EMULSION 7B | 75.000 | 0.029 | 133,290 | 0.022 | 0.263 | 14.153 | 131.987 | 29.490 |
| G68 — | GLASSINE | 25.000 | 0.005 | 133,240 | 0.005 | 0.004 | 14.158 | 131.991 | 29.495 |
| P60————* | EMULSION 7B | 75.000 | 0.029 | 133,215 | 0.022 | 0.263 | 14.179 | 132.254 | 29.524 |
| * | LUCITE BASE | 800.000 | 0.059 | 133,140 | 0.136 | 0.280 | 14.315 | 132.535 | 29.583 |
| * | EMULSION 7B | 75.000 | 0.029 | 132,340 | 0.022 | 0.263 | 14.337 | 132.798 | 29.612 |
| G69 — | GLASSINE | 25.000 | 0.005 | 132,265 | 0.005 | 0.004 | 14.342 | 132.802 | 29.617 |
| L9 | LEAD | 500.000 | 0.568 | 132,240 | 0.292 | 8.910 | 14.634 | 141.711 | 30.185 |
| G70 — | GLASSINE | 25.000 | 0.005 | 131,740 | 0.022 | 0.263 | 14.656 | 141.974 | 30.190 |
| P61————* | EMULSION 7B | 75.000 | 0.029 | 131,715 | 0.022 | 0.263 | 14.677 | 142.238 | 30.219 |
| * | LUCITE BASE | 800.000 | 0.059 | 131,640 | 0.136 | 0.280 | 14.813 | 142.518 | 30.278 |
| * | EMULSION 7B | 75.000 | 0.029 | 130,840 | 0.022 | 0.263 | 14.835 | 142.781 | 30.307 |
| G71 — | GLASSINE | 25.000 | 0.005 | 130,765 | 0.005 | 0.004 | 14.840 | 142.785 | 30.312 |
| CR9(P62)EC | CR-39 | 600.000 | 0.087 | 130,740 | 0.104 | 0.215 | 14.944 | 143.000 | 30.399 |
| G72 — | GLASSINE | 25.000 | 0.005 | 130,140 | 0.005 | 0.004 | 14.949 | 143.003 | 30.404 |
| P63————* | EMULSION 7B | 75.000 | 0.029 | 130,115 | 0.022 | 0.263 | 14.971 | 143.267 | 30.433 |
| * | LUCITE BASE | 800.000 | 0.059 | 130,040 | 0.136 | 0.280 | 15.107 | 143.547 | 30.492 |
| * | EMULSION 7B | 75.000 | 0.029 | 129,240 | 0.022 | 0.263 | 15.128 | 143.810 | 30.521 |
| | | | | 129,165 | | | 15.128 | 143.810 | 30.521 |
| | ********** | | | 129,165 | | | 15.128 | 143.810 | 30.521 |
| | PRODUCER | | | 129,165 | | | 15.128 | 143.810 | 30.521 |
| | 10TH CYCLE | | | 129,165 | | | 15.128 | 143.810 | 30.521 |
| | ********** | | | 129,165 | | | 15.128 | 143.810 | 30.521 |
| | | | | 129,165 | | | 15.128 | 143.810 | 30.521 |
| G73 — | GLASSINE | 25.000 | 0.005 | 129,165 | 0.005 | 0.004 | 15.133 | 143.814 | 30.526 |
| P64————* | EMULSION 7B | 200.000 | 0.772 | 129,140 | 0.058 | 0.702 | 15.191 | 144.516 | 31.298 |
| * | LUCITE BASE | 300.000 | 0.035 | 128,940 | 0.051 | 0.105 | 15.242 | 144.621 | 31.333 |
| * | EMULSION 6B | 200.000 | 0.772 | 128,640 | 0.058 | 0.702 | 15.300 | 145.322 | 32.105 |

# ECT MATERIALS COMPOSITION

| *NAME* | MATERIAL | THICKNESS | MASS | HEIGHT | mfp | r.l. | Sum mfp | Sum r.l. | Sum |
|---|---|---|---|---|---|---|---|---|---|
| | NAME | μm | g/cm2 | μm | % | % | % | % | g/cm2 |
| | | | | | | | | | |
| G74 — | GLASSINE | 25.000 | 0.005 | 128,440 | 0.005 | 0.004 | 15.305 | 145.326 | 32.110 |
| P65————* | EMULSION 7B | 75.000 | 0.029 | 128,415 | 0.022 | 0.263 | 15.326 | 145.589 | 32.139 |
| * | LUCITE BASE | 800.000 | 0.059 | 128,340 | 0.136 | 0.280 | 15.462 | 145.870 | 32.198 |
| * | EMULSION 7B | 75.000 | 0.029 | 127,540 | 0.022 | 0.263 | 15.484 | 146.133 | 32.227 |
| G75 — | GLASSINE | 25.000 | 0.005 | 127,465 | 0.005 | 0.004 | 15.489 | 146.137 | 32.232 |
| P66————* | EMULSION 7B | 75.000 | 0.029 | 127,440 | 0.022 | 0.263 | 15.511 | 146.400 | 32.261 |
| * | LUCITE BASE | 800.000 | 0.059 | 127,365 | 0.136 | 0.280 | 15.647 | 146.680 | 32.320 |
| * | EMULSION 7B | 75.000 | 0.029 | 126,565 | 0.022 | 0.263 | 15.668 | 146.943 | 32.349 |
| G76 — | GLASSINE | 25.000 | 0.005 | 126,490 | 0.005 | 0.004 | 15.673 | 146.947 | 32.354 |
| L10 | LEAD | 500.000 | 0.568 | 126,465 | 0.292 | 8.910 | 15.966 | 155.857 | 32.921 |
| G77 — | GLASSINE | 25.000 | 0.005 | 125,965 | 0.022 | 0.263 | 15.987 | 156.120 | 32.926 |
| P67————* | EMULSION 7B | 75.000 | 0.029 | 125,940 | 0.022 | 0.263 | 16.009 | 156.383 | 32.955 |
| * | LUCITE BASE | 800.000 | 0.059 | 125,865 | 0.136 | 0.280 | 16.145 | 156.663 | 33.014 |
| * | EMULSION 7B | 75.000 | 0.029 | 125,065 | 0.022 | 0.263 | 16.166 | 156.927 | 33.043 |
| G78— | GLASSINE | 25.000 | 0.005 | 124,990 | 0.005 | 0.004 | 16.171 | 156.930 | 33.048 |
| CR10(P68)E16 | CR-39 | 600.000 | 0.087 | 124,965 | 0.104 | 0.215 | 16.275 | 157.145 | 33.135 |
| G79— | GLASSINE | 25.000 | 0.005 | 124,365 | 0.005 | 0.004 | 16.281 | 157.149 | 33.140 |
| P69————* | EMULSION 7B | 75.000 | 0.029 | 124,340 | 0.022 | 0.263 | 16.302 | 157.412 | 33.169 |
| * | LUCITE BASE | 800.000 | 0.059 | 124,265 | 0.136 | 0.280 | 16.438 | 157.692 | 33.228 |
| * | EMULSION 7B | 75.000 | 0.029 | 123,465 | 0.022 | 0.263 | 16.460 | 157.956 | 33.257 |
| G79A — | GLASSINE | 25.000 | 0.050 | 123,390 | 0.005 | 0.004 | 16.465 | 157.959 | 33.307 |
| P70 | HRH-HR8 #2 | 3,500.000 | 0.812 | 123,365 | 0.920 | 5.466 | 17.385 | 163.426 | 34.119 |
| | | | | 119,865 | | | 17.385 | 163.426 | 34.119 |
| ********** | ********** | | | 119,865 | | | 17.385 | 163.426 | 34.119 |
| END PRODUCER | MODULE | | | 119,865 | | | 17.385 | 163.426 | 34.119 |
| ********** | ********** | | | 119,865 | | | 17.385 | 163.426 | 34.119 |
| | | | | 119,865 | | | 17.385 | 163.426 | 34.119 |
| ########## | ########## | | | 119,865 | | | 17.385 | 163.426 | 34.119 |
| DIVIDER PLATE | STAINLESS | 3,175.000 | 2.449 | 119,865 | 1.894 | 18.053 | 19.279 | 181.479 | 36.568 |
| ########## | ########## | | | 116,690 | | | 19.279 | 181.479 | 36.568 |
| | | | | 116,690 | | | 19.279 | 181.479 | 36.568 |
| ********** | ********** | | | 116,690 | | | 19.279 | 181.479 | 36.568 |
| CALORIMETER | MODULE (I) | | | 116,690 | | | 19.279 | 181.479 | 36.568 |
| ********** | ********** | | | 116,690 | | | 19.279 | 181.479 | 36.568 |
| | | | | 116,690 | | | 19.279 | 181.479 | 36.568 |
| RUBBER | SHIM | 2,000.000 | 0.528 | 116,690 | 0.600 | 3.520 | 19.879 | 184.999 | 37.096 |
| PLASTIC | N-MONITOR #2 | 600.000 | 0.085 | 114,690 | 0.102 | 0.210 | 19.981 | 185.209 | 37.181 |
| PLASTIC | N-MONITOR #1 | 600.000 | 0.085 | 114,090 | 0.102 | 0.210 | 20.083 | 185.419 | 37.266 |
| PLASTIC | SHIM | 800.000 | 0.211 | 113,490 | 0.240 | 1.408 | 20.322 | 186.828 | 37.477 |
| G80 — | GLASSINE | 25.000 | 0.005 | 112,690 | 0.005 | 0.004 | 20.327 | 186.832 | 37.482 |
| C00————* | EMULSION 7B | 200.000 | 0.772 | 112,665 | 0.058 | 0.702 | 20.385 | 187.533 | 38.254 |
| * | LUCITE BASE | 300.000 | 0.035 | 112,465 | 0.051 | 0.105 | 20.436 | 187.638 | 38.290 |
| * | EMULSION 7B | 200.000 | 0.772 | 112,165 | 0.058 | 0.702 | 20.494 | 188.340 | 39.062 |
| | | | | 111,965 | | | 20.494 | 188.340 | 39.062 |
| **1ST CYCLE* | | | | 111,965 | | | 20.494 | 188.340 | 39.062 |
| | | | | 111,965 | | | 20.494 | 188.340 | 39.062 |
| G81 — | GLASSINE | 25.000 | 0.005 | 111,965 | 0.005 | 0.004 | 20.499 | 188.344 | 39.067 |
| LC1 | LEAD | 1,000.000 | 1.135 | 111,940 | 0.585 | 17.820 | 21.083 | 206.163 | 40.202 |
| G82 — | GLASSINE | 25.000 | 0.005 | 110,940 | 0.005 | 0.004 | 21.088 | 206.167 | 40.207 |
| | | | | 110,915 | | | 21.088 | 206.167 | 40.207 |
| X1A | X-RAY FILM | 220.000 | 0.043 | 110,915 | 0.032 | 0.392 | 21.121 | 206.559 | 40.250 |
| X1B | X-RAY FILM | 220.000 | 0.043 | 110,695 | 0.032 | 0.392 | 21.153 | 206.951 | 40.293 |
| G83 — | GLASSINE | 25.000 | 0.005 | 110,475 | 0.005 | 0.004 | 21.158 | 206.955 | 40.298 |
| C01————* | EMULSION 7B | 75.000 | 0.029 | 110,450 | 0.022 | 0.263 | 21.179 | 207.218 | 40.327 |
| * | LUCITE BASE | 800.000 | 0.059 | 110,375 | 0.136 | 0.280 | 21.315 | 207.498 | 40.386 |

# ECT MATERIALS COMPOSITION

| *NAME* | MATERIAL | THICKNESS | MASS | HEIGHT | mfp | r.l. | Sum mfp | Sum r.l. | Sum |
|---|---|---|---|---|---|---|---|---|---|
| | NAME | μm | g/cm2 | μm | % | % | % | % | g/cm2 |
| | | | | | | | | | |
| * | EMULSION 7B | 75.000 | 0.029 | 109,575 | 0.022 | 0.263 | 21.337 | 207.761 | 40.415 |
| | | | | 109,500 | | | 21.337 | 207.761 | 40.415 |
| ***2ND CYCLE* | | | | 109,500 | | | 21.337 | 207.761 | 40.415 |
| | | | | 109,500 | | | 21.337 | 207.761 | 40.415 |
| G84— | GLASSINE | 25.000 | 0.005 | 109,500 | 0.005 | 0.004 | 21.342 | 207.765 | 40.420 |
| LC2 | LEAD | 1,000.000 | 1.135 | 109,475 | 0.585 | 17.820 | 21.926 | 225.584 | 41.555 |
| G85 — | GLASSINE | 25.000 | 0.005 | 108,475 | 0.005 | 0.004 | 21.932 | 225.588 | 41.560 |
| | | | | 108,450 | | | 21.932 | 225.588 | 41.560 |
| X2A | X-RAY FILM | 220.000 | 0.043 | 108,450 | 0.032 | 0.392 | 21.964 | 225.980 | 41.603 |
| X2B | X-RAY FILM | 220.000 | 0.043 | 108,230 | 0.032 | 0.392 | 21.996 | 226.372 | 41.646 |
| G86 — | GLASSINE | 25.000 | 0.005 | 108,010 | 0.005 | 0.004 | 22.001 | 226.376 | 41.651 |
| C02————* | EMULSION 7B | 75.000 | 0.029 | 107,985 | 0.022 | 0.263 | 22.023 | 226.639 | 41.680 |
| * | LUCITE BASE | 800.000 | 0.059 | 107,910 | 0.136 | 0.280 | 22.158 | 226.919 | 41.739 |
| * | EMULSION 7B | 75.000 | 0.029 | 107,110 | 0.022 | 0.263 | 22.180 | 227.182 | 41.768 |
| | | | | 107,035 | | | 22.180 | 227.182 | 41.768 |
| ***3RD CYCLE* | | | | 107,035 | | | 22.180 | 227.182 | 41.768 |
| | | | | 107,035 | | | 22.180 | 227.182 | 41.768 |
| G87 — | GLASSINE | 25.000 | 0.005 | 107,035 | 0.005 | 0.004 | 22.185 | 227.186 | 41.773 |
| LC3 | LEAD | 1,000.000 | 1.135 | 107,010 | 0.585 | 17.820 | 22.770 | 245.005 | 42.908 |
| G88 — | GLASSINE | 25.000 | 0.005 | 106,010 | 0.005 | 0.004 | 22.775 | 245.009 | 42.913 |
| | | | | 105,985 | | | 22.775 | 245.009 | 42.913 |
| X3A | X-RAY FILM | 220.000 | 0.043 | 105,985 | 0.032 | 0.392 | 22.807 | 245.401 | 42.956 |
| X3B | X-RAY FILM | 220.000 | 0.043 | 105,765 | 0.032 | 0.392 | 22.839 | 245.793 | 42.999 |
| G89 — | GLASSINE | 25.000 | 0.005 | 105,545 | 0.005 | 0.004 | 22.844 | 245.797 | 43.004 |
| C03————* | EMULSION 7B | 75.000 | 0.029 | 105,520 | 0.022 | 0.263 | 22.866 | 246.060 | 43.033 |
| * | LUCITE BASE | 800.000 | 0.059 | 105,445 | 0.136 | 0.280 | 23.002 | 246.340 | 43.092 |
| * | EMULSION 7B | 75.000 | 0.029 | 104,645 | 0.022 | 0.263 | 23.023 | 246.603 | 43.121 |
| | | | | 104,570 | | | 23.023 | 246.603 | 43.121 |
| ***4TH CYCLE* | | | | 104,570 | | | 23.023 | 246.603 | 43.121 |
| | | | | 104,570 | | | 23.023 | 246.603 | 43.121 |
| G90 — | GLASSINE | 25.000 | 0.005 | 104,570 | 0.005 | 0.004 | 23.028 | 246.607 | 43.126 |
| LC4 | LEAD | 1,000.000 | 1.135 | 104,545 | 0.585 | 17.820 | 23.613 | 264.426 | 44.261 |
| G91 — | GLASSINE | 25.000 | 0.005 | 103,545 | 0.005 | 0.004 | 23.618 | 264.430 | 44.266 |
| | | | | 103,520 | | | 23.618 | 264.430 | 44.266 |
| X4A | X-RAY FILM | 220.000 | 0.043 | 103,520 | 0.032 | 0.392 | 23.650 | 264.822 | 44.309 |
| X4B | X-RAY FILM | 220.000 | 0.043 | 103,300 | 0.032 | 0.392 | 23.682 | 265.214 | 44.352 |
| G92 — | GLASSINE | 25.000 | 0.005 | 103,080 | 0.005 | 0.004 | 23.687 | 265.218 | 44.357 |
| C04————* | EMULSION 7B | 75.000 | 0.029 | 103,055 | 0.022 | 0.263 | 23.709 | 265.481 | 44.386 |
| * | LUCITE BASE | 800.000 | 0.059 | 102,980 | 0.136 | 0.280 | 23.845 | 265.761 | 44.445 |
| * | EMULSION 7B | 75.000 | 0.029 | 102,180 | 0.022 | 0.263 | 23.866 | 266.024 | 44.474 |
| | | | | 102,105 | | | 23.866 | 266.024 | 44.474 |
| ***5TH CYCLE* | | | | 102,105 | | | 23.866 | 266.024 | 44.474 |
| | | | | 102,105 | | | 23.866 | 266.024 | 44.474 |
| G93 — | GLASSINE | 25.000 | 0.005 | 102,105 | 0.005 | 0.004 | 23.872 | 266.028 | 44.479 |
| LC5 | LEAD | 1,000.000 | 1.135 | 102,080 | 0.585 | 17.820 | 24.456 | 283.847 | 45.614 |
| G94 — | GLASSINE | 25.000 | 0.005 | 101,080 | 0.005 | 0.004 | 24.461 | 283.851 | 45.619 |
| | | | | 101,055 | | | 24.461 | 283.851 | 45.619 |
| X5A | X-RAY FILM | 220.000 | 0.043 | 101,055 | 0.032 | 0.392 | 24.493 | 284.243 | 45.663 |
| X5B | X-RAY FILM | 220.000 | 0.043 | 100,835 | 0.032 | 0.392 | 24.525 | 284.635 | 45.706 |
| G95 — | GLASSINE | 25.000 | 0.005 | 100,615 | 0.005 | 0.004 | 24.531 | 284.639 | 45.711 |
| C05————* | EMULSION 7B | 75.000 | 0.029 | 100,590 | 0.022 | 0.263 | 24.552 | 284.902 | 45.740 |
| * | LUCITE BASE | 800.000 | 0.059 | 100,515 | 0.136 | 0.280 | 24.688 | 285.182 | 45.799 |
| * | EMULSION 7B | 75.000 | 0.029 | 99,715 | 0.022 | 0.263 | 24.710 | 285.445 | 45.828 |
| G96 — | GLASSINE | 25.000 | 0.005 | 99,640 | 0.005 | 0.004 | 24.715 | 285.449 | 45.833 |
| B3(E15-E14) | CR39 | 600.000 | 0.087 | 99,615 | 0.104 | 0.215 | 24.819 | 285.664 | 45.920 |

| NAME | MATERIAL NAME | THICKNESS µm | MASS g/cm2 | HEIGHT µm | mfp % | r.l. % | Sum mfp % | Sum r.l. % | Sum g/cm2 |
|---|---|---|---|---|---|---|---|---|---|
| | | | | | | | | | |
| | | | | 99,015 | | | 24.819 | 285.664 | 45.920 |
| | | | | 99,015 | | | 24.819 | 285.664 | 45.920 |
| ********** | ********** | | | 99,015 | | | 24.819 | 285.664 | 45.920 |
| CALORIMETER | MODULE (II) | | | 99,015 | | | 24.819 | 285.664 | 45.920 |
| ********** | ********** | | | 99,015 | | | 24.819 | 285.664 | 45.920 |
| (6TH - 8TH CYCLES OMITTED) | | | | 99,015 | | | 24.819 | 285.664 | 45.920 |
| | | | | 99,015 | | | 24.819 | 285.664 | 45.920 |
| *9TH CYCLE | | | | 99,015 | | | 24.819 | 285.664 | 45.920 |
| | | | | 99,015 | | | 24.819 | 285.664 | 45.920 |
| G97 — | GLASSINE | 25.000 | 0.005 | 99,015 | 0.005 | 0.004 | 24.824 | 285.668 | 45.925 |
| LC9 | LEAD | 2,000.000 | 2.271 | 98,990 | 1.170 | 35.655 | 25.994 | 321.322 | 48.196 |
| G98 — | GLASSINE | 25.000 | 0.005 | 96,990 | 0.005 | 0.004 | 25.999 | 321.326 | 48.201 |
| | | | | 96,965 | | | 25.999 | 321.326 | 48.201 |
| X9A | X-RAY FILM | 220.000 | 0.043 | 96,965 | 0.032 | 0.392 | 26.031 | 321.718 | 48.244 |
| X9B | X-RAY FILM | 220.000 | 0.043 | 96,745 | 0.032 | 0.392 | 26.063 | 322.109 | 48.287 |
| G99 — | GLASSINE | 25.000 | 0.005 | 96,525 | 0.005 | 0.004 | 26.068 | 322.113 | 48.292 |
| C09————* | EMULSION 7B | 75.000 | 0.029 | 96,500 | 0.022 | 0.263 | 26.090 | 322.376 | 48.321 |
| * | LUCITE BASE | 800.000 | 0.059 | 96,425 | 0.136 | 0.280 | 26.226 | 322.657 | 48.380 |
| * | EMULSION 7B | 75.000 | 0.029 | 95,625 | 0.022 | 0.263 | 26.247 | 322.920 | 48.409 |
| G100 — | GLASSINE | 25.000 | 0.005 | 95,550 | 0.005 | 0.004 | 26.252 | 322.924 | 48.414 |
| B3(E15-E14) | CR39 | 600.000 | 0.087 | 94,950 | 0.104 | 0.215 | 26.356 | 323.138 | 48.501 |
| | | | | 94,350 | | | 26.356 | 323.138 | 48.501 |
| *10TH CYCLE | | | | 94,350 | | | 26.356 | 323.138 | 48.501 |
| | | | | 94,350 | | | 26.356 | 323.138 | 48.501 |
| G101 — | GLASSINE | 25.000 | 0.005 | 94,350 | 0.005 | 0.004 | 26.361 | 323.142 | 48.506 |
| LC10 | LEAD | 2,000.000 | 2.271 | 94,325 | 1.170 | 35.655 | 27.531 | 358.797 | 50.777 |
| G102 — | GLASSINE | 25.000 | 0.005 | 92,325 | 0.005 | 0.004 | 27.536 | 358.801 | 50.782 |
| | | | | 92,300 | | | 27.536 | 358.801 | 50.782 |
| X10A | X-RAY FILM | 220.000 | 0.043 | 92,300 | 0.032 | 0.392 | 27.568 | 359.193 | 50.825 |
| X10B | X-RAY FILM | 220.000 | 0.043 | 92,080 | 0.032 | 0.392 | 27.600 | 359.584 | 50.868 |
| G103 — | GLASSINE | 25.000 | 0.005 | 91,860 | 0.005 | 0.004 | 27.606 | 359.588 | 50.873 |
| C10 ————* | EMULSION 7B | 75.000 | 0.029 | 91,835 | 0.022 | 0.263 | 27.627 | 359.851 | 50.902 |
| * | LUCITE BASE | 800.000 | 0.059 | 91,760 | 0.136 | 0.280 | 27.763 | 360.131 | 50.961 |
| * | EMULSION 7B | 75.000 | 0.029 | 91,035 | 0.022 | 0.263 | 27.785 | 360.395 | 50.990 |
| | | | | 90,960 | | | 27.785 | 360.395 | 50.990 |
| *11TH CYCLE | | | | 90,960 | | | 27.785 | 360.395 | 50.990 |
| | | | | 90,960 | | | 27.785 | 360.395 | 50.990 |
| G104 — | GLASSINE | 25.000 | 0.005 | 90,960 | 0.005 | 0.004 | 27.790 | 360.398 | 50.995 |
| LC11 | LEAD | 2,000.000 | 2.271 | 90,935 | 1.170 | 35.655 | 28.959 | 396.053 | 53.266 |
| G105 — | GLASSINE | 25.000 | 0.005 | 88,935 | 0.005 | 0.004 | 28.965 | 396.057 | 53.271 |
| | | | | 88,910 | | | 28.965 | 396.057 | 53.271 |
| X11A | X-RAY FILM | 220.000 | 0.043 | 88,910 | 0.032 | 0.392 | 28.997 | 396.449 | 53.314 |
| X11B | X-RAY FILM | 220.000 | 0.043 | 88,690 | 0.032 | 0.392 | 29.029 | 396.840 | 53.357 |
| G106 — | GLASSINE | 25.000 | 0.005 | 88,470 | 0.005 | 0.004 | 29.034 | 396.844 | 53.362 |
| C11 ————* | EMULSION 7B | 75.000 | 0.029 | 88,445 | 0.022 | 0.263 | 29.055 | 397.107 | 53.391 |
| * | LUCITE BASE | 800.000 | 0.059 | 88,370 | 0.136 | 0.280 | 29.191 | 397.388 | 53.450 |
| * | EMULSION 7B | 75.000 | 0.029 | 87,570 | 0.022 | 0.263 | 29.213 | 397.651 | 53.479 |
| | | | | 87,495 | | | 29.213 | 397.651 | 53.479 |
| *12TH CYCLE | | | | 87,495 | | | 29.213 | 397.651 | 53.479 |
| | | | | 87,495 | | | 29.213 | 397.651 | 53.479 |
| G107 — | GLASSINE | 25.000 | 0.005 | 87,495 | 0.005 | 0.004 | 29.218 | 397.655 | 53.484 |
| LC12 | LEAD | 2,000.000 | 2.271 | 87,470 | 1.170 | 35.655 | 30.388 | 433.309 | 55.755 |
| G108 — | GLASSINE | 25.000 | 0.005 | 85,470 | 0.005 | 0.004 | 30.393 | 433.313 | 55.760 |
| | | | | 85,445 | | | 30.393 | 433.313 | 55.760 |
| X12A | X-RAY FILM | 220.000 | 0.043 | 85,665 | 0.032 | 0.392 | 30.425 | 433.705 | 55.803 |

# ECT MATERIALS COMPOSITION

| NAME | MATERIAL NAME | THICKNESS µm | MASS g/cm2 | HEIGHT µm | mfp % | r.l. % | Sum mfp % | Sum r.l. % | Sum g/cm2 |
|---|---|---|---|---|---|---|---|---|---|
| | | | | | | | | | |
| X12B | X-RAY FILM | 220.000 | 0.043 | 85,445 | 0.032 | 0.392 | 30.457 | 434.097 | 55.846 |
| G109 — | GLASSINE | 25.000 | 0.005 | 85,225 | 0.005 | 0.004 | 30.462 | 434.100 | 55.851 |
| C12 ——— * | EMULSION 7B | 75.000 | 0.029 | 85,200 | 0.022 | 0.263 | 30.484 | 434.364 | 55.880 |
| * | LUCITE BASE | 800.000 | 0.059 | 85,125 | 0.136 | 0.280 | 30.620 | 434.644 | 55.939 |
| * | EMULSION 7B | 75.000 | 0.029 | 84,325 | 0.022 | 0.263 | 30.641 | 434.907 | 55.968 |
| | | | | 84,250 | | | 30.641 | 434.907 | 55.968 |
| *13TH CYCLE | | | | 84,250 | | | 30.641 | 434.907 | 55.968 |
| | | | | 84,250 | | | 30.641 | 434.907 | 55.968 |
| G110 — | GLASSINE | 25.000 | 0.005 | 84,250 | 0.005 | 0.004 | 30.646 | 434.911 | 55.973 |
| LC13 | LEAD | 2,000.000 | 2.271 | 84,225 | 1.170 | 35.655 | 31.816 | 470.566 | 58.244 |
| G111 — | GLASSINE | 25.000 | 0.005 | 82,225 | 0.005 | 0.004 | 31.821 | 470.570 | 58.249 |
| | | | | 82,200 | | | 31.821 | 470.570 | 58.249 |
| X13A | X-RAY FILM | 220.000 | 0.043 | 82,200 | 0.032 | 0.392 | 31.853 | 470.961 | 58.292 |
| X13B | X-RAY FILM | 220.000 | 0.043 | 81,980 | 0.032 | 0.392 | 31.885 | 471.353 | 58.335 |
| G112 — | GLASSINE | 25.000 | 0.005 | 81,760 | 0.005 | 0.004 | 31.890 | 471.357 | 58.340 |
| C13 ——— * | EMULSION 7B | 75.000 | 0.029 | 81,735 | 0.022 | 0.263 | 31.912 | 471.620 | 58.369 |
| * | LUCITE BASE | 800.000 | 0.059 | 81,660 | 0.136 | 0.280 | 32.048 | 471.900 | 58.428 |
| * | EMULSION 7B | 75.000 | 0.029 | 80,935 | 0.022 | 0.263 | 32.070 | 472.163 | 58.457 |
| | | | | 80,860 | | | 32.070 | 472.163 | 58.457 |
| *14TH CYCLE | | | | 80,860 | | | 32.070 | 472.163 | 58.457 |
| | | | | 80,860 | | | 32.070 | 472.163 | 58.457 |
| G113 — | GLASSINE | 25.000 | 0.005 | 80,860 | 0.005 | 0.004 | 32.075 | 472.167 | 58.462 |
| LC14 | LEAD | 2,000.000 | 2.271 | 80,835 | 1.170 | 35.655 | 33.244 | 507.822 | 60.733 |
| G114 — | GLASSINE | 25.000 | 0.005 | 78,835 | 0.005 | 0.004 | 33.249 | 507.826 | 60.738 |
| | | | | 78,810 | | | 33.249 | 507.826 | 60.738 |
| X14A | X-RAY FILM | 220.000 | 0.043 | 78,810 | 0.032 | 0.392 | 33.281 | 508.217 | 60.781 |
| X14B | X-RAY FILM | 220.000 | 0.043 | 78,590 | 0.032 | 0.392 | 33.314 | 508.609 | 60.825 |
| G115— | GLASSINE | 25.000 | 0.005 | 78,370 | 0.005 | 0.004 | 33.319 | 508.613 | 60.830 |
| C14 ——— * | EMULSION 7B | 75.000 | 0.029 | 78,345 | 0.022 | 0.263 | 33.340 | 508.876 | 60.859 |
| * | LUCITE BASE | 800.000 | 0.059 | 78,270 | 0.136 | 0.280 | 33.476 | 509.156 | 60.918 |
| * | EMULSION 7B | 75.000 | 0.029 | 77,470 | 0.022 | 0.263 | 33.498 | 509.419 | 60.947 |
| G116 — | GLASSINE | 25.000 | 0.005 | 77,395 | 0.005 | 0.004 | 33.503 | 509.423 | 60.952 |
| B4(E19-E20) | CR-39 | 600.000 | 0.087 | 77,370 | 0.104 | 0.215 | 33.607 | 509.638 | 61.039 |
| | | | | 76,770 | | | 33.607 | 509.638 | 61.039 |
| *15TH CYCLE | | | | 76,770 | | | 33.607 | 509.638 | 61.039 |
| | | | | 76,770 | | | 33.607 | 509.638 | 61.039 |
| G117 — | GLASSINE | 25.000 | 0.005 | 76,770 | 0.005 | 0.004 | 33.612 | 509.642 | 61.044 |
| LC15 | LEAD | 2,000.000 | 2.271 | 76,745 | 1.170 | 35.655 | 34.782 | 545.297 | 63.315 |
| G118 — | GLASSINE | 25.000 | 0.005 | 74,745 | 0.005 | 0.004 | 34.787 | 545.301 | 63.320 |
| | | | | 74,720 | | | 34.787 | 545.301 | 63.320 |
| X15A | X-RAY FILM | 220.000 | 0.043 | 74,720 | 0.032 | 0.392 | 34.819 | 545.692 | 63.363 |
| X15B | X-RAY FILM | 220.000 | 0.043 | 74,500 | 0.032 | 0.392 | 34.851 | 546.084 | 63.406 |
| G119 — | GLASSINE | 25.000 | 0.005 | 74,280 | 0.005 | 0.004 | 34.856 | 546.088 | 63.411 |
| C15 ——— * | EMULSION 7B | 75.000 | 0.029 | 74,255 | 0.022 | 0.263 | 34.878 | 546.351 | 63.440 |
| * | LUCITE BASE | 800.000 | 0.059 | 74,180 | 0.136 | 0.280 | 35.014 | 546.631 | 63.499 |
| * | EMULSION 7B | 75.000 | 0.029 | 73,380 | 0.022 | 0.263 | 35.035 | 546.894 | 63.528 |
| | | | | 73,305 | | | 35.035 | 546.894 | 63.528 |
| *16TH CYCLE | | | | 73,305 | | | 35.035 | 546.894 | 63.528 |
| | | | | 73,305 | | | 35.035 | 546.894 | 63.528 |
| G120 — | GLASSINE | 25.000 | 0.005 | 73,280 | 0.005 | 0.004 | 35.040 | 546.898 | 63.533 |
| LC16 | LEAD + TLD | 2,000.000 | 2.271 | 73,255 | 1.170 | 35.655 | 36.210 | 582.553 | 65.804 |
| G121 — | GLASSINE | 25.000 | 0.005 | 71,255 | 0.005 | 0.004 | 36.215 | 582.557 | 65.809 |
| | | | | 71,230 | | | 36.215 | 582.557 | 65.809 |
| X16A | X-RAY FILM | 220.000 | 0.043 | 71,230 | 0.032 | 0.392 | 36.247 | 582.948 | 65.852 |
| X16B | X-RAY FILM | 220.000 | 0.043 | 71,010 | 0.032 | 0.392 | 36.279 | 583.340 | 65.895 |

# ECT MATERIALS COMPOSITION

| *NAME* | MATERIAL NAME | THICKNESS µm | MASS g/cm2 | HEIGHT µm | mfp % | r.l. % | Sum mfp % | Sum r.l. % | Sum g/cm2 |
|---|---|---|---|---|---|---|---|---|---|
| | | | | | | | | | |
| G122 – | GLASSINE | 25.000 | 0.005 | 70,790 | 0.005 | 0.004 | 36.285 | 583.344 | 65.900 |
| C16 ——— | EMULSION 7B | 75.000 | 0.029 | 70,765 | 0.022 | 0.263 | 36.306 | 583.607 | 65.929 |
| * | LUCITE BASE | 800.000 | 0.059 | 70,690 | 0.136 | 0.280 | 36.442 | 583.887 | 65.988 |
| * | EMULSION 7B | 75.000 | 0.029 | 69,890 | 0.022 | 0.263 | 36.464 | 584.150 | 66.017 |
| | | | | 69,815 | | | 36.464 | 584.150 | 66.017 |
| *17TH CYCLE* | | | | 69,815 | | | 36.464 | 584.150 | 66.017 |
| | | | | 69,815 | | | 36.464 | 584.150 | 66.017 |
| G123 – | GLASSINE | 25.000 | 0.005 | 69,815 | 0.005 | 0.004 | 36.469 | 584.154 | 66.022 |
| LC17 | LEAD | 2,000.000 | 2.271 | 69,790 | 1.170 | 35.655 | 37.638 | 619.809 | 68.293 |
| G124 – | GLASSINE | 25.000 | 0.005 | 67,790 | 0.005 | 0.004 | 37.643 | 619.813 | 68.298 |
| | | | | 67,765 | | | 37.643 | 619.813 | 68.298 |
| X17A | X-RAY FILM | 220.000 | 0.043 | 67,765 | 0.032 | 0.392 | 37.676 | 620.205 | 68.341 |
| X17B | X-RAY FILM | 220.000 | 0.043 | 67,545 | 0.032 | 0.392 | 37.708 | 620.596 | 68.384 |
| G125 – | GLASSINE | 25.000 | 0.005 | 67,325 | 0.005 | 0.004 | 37.713 | 620.600 | 68.389 |
| C17 ——— | EMULSION 7B | 75.000 | 0.029 | 67,300 | 0.022 | 0.263 | 37.734 | 620.863 | 68.418 |
| * | LUCITE BASE | 800.000 | 0.059 | 67,225 | 0.136 | 0.280 | 37.870 | 621.143 | 68.477 |
| * | EMULSION 7B | 75.000 | 0.029 | 66,425 | 0.022 | 0.263 | 37.892 | 621.407 | 68.506 |
| | | | | 66,350 | | | 37.892 | 621.407 | 68.506 |
| *18TH CYCLE* | | | | 66,350 | | | 37.892 | 621.407 | 68.506 |
| | | | | 66,350 | | | 37.892 | 621.407 | 68.506 |
| G126 – | GLASSINE | 25.000 | 0.005 | 66,350 | 0.005 | 0.004 | 37.897 | 621.411 | 68.511 |
| LC18 | LEAD | 2,000.000 | 2.271 | 66,325 | 1.170 | 35.655 | 39.067 | 657.065 | 70.782 |
| G127 – | GLASSINE | 25.000 | 0.005 | 64,325 | 0.005 | 0.004 | 39.072 | 657.069 | 70.787 |
| | | | | 64,300 | | | 39.072 | 657.069 | 70.787 |
| X18A | X-RAY FILM | 220.000 | 0.043 | 64,300 | 0.032 | 0.392 | 39.104 | 657.461 | 70.830 |
| X18B | X-RAY FILM | 220.000 | 0.043 | 64,080 | 0.032 | 0.392 | 39.136 | 657.852 | 70.873 |
| G128 – | GLASSINE | 25.000 | 0.005 | 63,860 | 0.005 | 0.004 | 39.141 | 657.856 | 70.878 |
| C18 ——— | EMULSION 7B | 75.000 | 0.029 | 63,835 | 0.022 | 0.263 | 39.163 | 658.119 | 70.907 |
| * | LUCITE BASE | 800.000 | 0.059 | 63,760 | 0.136 | 0.280 | 39.299 | 658.400 | 70.966 |
| * | EMULSION 7B | 75.000 | 0.029 | 62,960 | 0.022 | 0.263 | 39.320 | 658.663 | 70.995 |
| | | | | 62,885 | | | 39.320 | 658.663 | 70.995 |
| *19TH CYCLE* | | | | 62,885 | | | 39.320 | 658.663 | 70.995 |
| | | | | 62,885 | | | 39.320 | 658.663 | 70.995 |
| G129 – | GLASSINE | 25.000 | 0.005 | 62,885 | 0.005 | 0.004 | 39.325 | 658.667 | 71.000 |
| LC19 | LEAD | 2,000.000 | 2.271 | 62,860 | 1.170 | 35.655 | 40.495 | 694.321 | 73.271 |
| G130 – | GLASSINE | 25.000 | 0.005 | 60,860 | 0.005 | 0.004 | 40.500 | 694.325 | 73.276 |
| | | | | 60,835 | | | 40.500 | 694.325 | 73.276 |
| X19A | X-RAY FILM | 220.000 | 0.043 | 60,835 | 0.032 | 0.392 | 40.532 | 694.717 | 73.319 |
| X19B | X-RAY FILM | 220.000 | 0.043 | 60,615 | 0.032 | 0.392 | 40.564 | 695.109 | 73.362 |
| G131 – | GLASSINE | 25.000 | 0.005 | 60,395 | 0.005 | 0.004 | 40.569 | 695.112 | 73.367 |
| C19 ——— | EMULSION 7B | 75.000 | 0.029 | 60,370 | 0.022 | 0.263 | 40.591 | 695.376 | 73.396 |
| * | LUCITE BASE | 800.000 | 0.059 | 60,295 | 0.136 | 0.280 | 40.727 | 695.656 | 73.455 |
| * | EMULSION 7B | 75.000 | 0.029 | 59,495 | 0.022 | 0.263 | 40.748 | 695.919 | 73.484 |
| | | | | 59,420 | | | 40.748 | 695.919 | 73.484 |
| *20TH CYCLE* | | | | 59,420 | | | 40.748 | 695.919 | 73.484 |
| | | | | 59,420 | | | 40.748 | 695.919 | 73.484 |
| G132 – | GLASSINE | 25.000 | 0.005 | 59,420 | 0.005 | 0.004 | 40.754 | 695.923 | 73.489 |
| LC20 | LEAD | 2,000.000 | 2.271 | 59,395 | 1.170 | 35.655 | 41.923 | 731.578 | 75.760 |
| G133 – | GLASSINE | 25.000 | 0.005 | 57,395 | 0.005 | 0.004 | 41.928 | 731.582 | 75.765 |
| | | | | 57,370 | | | 41.928 | 731.582 | 75.765 |
| X20A | X-RAY FILM | 220.000 | 0.043 | 57,370 | 0.032 | 0.392 | 41.960 | 731.973 | 75.808 |
| X20B | X-RAY FILM | 220.000 | 0.043 | 57,150 | 0.032 | 0.392 | 41.993 | 732.365 | 75.852 |
| G134 – | GLASSINE | 25.000 | 0.005 | 56,930 | 0.005 | 0.004 | 41.998 | 732.369 | 75.857 |
| C20 ——— * | EMULSION 7B | 75.000 | 0.029 | 56,905 | 0.022 | 0.263 | 42.019 | 732.632 | 75.886 |
| * | LUCITE BASE | 800.000 | 0.059 | 56,830 | 0.136 | 0.280 | 42.155 | 732.912 | 75.945 |

# ECT MATERIALS COMPOSITION

| NAME | MATERIAL NAME | THICKNESS µm | MASS g/cm2 | HEIGHT µm | mfp % | r.l. % | Sum mfp % | Sum r.l. % | Sum g/cm2 |
|---|---|---|---|---|---|---|---|---|---|
| | | | | | | | | | |
| * | EMULSION 7B | 75.000 | 0.029 | 56,030 | 0.022 | 0.263 | 42.177 | 733.175 | 75.974 |
| | | | | 55,955 | | | 42.177 | 733.175 | 75.974 |
| *21ST CYCLE | | | | 55,955 | | | 42.177 | 733.175 | 75.974 |
| | | | | 55,955 | | | 42.177 | 733.175 | 75.974 |
| G135 — | GLASSINE | 25.000 | 0.005 | 55,955 | 0.005 | 0.004 | 42.182 | 733.179 | 75.979 |
| LC21 | LEAD | 2,000.000 | 2.271 | 55,930 | 1.170 | 35.655 | 43.352 | 768.834 | 78.250 |
| G136 — | GLASSINE | 25.000 | 0.005 | 53,930 | 0.005 | 0.004 | 43.357 | 768.838 | 78.255 |
| | | | | 53,905 | | | 43.357 | 768.838 | 78.255 |
| X21A | X-RAY FILM | 220.000 | 0.043 | 53,905 | 0.032 | 0.392 | 43.389 | 769.229 | 78.298 |
| X21B | X-RAY FILM | 220.000 | 0.043 | 53,685 | 0.032 | 0.392 | 43.421 | 769.621 | 78.341 |
| G137 — | GLASSINE | 25.000 | 0.005 | 53,465 | 0.005 | 0.004 | 43.426 | 769.625 | 78.346 |
| C21 ——— | EMULSION 7B | 75.000 | 0.029 | 53,440 | 0.022 | 0.263 | 43.448 | 769.888 | 78.375 |
| * | LUCITE BASE | 800.000 | 0.059 | 53,365 | 0.136 | 0.280 | 43.583 | 770.168 | 78.434 |
| * | EMULSION 7B | 75.000 | 0.029 | 52,565 | 0.022 | 0.263 | 43.605 | 770.431 | 78.463 |
| | | | | 52,490 | | | 43.605 | 770.431 | 78.463 |
| *22ND CYCLE | | | | 52,490 | | | 43.605 | 770.431 | 78.463 |
| | | | | 52,490 | | | 43.605 | 770.431 | 78.463 |
| G138 — | GLASSINE | 25.000 | 0.005 | 52,490 | 0.005 | 0.004 | 43.610 | 770.435 | 78.468 |
| LC22 | LEAD | 2,000.000 | 2.271 | 52,465 | 1.170 | 35.655 | 44.780 | 806.090 | 80.739 |
| G139 — | GLASSINE | 25.000 | 0.005 | 50,465 | 0.005 | 0.004 | 44.785 | 806.094 | 80.744 |
| | | | | 50,440 | | | 44.785 | 806.094 | 80.744 |
| X22A | X-RAY FILM | 220.000 | 0.043 | 50,440 | 0.032 | 0.392 | 44.817 | 806.486 | 80.787 |
| X22B | X-RAY FILM | 220.000 | 0.043 | 50,220 | 0.032 | 0.392 | 44.849 | 806.877 | 80.830 |
| G140 — | GLASSINE | 25.000 | 0.005 | 50,000 | 0.005 | 0.004 | 44.854 | 806.881 | 80.835 |
| C22 ———* | EMULSION 7B | 75.000 | 0.029 | 49,975 | 0.022 | 0.263 | 44.876 | 807.144 | 80.864 |
| * | LUCITE BASE | 800.000 | 0.059 | 49,900 | 0.136 | 0.280 | 45.012 | 807.425 | 80.923 |
| * | EMULSION 7B | 75.000 | 0.029 | 49,100 | 0.022 | 0.263 | 45.033 | 807.688 | 80.952 |
| | | | | 49,025 | | | 45.033 | 807.688 | 80.952 |
| *23RD CYCLE | | | | 49,025 | | | 45.033 | 807.688 | 80.952 |
| | | | | 49,025 | | | 45.033 | 807.688 | 80.952 |
| G141 — | GLASSINE | 25.000 | 0.005 | 49,025 | 0.005 | 0.004 | 45.038 | 807.692 | 80.957 |
| LC23 | LEAD | 2,000.000 | 2.271 | 49,000 | 1.170 | 35.655 | 46.208 | 843.346 | 83.228 |
| G142 — | GLASSINE | 25.000 | 0.005 | 47,000 | 0.005 | 0.004 | 46.213 | 843.350 | 83.233 |
| | | | | 46,975 | | | 46.213 | 843.350 | 83.233 |
| X23A | X-RAY FILM | 220.000 | 0.043 | 46,975 | 0.032 | 0.392 | 46.245 | 843.742 | 83.276 |
| X23B | X-RAY FILM | 220.000 | 0.043 | 46,755 | 0.032 | 0.392 | 46.277 | 844.133 | 83.319 |
| G143 — | GLASSINE | 25.000 | 0.005 | 46,535 | 0.005 | 0.004 | 46.283 | 844.137 | 83.324 |
| C23 ———* | EMULSION 7B | 75.000 | 0.029 | 46,510 | 0.022 | 0.263 | 46.304 | 844.400 | 83.353 |
| * | LUCITE BASE | 800.000 | 0.059 | 46,435 | 0.136 | 0.280 | 46.440 | 844.681 | 83.412 |
| * | EMULSION 7B | 75.000 | 0.029 | 45,635 | 0.022 | 0.263 | 46.462 | 844.944 | 83.441 |
| | | | | 45,560 | | | 46.462 | 844.944 | 83.441 |
| *24TH CYCLE | | | | 45,560 | | | 46.462 | 844.944 | 83.441 |
| | | | | 45,560 | | | 46.462 | 844.944 | 83.441 |
| G144 — | GLASSINE | 25.000 | 0.005 | 45,560 | 0.005 | 0.004 | 46.467 | 844.948 | 83.446 |
| LC24 | LEAD | 2,000.000 | 2.271 | 45,535 | 1.170 | 35.655 | 47.636 | 880.602 | 85.717 |
| G145 — | GLASSINE | 25.000 | 0.005 | 43,535 | 0.005 | 0.004 | 47.642 | 880.606 | 85.722 |
| | | | | 43,510 | | | 47.642 | 880.606 | 85.722 |
| X24A | X-RAY FILM | 220.000 | 0.043 | 43,510 | 0.032 | 0.392 | 47.674 | 880.998 | 85.765 |
| X24B | X-RAY FILM | 220.000 | 0.043 | 43,290 | 0.032 | 0.392 | 47.706 | 881.390 | 85.808 |
| G146 — | GLASSINE | 25.000 | 0.005 | 43,070 | 0.005 | 0.004 | 47.711 | 881.394 | 85.813 |
| C24 ———* | EMULSION 7B | 75.000 | 0.029 | 43,045 | 0.022 | 0.263 | 47.732 | 881.657 | 85.842 |
| * | LUCITE BASE | 800.000 | 0.059 | 42,970 | 0.136 | 0.280 | 47.868 | 881.937 | 85.901 |
| * | EMULSION 7B | 75.000 | 0.029 | 42,170 | 0.022 | 0.263 | 47.890 | 882.200 | 85.930 |
| | | | | 42,095 | | | 47.890 | 882.200 | 85.930 |
| *25TH CYCLE | | | | 42,095 | | | 47.890 | 882.200 | 85.930 |

| *NAME* | MATERIAL NAME | THICKNESS µm | MASS g/cm2 | HEIGHT µm | mfp % | r.l. % | Sum mfp % | Sum r.l. % | Sum g/cm2 |
|---|---|---|---|---|---|---|---|---|---|
| | | | | | | | | | |
| | | | | 42,095 | | | 47.890 | 882.200 | 85.930 |
| G147 – | GLASSINE | 25.000 | 0.005 | 42,095 | 0.005 | 0.004 | 47.895 | 882.204 | 85.935 |
| LC25 | LEAD | 2,000.000 | 2.271 | 42,070 | 1.170 | 35.655 | 49.065 | 917.859 | 88.206 |
| G148 – | GLASSINE | 25.000 | 0.005 | 40,070 | 0.005 | 0.004 | 49.070 | 917.863 | 88.211 |
| | | | | 40,045 | | | 49.070 | 917.863 | 88.211 |
| X25A | X-RAY FILM | 220.000 | 0.043 | 40,045 | 0.032 | 0.392 | 49.102 | 918.254 | 88.254 |
| X25B | X-RAY FILM | 220.000 | 0.043 | 39,825 | 0.032 | 0.392 | 49.134 | 918.646 | 88.297 |
| G149 – | GLASSINE | 25.000 | 0.005 | 39,605 | 0.005 | 0.004 | 49.139 | 918.650 | 88.302 |
| C25———* | EMULSION 7B | 75.000 | 0.029 | 39,580 | 0.022 | 0.263 | 49.161 | 918.913 | 88.331 |
| * | LUCITE BASE | 800.000 | 0.059 | 39,505 | 0.136 | 0.280 | 49.297 | 919.193 | 88.390 |
| * | EMULSION 7B | 75.000 | 0.029 | 38,705 | 0.022 | 0.263 | 49.318 | 919.456 | 88.419 |
| G150 – | GLASSINE | 25.000 | 0.005 | 38,630 | 0.005 | 0.004 | 49.323 | 919.460 | 88.424 |
| B5(E34-E39) | CR-39 | 600.000 | 0.087 | 38,605 | 0.104 | 0.215 | 49.427 | 919.675 | 88.511 |
| | | | | 38,005 | | | 49.427 | 919.675 | 88.511 |
| **26TH CYCLE* | | | | 38,005 | | | 49.427 | 919.675 | 88.511 |
| | | | | 38,005 | | | 49.427 | 919.675 | 88.511 |
| G151 – | GLASSINE | 25.000 | 0.005 | 38,005 | 0.005 | 0.004 | 49.433 | 919.679 | 88.516 |
| LC26 | LEAD | 2,000.000 | 2.271 | 37,980 | 1.170 | 35.655 | 50.602 | 955.333 | 90.787 |
| G152 – | GLASSINE | 25.000 | 0.005 | 35,980 | 0.005 | 0.004 | 50.607 | 955.337 | 90.792 |
| | | | | 35,955 | | | 50.607 | 955.337 | 90.792 |
| X26A | X-RAY FILM | 220.000 | 0.043 | 35,955 | 0.032 | 0.392 | 50.639 | 955.729 | 90.835 |
| X26B | X-RAY FILM | 220.000 | 0.043 | 35,735 | 0.032 | 0.392 | 50.672 | 956.121 | 90.878 |
| G153 – | GLASSINE | 25.000 | 0.005 | 35,515 | 0.005 | 0.004 | 50.677 | 956.125 | 90.883 |
| C26———* | EMULSION 7B | 75.000 | 0.029 | 35,490 | 0.022 | 0.263 | 50.698 | 956.388 | 90.912 |
| * | LUCITE BASE | 800.000 | 0.059 | 35,415 | 0.136 | 0.280 | 50.834 | 956.668 | 90.971 |
| * | EMULSION 7B | 75.000 | 0.029 | 34,615 | 0.022 | 0.263 | 50.856 | 956.931 | 91.000 |
| | | | | 34,540 | | | 50.856 | 956.931 | 91.000 |
| **27TH CYCLE* | | | | 34,540 | | | 50.856 | 956.931 | 91.000 |
| | | | | 34,540 | | | 50.856 | 956.931 | 91.000 |
| G154 – | GLASSINE | 25.000 | 0.005 | 34,540 | 0.005 | 0.004 | 50.861 | 956.935 | 91.005 |
| LC27 | LEAD | 2,000.000 | 2.271 | 34,515 | 1.170 | 35.655 | 52.030 | 992.590 | 93.276 |
| G155 – | GLASSINE | 25.000 | 0.005 | 32,515 | 0.005 | 0.004 | 52.036 | 992.594 | 93.281 |
| | | | | 32,490 | | | 52.036 | 992.594 | 93.281 |
| X27A | X-RAY FILM | 220.000 | 0.043 | 32,490 | 0.032 | 0.392 | 52.068 | 992.985 | 93.325 |
| X27B | X-RAY FILM | 220.000 | 0.043 | 32,270 | 0.032 | 0.392 | 52.100 | 993.377 | 93.368 |
| G156 – | GLASSINE | 25.000 | 0.005 | 32,050 | 0.005 | 0.004 | 52.105 | 993.381 | 93.373 |
| C27———* | EMULSION 7B | 75.000 | 0.029 | 32,025 | 0.022 | 0.263 | 52.127 | 993.644 | 93.402 |
| * | LUCITE BASE | 800.000 | 0.059 | 31,950 | 0.136 | 0.280 | 52.262 | 993.924 | 93.461 |
| * | EMULSION 7B | 75.000 | 0.029 | 31,150 | 0.022 | 0.263 | 52.284 | 994.187 | 93.490 |
| | | | | 31,075 | | | 52.284 | 994.187 | 93.490 |
| **28TH CYCLE* | | | | 31,075 | | | 52.284 | 994.187 | 93.490 |
| | | | | 31,075 | | | 52.284 | 994.187 | 93.490 |
| G157 – | GLASSINE | 25.000 | 0.005 | 31,075 | 0.005 | 0.004 | 52.289 | 994.191 | 93.495 |
| LC28 | LEAD | 2,000.000 | 2.271 | 31,050 | 1.170 | 35.655 | 53.459 | 1,029.846 | 95.766 |
| G158 – | GLASSINE | 25.000 | 0.005 | 29,050 | 0.005 | 0.004 | 53.464 | 1,029.850 | 95.771 |
| | | | | 29,025 | | | 53.464 | 1,029.850 | 95.771 |
| X28A | X-RAY FILM | 220.000 | 0.043 | 29,025 | 0.032 | 0.392 | 53.496 | 1,030.241 | 95.814 |
| X28B | X-RAY FILM | 220.000 | 0.043 | 28,805 | 0.032 | 0.392 | 53.528 | 1,030.633 | 95.857 |
| G159 – | GLASSINE | 25.000 | 0.005 | 28,585 | 0.005 | 0.004 | 53.533 | 1,030.637 | 95.862 |
| C28———* | EMULSION 7B | 75.000 | 0.029 | 28,560 | 0.022 | 0.263 | 53.555 | 1,030.900 | 95.891 |
| * | LUCITE BASE | 800.000 | 0.059 | 28,485 | 0.136 | 0.280 | 53.691 | 1,031.180 | 95.950 |
| * | EMULSION 7B | 75.000 | 0.029 | 27,685 | 0.022 | 0.263 | 53.712 | 1,031.443 | 95.979 |
| | | | | 27,610 | | | 53.712 | 1,031.443 | 95.979 |
| | | | | 27,610 | | | 53.712 | 1,031.443 | 95.979 |
| **29TH CYCLE* | | | | 27,610 | | | 53.712 | 1,031.443 | 95.979 |

| NAME | MATERIAL NAME | THICKNESS μm | MASS g/cm2 | HEIGHT μm | mfp % | r.l. % | Sum mfp % | Sum r.l. % | Sum g/cm2 |
|---|---|---|---|---|---|---|---|---|---|
| | | | | | | | | | |
| | | | | 27,610 | | | 53.712 | 1,031.443 | 95.979 |
| G160 — | GLASSINE | 25.000 | 0.005 | 27,610 | 0.005 | 0.004 | 53.717 | 1,031.447 | 95.984 |
| LC29 | LEAD + TLD | 2,000.000 | 2.271 | 27,585 | 1.170 | 35.655 | 54.887 | 1,067.102 | 98.255 |
| G161 — | GLASSINE | 25.000 | 0.005 | 25,585 | 0.005 | 0.004 | 54.892 | 1,067.106 | 98.260 |
| | | | | 25,560 | | | 54.892 | 1,067.106 | 98.260 |
| X29A | X-RAY FILM | 220.000 | 0.043 | 25,560 | 0.032 | 0.392 | 54.924 | 1,067.498 | 98.303 |
| X29B | X-RAY FILM | 220.000 | 0.043 | 25,340 | 0.032 | 0.392 | 54.956 | 1,067.889 | 98.346 |
| G162 — | GLASSINE | 25.000 | 0.005 | 25,120 | 0.005 | 0.004 | 54.962 | 1,067.893 | 98.351 |
| C29———* | EMULSION 7B | 75.000 | 0.029 | 25,170 | 0.022 | 0.263 | 54.983 | 1,068.156 | 98.380 |
| * | LUCITE BASE | 800.000 | 0.059 | 25,095 | 0.136 | 0.280 | 55.119 | 1,068.437 | 98.439 |
| * | EMULSION 7B | 75.000 | 0.029 | 24,295 | 0.022 | 0.263 | 55.141 | 1,068.700 | 98.468 |
| | | | | 24,220 | | | 55.141 | 1,068.700 | 98.468 |
| | | | | 24,220 | | | 55.141 | 1,068.700 | 98.468 |
| *30TH CYCLE | | | | 24,220 | | | 55.141 | 1,068.700 | 98.468 |
| | | | | 24,220 | | | 55.141 | 1,068.700 | 98.468 |
| G163 — | GLASSINE | 25.000 | 0.005 | 24,220 | 0.005 | 0.004 | 55.146 | 1,068.704 | 98.473 |
| LC30 | LEAD | 2,000.000 | 2.271 | 24,195 | 1.170 | 35.655 | 56.315 | 1,104.358 | 100.744 |
| G164 — | GLASSINE | 25.000 | 0.005 | 22,195 | 0.005 | 0.004 | 56.320 | 1,104.362 | 100.749 |
| | | | | 22,170 | | | 56.320 | 1,104.362 | 100.749 |
| X30A | X-RAY FILM | 220.000 | 0.043 | 22,170 | 0.032 | 0.392 | 56.353 | 1,104.754 | 100.792 |
| X30B | X-RAY FILM | 220.000 | 0.043 | 21,950 | 0.032 | 0.392 | 56.385 | 1,105.145 | 100.835 |
| G165 — | GLASSINE | 25.000 | 0.005 | 21,730 | 0.005 | 0.004 | 56.390 | 1,105.149 | 100.840 |
| C30———* | EMULSION 7B | 75.000 | 0.029 | 21,705 | 0.022 | 0.263 | 56.411 | 1,105.412 | 100.869 |
| * | LUCITE BASE | 800.000 | 0.059 | 21,630 | 0.136 | 0.280 | 56.547 | 1,105.693 | 100.928 |
| * | EMULSION 7B | 75.000 | 0.029 | 20,830 | 0.022 | 0.263 | 56.569 | 1,105.956 | 100.957 |
| | | | | 20,755 | | | 56.569 | 1,105.956 | 100.957 |
| | | | | 20,755 | | | 56.569 | 1,105.956 | 100.957 |
| *31ST CYCLE | | | | 20,755 | | | 56.569 | 1,105.956 | 100.957 |
| | | | | 20,755 | | | 56.569 | 1,105.956 | 100.957 |
| G166 — | GLASSINE | 25.000 | 0.005 | 20,755 | 0.005 | 0.004 | 56.574 | 1,105.960 | 100.962 |
| LC31 | LEAD | 2,000.000 | 2.271 | 20,730 | 1.170 | 35.655 | 57.744 | 1,141.614 | 103.233 |
| G167 — | GLASSINE | 25.000 | 0.005 | 18,730 | 0.005 | 0.004 | 57.749 | 1,141.618 | 103.238 |
| | | | | 18,705 | | | 57.749 | 1,141.618 | 103.238 |
| X31A | X-RAY FILM | 220.000 | 0.043 | 18,705 | 0.032 | 0.392 | 57.781 | 1,142.010 | 103.281 |
| X31B | X-RAY FILM | 220.000 | 0.043 | 18,485 | 0.032 | 0.392 | 57.813 | 1,142.402 | 103.324 |
| G168 — | GLASSINE | 25.000 | 0.005 | 18,265 | 0.005 | 0.004 | 57.818 | 1,142.406 | 103.329 |
| C31 ———* | EMULSION 7B | 75.000 | 0.029 | 18,240 | 0.022 | 0.263 | 57.840 | 1,142.669 | 103.358 |
| * | LUCITE BASE | 800.000 | 0.059 | 18,165 | 0.136 | 0.280 | 57.976 | 1,142.949 | 103.417 |
| * | EMULSION 7B | 75.000 | 0.029 | 17,365 | 0.022 | 0.263 | 57.997 | 1,143.212 | 103.446 |
| | | | | 17,290 | | | 57.997 | 1,143.212 | 103.446 |
| | | | | 17,290 | | | 57.997 | 1,143.212 | 103.446 |
| *32ND CYCLE | | | | 17,290 | | | 57.997 | 1,143.212 | 103.446 |
| | | | | 17,290 | | | 57.997 | 1,143.212 | 103.446 |
| G169 — | GLASSINE | 25.000 | 0.005 | 17,290 | 0.005 | 0.004 | 58.002 | 1,143.216 | 103.451 |
| LC32 | LEAD | 2,000.000 | 2.271 | 17,265 | 1.170 | 35.655 | 59.172 | 1,178.871 | 105.722 |
| G170 — | GLASSINE | 25.000 | 0.005 | 15,265 | 0.005 | 0.004 | 59.177 | 1,178.875 | 105.727 |
| | | | | 15,240 | | | 59.177 | 1,178.875 | 105.727 |
| X32A | X-RAY FILM | 220.000 | 0.043 | 15,240 | 0.032 | 0.392 | 59.209 | 1,179.266 | 105.770 |
| X32B | X-RAY FILM | 220.000 | 0.043 | 15,020 | 0.032 | 0.392 | 59.241 | 1,179.658 | 105.813 |
| G171 — | GLASSINE | 25.000 | 0.005 | 14,800 | 0.005 | 0.004 | 59.246 | 1,179.662 | 105.818 |
| C32———* | EMULSION 7B | 75.000 | 0.029 | 14,775 | 0.022 | 0.263 | 59.268 | 1,179.925 | 105.847 |
| * | LUCITE BASE | 800.000 | 0.059 | 14,700 | 0.136 | 0.280 | 59.404 | 1,180.205 | 105.906 |
| * | EMULSION 7B | 75.000 | 0.029 | 13,900 | 0.022 | 0.263 | 59.425 | 1,180.468 | 105.935 |
| G172 — | GLASSINE | 25.000 | 0.005 | 13,825 | 0.005 | 0.004 | 59.431 | 1,180.472 | 105.940 |
| B6(E12-E05) | CR-39 | 600.000 | 0.087 | 13,800 | 0.104 | 0.215 | 59.535 | 1,180.687 | 106.027 |

# ECT MATERIALS COMPOSITION

| NAME | MATERIAL NAME | THICKNESS µm | MASS g/cm2 | HEIGHT µm | mfp % | r.l. % | Sum mfp % | Sum r.l. % | Sum g/cm2 |
|---|---|---|---|---|---|---|---|---|---|
| | | | | | | | | | |
| | | | | 13,200 | | | 59.535 | 1,180.687 | 106.027 |
| *33RD CYCLE | | | | 13,200 | | | 59.535 | 1,180.687 | 106.027 |
| | | | | 13,200 | | | 59.535 | 1,180.687 | 106.027 |
| G173 – | GLASSINE | 25.000 | 0.005 | 13,200 | 0.005 | 0.004 | 59.540 | 1,180.691 | 106.032 |
| LC33 | LEAD | 2,000.000 | 2.271 | 13,175 | 1.170 | 35.655 | 60.709 | 1,216.345 | 108.303 |
| G174 – | GLASSINE | 25.000 | 0.005 | 11,175 | 0.005 | 0.004 | 60.715 | 1,216.349 | 108.308 |
| | | | | 11,150 | | | 60.715 | 1,216.349 | 108.308 |
| X33A | X-RAY FILM | 220.000 | 0.043 | 11,150 | 0.032 | 0.392 | 60.747 | 1,216.741 | 108.352 |
| X33B | X-RAY FILM | 220.000 | 0.043 | 10,930 | 0.032 | 0.392 | 60.779 | 1,217.133 | 108.395 |
| G175 – | GLASSINE | 25.000 | 0.005 | 10,710 | 0.005 | 0.004 | 60.784 | 1,217.137 | 108.400 |
| C33———* | EMULSION 7B | 75.000 | 0.029 | 10,685 | 0.022 | 0.263 | 60.806 | 1,217.400 | 108.429 |
| * | LUCITE BASE | 800.000 | 0.059 | 10,610 | 0.136 | 0.280 | 60.941 | 1,217.680 | 108.488 |
| * | EMULSION 7B | 75.000 | 0.029 | 9,810 | 0.022 | 0.263 | 60.963 | 1,217.943 | 108.517 |
| | | | | 9,735 | | | 60.963 | 1,217.943 | 108.517 |
| *34TH CYCLE | | | | 9,735 | | | 60.963 | 1,217.943 | 108.517 |
| | | | | 9,735 | | | 60.963 | 1,217.943 | 108.517 |
| G176 – | GLASSINE | 25.000 | 0.005 | 9,735 | 0.005 | 0.004 | 60.968 | 1,217.947 | 108.522 |
| LC34 | LEAD + TLD | 2,000.000 | 2.271 | 9,710 | 1.170 | 35.655 | 62.138 | 1,253.602 | 110.793 |
| G177 – | GLASSINE | 25.000 | 0.005 | 7,710 | 0.005 | 0.004 | 62.143 | 1,253.606 | 110.798 |
| | | | | 7,685 | | | 62.143 | 1,253.606 | 110.798 |
| X34A | X-RAY FILM | 220.000 | 0.043 | 7,685 | 0.032 | 0.392 | 62.175 | 1,253.997 | 110.841 |
| X34B | X-RAY FILM | 220.000 | 0.043 | 7,465 | 0.032 | 0.392 | 62.207 | 1,254.389 | 110.884 |
| G178 – | GLASSINE | 25.000 | 0.005 | 7,245 | 0.005 | 0.004 | 62.212 | 1,254.393 | 110.889 |
| C34———* | EMULSION 7B | 75.000 | 0.029 | 7,220 | 0.022 | 0.263 | 62.234 | 1,254.656 | 110.918 |
| * | LUCITE BASE | 800.000 | 0.059 | 7,145 | 0.136 | 0.280 | 62.370 | 1,254.936 | 110.977 |
| * | EMULSION 7B | 75.000 | 0.029 | 6,420 | 0.022 | 0.263 | 62.391 | 1,255.199 | 111.006 |
| | | | | 6,345 | | | 62.391 | 1,255.199 | 111.006 |
| *35TH CYCLE | | | | 6,345 | | | 62.391 | 1,255.199 | 111.006 |
| | | | | 6,345 | | | 62.391 | 1,255.199 | 111.006 |
| G179 – | GLASSINE | 25.000 | 0.005 | 6,345 | 0.005 | 0.004 | 62.396 | 1,255.203 | 111.011 |
| LC35 | LEAD + THERM | 2,000.000 | 2.271 | 6,320 | 1.170 | 35.655 | 63.566 | 1,290.858 | 113.282 |
| G180 – | GLASSINE | 25.000 | 0.005 | 4,320 | 0.005 | 0.004 | 63.571 | 1,290.862 | 113.287 |
| | | | | 4,295 | | | 63.571 | 1,290.862 | 113.287 |
| X35A | X-RAY FILM | 220.000 | 0.043 | 4,295 | 0.032 | 0.392 | 63.603 | 1,291.253 | 113.330 |
| X35B | X-RAY FILM | 220.000 | 0.043 | 4,075 | 0.032 | 0.392 | 63.635 | 1,291.645 | 113.373 |
| G181 – | GLASSINE | 25.000 | 0.005 | 3,855 | 0.005 | 0.004 | 63.640 | 1,291.649 | 113.378 |
| C35———* | EMULSION 7B | 75.000 | 0.029 | 3,830 | 0.022 | 0.263 | 63.662 | 1,291.912 | 113.407 |
| * | LUCITE BASE | 800.000 | 0.059 | 3,755 | 0.136 | 0.280 | 63.798 | 1,292.192 | 113.466 |
| * | EMULSION 7B | 75.000 | 0.029 | 2,955 | 0.022 | 0.263 | 63.820 | 1,292.455 | 113.495 |
| | | | | 2,880 | | | 63.820 | 1,292.455 | 113.495 |
| ********** | ********** | | | 2,880 | | | 63.820 | 1,292.455 | 113.495 |
| **** END OF | CALORIMETER | | | 2,880 | | | 63.820 | 1,292.455 | 113.495 |
| ********** | ********** | | | 2,880 | | | 63.820 | 1,292.455 | 113.495 |
| | | | | 2,880 | | | 63.820 | 1,292.455 | 113.495 |
| G182 – | GLASSINE | 25.000 | 0.005 | 2,880 | 0.005 | 0.004 | 63.825 | 1,292.459 | 113.500 |
| C36———* | EMULSION 7B | 200.000 | 0.772 | 2,855 | 0.058 | 0.702 | 63.882 | 1,293.161 | 114.272 |
| * | LUCITE BASE | 300.000 | 0.035 | 2,655 | 0.051 | 0.105 | 63.933 | 1,293.266 | 114.307 |
| * | EMULSION 7B | 200.000 | 0.772 | 2,355 | 0.058 | 0.702 | 63.991 | 1,293.968 | 115.079 |
| G183 – | GLASSINE | 25.000 | 0.005 | 2,155 | 0.005 | 0.004 | 63.996 | 1,293.972 | 115.084 |
| B7(E04-E01) | CR39 | 600.000 | 0.087 | 2,130 | 0.104 | 0.215 | 64.100 | 1,294.186 | 115.171 |
| G184 – | GLASSINE | 25.000 | 0.005 | 1,530 | 0.005 | 0.004 | 64.105 | 1,294.190 | 115.176 |
| | | 0.000 | | 1,505 | | | 64.105 | 1,294.190 | 115.176 |
| *TEST ITEMS | | 0.000 | | 1,505 | | | 64.105 | 1,294.190 | 115.176 |
| | | 0.000 | | 1,505 | | | 64.105 | 1,294.190 | 115.176 |
| G185 – | GLASSINE | 25.000 | 0.005 | 1,505 | 0.005 | 0.004 | 64.110 | 1,294.194 | 115.181 |

# ECT MATERIALS COMPOSITION

| *NAME* | MATERIAL NAME | THICKNESS µm | MASS g/cm2 | HEIGHT µm | mfp % | r.l. % | Sum mfp % | Sum r.l. % | Sum g/cm2 |
|---|---|---|---|---|---|---|---|---|---|
| | | | | | | | | | |
| S-1 — | SEALON FILM | 100.000 | 0.015 | 1,480 | 0.011 | 0.035 | 64.121 | 1,294.229 | 115.196 |
| X1 TEST | X-RAY FILM | 220.000 | 0.043 | 1,380 | 0.032 | 0.392 | 64.153 | 1,294.621 | 115.239 |
| G186 — | GLASSINE | 25.000 | 0.005 | 1,160 | 0.005 | 0.004 | 64.158 | 1,294.625 | 115.244 |
| S-2 — | SEALON FILM | 100.000 | 0.015 | 1,135 | 0.011 | 0.035 | 64.169 | 1,294.660 | 115.258 |
| X2 TEST | X-RAY FILM | 220.000 | 0.043 | 1,035 | 0.032 | 0.392 | 64.201 | 1,295.051 | 115.301 |
| G187 — | GLASSINE | 25.000 | 0.005 | 815 | 0.005 | 0.004 | 64.206 | 1,295.055 | 115.306 |
| S-3 — | SEALON FILM | 100.000 | 0.015 | 790 | 0.011 | 0.035 | 64.217 | 1,295.090 | 115.321 |
| X3 TEST | X-RAY FILM | 220.000 | 0.043 | 690 | 0.032 | 0.392 | 64.249 | 1,295.482 | 115.364 |
| G188 — | GLASSINE | 25.000 | 0.005 | 470 | 0.005 | 0.004 | 64.254 | 1,295.486 | 115.369 |
| S-4 — | SEALON FILM | 100.000 | 0.015 | 445 | 0.011 | 0.035 | 64.265 | 1,295.521 | 115.384 |
| X4 TEST | X-RAY FILM | 220.000 | 0.043 | 345 | 0.032 | 0.392 | 64.297 | 1,295.913 | 115.427 |
| G189 — | GLASSINE | 25.000 | 0.005 | 125 | 0.005 | 0.004 | 64.302 | 1,295.916 | 115.432 |
| S-5 — | SEALON FILM | 100.000 | 0.015 | 100 | 0.011 | 0.035 | 64.313 | 1,295.951 | 115.446 |
| | | 0.000 | 0.000 | 0 | | | 64.313 | 1,295.951 | 115.446 |
| | | | | | | | | | |
| ********** | ********** | | | | | | | | |
| BOTTOM OF THE CHAMBER | | | | | | | | | |
| ********** | ********** | | | | | | | | |